

**Preclinical studies on
holmium-166 poly(L-lactic acid)
microspheres
for hepatic arterial radioembolization**

Maarten A.D. Vente

Preclinical studies on holmium-166 poly(L-lactic acid) microspheres for hepatic arterial radioembolization

PhD thesis, Utrecht University – with a summary in Dutch

© M.A.D. Vente, Bosch en Duin, 2009

The copyright of the articles that have been published or have been accepted for publication has been transferred to the respective journals.

ISBN: 978-90-393-5096-6

The research described in this thesis was carried out at the department of Radiology and Nuclear Medicine, University Medical Center Utrecht (Utrecht, The Netherlands), under the auspices of ImagO, the Graduate Programme Medical Imaging. The project was financially supported by the Dutch Technology Foundation STW under grant 06069.

Layout: Karin van Rijnbach

Printing: Ipskamp Drukkers B.V., Enschede, The Netherlands

Cover: Isodose curves calculated with Monte Carlo software, derived from an autoradiography image acquired *ex vivo* from a liver (slice) of a pig in which holmium-166 poly(L-lactic acid) microspheres had been instilled.

**Preclinical studies on
holmium-166 poly(L-lactic acid)
microspheres
for hepatic arterial radioembolization**

Preklinische studies aan holmium-166
poly(L-melkzuur) microsferen
voor radioembolisatie van de leverslagader

(met een samenvatting in het Nederlands)

Proefschrift

ter verkrijging van de graad van doctor
aan de Universiteit Utrecht
op gezag van de rector magnificus, prof. dr. J.C. Stoof,
ingevolge het besluit van het college voor promoties
in het openbaar te verdedigen
op donderdag 9 juli 2009 des middags te 2.30 uur

door

Maarten Albert Dirk Vente

geboren op 15 juli 1970 te Amstelveen

Promotor: Prof. dr. P.P. van Rijk

Co-promotoren: Dr. A.D. van het Schip
Dr. J.F.W. Nijsen

Manuscriptcommissie: Prof. dr. P.R. Lijten (voorzitter)
Prof. dr. W.P.Th.M. Mali
Prof. dr. L. Defreyne
Prof. dr. H.Th. Wolterbeek

Publication of this thesis was financially supported by:
Advanced Accelerator Applications
Covidien Nederland B.V.
IDB-Holland B.V.
Stichting Nationaal Fonds tegen Kanker – voor onderzoek naar reguliere en
aanvullende therapieën te Amsterdam
Veenstra Instruments B.V.

Ter nagedachtenis aan mijn moeder
Voor mijn vader

CONTENTS

Chapter 1	Introduction and outline of the thesis	9
Chapter 2	Radionuclide liver cancer therapies: from concept to current clinical status	17
Chapter 3	Neutron activation of holmium poly(L-lactic acid) microspheres for hepatic arterial radioembolization: a validation study	81
Chapter 4	Clinical effects of transcatheter hepatic arterial radioembolization with holmium-166 poly(L-lactic acid) microspheres in healthy pigs	103
Chapter 5	Holmium-166 poly(L-lactic acid) microsphere radioembolization of the liver: technical aspects studied in a large-animal model	129
Chapter 6	Hepatic dosimetry for holmium-166 and yttrium-90 radioembolization: comparison of MIRD, dose-point kernel, and MCNP	149
Chapter 7	Yttrium-90 microsphere radioembolization for the treatment of liver malignancies: a structured meta-analysis	173
Chapter 8	Interstitial microbrachytherapy using small holmium-166 acetylacetonate microspheres for radioablation of intrahepatic malignancies	193
Chapter 9	Summary and future directions	213
	Samenvatting in het Nederlands	221
	Dankwoord	229
	Curriculum vitae and list of publications	237

CHAPTER 1

Introduction and outline of the thesis



Chapter 1

1 INTRODUCTION

Liver cancer, whether primary or metastatic, represents a major cause of death [1]. The treatment option of choice is partial hepatectomy, but unfortunately a high percentage of patients is not eligible for complete surgical resection [2]. Despite recent improvements in response rates and in median survival, the effect of systemic chemotherapy on overall survival in patients with malignant liver disease remains insignificant for most tumor types [3,4]. The third classic treatment modality is external beam radiation therapy of which the role is limited because of the low whole-liver tolerance to radiation [5]. The need therefore exists for effective liver-directed treatment options. One relatively novel treatment modality, which is increasingly applied in patients with unresectable liver malignancies, consists of the hepatic arterial instillation of embolic microspheres, loaded with the high-energy beta-emitting radio-isotope yttrium-90 (^{90}Y) [6-8]. Efficacy of this type of internal radiation therapy, often referred to as ^{90}Y radioembolization, relies on the difference in blood supply between liver tumors and the normal liver parenchyma. Whereas the normal liver receives its blood mainly from the portal vein, liver tumors are exclusively dependent on arterial blood supply [9,10]. The microspheres are administered *via* a catheter placed in the hepatic artery and will therefore be passively targeted mainly to the liver tumors which will subsequently receive a high radiation dose [7]. Currently, over 10,000 patients have undergone ^{90}Y radioembolization and high response rates have been reported, but the effect on overall survival has not yet been established [11,12]. Post-administration visualization of the ^{90}Y microspheres' biodistribution is hampered by ^{90}Y 's lack of gamma emission. Bremsstrahlung scintigraphy can be performed, but the image quality is poor and quantitative analysis was demonstrated to be not feasible [13,14].

At the nuclear medicine department of the University Medical Center Utrecht, work started in the mid-nineties on the development of poly(L-lactic acid) microspheres loaded with the radioisotope holmium-166 (^{166}Ho -PLLA-MS) [15]. The main advantages of the use of ^{166}Ho over ^{90}Y lie in its medical imaging possibilities. Next to high-energy beta particles, ^{166}Ho emits low-energy gamma rays, which allows for nuclear imaging of a quality sufficient for quantitative analysis [16]. It is also a highly paramagnetic element, therefore permitting magnetic resonance imaging (MRI) [17]. These imaging possibilities are

particularly useful for patient dosimetry purposes. The preparation under Good Manufacturing Practice conditions of the 'cold' ^{165}Ho -PLLA-MS, the effects on the PLLA matrix of the neutron activation in a nuclear reactor, the *in vitro* and *in vivo* degradation behavior, qualitative and quantitative MRI analysis, and *in vivo* efficacy and biocompatibility of this microdevice, have all been extensively investigated in previous research. A key result of this research was the observation that only minute amounts of radioactivity eluded from the microspheres, both *in vitro* and *in vivo* [18,19]. In rats, it was observed that the implantation of rods consisting of ^{165}Ho -PLLA-MS or ^{166}Ho -PLLA-MS into the liver did not elicit a response of the body's immune system and that the ^{166}Ho -PLLA-MS degraded very slowly [20]. Another relevant finding was that the chloroform, that still resides in the ^{165}Ho -PLLA-MS following formation, is completely removed during neutron activation, as a result of radiolysis [21]. It was demonstrated in tumor-bearing rabbits that hepatic arterial infusion of ^{166}Ho -PLLA-MS resulted in tumoricidal doses whereas the normal liver remained largely unaffected [22]. Both in phantoms and in animals, it was shown that Ho-PLLA-MS can be visualized by MRI [23]. Methods for quantitative MRI analysis of Ho-PLLA-MS have also been developed [17]. It was furthermore demonstrated that real-time visualization of the administration of Ho-PLLA-MS by MRI is feasible [24].

However, before a patient study would be allowed to be initiated, more work needed to be done. The most important issues that still needed to be addressed included the toxicity of liver radioembolization with ^{166}Ho -PLLA-MS in a large-animal model, a validation study of the neutron activation of the ^{165}Ho -PLLA-MS in a nuclear reactor, validation of the concept that the biodistribution of a therapeutic dose of the ^{166}Ho -PLLA-MS can be predicted based on the distribution of a small scout dose of the same microspheres, and the development of a dedicated administration system and vial. The results of studies in which these subjects were investigated are presented in this thesis.

2 OUTLINE OF THIS THESIS

This thesis is organized as follows. **Chapter 2** describes the concept, rise and clinical status of microsphere- and lipiodol-based radioembolization, developed for the treatment of patients with liver malignancies not amenable to surgical resection. Potential liver cancer animal models are discussed as well.

In **Chapter 3**, the standardization and objective validation of the neutron activation of ^{165}Ho -PLLA-MS in a specific nuclear reactor is presented. Methods that were used included photon and neutron energy deposition calculations, neutron flux measurements, light microscopy, scanning electron microscopy, dilute-solution viscometry, and differential scanning calorimetry. **Chapter 4** describes the results of a comprehensive toxicity study in healthy pigs. The animals were hepatic arterially injected with (non-radioactive) ^{165}Ho -PLLA-MS or (radioactive) ^{166}Ho -PLLA-MS and the biodistribution was assessed with SPECT and/or MRI. The pigs were monitored clinically, hematologically, and biochemically, for one or two months post-administration. The animals were then euthanized and a complete necropsy was performed, and tissue samples were processed for histological examination. In **Chapter 5**, several technical aspects of radioembolization with ^{166}Ho -PLLA-MS are studied. The concept of a small scout dose of ^{166}Ho -PLLA-MS employed to predict the biodistribution of the therapeutic dose of ^{166}Ho -PLLA-MS is investigated in the porcine model. The applicability of a dedicated administration system and multimodal medical imaging is also investigated. The accuracy of quantitative ^{166}Ho SPECT analysis in an inhomogeneous model is also evaluated. In **Chapter 6**, the applicability and value for ^{166}Ho dosimetry of several acknowledged dosimetry methods are assessed, using a 3-dimensional dose distribution derived from storage-phosphor autoradiography of slices of an *ex vivo* pig liver in which ^{166}Ho -PLLA-MS had been instilled. These methods were the MIRD (Medical Internal Radiation Dose committee) dose estimation schema, Monte Carlo simulation, and the dose point-kernel convolution method. **Chapter 7** reports on the results of a structured meta-analysis that was performed of the available literature on tumor response and survival of patients with unresectable primary liver cancer or colorectal liver metastases, who underwent ^{90}Y radioembolization, in a salvage setting or in the first-line, as monotherapy or in conjunction with systemic chemotherapy. In **Chapter 8**, ^{166}Ho acetylacetonate microspheres with an especially high loading rate are proposed as an interstitial microbrachytherapy device for the ablation of intrahepatic malignancies in which radiofrequency ablation is not successful due to tissue cooling by blood flow from adjacent vessels. The results of the experimental treatment of a house cat with primary liver cancer are also described. **Chapter 9** provides a summary of the previous chapters and discusses possible future directions of liver radioembolization with ^{166}Ho -PLLA-MS.

REFERENCES

1. Parkin DM, Bray F, Ferlay J, Pisani P. Global cancer statistics, 2002. *Ca Cancer J. Clin.* **2005**;55:74-108.
2. Yamane B, Weber S. Liver-directed treatment modalities for primary and secondary hepatic tumors. *Surg. Clin. North Am.* **2009**;89:97-113.
3. Edeline J, Raoul JL, Vauleon E, Guillygomach A, *et al.* Systemic chemotherapy for hepatocellular carcinoma in non-cirrhotic liver: A retrospective study. *World J. Gastroenterol.* **2009**;15:713-716.
4. Adam R, Wicherts DA, De Haas RJ, Ciaccio O, *et al.* Patients with initially unresectable colorectal liver metastases: Is there a possibility of cure? *J. Clin. Oncol.* **2009**;27:1829-1835.
5. Cromheecke M, Konings AW, Szabo BG, Hoekstra HJ. Liver tissue tolerance for irradiation: experimental and clinical investigations. *Hepatogastroenterology* **2000**;47:1732-1740.
6. Sato KT, Lewandowski RJ, Mulcahy MF, Atassi B, *et al.* Unresectable chemorefractory liver metastases: radioembolization with ⁹⁰Y microspheres—safety, efficacy, and survival. *Radiology* **2008**;247:507-515.
7. Gulec SA, Fong Y. Yttrium 90 microsphere selective internal radiation treatment of hepatic colorectal metastases. *Arch. Surg.* **2007**;142:675-682.
8. Salem R, Thurston KG. Radioembolization with yttrium-90 microspheres: a state-of-the-art brachytherapy treatment for primary and secondary liver malignancies: part 3: comprehensive literature review and future direction. *J. Vasc. Interv. Radiol.* **2006**;17:1571-1593.
9. Breedis C, Young G. The blood supply of neoplasms in the liver. *Am. J. Pathol.* **1954**;30:969-977.
10. Bierman HR, Byron RL, Jr., Kelley KH, Grady A. Studies on the blood supply of tumors in man. III. Vascular patterns of the liver by hepatic arteriography in vivo. *J. Natl. Cancer Inst.* **1951**;12:107-131.
11. Salem R, Hunter RD. Yttrium-90 microspheres for the treatment of hepatocellular carcinoma: a review. *Int. J. Radiat. Oncol. Biol. Phys.* **2006**;66:S83-S88.
12. Van Hazel G, Blackwell A, Anderson J, Price D, *et al.* Randomised phase 2 trial of SIR-Spheres plus fluorouracil/leucovorin chemotherapy versus fluorouracil/leucovorin chemotherapy alone in advanced colorectal cancer. *J. Surg. Oncol.* **2004**;88:78-85.
13. Sarfaraz M, Kennedy AS, Lodge MA, Li XA, *et al.* Radiation absorbed dose distribution in a patient treated with yttrium-90 microspheres for hepatocellular carcinoma. *Med. Phys.* **2004**;31:2449-2453.
14. Sandström M, Lubberink M, Lundquist H. Quantitative SPECT with yttrium-90 for radionuclide therapy dosimetry. *Eur. J. Nucl. Med. Mol. Imaging* **2007**;32:S260.
15. Nijssen JFW, Zonnenberg BA, Woittiez JR, Rook DW, *et al.* Holmium-166 poly lactic acid microspheres applicable for intra-arterial radionuclide therapy of hepatic malignancies: effects of preparation and neutron activation techniques. *Eur. J. Nucl. Med.* **1999**;26:699-704.

16. De Wit TC, Xiao J, Nijsen JF, Van het Schip FD, *et al.* Hybrid scatter correction applied to quantitative holmium-166 SPECT. *Phys. Med. Biol.* **2006**;51:4773-4787.
17. Seppenwoolde JH, Nijsen JFW, Bartels LW, Zielhuis SW, *et al.* Internal radiation therapy of liver tumors: Qualitative and quantitative magnetic resonance imaging of the biodistribution of holmium-loaded microspheres in animal models. *Magn Reson. Med.* **2004**;53:76-84.
18. Zielhuis SW, Nijsen JFW, Krijger GC, Van het Schip AD, Hennink WE. Holmium-loaded poly(L-lactic acid) microspheres: In vitro degradation study. *Biomacromolecules* **2006**;7:2217-2223.
19. Van Es RJ, Nijsen JFW, Van het Schip AD, Dullens HF, *et al.* Intra-arterial embolization of head-and-neck cancer with radioactive holmium-166 poly(L-lactic acid) microspheres: an experimental study in rabbits. *Int. J. Oral Maxillofac. Surg.* **2001**;30:407-413.
20. Zielhuis SW, Nijsen JFW, Seppenwoolde JH, Bakker CJG, *et al.* Long-term toxicity of holmium-loaded poly(L-lactic acid) microspheres in rats. *Biomaterials* **2007**;28:4591-4599.
21. Zielhuis SW, Nijsen JFW, Dorland L, Krijger GC, *et al.* Removal of chloroform from biodegradable therapeutic microspheres by radiolysis. *Int. J. Pharm.* **2006**;315:67-74.
22. Nijsen JFW. Radioactive holmium poly(L-lactic acid) microspheres for treatment of liver malignancies. PhD thesis, Utrecht University, The Netherlands. **2001**;109-122.
23. Nijsen JFW, Seppenwoolde JH, Havenith T, Bos C, *et al.* Liver tumors: MR imaging of radioactive holmium microspheres—phantom and rabbit study. *Radiology* **2004**;231:491-499.
24. Seppenwoolde JH, Bartels LW, Van der Weide R, Nijsen JFW, *et al.* Fully MR-guided hepatic artery catheterization for selective drug delivery: a feasibility study in pigs. *J. Magn. Reson. Imaging* **2006**;23:123-129.

Chapter 1

CHAPTER 2

Radionuclide liver cancer therapies: from concept to current clinical status

Maarten A.D. Vente
Monique G.G. Hobbelink
Alfred D. van het Schip
Bernard A. Zonnenberg
Johannes F.W. Nijsen

Anti-Cancer Agents in Medicinal Chemistry 2007;7:441-459

ABSTRACT

Primary and secondary liver cancer have longtime been characterized by an overall poor prognosis, since the majority of patients are not candidates for surgical resection with curative intent, systemic chemotherapy alone has rarely resulted in long-term survival, and the role of conventional external beam radiation therapy has traditionally been limited due to the relatively high sensitivity of the liver parenchyma to ionizing radiation. Therefore, a host of new treatment options has been developed and clinically introduced, including radioembolization techniques, which constitute the main topic of this paper. These internal radiation techniques consist of injecting either yttrium-90 (^{90}Y) microspheres, or iodine-131 (^{131}I) or rhenium-188 (^{188}Re) labeled lipiodol into the hepatic artery. Liver malignancies are passively targeted because, unlike the normal liver, the blood supply of intrahepatic tumors is almost exclusively derived from the hepatic artery. Radioactive lipiodol is used only for treatment of primary liver cancer, whereas ^{90}Y microsphere radioembolization is applied for treatment of both primary and metastatic liver cancers. Favorable clinical results have been achieved, particularly when ^{90}Y microspheres were used in conjunction with systemic chemotherapy. The main advantages of radiolabeled lipiodol treatment are that it is relatively inexpensive (especially ^{188}Re -HDD-lipiodol) and that the pretreatment assessment and the administration procedure are somewhat less complex than in ^{90}Y microsphere radioembolization. Holmium-166 (^{166}Ho) loaded poly(L-lactic acid) microspheres have also been developed and are about to be clinically introduced. Since ^{166}Ho is a combined beta-gamma emitter and highly paramagnetic as well, it allows for both (quantitative) scintigraphic and magnetic resonance imaging.

1. INTRODUCTION

Nuclear medicine is the branch of medicine specializing in the use of radionuclides for diagnostic and therapeutic purposes. However, traditionally it has been a primarily diagnostic discipline, with one important exception, namely the radioiodine (^{131}I sodium iodide) based treatments for thyroid disease, both thyroid cancer (especially well differentiated follicular and papillary carcinoma) and hyperthyroidism (toxic nodular thyroid disease and Graves' disease). As yet the lion's share of patients that have been presented to nuclear medicine physicians was referred for disease diagnosis, staging and/or treatment response assessment.

That said, in recent decades, a number of radionuclide therapies for oncological indications have been developed and evermore promising treatments are emerging from preclinical research. One important oncological indication that has received a lot of attention in research is unresectable liver cancer, which holds a grave prognosis and remains a ubiquitous medical problem. Since systemic chemotherapy has traditionally been relatively ineffective in treating malignant liver disease, and the liver parenchyma has an intolerance to tumoricidal radiation doses diminishing the role of conventional external beam radiation therapy, new treatment modalities have been put forward and clinically introduced. The proposed therapies can be categorized in three groups:

1. Percutaneous/laparoscopic/intraoperative ablation techniques: thermal ablation (radiofrequency, laser, microwave and focused ultrasound coagulation), cryoablation, ethanol injections, and interstitial brachytherapy;
2. Regional techniques: hepatic dearterialization, hepatic arterial infusion (HAI), isolated hepatic perfusion (IHP), trans(catheter)arterial chemoembolization (TACE), radiolabeled lipiodol therapy, and radioactive microsphere therapy;
3. Biological and targeted therapies: cancer vaccines, gene therapy, pro-apoptotic drugs, and angiogenesis inhibitors.

In this chapter, the main focus is on radionuclide based therapies for liver malignancies, from concepts and preclinical investigations to clinical implementation and current status.

The road from discovery or concept to approved drug or device is often long

and costly. One important aspect herein is *in vivo* research in animals, essential for demonstrating safety and efficacy of the drug or device. Therefore, a critical factor is to employ the appropriate laboratory animal model(s). For this reason, a section is devoted to potential animal models in preclinical investigations on (loco)regional techniques.

2. LIVER CANCER

Liver malignancies, primary as well as secondary, have a high incidence. Each year, worldwide over 600,000 people develop hepatocellular carcinoma (HCC) and cancer of the biliary tree (cholangiocarcinoma) while at least as much are diagnosed with liver metastases, often originating from tumors, arising in organs drained by the portal vein. The most commonly diagnosed of such tumors is colorectal carcinoma, with about one million new cases every year [1], of which up to 25% will present with liver metastases at time of diagnosis, whereas in due time more than 50% will develop hepatic metastases [2,3]. For both primary liver cancer and colorectal cancer mortality is high; it was estimated that in 2002 close to 600,000 persons died from primary liver cancer and over 500,000 from colorectal cancer (Table 1). Noteworthy is that for HCC 82% of cases are in developing countries, with the high incidence in sub-Saharan Africa, eastern and southeastern Asia, and Melanesia associated with the high prevalence of hepatitis B and C virus infections. In contrast, the incidence of colon and rectum cancer is highest in the Western world, which is explained by several lifestyle factors (especially certain dietary habits, *e.g.*, high meat and animal fat intake, smoking and physical inactivity) [1,4,5].

3. CONVENTIONAL TREATMENT MODALITIES

3.1 *Surgical resection*

Subtotal hepatic resection is the treatment of choice for both primary and secondary liver cancer and the only potentially curative treatment, yet only a small percentage of patients is eligible for surgical intervention, namely those with solitary or small numbers of tumors, and with favorable lesion localization. With respect to colorectal liver metastases, it was estimated that the percentage of patients amenable for surgical treatment with curative intent is in the order

Table 1 Primary liver cancer and colorectal cancer statistics

	Incidence	Mortality	5-year survival rate
Primary liver cancer	626,162	598,321	3-5%
Colorectal cancer	1,023,152	528,978	Western world 55% Developing areas 39%

Estimated data [1]

of 20-30% [6]. Scheele *et al.* [7,8] found that resectability was high if four or less lesions were present and in patients with five to seven metastases the probability of curation following surgical intervention to be rare, whereas a number of nine or more was unexceptionally associated with residual disease. They reported a 33% 5-year survival if resection was performed with curative intent, which is in agreement with the literature. Presence of extrahepatic metastases dramatically worsens prognosis. Of course, sufficient healthy liver remnant must be present following resection. Next to multinodularity, overt fibrotic or cirrhotic liver disease (and therefore compromised liver function), often coexistent in HCC, especially in Europe and Japan [9], is the most important contraindication for surgical resection. Merely 10-15% of newly diagnosed cases of HCC are eligible for partial hepatectomy [10]. Reported 5-year survival rates after resection vary between 32-70% [11].

3.2 Systemic chemotherapy

Hepatocellular carcinomas are known to be resistant to chemotherapy and, if considered unresectable, rapidly fatal. If no specific treatment was given, a median survival of just 1.6 months (regardless of stage classification) has been reported in the literature [12]. However, in the more recent literature considerably better survival has been reported. For example, Llovet *et al.* [13] reported a median survival of 17 months in 102 cirrhotic patients with unresectable HCC managed with symptomatic treatment (at 60 months when 77% of patients had died). This improvement was, among other things, caused by advancement of the time of diagnosis, the so-called 'lead-time bias'. The most widely used cytotoxic agent

for treating HCC is the anthracycline doxorubicin. Cisplatin has been frequently employed as well [14]. Tamoxifen, an orally taken estrogen antagonist, has been investigated extensively and, although in the early 1990s a survival benefit was suggested, a recently published meta-analysis study showed no improvement in overall survival [15]. New cytotoxic agents and chemotherapy regimens are constantly developed and clinically introduced, yet response rates seldom are >20%, without improved overall survival [16].

Standard first-line chemotherapy in the last two decades for advanced colorectal cancer has consisted of 5-fluorouracil, a fluoropyrimidine, clinically introduced in 1957, in combination with leucovorin (syn.: folinic acid) (5-FU/LV) [17]. A meta-analysis study of 13 randomized controlled trials, nine of which 5-FU based, by the Colorectal Cancer Collaborative Group, published in 2000, showed a mean survival benefit for (systemic) chemotherapy of a mere 3.7 months [18]. Nowadays, oxaliplatin or irinotecan usually are added to 5-FU/LV. These regimens are referred to as FOLFOX (5-FU/LV + oxaliplatin) and FOLFIRI (5-FU/LV + irinotecan), and have become the preferred first-line protocols for the treatment of metastasized colorectal cancer. Whilst traditionally median survival with 5-FU/LV therapy has been approximately 12 months, with FOLFOX and FOLFIRI median survival has reached 20 months [19,20]. Another new cytotoxic agent for this indication is capecitabine, a 5-FU prodrug, which has the advantage that it can be taken orally. Following data analysis from two large, randomized phase III trials, comparing efficacy of oral capecitabine and intravenous 5-FU/LV, it was concluded that capecitabine had a superior response rate, and equivalent time to progression and overall survival, accompanied by a better safety profile and improved convenience [21,22].

3.3 External beam radiation therapy

The role of conventional radiation therapy is limited as the tolerance of the liver to radiation is relatively low; the healthy liver can tolerate a fractionated whole-organ dose of up to approximately 30-35 Gy¹ [23,24]. However, radiation-induced liver disease (RILD), also called “radiation hepatitis” – a severe veno-occlusive liver disease from which patients can recover but which may also lead

¹ Gy (Gray); the SI unit of the energy absorbed from ionizing radiation, equal to one joule per kilogram. After Louis Harold Gray (1905-1965).

to fulminant liver failure – is seen in 5-10% of patients receiving an equivalent radiation dose [25,26]. Unfortunately, in order to achieve consistent tumoricidal effects a dose of at least 50 Gy is needed making conventional external beam radiation therapy not well suited for the treatment of intrahepatic malignancies [27,28].

In the last 10-15 years, external beam radiation therapy has advanced to a higher level, due to the invention of three-dimensional conformal radiation therapy (3DCRT) [28]. This technique uses computer technology to create a three-dimensional picture of the tumor so multiple radiation beams can be shaped exactly (conform) to the contour of the treatment area (tumor). Compared to conventional techniques, 3DCRT allows for a significantly higher radiation dose delivered to the tumor, while the dose to the normal liver (and kidneys) is decreased [29]. At this moment, 3DCRT is regarded mainly as a salvage therapy for which substantial response rates with acceptable overall toxicity have been reported [30]. Nonetheless, a recently published study in which patients with unresectable liver cancer (primary hepatobiliary cancer and colorectal metastases) were treated with 3DCRT with concurrent hepatic arterial infusion of floxuridine (chemoradiotherapy) suggested a survival benefit for this treatment combination [31]. Median survival for HCC, cholangiocarcinoma, and metastasized colorectal cancer at time of analysis, when 85% of patients had died, was 15.2, 13.3, and 17.2 months, respectively. Widespread application of this technique for liver cancer treatment is hampered by the fact that this technique is apt only for treating patients with a limited number of tumors and unsuitable for the treatment of diffuse liver disease [32].

Meanwhile the concept of 3DCRT has been further improved; novel external radiation techniques include intensity-modulated radiation therapy (IMRT), image-guided radiation therapy (IGRT), and stereotactic body radiation therapy (SBRT). In IMRT, which was introduced in 1994, the radiation ports are divided into many so-called ‘pencil beams’, each of which can be individually allocated a certain radiation intensity, or fluence, allowing for very precise radiation doses to be delivered to tumors or specific areas within tumors while collateral damage to the adjacent normal tissues is reduced. IGRT is complementary to IMRT; whereas IMRT is used to enhance precision of the radiation dose delivery, IGRT is guided by imaging techniques (often, but not exclusively, X-ray computed

tomography (CT)), consequently improving radiation accuracy. Explicitly, it is a tool to detect and correct for patient set-up errors, patient movement errors (breathing), organ movement and organ changes [27]. SBRT is an external radiation technique dedicated to the ablation of intrahepatic and intrapulmonary malignancies. This technique employs stereotactic localization and targeting, resembling those developed and established in intracranial radiosurgery [33]. Several phase I, II, and III trials have been conducted or are ongoing, in which predominantly patients with solitary or a few lesions were treated. The main objectives of these studies are on dose scheduling, maximum tolerated dose, and dose limiting toxicity. Schefter *et al.* [34] reported that in SBRT doses of 60 Gy (in three fractions), hence in the therapeutic range, were well tolerated by patients with up to three lesions and adequate liver function. As in standard 3DCRT, eligibility is limited. At this time, the impact of these new external radiation techniques on clinical outcome can only be speculated on.

3.4 Liver transplantation

If the correct enrollment criteria, the so-called Milan criteria, are met, a subpopulation of HCC patients is eligible for orthotopic liver transplantation. These selection criteria are: no more than three lesions, of which none more than 3 cm in diameter, or presence of a solitary mass, 5 cm or less in diameter, absence of macroscopic portal vein invasion, and absence of recognizable extrahepatic tumor involvement [35]. Unfortunately, most patients with unresectable HCC do not meet these inclusion criteria. For patients who do, outcome is excellent with 5-year survival rates of 70% [36]. Although a few centers are accepting patients with extended criteria, the University of California, San Francisco criteria (UCSF criteria) (Table 2) [37,38], it is obvious that the role of liver transplantation is limited in unresectable HCC. The therapeutic value of liver transplantation for unresectable cholangiocarcinoma and cholangiohepatoma has been explored as well. The procedure itself is technically more straightforward for the absence of portal hypertension, but down to the very high recurrence rates (usually in the allograft or the lung), hence poor survival rates (5-year survival: 18-25%), liver transplantation has been abandoned for this indication [39]. With regard to metastatic liver disease, liver transplantation is suited only for the treatment

Table 2 Liver transplantation criteria

Milan criteria	UCSF criteria
solitary lesion ≤ 5 cm, or ≤ 3 lesions none > 3 cm	solitary lesion ≤ 6.5 cm, or ≤ 3 lesions none > 4.5 cm
	total tumor diameter ≤ 8 cm
no indications of portal vein invasion	
no extrahepatic tumor deposits	

of selected patients with unresectable metastasized neuroendocrine tumors (if not responding to conventional treatment). These tumors can remain confined to the liver for a long time and usually exhibit slow growth. Impressive 5-year survival rates ($>80\%$) have been reported in liver-transplanted neuroendocrine tumor patients, especially in carcinoid patients [40-44].

4. ALTERNATIVE TREATMENT MODALITIES

4.1 Local ablation techniques

A wide array of local ablation techniques has been developed, which are aimed to achieve tumor reductive effects by means of hyperthermia (radiofrequency ablation (RFA), interstitial laser thermotherapy (ILT), microwave coagulation, high-intensity focused ultrasound (HIFU)), hypothermia (cryotherapy) or, in case of percutaneous ethanol injections (PEI), (mainly) through cytoplasmic dehydration. These procedures can be performed percutaneously, laparoscopically and/or during open surgery. Of these minimally invasive therapies, PEI has been used the longest but is now considered inferior to RFA [45]. After percutaneous treatments local recurrence rates are usually higher than after intra-operative RFA. The laparoscopic approach delivers intermediate results. Between RFA and ILT seems to be little difference in outcome [46]. Microwave coagulation therapy (during laparotomy) for multiple colorectal liver metastases is suggested to be equally effective to hepatic resection [47]. Preliminary results on the safety and feasibility of extracorporeal HIFU have been published, not yet on efficacy [48]. At the present time, no prospective, randomized studies on these local ablation

techniques have been published, making it difficult to assess their influence on survival. These techniques all have distinct limitations regarding tumor location, number and/or size of lesions; to name a few, in larger tumors the local recurrence rate is much higher due to incomplete coagulative necrosis in the tumor periphery. Therefore, in RFA post-treatment survival negatively correlates with lesion size. Preferably, tumor diameter should not exceed 3 cm. However, when multiple array hook electrodes are deployed tumors up to 5 cm in size can be completely ablated. If located high in the dome of the liver, tumors are sometimes not accessible for percutaneous techniques. Hilar located lesions are not eligible for treatment with RFA either. It has been stated that there is no survival benefit in RFA of more than five metastases or three HCC lesions [49-51].

Interstitial brachytherapy – the intratumoral insertion of radioactive seeds – has been successfully applied in the treatment of prostate carcinoma. The most commonly used form of prostate brachytherapy is permanent seed implantation, using the low-energy gamma emitter iodine-125 (^{125}I : $E_\gamma = 35.5 \text{ keV}^2$, $I_\gamma = 6.68\%$; $T_{1/2} = 59.4 \text{ d}$) [52]. Be it infrequently, ^{125}I brachytherapy has been applied in the treatment of intrahepatic malignancies as well, as an adjuvant treatment to surgical resection. In a recently published study by Nag and co-workers [53] an improvement of local control following incomplete surgical resection of (primary or metastatic) intrahepatic malignancies was suggested. Local control was significantly better in patients with up to three lesions than in patients who had four or more lesions (5-year local control: 32% and 0%, respectively) and coupled with a very low complication rate. Ricke *et al.* [54,55] have explored CT-guided high-dose-rate interstitial brachytherapy using iridium-192 (^{192}Ir : $E_{\beta\text{max}} = 539 \text{ keV}$ and 675 keV , $I_\beta = 41.8\%$ and 48.0% , respectively; $E_\gamma = 317 \text{ keV}$ and 468 keV , $I_\gamma = 82.8\%$ and 47.8% , respectively; $T_{1/2} = 73.8 \text{ d}$), specifically for the treatment of patients with very large liver tumors ($>5 \text{ cm}$), or lesions ($\leq 5 \text{ cm}$) inoperable due to close adjacency to the liver hilum, common bile duct, or hepatic bifurcation, alone or in combination with ILT. The attained local control rates were better for brachytherapy than for combined ILT and brachytherapy treatment (88% and

² keV (kilo-electron volt) = $10^3 \cdot \text{eV}$ (electron volt); unit of energy where 1 eV (which corresponds to $1.60217653 \cdot 10^{-19} \text{ J}$) is the amount of kinetic energy gained by a single unbound electron when it passes through an electrostatic potential difference of one volt, in vacuum.

72% at 6 months, respectively). Further patient studies are warranted to assess the value of this treatment modality for this indication.

4.2 Regional techniques

Almost the entire blood supply of liver tumors is derived from the hepatic artery, whereas the liver parenchyma receives 70% of its blood from the portal vein [56]. For this reason, since the 1960s hepatic dearterialization has been carried out in patients with intrahepatic malignancies [57,58]. Tumor blood supply can be halted through ligation of the hepatic artery, by placing coils, or *via* injection of an embolizing agent (*e.g.*, polyvinyl alcohol particles), which expectedly would lead to tumor ischemia and necrosis. To some degree tumor necrosis may be achieved, but an effect on survival has been reported to be absent, among several reasons thought to be caused by reinforcement of tumor blood supply by neoangiogenesis [59]. However, for patients with hepatic metastases from gastrointestinal stromal tumors (GIST), the most common mesenchymal neoplasm of the gastrointestinal tract and often hypervascular, hepatic artery occlusion has proven to be an effective palliative therapy [60].

This anatomical circumstantiality is also made use of in (loco)regional chemotherapy procedures: hepatic arterial infusion (HAI), isolated hepatic perfusion (IHP), and trans(catheter)arterial chemoembolization (TACE). These administration techniques allow tumors to be exposed to much higher drug concentrations than can be achieved in systemic delivery. The response rates of HAI are undoubtedly higher than those seen with systemic chemotherapy, but there is no convincing evidence at present that overall survival is affected [61]. For the reason that there is complete vascular isolation of the liver in IHP, very high doses of chemotherapy (typically mitomycin C, or melphalan with or without tumor necrosis factor alpha (TNF- α)) can be given. An important disadvantage of this technique, compared to HAI and TACE, is that it is a complex procedure, which requires a major laparotomy [62]. It is therefore currently being investigated if IHP could be performed percutaneously instead. Nonetheless, impressive clinical results, including complete remissions and 5-year survivors, have been reported in selected patients with unresectable colorectal liver metastases after receiving IHP treatment [63]. Although considered a palliative treatment, TACE has been shown to offer a survival benefit in two separate

randomized controlled trials [64,65]. A meta-analysis study by Llovet *et al.* [66] supported this. Notwithstanding its effectiveness, TACE is also associated with considerable morbidity rates; most patients receiving TACE suffer from the self-limited so-called 'post-embolization syndrome', which typically includes right upper quadrant pain, nausea, vomiting, and fever [67]. Complications such as (sometimes fatal) liver failure, peptic ulcer, gastrointestinal bleeding, liver abscesses, and ischemic cholecystitis have been reported in the literature [68,69].

4.3 Biological and targeted therapies

It is an appealing idea to deploy the patients' own immune system in combating cancer. In recent years a lot of different colorectal cancer vaccines have been developed and compelling results have been reported in animal models, and accordingly quite a few clinical trials have been carried out. However, the clinical results have remained limited, thus far [70].

Essentially, chemotherapies exert their antitumor effect by induction of apoptosis (programmed cell death). Unfortunately, suppression of apoptosis itself is implicated in tumorigenesis. In fact, resistance to apoptosis may be a key factor in limiting the effectiveness of anticancer therapy [71]. Therefore, a strong rationale existed to develop apoptosis-inducing agents. These drugs induce apoptosis indirectly by targeting cell-proliferative or cell-survival signals [72]. Examples of targets for apoptosis modulation are Bcl-2 (B-cell lymphoma-2), p53 (tumor suppressor gene), caspases, protein kinases, inhibitor of apoptosis proteins (IAPs), and COX-2 (cyclooxygenase-2). Clinical trials have started, but few have been published as yet [73,74].

A further biological treatment modality for cancer is gene therapy, which stands for the introduction of specific engineered genes into a patient's cells. Administration of a gene delivery vector, either viral or non-viral, can be done intratumorally, intracavitary, or intravascularly. Cancer gene therapy strategies include: restoring the function of suppressor genes, selectively activating prodrugs inside of tumor cells, immune stimulation, genetically modified oncolytic virus therapy, and antisense oligonucleotide therapy. In animal studies positive results have been achieved, and during the last 15 years close to 700 cancer gene therapy trials have been conducted, of which about half involved oncolytic viruses [75]. The vast majority has been phase I studies and less than 1% were phase III trials.

This has to do with the disappointing results, thus far; little clinically significant efficacy has been shown. Lack of efficacy is mostly due to inefficient gene transfer and low levels of gene expression [76].

Generally thought to be a major breakthrough in the treatment of solid tumors is antiangiogenesis. The growth of new blood vessels, angiogenesis or neovascularization, is necessary for tumors to grow past a critical size of several mm and also for tumor invasion and metastasis [77,78]. It is Folkman who has done a lot of research in this field, and the first to have isolated a tumor angiogenic factor and to propose the concept of antiangiogenesis in cancer therapy [79]. In the 1980s, the first molecules that mediate angiogenesis were identified, including vascular endothelial growth factor (VEGF) [80,81]. This endothelial cell-specific mitogen is the target of the first FDA-approved (in February 2004) angiogenesis inhibitor: bevacizumab (Avastin[®], Genentech Inc., South San Francisco, CA, USA), a recombinant, humanized monoclonal antibody. It is the first angiogenesis inhibitor to have demonstrated a statistically significant and clinically meaningful prolongation of survival in unresectable metastasized colorectal cancer, when added to a chemotherapy protocol (FOLFIRI) [82]. Thus, angiogenesis inhibition indeed seems worthwhile for further investigations and many novel antiangiogenic agents are currently in various phases of clinical testing. To improve efficacy, it is thought essential to complement current VEGF-based therapies with agents that target other proangiogenic factors, or drugs that indirectly affect angiogenesis [83].

5. ANIMAL MODELS IN LIVER CANCER RESEARCH

5.1 The ideal animal model

As a rule, before a hospital's research ethics board is prepared to give permission for initiating a clinical trial and also for registration purposes, next to pharmaceutical quality, efficacy and especially safety of the drug or device must have been demonstrated in an animal model, preferably in more than one species. In general, for an animal model to be regarded suitable, it should fulfill certain demands, wholly depending on the research question at hand. In case of the internal radiotherapy techniques, some specific requirements have to be met. First, since a catheterization procedure is involved in delivering the device, vessel

size should be large enough to allow for the use of catheters of sufficient size (3F³ or greater). Therefore, the animal model should be of a certain minimum size. Then, in being able to demonstrate efficacy of the therapy, *i.e.*, evaluation of its tumoricidal effect, hepatic tumor induction or implantation has to be feasible. In tumor cell implantation, tumor “take rate” should ideally be 100%. After tumor induction or implantation, the time for macroscopic nodules to be developed should be predictable, reproducible and not too long, and no extrahepatic tumor growth ought to occur.

5.2 Mouse and rat models

In biomedical research the most used animal model is the mouse. Several strategies exist for triggering hepatic tumor growth in mice. The most straightforward approach is implantation of murine tumor cells into recipient mice. Hepatitis B or C transgenic mice and infectious agents like *Helicobacter hepaticus* are especially useful in studies on oncogenesis, immunobiology, and pathogenesis of HCC [84]. Multiple murine models of chemically induced colorectal cancer have been developed, but major disadvantages of carcinogen-induced colorectal cancer are the low incidence of tumor development and the slow and infrequent metastases formation [85]. Ideally suited for cancer research are nude mice and SCID (severe combined immunodeficiency) mice. The nude mouse is a hairless mutant mouse strain, which lacks a thymus and therefore T lymphocytes. SCID mice lack both T and B cells. This disorder is inherited as an autosomal recessive trait. Due to being immunologically deficient, these mouse strains will accept an organ transplant or cell inoculation, either from another mouse (allograft) or from another species (xenograft), without rejecting it, *e.g.*, human colon cancer tissue [86-88]. Evidently, this makes these mouse strains well fitted *in vivo* models for testing new anticancer drugs. An interesting mutant mouse model for metastatic colorectal cancer, specifically familial adenomatous polyposis (FAP), are *Smad3*^{-/-} mice [89]. These mice lack the Smad3 protein – a second messenger for the transforming growth factor beta (TGF-β), a tumor suppressing cytokine with growth inhibitory effects in many epithelial cells, including colonic epithelium – and develop colorectal cancer, metastatic to the lymph nodes, before the age

³ F (French); catheter scale, where 3F corresponds to 1.0 mm or 0.039 inch outer diameter size catheter.

of 24 weeks. The most widely used liver metastases animal models are athymic mice in which tumor cells are injected either intrasplenic, into the portal vein, or implanted in the colon wall.

Obviously, for its significantly larger size, the rat would seem predestinated for research on new cancer treatments including novel surgical and ablative techniques. Therefore, transplantable rat colon carcinoma cell lines, chemically induced, have been developed [90]. Nude rats, *i.e.*, athymic rats, which support the growth of xenogeneic tumor cells, *e.g.*, human colorectal carcinoma cells, have been developed as well [91,92]. In contrast to nude mice, nude rats still possess some immune responsiveness. To surmount this remaining immunoreactivity, and improve tumor take rate, whole-body gamma irradiation or chemotherapeutic immunomodulation, preceding tumor cell implantation, is advisable [93].

However, for testing regional liver cancer therapies (especially microsphere techniques), which require a catheterization procedure, both the mouse and rat model are not the optimal choice, for several reasons. First the unavailability of catheters, which are small enough to be inserted into especially the murine hepatic artery, yet not so small that the microspheres get stuck in it, or require too much force to get flushed out in a controlled manner. For microspheres to be flushed out of the administration device (syringe, vial) and into the liver vasculature a certain amount of flushing fluid has to be used, coupled with the appliance of force in doing so. Both the volume of fluid and the flushing force needed quickly outplay the strength of the vessels, which have to deal with both these aspects of the flushing procedure. A final problem is that microspheres would most likely lodge relatively too proximally from the tumor microvasculature, again due to the small vessel size in these rodents. In other words, both the mouse and (in lesser extent) the rat are just too small for the administration technique, although in relative biodistribution assessment, where only low doses of radioactivity and therefore small amounts of microspheres need to be administered, the rat model has proven useful [94].

5.3 Rabbit models

The rabbit is a significantly larger animal than the mouse and the rat making it, at first sight, a better suited animal model for preclinical research on the described

techniques. However, an immune deficient rabbit strain that does not reject xenograft tumor cells does not exist. Nonetheless, a rabbit tumor model is available, owing to the transplantable Vx2 (squamous cell) carcinoma. Vx2 carcinoma cell lines are originally derived from transmissible cutaneous papillomas, naturally occurring in eastern cottontail rabbits (*Sylvilagus floridanus*) [95-98]. Since the 1960s, Vx2 cell lines have been widely used in preclinical oncology research, *e.g.*, in treatment efficacy studies and tumor angiogenesis studies. Vx2 carcinoma is a highly malignant tumor, has a high take rate and is lethal within one month post-inoculation (in the liver).

With regard to catheterization of the hepatic artery and administration of microspheres into this blood vessel, it is the authors' experience, that even if the rabbit vessels are somewhat larger in diameter than those in the rodents, the risk of vessel trauma is quite high, and since the complication rate of this type of treatments is highly dependent of the catheterization/administration procedure and not particularly device dependent, we would advocate that this kind of therapies is tested in rather larger and more anthropomorphic species, *i.e.*, the dog or the pig.

5.4 Dog models

The first transplantable canine tumor, transmissible venereal tumor (TVT), was initially described by Russian veterinarian Novinsky in 1876, when he demonstrated that the tumor could be transplanted from one dog to another. Some allogeneic canine cell lines have been developed, especially brain tumor (glioma, syn.: astrocytoma) cell lines [99,100]. A transplantable canine liver tumor cell line did not exist, until recently, when Boomkens *et al.* [101] reported on the establishment and characterization of the first canine hepatocyte tumor cell line, which they had derived from a spontaneous canine HCC. The authors proposed this cell line to be used in studies on the molecular pathogenesis of HCC, but one might speculate this cell line to be also suitable as a large laboratory animal research tool in testing (locoregional) tumor reductive techniques. In theory, it might seem to be an attractive animal model; however, a strict condition would be that the recipient dog's immune system is heavily suppressed by high-dose corticosteroids and/or other immunosuppressant agents, or virtually absent due to a genetic condition. SCID not only occurs in mice but is also an autosomal

recessively inherited disorder in horses, exclusively Arabian foals [102], and has been described in dogs as well (X-linked inheritance in the Basset Hound [103], autosomal recessive inheritance in Cardigan Welsh Corgis [104,105] and Jack Russell Terriers [106]). The latter constitutes a highly anthropomorphic model for basic immunological research, yet is an impractical model with regard to testing experimental cancer treatments, since severely immunocompromised animals, including SCID animals, have to be kept in a housing facility dedicated to immunocompromised animals and the pups have to be born in a germfree environment.

5.5 Pig models

Not including (non-human) primates and monkeys, the pig is the most anthropomorphic (laboratory) animal species and could therefore be considered a first-rate choice for testing tumor ablative and locoregional treatments. Alas, no porcine liver tumor cell lines are available, and in a recently published paper it was reported that xenogeneic tumor cell (human HCC cell line HepG2) transplantation in the portal vein (for the sake of immunological tolerance in the liver towards soluble antigens [107]), under vigorous immune suppression, remained unsuccessful in two mini-pigs [108].

However, chemically induced HCC in pigs has been reported in the literature. Graw and co-workers [109] orally administered five Göttingen mini-pigs diethylnitrosamine (DENa, syn.: *N*-nitrosodiethylamine), a nitrosamine derivative with alkylating, carcinogenic, and mutagenic properties, in a low dose for the duration of five years, after which the pigs each had taken a total of 420 mg/kg DENa. During postmortem examination, the livers of all animals showed blatant neoplastic and non-neoplastic structural changes, including, in 4 of 5 animals, HCC. In all five pigs regional lymph node metastases and in one animal multiple lung metastases were observed. In addition, histological examination showed, among other findings, a renal cell carcinoma and a complex brain tumor. In a recently published study by Li and co-workers [110], six Taihu pigs were intraperitoneally injected with DENa, 10 mg/kg, once a week, for the duration of three months, followed by another 10-12 months during which DENa treatment was withheld. CT examinations were carried out to screen the pigs for liver tumors. Necropsy showed multiple tumor nodules of various sizes and varying

degree of differentiation. On histological and ultrastructural examination, the tumor cells resembled human HCC arising in a cirrhotic background. Clearly, this porcine tumor model represents a very interesting animal model for deployment in preclinical investigations on liver cancer therapies, not only those which require a catheterization procedure, the only drawback being the long time it takes for HCC nodules to be developed. Not just for this long lag time before tumor appearance, but also for animal discomfort considerations and practical reasons like the necessity of frequently handling a highly carcinogenic substance, it would be worthwhile to investigate the possibilities of allogeneic tumor cell transplantation in pigs.

6 RADIONUCLIDE LIVER CANCER THERAPIES

6.1 Yttrium-90 loaded microspheres

Concerning its vascular anatomy, the liver is a peculiar organ; usually the afferent blood vessel of an organ is an artery supplying oxygenated blood, and the efferent blood vessel a vein, which drains deoxygenated blood back into the direction of the heart. Unique to the liver is that whereas it does indeed receive (some of its) blood from an artery, the hepatic artery, and its blood is drained by the hepatic veins, over seventy percent of the liver's blood supply is derived by a vein, the portal vein, which conveys the blood from the greater part of the abdominal part of the digestive tract and from the spleen, pancreas, and gall bladder. One of the first to have systematically studied the vascularization of intrahepatic tumors were Bierman *et al.* [56], who performed angiography studies of the common hepatic artery in patients, mainly with secondary liver tumors, and in patients with uninvolved livers. The conclusions drawn were that the flow rate in tumor bearing livers is significantly higher than in normal livers and, most important, that in contradistinction to the normal liver tissue the blood supply of neoplasia in the liver is predominantly of arterial origin.

The first study in which radioactive microspheres were tested in an *in vivo* model for liver tumor treatment was conducted by LaFave *et al.* [111]. In New Zealand White rabbits, yttrium-90 (^{90}Y : $E_{\beta\text{max}} = 2.28 \text{ MeV}$, $I_{\beta} = 100\%$; $T_{1/2} = 64.1 \text{ h}$) (Table 3) loaded ceramic microspheres 40-60 μm in size and Vx2 carcinoma

cells were injected semi-simultaneously in a mesenteric vein (which leads into the portal vein, consequently into the liver) or in an ear vein (for pulmonary inoculation). The aim of this study apparently was to prove that this form of internal radiation delivery can hinder tumor growth. It was observed that administration of microspheres prior to inoculation elicits better tumor growth inhibitory effects than vice versa. This is what could have been expected, since the Vx2 cells will have lodged far deeper into the microvasculature (capillary) than the considerably larger microspheres, which will have embolized much more proximally (arteriolar), hence the distance between the cells and the beta-particle emitting microparticles was of course significantly longer than was the case when the microspheres were administered first instead of the cells. Also, it can be assumed that the conditions proximally of the microvasculature are less favorable for tumor growth. The authors also commented on the radiation dose tolerance; the animals were terminated 28 days post-procedure and apparently no signs of RILD had been observed during that period. From literature on human patients who had undergone (external) radiation therapy it is known that if RILD occurs this typically does between four to eight weeks after radiation therapy completion, yet it has also been described to occur as early as two weeks and as late as 16 weeks following radiation therapy [25]. A long-term toxicity study in rabbits (undergoing pulmonary inoculation) was supposedly carried out at the time but never published. Perhaps this has to do with the fact that the discussed rabbit study was based on a faulty hypothesis: malignant tumors in organs drained by the portal vein usually disseminate to the liver *via* this blood vessel but, as pointed out earlier in this paragraph, hepatic tumors derive their blood supply almost exclusively from the hepatic artery, which ought to have been a known fact to the authors, at the time already. And maybe it was indeed known to them, but if that is the case the rationale behind this rabbit study becomes unclear, perhaps it was to demonstrate that beta irradiation can prevent tumor growth.

Following this 'portal vein radioembolization study', a study by this group was published in which the concept of delivering radioactive microspheres to liver tumors *via* the hepatic artery was tested for the first time [112]. The same animal model (New Zealand White rabbit) and tumor cell line (Vx2 carcinoma) were employed. The (plastic) ^{90}Y loaded microspheres used this time were much

smaller in diameter ($15\pm 3\ \mu\text{m}$) than the microspheres in the preceding 'tumor growth inhibition study'. Inoculation was performed by injecting Vx2 carcinoma cells into the appendiceal veins. An explorative laparotomy was performed two weeks later to assess the extent of hepatic tumor burden. Eighteen animals received treatment with ^{90}Y loaded microspheres (radioactivity dose/animal ca. $110\ \text{MBq}^4$) and a same number of animals, the control group, was injected with non-radioactive microspheres. It is not clear why it was considered necessary to utilize such a large control group, but perhaps the authors anticipated some therapeutic effect from the 'cold' microsphere treatment. The authors did not specify on how many microspheres were injected, which would have been interesting to know, since injection of enough microspheres (or of microspheres of sufficient size, for that matter) could have a (temporary) tumor reductive effect, due to the embolic effect resulting in ischemia of tumorous tissue. Two weeks after administration of the microspheres, the animals were sacrificed and the T/L ratio (the ratio weight of tumor/weight of liver) of treated animals calculated and expressed as a percentage of that of control animals. It was concluded that either progression of the liver tumors was halted or that the tumors were completely eliminated whilst in the control animals tumor growth had progressed.

At the same time, a study was carried out by the same group in Vx2 carcinoma-bearing rabbits (New Zealand White) with the aim to expose the source of liver tumor vasculature [113]. Scandium-46 (^{46}Sc : $E_{\beta\text{max}} = 357\ \text{keV}$, $I_{\beta} = 100\%$; $E_{\gamma} = 0.889$ and $1.121\ \text{MeV}$, $I_{\gamma} = 100\%$ and 100% , respectively; $T_{1/2} = 83.3\ \text{d}$) containing ceramic or plastic microspheres were injected in either the hepatic artery or the mesenteric vein. Whether injected into the hepatic artery or the mesenteric vein did not result in a noteworthy difference for the average counts in liver tissue. However, the average counts in tumor samples of the animals in which the ^{46}Sc loaded microspheres had been administered *via* the hepatic artery were much higher than the counts measured after administration *via* the mesenteric vein. These findings were in agreement with the research by Bierman *et al.* [56], described earlier, and also demonstrated that Vx2 carcinoma-bearing rabbits are a valid liver cancer model, in that the blood supply of Vx2 tumors in the liver is arterial from origin, as it is in patients.

⁴ MBq ($\text{Bq} \cdot 10^6$); SI unit for radioactivity; 1 Bq (Becquerel) = 1 disintegration/s. After Antoine Henri Becquerel (1852-1908).

Radioactive microsphere embolization for the treatment of liver cancer may be a promising concept but it is not a very recent concept. Already in the early 1960s, cancer patients have been treated with ^{90}Y microspheres [114]. This group of 31 patients was a very heterogeneous group, having inoperable cancer as the only common denominator. Twenty-six patients with carcinomas of various locations and five patients suffering from glioblastoma were treated with ceramic ^{90}Y microspheres 40-60 μm in diameter (ca. 550-14,000 MBq). Four modes of administration were utilized: (1) infusion into the blood stream (either intravenously or intra-arterially); (2) direct intratumoral injection; (3) incorporated in a silastic patch sutured over the tumor; (4) impregnated in a gelatin sponge implanted in the tumor cavity (brain tumors only). Although 30% of patients seemed to have benefited from the treatment, as many suffered from complications, the nature of which varied extensively. However, in none of the treated patients with liver cancer complications were observed. The authors commented that too little patients had been included in this study and the trial set-up unfit to be able to draw hard conclusions on survival or even quality of life, but that the results were comparable to those achieved with chemotherapy, with lower morbidity and mortality rates. In this study five patients suffering from malignant liver disease were treated with ^{90}Y microspheres, not instilled into the hepatic artery but into the mesenteric vein or into an omental vein, consequently embolizing the portal vein's microvasculature, which is obviously the incorrect route. The authors pointed out this 'slip-up' as well and referred to publications on the matter. Apparently, the physicians involved in the treatment of these patients must have been unaware of the predominantly arterial dependency of (liver) tumors. This is remarkable, since around the same time these authors had conducted the previously described Vx2 carcinoma blood supply study [113].

Although sporadically patients with liver cancer have been treated with ^{90}Y microspheres in the 1960s [115] and 70s [116,117], and with remarkable results, it all came to a temporary halt in 1980, when the U.S. Food and Drug Administration (FDA) removed the ^{90}Y microspheres from clinical use because of an incident involving a batch from which radioactivity had leached, which had led to lethal myelosuppression in several patients [116,118,119]. In 1986, the Theragenics Corporation introduced a glass microsphere from which ^{90}Y cannot elute, TheraSphere[®]. Next to its radiochemical stability, an advantage of glass

microspheres is that extremely high specific activities can be reached [120,121]. A disadvantage of the glass microspheres is the high density (3.29 g/ml [121,122]), thereby increasing the chance of premature intravascular settling [123]. Before initiating a clinical trial, a dose escalation study in eight healthy dogs was conducted [119]. Maximally 4,150 MBq ^{90}Y was instilled into the hepatic artery, equating to a liver absorbed dose of about 350 Gy, which was well tolerated, save two animals, which suffered from complications due to inadvertent extrahepatic deposition of microspheres, namely gastric and duodenal ulceration, respectively, even though the gastroduodenal artery was occluded preceding the administration, using coils. If no complications occurred, the only side effect observed was a transient decline in appetite and weight in the two dogs that received the highest doses. The finding that healthy dogs seem to be able to withstand a liver absorbed dose of over 300 Gy was impressive but an essential finding was the absolute absence of signs of myelosuppression confirming that no leakage of ^{90}Y had occurred.

Owing to this study's favorable outcome, clinical trials were allowed to start and initial results of the first pilot trial for toxicity assessment involving seven patients with HCC were published in 1989 by Houle *et al.* [124]. Administered amounts were based on the volume of the patient's liver and the intended liver absorbed dose to be given, and ranged from 1.6 to 6.3 GBq ^{90}Y ; assuming a uniform intrahepatic distribution, a liver absorbed dose of 50, 75, or 100 Gy was delivered. It is obviously of paramount importance to dismiss or quantify extrahepatic shunting, specifically to the lungs and/or stomach, before administering a therapeutic dose of microspheres loaded with a high-energy beta-emitting radioisotope. For this reason, the biodistribution of the glass ^{90}Y microspheres was predicted by the injection of technetium-99m ($^{99\text{m}}\text{Tc}$)⁵ labeled human albumin microspheres beforehand. The assumption that the glass ^{90}Y microspheres' distribution would be identical to that of the $^{99\text{m}}\text{Tc}$ microspheres was uncertain, as the authors commented, since the $^{99\text{m}}\text{Tc}$ microspheres had a similar size yet were of a much lower density than the glass ^{90}Y microspheres,

⁵ Technetium-99m; a generator-produced (Mo-99/Tc-99m) radioisotope of technetium, emitting a gamma ray of 140.5 keV ($T_{1/2} = 6.01$ h), and capable of binding chemically to many biologically active molecules. It is the workhorse of nuclear medicine, used for imaging the brain, parotid gland, thyroid gland, skeleton, kidney, and many other organs/tissues.

which probably would have had some implications on the (dis)similarity of the biodistribution of the respective microparticles. However, to refrain from performing ^{99m}Tc scintigraphy for the reason that the distribution may not be entirely identical would have been unwise, and currently, preceding the administration of ^{90}Y microspheres, injection of a dose of ^{99m}Tc macroaggregated albumin (MAA) still is standard operating procedure. Apart from one patient with partially compromised liver function from diffuse HCC, in whom a transient rise in liver enzymes serum levels was seen, signs of toxicity were observed in none of the other patients. No signs of bone marrow suppression were seen. Changes in tumor size were monitored by means of ultrasound examinations and, if significant changes were found, CT images were acquired as well. Disease progression was observed in all four patients who received the lower absorbed doses (50 Gy), stable disease was achieved in two patients and in one a slight reduction in tumor size was observed (75 and 100 Gy liver absorbed doses).

In 1998, MDS Nordion Inc. (Kanata, Ontario, Canada), which holds an exclusive worldwide sublicense to produce and distribute the glass ^{90}Y microspheres, submitted an application at the FDA's Office of Orphan Products Development to have TheraSphere[®] approved as a 'humanitarian use device' (HUD) specifically "for use in radiation treatment or as a neoadjuvant to surgery or transplantation in patients with unresectable hepatocellular carcinoma who can have placement of appropriately positioned hepatic arterial catheters." An HUD is a device that is aimed to treat or diagnose a disease or condition with an incidence of less than 4,000 patients in the United States per year, making it often not financially worthwhile for a manufacturer to attain FDA marketing approval, which usually is a very time-consuming and costly feat. A 'humanitarian device exemption' (HDE) application is similar to a premarket approval (PMA) in that quality and safety have to meet certain standards but, in contrast to a PMA application, for the submission of an HDE the regulation does not require that efficacy of the device is proved clinically. Also, the manufacturer must demonstrate that no comparable devices are available to treat or diagnose the particular disease or condition and that they could not otherwise bring the device to market. TheraSphere[®] was granted FDA approval for humanitarian use in 2000.

One other similar microdevice in clinical use in which ^{90}Y is incorporated

is SIR-Spheres[®] (SIRTeX Medical Ltd., Sydney, New South Wales, Australia). These microspheres are resin based, have a slightly greater diameter (SIR-Spheres[®]: 32±10 µm; TheraSphere[®]: 25±10 µm [121]) and are of a markedly lower density (1.6 g/ml [121]), which allows for a lower risk of intravascular settling. SIR-Spheres[®] were granted FDA premarket approval in 2002, in analogy to TheraSphere[®] for a single indication, namely the treatment of hepatic metastasized colorectal cancer with adjuvant hepatic arterial infusion of floxuridine (syn.: 5-fluorodeoxyuridine), a deoxyribonucleoside derivative of 5-FU. Outside the United States quite a large number of centers, especially in Europe and Australia, have started treating patients with the resin ⁹⁰Y microspheres as well, usually not discriminating between primary and secondary liver cancer.

In the meantime, over 10,000 doses of ⁹⁰Y microspheres (both the glass and the resin-based microspheres) have been administered to patients, and promising results have been reported [120]. In one study, patients with unresectable colorectal liver metastases underwent standard systemic 5-FU/LV chemotherapy or, in the experimental arm, chemotherapy in combination with a single dose of the resin ⁹⁰Y microspheres [125]. One patient, in the combined-treatment arm, died from neutropenia-related sepsis, which was ascribed to the chemotherapy. Another patient, also from the combination group, developed a liver abscess but subsequent to abscess drainage quickly recovered. One patient developed RILD at approximately one year after the start of treatment, which was attributed to a disproportionately high amount of activity (2.5 GBq) administered, since this patient weighed just 43 kg. Four patients experienced abdominal pain following administration of the microspheres. Although the safety and tolerance profile might have been marginally better for the chemotherapy-alone arm, and no (proven) complete responses were achieved in either group, the response rate for the patients receiving the combination treatment was significantly ($p<0.001$) higher than for the standard treatment, which yielded no partial responses. Median time to progression was significantly ($p<0.0005$) longer for the experimental arm (18.6 months) than for the control group (3.6 months), and median survival was considerably better for the combination group (29.4 months *versus* 12.8 months; $p=0.025$). The results of this phase II trial were encouraging yet statistically rather weak due to the small number of patients ($n=21$). Meanwhile phase I/II studies are in progress in which radioembolization with the resin ⁹⁰Y microspheres is

combined with FOLFOX [126] or irinotecan [127].

Kennedy *et al.* [128] recently reported on the results of resin ^{90}Y microsphere treatment of 208 heavily pretreated patients with colorectal liver metastases, all refractory to oxaliplatin and irinotecan and not candidates for any other palliative treatment. The mean activity delivered was $1.7 \pm 0.5 \text{ GBq } ^{90}\text{Y}$ (0.4-2.9 GBq). The most commonly observed post-embolization symptoms were fatigue (39%), abdominal pain (13%), nausea (10%), and emesis (7%). Steroid therapy was beneficial in one-third of the patients. Overall, biochemical side effects were very mild, and no treatment-related deaths occurred. Response to treatment was evaluated on CT and/or ^{18}F -FDG-PET⁶ scans and/or biochemically (CEA⁷). CT showed partial response in 35% of patients and stable disease in 55%. In 10% of patients CT indicated disease progression. PET scans showed response in 85% of patients and no response or progression in 15%. Median survival was 10.5 months for responders and 4.5 months for nonresponding patients ($p=0.0001$).

Thus, ^{90}Y microsphere radioembolization appears to be an effective treatment option for patients with unresectable liver malignancies. However, the procedure can be associated with severe adverse events if microspheres are unintentionally deposited in organs other than the liver. Complications that have been described in this regard are radiation pneumonitis [129,130], radiation cholecystitis [131], and gastric and duodenal ulceration [118,132-134]. If too high a dose is given and/or liver cirrhosis coexists (usually present in HCC), RILD [125] and impaired liver function related symptoms (*e.g.*, hepato-encephalopathy) and even death can occur [129]. Following ^{90}Y microsphere treatment, the incidence of post-embolization symptoms, when compared to TACE, is very low, especially for the glass microspheres [135]. This is probably due to the lack of macroscopic embolization as assessed by post-treatment arteriography [136].

Contraindications for treatment with ^{90}Y microspheres definitely exist.

⁶ ^{18}F -FDG-PET: fluorine-18-2-fluoro-2-deoxy-D-glucose positron emission tomography; a nuclear imaging technique in which ^{18}F (a positron emitter) labeled glucose is intravenously injected. It is used in tumor detection and tumor response assessment, and to study the brain.

⁷ CEA: carcinoembryonic antigen; a glycoprotein present in fetal gastrointestinal tissue and in the cells or serum of adults having certain types of cancer, particularly colorectal carcinoma. CEA is used as a tumor marker, to monitor treatment effectiveness, or to detect cancer recurrence.



Figure 1 Angiographic image of the selective occlusion of the gastroduodenal artery with coils

The package insert of the glass ^{90}Y microspheres names the following. First of all, a high risk of excessive extrahepatic microsphere delivery; the $^{99\text{m}}\text{Tc}$ -MAA scintigram should not show any deposition of radioactivity in the gastrointestinal tract not correctable by angiographic techniques. Obviously, it is imperative that the relevant vascular anatomy (specifically, the superior mesenteric artery, the celiac axis, the gastroduodenal artery, and the proper hepatic artery) of the individual patient is mapped out minutely to determine the risk of radioembolization of particularly the gastroduodenal artery and right gastric artery. It can be decided to occlude these arteries with coils to inhibit inadvertent microsphere flow altogether (Fig. 1). A planar $^{99\text{m}}\text{Tc}$ -MAA image is acquired for detection of excessive hepatopulmonary shunting. If needed the intended dose is reduced. For the glass ^{90}Y microspheres the indicated upper limit of injected activity to the lungs is 600 MBq of ^{90}Y . The supplier of the resin ^{90}Y microspheres stipulates that the amount of radioactivity must be reduced if the percentage lung shunting is more than 10% while over 20% shunting is regarded as an absolute contraindication. In a study by Ngan *et al.* [137] on the prevalence of arteriovenous shunting in patients presenting with HCC, in 31.2% (91/292) of

patients was arteriovenous shunting into hepatic veins or (branches of) the portal vein observed. Naturally, liver function should be considered (biochemically) adequate (aspartate aminotransferase (AST) or alanine aminotransferase (ALT) ≤ 5 times ULN (upper limit of normal) value, bilirubin ≤ 2 mg/dl) and tumor burden not excessive; tumor load is considered excessive if tumor volume is $\geq 70\%$, or $\geq 50\%$ if albumin ≤ 3 g/dl. Also, pulmonary function must not be compromised. Patients suffering from vascular abnormalities, bleeding diathesis, or portal vein thrombosis should normally be withheld treatment as well. Patients with portal vein thrombosis are assumed to be prone for ischemic liver disease after embolization of the hepatic artery. However, a study was published in which it was demonstrated that patients with portal vein thrombosis, albeit without evidence of cavernous transformation, were able to tolerate the procedure well [138]. It has to be stressed that in this study glass ^{90}Y microspheres were applied, of which considerably lower amounts need to be administered, compared to the resin ^{90}Y microspheres [121] (Table 4). Additional contraindications mentioned in the package insert of the resin ^{90}Y microspheres are: previous external beam radiation therapy (to the liver), disseminated extrahepatic disease, and (pre/post-)treatment with capecitabine of which the most significant adverse events reported are gastrointestinal disorders.

For the glass ^{90}Y microspheres the radioactivity required (A) to deliver the desired dose to the liver (maximum absorbed liver dose = 150 Gy) may be calculated using the following formula:

$$A \text{ (GBq)} = [\text{Desired Dose (Gy)} \cdot \text{Liver Mass (kg)}] / 50 \text{ (Gy kg GBq}^{-1}\text{)}$$

Then, the required amount of activity has to be corrected for the fraction of injected radioactivity that, based on the $^{99\text{m}}\text{Tc-MAA}$ image, is presumed to shunt into the lungs (F):

$$\text{Dose (Gy)} = 50 \cdot A \text{ (GBq)} \cdot [1 - F] / \text{Liver Mass (kg)}$$

While in the glass ^{90}Y microspheres dose calculation a uniform distribution is assumed, in the resin ^{90}Y microspheres dose calculation (empirical model) the extent of hepatic tumor involvement is taken into account, as well as the degree of hepatopulmonary shunting; the recommended implanted activity is 2.0 GBq in case of $<25\%$ tumor involvement, 2.5 GBq for 25-50%, and 3.0 GBq

if >50% consists of tumorous tissue. Apart from dose calculation according to the described empirical model, which accepts the safety margins of the dose known from published clinical data and selects the most safe and effective dose, the individual dose can also be calculated using the body surface area (BSA) model, which determines the maximum amount of radioactivity tolerable by the patient based on the BSA (m²) and the percentage of tumor involvement:

$$BSA = 0.20247 \cdot h^{0.725} \cdot w^{0.425}$$

where *h* is height in meters and *w* is body weight in kilograms. Relative tumor involvement of the liver (TI) is calculated as:

$$TI (\%) = (\text{Tumor Volume} \cdot 100) / (\text{Tumor Volume} + \text{Liver Volume})$$

Subsequently, the to be injected amount of radioactivity (A) may be calculated:

$$A (\text{GBq}) = (BSA (\text{m}^2) - 0.2) + (TI (\%) / 100)$$

Table 3 Characteristics of radionuclides for internal radiation therapies

Radionuclide	Cross section (barn)	T _{1/2} (h)	γ-emission (keV)		β-emission (keV)		Mean tissue range (mm)
iodine-131 (¹³¹ I)	– (fission product)	56.1	80.2	2.6%	247.9	2.1%	2.4
			284.3	6.1%	303.9	0.7%	
			364.5	81.7%	333.8	7.3%	
			637.0	7.2%	606.31	89.9%	
			722.9	1.8%			
rhenium-188 (¹⁸⁸ Re)	¹⁸⁶ W: 38 ¹⁸⁷ W: 14.5	17.0	155.0	15.1%	1487.4	1.7%	3.5
			478.0	1.0%	1965.4	25.6%	
			633.0	1.3%	2120.4	71.1%	
			931.3	0.6%			
yttrium-90 (⁹⁰ Y)	⁸⁹ Y: 1.3	64.2	none		2280.1	100%	3.9
holmium-166 (¹⁶⁶ Ho)	¹⁶⁵ Ho: 64	26.8	80.6	6.7%	1774.3	48.7%	3.2
			1379.4	0.9%	1854.9	50.0%	

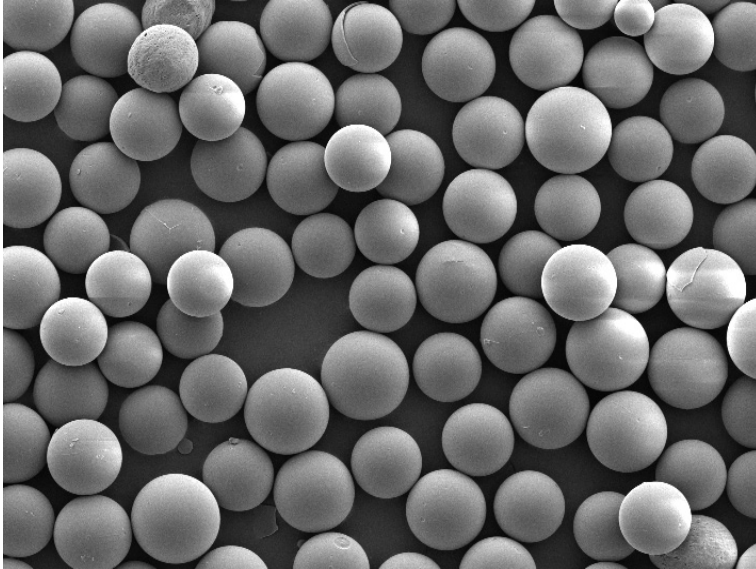


Figure 2 Scanning electron micrograph of ^{165}Ho loaded poly(L-lactic acid) microspheres

6.2 Holmium-166 poly(L-lactic acid) microspheres

Intra-arterial radioembolization with ^{90}Y microspheres undeniably is an effective new treatment modality for which encouraging clinical results have been reported. Yet, the ^{90}Y microspheres lack one important aspect, namely possibilities for good quality medical imaging, which would be very useful in dosimetry and biodistribution assessment. The only possibility of imaging is through means of Bremsstrahlung scintigraphy, of which the attained imaging quality is rudimentary and quantitative SPECT (single photon emission computed tomography) analysis is not possible [139].

The lack of medical imaging possibilities of ^{90}Y was the main reason for holmium-166 (^{166}Ho) loaded polymer-based microspheres (Fig. 2), originally proposed by Mumper *et al.* [140,141], to be further developed at the authors' nuclear medicine department [142]. These poly(L-lactic acid) (PLLA) microspheres are preloaded with ^{165}Ho acetylacetonate and prepared by a straightforward solvent evaporation method. ^{166}Ho has several advantageous properties when compared to ^{90}Y . Its beta energy may be marginally lower than ^{90}Y 's ($E_{\beta\text{max}} = 1.74$ and 1.85 MeV; $I_{\beta} = 48.7\%$ and 50.0%, respectively), but ^{166}Ho is a gamma emitter as well

Table 4 Characteristics of radionuclide loaded microspheres

Particle	Radio-nuclide	Matrix material	Density (g/ml)	Diameter (μm)	Administered amount of particles (mg)	Administered amount of particles	Standard dose (MBq)	Activity per microsphere (Bq)
TheraSphere [®] (MDS Nordion)	yttrium-90	glass	3.3	25 \pm 10	110*	4,000,000	5,000	1,250*-2,500
SIR-Spheres [®] (SIRTeX)	yttrium-90	polymer	1.6	32 \pm 10	1,370*	50,000,000	3,000	40*
Holmium microspheres (UMC Utrecht)	holmium-166	PLLA	1.4	30 \pm 5	700	33,000,000	15,000	400*

* Calculated values

($E_\gamma = 81 \text{ keV}$; $I_\gamma = 6.7\%$) (Table 3) making nuclear imaging possible. The dose rate is higher ($T_{1/2} = 26.8 \text{ h}$), which is a propitious feature as well [143]. These ^{166}Ho microspheres are also substantially less costly than the existing ^{90}Y microspheres, mainly for the reason that the thermal neutron capture cross section (σ) of ^{165}Ho is much higher than ^{89}Y 's (^{165}Ho : $\sigma = 64 \text{ barn}$; ^{89}Y : $\sigma = 1.3 \text{ barn}$) as a consequence of which considerably less (utterly expensive) nuclear reactor time is needed (Table 3). Furthermore, these ^{166}Ho microspheres are preloaded dismissing the need of a 'hot lab'. The neutron bombardment on the PLLA-based microspheres obviously has implications on the maximum activation time hence attainable specific activity, since neutron irradiation does damage the polymer matrix [144]. The maximum neutron irradiation time is 1 h in a high-flux reactor (neutron flux: $3 \times 10^{13} \text{ cm}^{-2} \text{ s}^{-1}$; Petten, The Netherlands [142]) and 6 h in a medium-flux reactor (neutron flux: $5 \times 10^{12} \text{ cm}^{-2} \text{ s}^{-1}$; Delft, The Netherlands [145]), which results in a sufficiently high amount of radioactivity: 15 GBq ^{166}Ho , which would translate, for a liver weight of 1,500 g, to a mean liver absorbed dose of 150 Gy. For the reasons that the beta energy of ^{166}Ho is slightly lower than ^{90}Y 's and the physical half-life is significantly shorter, the absorbed radiation dose of ^{166}Ho is notably lower than that of ^{90}Y (^{166}Ho : 8.7 mGy MBq^{-1} ; ^{90}Y : 28 mGy MBq^{-1}). Therefore, to deliver a radiation dose on tissue equivalent to ^{90}Y , roughly three times the amount of radioactivity has to be administered [141]. Particle size distribution analysis performed by using a Coulter Counter Multisizer 3 apparatus (Beckman Coulter Nederland, Mijdrecht, The Netherlands) on a known amount of ^{166}Ho microspheres showed that 700 mg corresponds with approximately 33 million particles. Consequently, the calculated specific activity of the ^{166}Ho microspheres is around 450 Bq/sphere. The specific activity of the preloaded glass ^{90}Y microspheres is considerably higher, whereas the specific activity of the resin ^{90}Y microspheres, which are afterloaded, is relatively low: resin ^{90}Y microspheres: 50 Bq/sphere; glass ^{90}Y microspheres: 2,500 Bq/sphere [120,121] (Table 4). The procedure by which the labeling of the resin microspheres is done has never been made public by the manufacturer, SIRTEx Medical. Evidently, the specific activity will have a direct effect on the to be administered amounts of microspheres; for the resin ^{90}Y microspheres, it can be calculated that for a standard dose of 2,000 MBq of ^{90}Y (ca. 60 Gy liver absorbed dose) to be given, corresponding with 50 million particles (density: 1.6 g/ml) [121], over 1,300 mg of microspheres have to be instilled. Importantly, this

can lead to failure in delivering the intended dose, when retrograde flow occurs during the administration procedure due to the macroscopic embolic effect of the high number of microspheres [146]; Pöpperl *et al.* [147] reported that in one-third of patients the administration procedure had to be halted prematurely due to this phenomenon. This complication has not been reported for the glass ^{90}Y microspheres, of which a considerably lower amount of microspheres has to be administered; it has been reported that 4 million spheres are needed to administer a standard liver absorbed dose of 5 GBq ^{90}Y [120,121]. For the ^{166}Ho microspheres, owing to the intermediate specific activity, difficulties in delivering the entire dose are not expected to become an issue either. A favorable feature of both the resin ^{90}Y microspheres and the ^{166}Ho microspheres is the near-plasma density (resin ^{90}Y microspheres: 1.6 g/ml [121]; ^{166}Ho PLLA microspheres: 1.4 g/ml [142]), reducing the risk of premature intravascular settling. During a biodistribution study in rats, a T/L ratio of 6.1 ± 2.9 for the ^{166}Ho microspheres was observed [94]. Radioactivity measurements demonstrated 95% retention of the injected activity in the liver and its resident tumor. The average activity detected in other tissues was $\leq 0.1\%$ injected dose/g. An efficacy study was conducted in Vx2 carcinoma-bearing rabbits [148]. After administration of the ^{166}Ho microspheres into the proper hepatic artery, the biodistribution was assessed with a gamma camera and tumor growth followed by ultrasound. The ^{166}Ho microspheres were heterogeneously distributed in the liver and accumulated preferentially in the tumor area, which was confirmed by histological analysis. Sham-treated rabbits (n=3) and rabbits treated with 'cold' microspheres (n=3) exhibited exponential tumor growth. Therapeutic doses (900 MBq ^{166}Ho ; 100 Gy liver absorbed dose) arrested growth and resulted in massive tumor necrosis (n=2).

Instead of performing $^{99\text{m}}\text{Tc}$ -MAA scintigraphy, as is customary in ^{90}Y microsphere radioembolization, prior to administration of the ^{166}Ho microspheres treatment dose, a small scout dose (10% of the total dose) of the same microspheres could be administered and gamma scintigraphy (planar and SPECT) acquired. The nuclear medicine studies would be used to screen for arteriosystemic shunting and for extrahepatic administration but would also allow for dosimetric analysis. Currently, at the authors' department, research is carried out on quantitative ^{166}Ho SPECT [149]. Next to emitting gamma rays suitable for nuclear imaging, holmium is a highly paramagnetic element as well, which allows

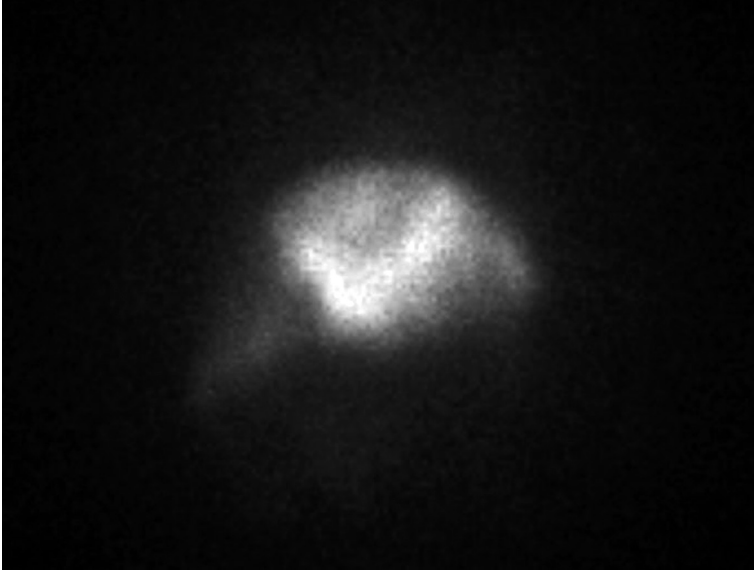


Figure 3 Planar nuclear image (anterior view) of a pig demonstrating selective hepatic deposition of radioactivity (ca. 300 MBq of ^{166}Ho at time of acquisition)

for (quantitative) magnetic resonance imaging (MRI). The imaging protocol would include anatomic T_1 -weighted SE (spin-echo) MRI in combination with a holmium-sensitive dual-echo T_2^* -weighted FFE (fast field echo) MRI [150,151]. Catheterization and administration of ^{166}Ho microspheres under real-time MRI guidance has been investigated in rabbits and pigs [150,152]. Dynamic imaging of ^{166}Ho microspheres accumulating in the tumor(s) could allow for supraseductive administration, if desired. Presently, a comprehensive toxicity study on the ^{166}Ho microspheres is conducted in healthy pigs (Fig.3), in which liver absorbed doses of up to 150 Gy are delivered. Preliminary results show that if the catheterization/administration procedure is performed correctly, neither serious clinical side-effects nor (extensive) pathological consequences or persistent alterations in serum levels of relevant blood parameters or myelosuppression are observed. The explanation for the capability of the (porcine) liver of withstanding absorbed organ doses this high is that the arterially administered radioactivity is in fact distributed inhomogeneously, as demonstrated by MRI and SPECT.

6.3 Lipiodol

Another form of radioembolization is hepatic arterial administration of radionuclide tagged lipiodol (syn.: ethiodol; Lipiodol® Ultrafluide, Guerbet Inc., Villepinte, France). Lipiodol, an iodinated ethyl ester of the fatty acids of poppy seed oil (37-39% by weight of iodine), was developed in 1901 by Marcel Guerbet, and in 1918 its radiocontrast properties were firstly recognized. In 1921, it was clinically applied for the first time, when Jean Sicard performed a positive contrast myelography using lipiodol (an indication for which it is now banned, as a consequence of its neurotoxicity).

In 1966, Idezuki *et al.* [153] injected lipiodol into the portal vein for visualization of liver malignancies on plain X-ray films. During the first two days following administration, hepatography showed good visualization of portal retention of lipiodol, whilst sinusoidal retention was demonstrated to last for several weeks. In the late 1970s, lipiodol was proposed as an intravascular contrast agent for CT imaging of the liver and spleen [154], and in 1984 Iwai *et al.* [155] demonstrated, using low-kVp⁸ X-ray examination, that in Vx2 carcinoma-bearing rabbits lipiodol, when injected into the proper hepatic artery, distributed throughout the entire hepatic arterial vascular bed. Lipiodol was retained in the liver parenchyma for 24 h, while in the tumor tissue (intracellularly) and tumor vasculature retention was maintained for at least seven days. Using a ¹⁴C-labeled lipiodol analogue for the sake of autoradiography, they demonstrated lipiodol accumulation in tumor tissue to be 1000 times more at 15 minutes and 100 times more at three days post-injection than in most other organs or plasma. Furthermore, they dissolved poly(styrene-co-maleic acid anhydride) conjugated to the cytostatic agent neocarzinostatin, named SMANCS, in lipiodol, and compared the survival period and tumor size in rabbits treated with SMANCS-lipiodol emulsion with these efficacy parameters of rabbits treated with lipiodol alone. Survival was significantly better in the SMANCS-lipiodol group whereas difference in tumor size was not. However, histological examination showed massive tumor necrosis in the SMANCS-lipiodol treated rabbits and only minimal tumor necrosis in the lipiodol treated animals. Preceding this animal study, the preliminary findings of a clinical study conducted by the same group

⁸ kVp (kilovolts peak); peak tube potential, the maximum value of the X-ray tube potential in a specified time interval.

on SMANCS-lipiodol in 44 patients suffering from (mostly) unresectable HCC were published [156]. Similarly to the findings in the rabbit study, it was shown in these patients that SMANCS-lipiodol accumulated highly selectively and was retained much longer (over three weeks) in hepatoma tissue than in the non-tumorous liver parenchyma or in other organs. Although a preliminary study and no survival rates available at the time, a significant tumoricidal effect was observed in most of the patients, as demonstrated by CT and other imaging techniques, and by a decrease in serum AFP⁹. As described in the section on microsphere radioembolization, transient side-effects (fever, abdominal pain, raise in liver enzymes serum levels) following embolization were seen. There was no myelosuppression or liver toxicity.

Also in 1983, Nakakuma *et al.* [157] carried out a similar study, the aim of which was to determine the distribution and retention of a cytostatic drug in an oily form in tumor-bearing livers, and furthermore whether this method of administration could enhance the cytoreductive effect of proper hepatic artery ligation. They investigated this concept experimentally and clinically, in rabbits and in patients suffering from unresectable liver cancer, respectively. Vx2 carcinoma-bearing rabbits were administered lipiodol, with or without ligation and transection, for distribution and retention assessment, or were injected with either a saline solution of bleomycin or a bleomycin sesame oil suspension, with ligation and transection. The effect of hepatic arterial injection of lipiodol on liver function (AST, total bilirubin) was evaluated in non-tumor bearing rabbits. Soft X-ray films and histological examination (Sudan III staining) showed that within one week almost all the lipiodol had dissipated from the normal liver, but intratumorally the lipiodol was retained. The mean survival time in the rabbits treated with a bleomycin sesame oil suspension was significantly longer than the survival time in the animals treated with a saline solution of bleomycin. No effect on liver function was seen as a consequence of lipiodol embolization. Six patients suffering from unresectable (either primary or secondary) liver cancer underwent ligation and transection of the right hepatic artery and received a subsequent injection of 5-20 ml lipiodol into the hepatoproximal lumen of the ligated artery. They also received continuous hepatic arterial infusion of 5-FU for

⁹ AFP: α -fetoprotein; a tumor marker for HCC and germ cell tumors. The sensitivity of AFP for HCC is around 60%.

the period of 22.0 ± 7.9 days. Like in the rabbits, as was demonstrated on X-ray films, lipiodol was washed out of the noncancerous part of the liver within seven days, and retention in the tumorous tissue for up to 16 months was observed. No significant difference in the liver function tests (liver enzymes, total bilirubin) was observed when compared to patients receiving only 5-FU. On the very distinct discrepancy in retention of lipiodol between tumorous tissue and normal liver parenchyma, the authors commented that, due to formation of collaterals and/or arteriovenous shunts, the lipiodol is rapidly cleared from nontumorous areas, whereas the blood flow in tumors is slow as a consequence of the tortuous and irregular tumor angioarchitecture. In addition, neoplastic vessels often lack a well developed *Tunica intima et media*, i.e., the muscular layer and elastic lamellae are less prominently present, aiding in long-term retention of the adhesive lipiodol. Ohishi *et al.* [158] contemplated on the absence of reticuloendothelial cells and lymphatic flow in tumors, which might inhibit decomposition and absorption of oil. Based on lack of histological confirmation of lymphatic clearance of lipiodol from the normal liver, the latter hypothesis was dismissed by Miller *et al.* [159]. Kobayashi *et al.* [160] suggested that lipiodol droplets adhere to the neovascular vessel inner wall due to its reversed electric charge. At last, Bhattacharya *et al.* [161] found, through light microscopic and ultrastructural examination of HepG2 (human HCC cell line) and HUVECs (human umbilical vein endothelial cells) monolayers, after exposure to lipiodol, that the tumor cells showed a slow rate of uptake followed by progressive intracellular accumulation whilst HUVECs demonstrated a rapid initial uptake followed by a short retention time. Histological examination of resected HCCs and explanted HCC-bearing livers showed that after lipiodol embolization of tumor vasculature, lipiodol uptake, possibly by pinocytosis, into endothelial cells and liver tumor cells takes place. In the mid-eighties the value of lipiodol as a CT contrast agent for the detection of liver malignancies, especially small (satellite) lesions, was assessed [162,163]. It was demonstrated to greatly increase the sensitivity of CT for (early) detecting daughter nodules only a few mm in size, and could therefore affect the decision to perform resection and aid in determining the proper surgical technique. For about 15 years, lipiodol-enhanced CT has been widely used for the detection of intrahepatic tumors (especially HCC), until it was demonstrated that its sensitivity and specificity are in fact rather low [164]. For its better accuracy, triple-phase

helical CT is a superior modality [165]. However, it has been demonstrated that 3-D MRI angiography is the optimal radiological technique for HCC staging [166].

6.4 Iodine-131 lipiodol

Instead of mixing lipiodol with antitumor drugs for TACE, it can be labeled with a radionuclide, for internal radiation therapy. The most obvious choice in the matter naturally is iodine-131 (^{131}I), a combined beta-gamma emitter ($E_{\beta\text{max}} = 606$ keV, $I_{\beta} = 89.9\%$; $E_{\gamma} = 364$ keV, $I_{\gamma} = 81.7\%$) (Table 3). On ^{131}I -labeled lipiodol, which is obtained by an isotopic exchange reaction, initial research has been carried out in Japan. The first clinical series was conducted by Kobayashi *et al.* [167], who treated seven HCC patients with multinodular disease by selective infusion of ^{131}I -lipiodol (281-592 MBq; 2.0-3.5 ml) into the right or left hepatic artery, or into a distal segmental branch. The estimated absorbed tumor doses ranged between 40-190 Gy. Tumor regression was achieved, according to a decrease in AFP serum levels (6/7) and reduction in tumor size on CT (7/7). Following treatment some side effects were observed, not dissimilar to those reported after ^{90}Y microsphere embolization, namely transient fever (4/7), temporary abdominal pain (1/7), and elevations in AST and/or ALT serum levels for a few days (3/7).

Raoul *et al.* [168] conducted a biodistribution study on ^{131}I -lipiodol in 23 patients with HCC, 14 with liver metastases (in most cases of colorectal origin), and 10 without hepatic tumors (control group). All patients had 3 ml lipiodol labeled with 70 MBq ^{131}I injected into the hepatic artery, followed by gamma scintigraphy 24 h post-injection. In contrast to what was reported by Kobayashi *et al.* [167], no post-embolic side effects were observed in this study. Tumor uptake was intense in the HCC patients and in the metastases group as well. Liver uptake was at least 75% of the injected dose, with most of the extrahepatic deposition into the lungs. The tumor/non-tumor activity ratio (T/NT ratio) was significantly higher in the HCC group (4.3 ± 2.6) than in the secondary liver cancer and control groups (2.4 ± 0.7 and 1.7 ± 0.5 , respectively). The authors held the poor vascularization of liver metastases, particularly if large and with necrotic, hence avascular cores, responsible for the lower T/NT ratio for this group. Between 30-50% of ^{131}I was eliminated through the urine, when measured over an eight-day period. Ten patients received a second dose within four weeks of the first for reproducibility

assessment purposes; no significant changes were seen in the distribution of the radioactivity. Furthermore, as was to be expected based on observations by other researchers [156-158], in the (primary and secondary) tumor groups an increase in the T/NT ratio over time was noticed.

Subsequent to this biodistribution study, the same group conducted a phase I trial to evaluate the toxicity and efficacy of internal radiation therapy with ¹³¹I-lipiodol [169]. Twenty-three patients, none pretreated with chemotherapy, including 15 with HCC and eight patients suffering from hepatic metastases from gastrointestinal primaries, were enrolled in this study. In all patients surgical resection was contraindicated, due to excessive tumor load or severity of cirrhosis. Doses between 900-2,400 MBq in 3 ml were injected into the hepatic artery. On day 7 post-injection, all patients underwent scintigraphic and CT examinations. The biodistribution (lung fraction and T/NT ratio) of the therapeutic doses was found to be not significantly different from the biodistribution of the scout doses. The treatment was well tolerated; two patients experienced pain during administration and three developed a mild, transient fever. In patients with liver metastases, no bone marrow toxicity was observed and no significant changes in levels of relevant serum parameters (uric acid, creatinine, liver enzymes and bilirubin) were measured. However, in all patients with HCC a slight and transient elevation in bilirubin levels, and in three patients in AST, was measured. Two patients died eight and ten days post-treatment, respectively, which was attributed to the severity of cirrhotic disease. In both patient groups, in patients with painful tumors durable pain relief was achieved. In the HCC group, serum AFP levels were monitored in 12 patients; in 11 of the 12 a rapid but temporary decrease was seen, and in the patients who received additional injections (5/15) these levels decreased again. CT was performed in nine patients and demonstrated a reduction in tumor size, characterized by shrinkage of the lipiodol retention areas, in all nine, ranging from 17-92% (median: 50%). After a follow-up of 5-12 months, six patients were still alive, including two who had undergone liver transplantation four and six months after the first ¹³¹I-lipiodol treatment. In contrast, in the metastatic liver cancer group the results were disappointing; CT evaluations showed no significant reduction in tumor size in any of the patients. According to the authors, this was associated with the lower and peripheral tumor uptake of ¹³¹I-lipiodol and the larger size of these lesions. Because of this lack of success in treating metastatic liver disease, since then

^{131}I -lipiodol radioembolization has been abandoned for this indication. Brans *et al.* [170] believed these poor results to be related to the considerably lower β -energy, *i.e.*, lower particle radiation range and therefore less 'crossfire' action, as compared to, for instance, ^{90}Y (^{131}I : $E_{\beta\text{max}} = 0.606 \text{ MeV}$; ^{90}Y : $E_{\beta\text{max}} = 2.28 \text{ MeV}$) (Table 3).

On the palliative treatment with ^{131}I -lipiodol of inoperable HCC sixteen original papers have been published [171]. Administered amounts of activity varied extensively (74-6,220 MBq), consequently did delivered tumor absorbed doses (10-260 Gy); the reported response rates varied from 17-92%.

In a randomized study conducted by Raoul and co-workers [172], the efficacy and tolerance of TACE (lipiodol-cisplatin) and ^{131}I -lipiodol radioembolization (2.2 GBq) were compared. A total of 142 patients with unresectable HCC were enrolled in the study, 129 of whom were available for analysis, 65 in the ^{131}I -lipiodol arm and 64 in the TACE arm; the overall survival rates at six months, 1, 2, 3, and 4 years of 69%, 38%, 22%, 14%, and 10%, and 66%, 42%, 22%, 3%, and 0% in the ^{131}I -lipiodol group and the TACE group, respectively, were similar as were complete and partial response rates. Conversely, in terms of clinical tolerance the two groups differed considerably; limited to a 15-day period post-treatment, for the TACE group 29 major side effects were reported, including 17 life-threatening events, against three major side effects for the ^{131}I -lipiodol group, none of which were life threatening. Six treatment-related deaths occurred in the TACE group, representing a 9% mortality rate. This considerable difference in morbidity and mortality rates might be (partially) associated with the substantially larger volume of lipiodol instilled in TACE (10 ml *versus* 3 ml in ^{131}I -lipiodol radioembolization) and the subsequent injection of gel-sponge fragments, greatly impairing hepatic arterial blood flow.

Certainly, ^{131}I -lipiodol therapy can be associated with (severe) adverse events as well; recently, CIS bio international (Gif-sur-Yvette, France), manufacturer of ^{131}I -lipiodol (Lipiodis[®]), has informed health care professionals that the incidence of radiation pneumonitis associated with the use of Lipiodis[®] appears notably higher (2%) than initially observed in clinical trials (0.5%) [173]. These interstitial pneumopathies usually manifest themselves approximately one month following the second ^{131}I -lipiodol injection and constitute a severe clinical condition that generally leads to respiratory failure.

Albeit to a limited extent, ^{131}I -lipiodol radioembolization as a neoadjuvant treatment in HCC patients awaiting liver transplantation has been explored as well. The first (pilot) study published on this use of ^{131}I -lipiodol was by Brans *et al.* [174]. Ten HCC patients, not amenable for partial hepatectomy and awaiting liver transplantation, four of ten previously treated with chemoembolization, received intra-arterial ^{131}I -lipiodol. The applied doses of radioactivity depended on the attainable selectivity of the catheterization and ranged from 1,332-2,146 MBq (mean: 1,887 MBq) of ^{131}I . Except for one patient who received a second instillation, a single treatment was given. Tumor response was evaluated based on pre- and post-therapy AFP serum levels and MRI, and on pathological examination of explanted liver samples; in five of ten patients antitumor activity was demonstrated. Of these five responders, two had undergone TACE previously, seven and 12 months preceding ^{131}I -lipiodol treatment, and a 'combined effect' cannot with absolute certainty be discarded.

In a trial led by Raoul *et al.* [175], eligible patients received 1-3 hepatic arterial instillations of ^{131}I -lipiodol (2,400 MBq/injection), with 2-3 months intervals. CT was performed seven days post-treatment to assess tumor number and size. Thirty-four HCC patients were included in the study, including 29 with cirrhosis. Subsequent to the ^{131}I -lipiodol injections, 14 underwent liver transplantation, 19 underwent partial hepatectomy, and one patient had explorative laparotomy during which it was decided that resection was not feasible. The catheterization/radioembolization procedure was well tolerated, except for one patient who developed acute ischemia of the small bowel, which resolved with intestinal resection. AFP levels, CT examinations, and measurements on operative specimens were used for treatment response assessment; none had a complete response, but an objective tumor response or necrosis, involving more than 90% of the tumor, was observed in 25 of 34 patients. The 1-, 3-, and 5-year overall survival rates were 85%, 59%, and 48%, respectively. When discriminating between resection and transplantation, the second category had a significantly higher 5-year survival rate (36% *versus* 69%) and recurrence-free survival (48% *versus* 83% 3-year recurrence-free survival).

Lambert *et al.* [176] have also treated HCC patients awaiting liver transplantation with radioactive lipiodol, initially ^{131}I -lipiodol, and later on Re-188-HDD-lipiodol (^{188}Re : $E_{\beta\text{max}} = 2.12 \text{ MeV}$, $I_{\beta} = 71.1\%$; $E_{\gamma} = 155 \text{ keV}$, $I_{\gamma} = 15\%$; $T_{1/2}$

= 17.0 h) (Table 3). Thirty-seven patients (Child-Pugh¹⁰ class A or B) enrolled and mean activities of 2.1 GBq ¹³¹I-lipiodol or 4.1 GBq ¹⁸⁸Re-HDD-lipiodol were instilled into the proper hepatic artery or into its right and/or left branches. Patients received 1-3 treatments. Nine patients were not exclusively pretreated with radiolabeled lipiodol and therefore excluded from further analysis. Two patients died while on the waiting list, and of the remaining 26 patients who underwent a liver transplantation, six were not available for long-term outcome assessment, either because of failure to confirm HCC diagnosis in the explanted liver (4/26) or due to perioperative death from surgical complications (2/26). Four of 20 patients suffered from recurrent disease. The overall recurrence-free survival was 19.7 months, with a mean follow-up of 20.1 months. Pathological examination revealed tumor necrosis (in the largest lesion) exceeding 90% in only four patients, which accounts for less than 25% of patients, which is a drastically lower result than reported in the before discussed papers by Brans *et al.* [174], who included pretreated patients in their analysis as well, and by Raoul *et al.* [175], who did not report whether enrolled patients had been pretreated or not.

In an *in vitro* study by Chenoufi *et al.* [177], it was demonstrated that the radiosensitivity of HepG2 cells is significantly enhanced in a synergistic manner when next to ¹³¹I additionally exposed to a cytostatic agent (doxorubicin or cisplatin). Recently, the results of a phase II trial were published in which 41 patients suffering from unresectable HCC, and Child-Pugh class B7 or less, were hepatic intra-arterially injected with ¹³¹I-lipiodol (mean activity 2.22 GBq ¹³¹I), preceded and followed by low-dose intravenous cisplatin infusion (20 mg/m², and 6 mg/m²/d for 5 days, respectively) [178]. Depending on response, general status, and liver function, up to four cycles were given. Response was evaluated on CT, and in patients with measurable tumors (38/41) an objective response was observed in 18 patients (47%), including one complete response. In 15 patients, stable disease was observed, whereas two displayed progressive disease. Four patients were not available for response assessment. One-year and 2-year survival rates were 73% and 48%, respectively. Fifteen patients developed grade 3 or 4 adverse events, mainly hematological disorders (thrombocytopenia,

¹⁰ Child-Pugh (syn.: Child-Turcotte-Pugh) classification (graded A-C); a scoring system used to determine prognosis of chronic liver disease, mainly cirrhosis. The score employs five clinical parameters of liver disease: serum bilirubin, serum albumin, INR (PT prolongation), ascites, and hepatoencephalopathy.

neutropenia) and post-embolization syndrome symptoms. One patient with neutropenia succumbed from a fatal *Chlamydia pneumoniae* infection. In eight patients, the adverse effects were ascribed to the chemotherapy. Four patients developed major lung complications: interstitial pneumonitis in two patients, and infection or tumor spread in the other two. Three patients died of pulmonary complications, which accounts for 7% of treated patients. Nonetheless, the authors concluded that toxicity was not increased by the addition of cisplatin, and that this combination treatment appeared to yield better response rates than ^{131}I -lipiodol alone.

^{131}I -lipiodol injections indeed have proven to be a valuable palliative treatment option in the management of HCC, with a lower complication rate than chemoembolization. However, for proper evaluation of its employment as a neo-adjuvant treatment in HCC, larger, randomized studies are warranted.

6.5 Yttrium-90-EDTB-lipiodol

In the late 1980s, it was suggested that, for its higher-energy β -particles and shorter half-life (Table 3), ^{90}Y might be a better suited isotope for radiolabeled lipiodol therapy [179]. In 1994, Wang *et al.* [180] conjugated lipiodol with the chelator *N,N,N,N*-tetrakis(2-benzimidazolmethyl)-1,2-ethanediamine (EDTB), which was synthesized through condensation of 1,2-benzenediamine and ethylene diamine tetra-acetic acid (EDTA). Subsequently, ^{90}Y , which had been separated from strontium-90 (^{90}Sr) using a RP-18 column, was eluted from the column with EDTB-lipiodol, yielding ^{90}Y -EDTB-lipiodol. They carried out a biodistribution study in 16 healthy rats subsequent to hepatic arterial administration of approximately 0.37 MBq ^{90}Y -EDTB-lipiodol. The rats were terminated at 1 h, 24 h, 48 h, and 72 h post-injection, and the average tissue concentrations (% injected dose/g) in organ samples (liver, spleen, muscle, lung, kidney, bone, whole blood, and testis) were calculated; at 1 h most of the radioactivity was confined to the liver, however, at 48 h >50% of the activity had been released from the liver. Radioactivity concentrations in kidney samples were low initially (0.12%/g at 1 h), but peaked at 24 h (0.87%/g), suggesting that ^{90}Y is predominantly renally excreted. However, the ^{90}Y bone concentrations started to dramatically increase after 24 h (>0.40%/g) to remain at the same level for the duration of the study, a finding that brought research on ^{90}Y -EDTB-lipiodol to a standstill, since bone

marrow is highly sensitive for radiation. Also, skeletal retention would not be accurately measurable by SPECT, due to ^{90}Y 's absence of gamma emission. Of course, this lack of gamma emission could be looked upon as an advantage as well, since no hospitalization is required for radiation safety reasons. Then again, gamma rays suitable for nuclear imaging, *i.e.*, of a low or medium energy and sufficient abundance, can be very useful in biodistribution assessment.

6.6 Rhenium-188-HDD-lipiodol

^{188}Re has several advantages over both ^{131}I and ^{90}Y : its beta energy is similar to that of ^{90}Y (^{188}Re : $E_{\beta\text{max}} = 2.12$ MeV; ^{90}Y : $E_{\beta\text{max}} = 2.28$ MeV; ^{131}I : $E_{\beta\text{max}} = 0.606$ MeV) and it emits gamma rays as well that allow for nuclear imaging ($E_{\gamma} = 155$ keV, $I_{\gamma} = 15\%$) (Table 3). In addition, the dose rate is higher due to its shorter half-life ($T_{1/2} = 16.9$ h), and it is generator-produced (tungsten-188/rhenium-188 ($^{188}\text{W}/^{188}\text{Re}$)-generator) making it a relatively inexpensive radioisotope. In 1996, Wang *et al.* [181] reported on the preparation and biodistribution of ^{188}Re -EDTB-lipiodol. Lipiodol was labeled with ^{188}Re by sonicating EDTB-lipiodol with an aqueous solution of ^{188}Re in ammonium acetate buffer containing EDTB for 2 h at 70°C , followed by filtration through a 0.2 micrometer Millipore® filter. In this study, 12 liver-tumor-bearing rats were injected into the hepatic artery with 7.4 MBq ^{188}Re -lipiodol (0.1 ml). At 1 h, 24 h, or 48 h the rats were sacrificed and the tissue distribution assessed (% injected dose/g, in tumor, liver, kidney, spleen, testis, muscle, bone and blood). The mean tumor/normal-liver ratio was 5.15 at 1 h, and 7.70 and 10.84 at 24 h and 48 h post-injection, respectively. At 1 h the relative lung dose was high – which was ascribed to intrahepatic arterioportal shunting – but rapidly declined in time, in contrast to the kidneys, in which radioactivity levels were higher at 24 h than at 1 h. Tissue concentrations were low in the other samples, including the bone. It was concluded that ^{188}Re -EDTB-lipiodol might be a more effective and, in contradistinction to ^{90}Y -EDTB-lipiodol, safe alternative to ^{131}I -lipiodol.

In the meantime, clinical trials on ^{188}Re -labeled lipiodol have been conducted, all pertaining to ^{188}Re -4-hexadecyl-TDD-lipiodol (^{188}Re -HDD-lipiodol); ^{188}Re -HDD-lipiodol is obtained by heating the concentrated eluate from a $^{188}\text{W}/^{188}\text{Re}$ -generator with lyophilized HDD for 1 h, followed by addition of lipiodol and separation by centrifugation.

In 2002, the results of a phase I study were published in which 16 HCC patients had been included for ^{188}Re -HDD-lipiodol treatment [182]. Prior to the treatment dose, a scout dose of about 200 MBq was infused and planar nuclear images were acquired to assess biodistribution and to calculate the maximum tolerated dose (determined by the liver absorbed dose and the lung absorbed dose). The main limiting factor was shown to be the liver dose. In the first five patients, radioactivity levels in blood samples were measured to assess the bone marrow dose, but this was refrained from when the dose was found to be negligible. A mean treatment dose of 4.0 GBq (1.8-7.5 GBq) was administered, resulting in a mean total dose of 4.2 GBq of ^{188}Re -HDD-lipiodol. Following treatment, AFP serum levels generally decreased, and CT showed 10-50% reduction in tumor size in four of 16 and no change in 12 patients; one patient had a partial response, 13 patients had stable disease, and two had progressive disease. The treatment was well tolerated by most patients; in most patients, a minor elevation in AST and ALT levels at 24 h post-instillation was observed, whereas bilirubin serum levels remained unchanged. During a three-month follow-up, no signs of myelosuppression were observed in any of the patients. Reported side effects, all transient, included mild nausea, mild right upper quadrant pain, low-grade fever, and emesis. Still, performance status was good; all patients were discharged within 48-72 h and able to resume their work within a week. The authors pointed out the good cost-effectiveness of ^{188}Re -HDD-lipiodol therapy when compared to ^{90}Y microsphere and ^{131}I -lipiodol radioembolization, which is mainly due to the low cost, on-site availability and long shelf life (4-6 months) of the $^{188}\text{W}/^{188}\text{Re}$ -generator. Yet, they also commented on the occasional failure in obtaining adequate doses of radioactivity due to problems in eluting and labeling.

Subsequent to this rather small study, a second, larger trial was conducted, in which safety and efficacy of HCC treatment with ^{188}Re -HDD-lipiodol was assessed [183]. The trial was subdivided in a dose escalation study (16 patients), in which from 1.8-7.7 GBq ^{188}Re -HDD-lipiodol was administered, and an efficacy study (54 patients), in which up to 9.8 GBq (mean: 4.6 GBq) was injected as selectively as possible. At three months post-treatment, based on CT, almost half of the patients (34/70) had stable disease, 13 showed a partial response and 23 patients had disease progression. Sixty-three patients (90%) were alive at three months, and 13 (19%) at one year. One patient, who received three instillations of

^{188}Re -HDD-lipiodol, had a complete response at 16 months. The side effects, both clinical, biochemical, and hematological were of similar nature and duration as in the described safety trial [182]. Twenty patients had repeated treatments, which did not appear to have had any repercussions on liver function. Two months post-treatment, two patients developed mild pleural effusion, most likely associated with radiation pneumonitis, which resolved with steroid treatment .

Lambert *et al.* [184] have conducted a phase I trial on ^{188}Re -HDD-lipiodol as well, in which its pharmacokinetics, organ dosimetry, and toxicity were investigated. Eleven HCC patients, five pretreated with ^{131}I -lipiodol, received 1-3 injections (total of 16 injections) of ^{188}Re -HDD-lipiodol. The mean administered activity was 3.60 GBq ^{188}Re (1.86-4.14 GBq) per session. Blood and urine samples were taken within 76 h following administration and it was observed that radioactivity, that eluded from the injected ^{188}Re -HDD-lipiodol, was rapidly cleared from the blood; a mean effective half-life of 7.6 ± 2.2 h was calculated. A mean $25.9 \pm 6.3\%$ and $44.1 \pm 11.7\%$ of the administered activity was renally excreted within 21 and 76 h post-treatment, respectively. Except for one patient, who developed a transient leukopenia and thrombocytopenia, there were no significant changes in the hematological parameters. One patient with preexisting hyperbilirubinemia developed a progression of his jaundice, hence liver dysfunction, but overall no liver biochemical abnormalities (bilirubin, AST, ALT) were seen. One patient, following a second instillation of ^{188}Re -HDD-lipiodol, developed diffuse fibrotic lung disease (Fig. 4). A mean absorbed lung dose of 4.07 Gy (range: 1.38-5.96 Gy), or distinctly in the safe range, was calculated. Tumor response was evaluated on MRI (six weeks post-treatment): three patients were not eligible for response assessment, one patient had progressive disease following the third treatment, in one patient a partial response was observed, while the remainder of patients had stable disease. Serum AFP was elevated pretreatment in eight treatment sessions; at week 6, in five of these treatments a reduction in AFP serum levels (range: 19-90%) was measured. In contradistinction to the before described studies conducted by Sundram *et al.* [182,183], who aimed to inject the activity as near to the tumor feeding artery as possible, Lambert and co-workers preferred a relatively nonselective administration into the proper hepatic artery in order to be able to deliver a dose to occult tumors in other liver segments or lobes (metachronous HCC) as well. As the authors commented, this



Figure 4 Whole-body scan (anterior view, acquired 28 h post-administration) of a patient with HCC who received 3.7 GBq ^{188}Re -HDD-lipiodol. Significant uptake is seen in HCC (right lobe) and in the urine bladder. Some lung uptake is observed as well.

(Image courtesy of Dr. B. Lambert, Ghent University Hospital, Ghent, Belgium)

'whole-liver treatment' approach may of course have had implications on the incidence of adverse events.

In the before described studies, with respect to liver function status, essentially stage of cirrhosis, mixed patient groups were treated. Since cirrhosis is often coexistent with HCC, it would obviously be worthwhile to further examine the value of ^{188}Re -HDD-lipiodol treatment in patients with advanced cirrhotic liver disease. Therefore, Lambert *et al.* [185] performed a feasibility study in HCC patients, concomitantly suffering from moderate hepatic impairment (Child-Pugh B). Twelve patients, of whom four with portal vein thrombosis, underwent single instillations of ^{188}Re -HDD-lipiodol (3.7 ± 0.2 GBq) into either the proper hepatic artery or the left and right hepatic artery separately. Tumor response was assessed using AFP serum levels and MRI. Four patients were not available for radiological response assessment at week 6 post-treatment; one patient had undergone liver transplantation at week 5, and the conditions of three patients had drastically worsened, prohibiting attending follow-up visits. One patient had a partial response and underwent liver transplantation at week 12. The remaining seven patients had stable disease. Following treatment, ten of 12 patients experienced adverse events, eight of which grade 3 or 4 events. Adverse events, not all strictly treatment-related, included elevations in bilirubin, AST, or ALT serum levels, myelosuppression, peritoneal effusion, and pulmonary fibrosis. The authors concluded that, given the clinical outcome, namely that seven of 12 patients had a worsening of their general condition following treatment, the administration of 3.7 GBq of ^{188}Re -HDD-lipiodol to patients with Child-Pugh B disease, at least in the way it was carried out in this study, *i.e.*, not supraselectively, was not supported.

Recently, the same group published the results of a dose-escalation study in HCC patients with well-compensated cirrhosis (Child-Pugh A) [186]. Thirty-five doses of ^{188}Re -HDD-lipiodol, from 4.8-7.0 GBq, were instilled in 28 patients, of whom five had undergone previous anti-cancer treatment and five had portal vein thrombosis. The ^{188}Re -HDD-lipiodol was preferably injected into the proper hepatic artery or into both the left and right hepatic artery, but in two patients with aberrant vascular anatomy and unilobar disease the radioconjugate was selectively injected the right branch. According to measurements in urine samples obtained from 25 patients, a mean of 41.7% of the administered activity

was renally excreted within 46 h. Estimated organ absorbed doses were linearly related to the administered amounts of radioactivity and remained well below the threshold levels for radiation-induced effects. There were no hematological side effects, except for a slight but statistically significant decrease in white blood cell counts at week 6. No clinical liver toxicity was observed, although it was noticed that, at discharge, in all patients AST and bilirubin serum levels were elevated. Like in the described Child-Pugh B-study, lung conditions were reported; two patients experienced pulmonary symptoms 2-5 weeks following a second treatment, of which the relation to the radioconjugate treatments remained unclear, since fibrotic lung changes were not detected on CT. Also, the estimated absorbed lung doses in these patients (10.4 and 11.5 Gy) were held too low for radiation pneumonitis to be induced. One of these patients, who was known to have pre-existing chronic obstructive pulmonary disease, had to be treated with corticosteroids, after which the condition resolved. Further reported treatment-related side effects were fever and fatigue. Treatment response could be assessed in 25 patients (31 treatment sessions); partial response, stable disease, and disease progression was observed following one, 28, and two treatments, respectively. Thus, based on CT, stable disease was the generally observed outcome; however, examinations of explanted livers showed massive necrosis in some tumors, whereas imaging (CT or MRI) had suggested disease stabilization. The authors commented on the inability of synthesizing over 7.0 GBq ^{188}Re -HDD due to limitations of the labeling procedure, and concluded that investigations on superior chelating compounds and on SPECT dosimetry were considered of the essence.

7 DISCUSSION

An evident advantage of the described locoregional radionuclide treatments is that these are minimally-invasive techniques, as are ablation techniques like RFA (if performed percutaneously). However, in contradistinction to the latter, the radionuclide therapies are not restricted by the number, location, or size of tumors. Two further advantages, when set alongside to systemic chemotherapy, are the absence of systemic toxicity (*e.g.*, myelosuppression) and the improved patient convenience and quality of life since these techniques are usually performed once or, in case of radiolabeled lipiodol, sometimes repeated 1-3 times, whereas

a chemotherapy regimen like for instance FOLFOX typically consists of 12 cycles, each of which lasts two weeks. With regard to efficacy, radioembolization techniques are at least equivalent to chemoembolization and, according to the results of one randomized trial (TACE *versus* ^{131}I -lipiodol), also significantly better tolerated [172]. This has probably mainly to do with the fact that embolization in radioembolization techniques is incomplete, whereas hepatic arterial blood flow is arrested completely in TACE. Addition of systemic chemotherapy appears to improve clinical efficacy of ^{90}Y microsphere and radiolabeled lipiodol treatment [125,178], and the results of studies underway, in which resin ^{90}Y microspheres are combined with the latest chemotherapy protocols, are awaited with interest [126,127]. An obvious downside of these radionuclide treatments, and high-dose therapeutic nuclear medicine procedures in general, especially in a palliative setting, is the necessity to isolate the patient for a certain length of time for radiation safety considerations to limit the radiation dose to relatives, nursing staff and members of the public. The required isolation periods vary between countries but can be up to seven days, in the case of ^{131}I .

Microsphere and lipiodol radioembolization are based on the same underlying principle, but put side by side, there are some remarkable differences to be noted. First, as a consequence of the results of a single patient study [169], lipiodol based radionuclide treatments are considered ineffective for metastatic liver cancer. This conclusion is based on the disappointing clinical results in just eight patients where the low intratumoral penetration of ^{131}I -lipiodol was deemed the key factor responsible for this outcome. Since then, treatment of secondary liver cancer with radiolabeled lipiodol has not been reported in the literature. However, it could be postulated that better efficacy might be sorted if ^{188}Re -HDD-labeled lipiodol were used for this indication, owing to the considerably higher energy of this radionuclide's beta particles. The longer tissue range of these particles could perhaps result in tumor reductive effects in lesions of larger dimensions and/or with a necrotic core.

One other important difference is that, in contrast to radiolabeled lipiodol, almost no radioactivity eludes from the ^{90}Y microspheres nowadays available, whereas a significant portion of the radionuclide fraction is released from the lipiodol following administration [184,187]. Reported calculated organ absorbed doses remained below the level where radiation-induced effects can

be expected. However, according to the manufacturer, severe lung conditions have been reported to arise in 2% of patients treated with ^{131}I -lipiodol [173]. Hematosuppression was absent or mild in most patients treated with either ^{131}I - or ^{188}Re -HDD-labeled lipiodol, and is directly dose related. Both Lambert *et al.* [186], who have administered up to 7.0 GBq of ^{188}Re -HDD-lipiodol to patients, and Sundram *et al.* [183], who injected activities up to 9.8 GBq of ^{188}Re -HDD-lipiodol, observed that bone marrow toxicity was negligible. It would be very useful to determine which would be the maximum tolerated administered dose of ^{188}Re -HDD-lipiodol since significantly higher amounts of radioactivity might elicit better tumoricidal effects and perhaps be effective in metastatic liver disease as well. However, in order to enhance the labeling efficiency, *i.e.*, specific activity, as Lambert *et al.* [186] commented, improved chelators are needed.

There seems to be no consensus on whether the radiolabeled lipiodol or ^{90}Y microspheres ought best be injected supraselectively, *i.e.*, the tip of the catheter positioned as near to the tumor feeding artery as possible, or if administration should be performed relatively proximally, in the proper or left or right hepatic artery. The first approach, in theory, might accomplish in delivering a higher dose on the selected lesion and limit the dose on normal-liver tissue but, as Lambert *et al.* [184] rightly commented, would also suspend treatment of metachronous lesions. The second method might indeed deliver a higher dose on the non-tumorous tissue but would not spare occult tumors either. We would propose that the second approach is probably best suited for patients with sufficient liver function and the first to be reserved for patients with decreased liver function. In effect, the resin ^{90}Y microspheres are prescribed to be instilled supraselectively, and this, coupled with the high number of microspheres applied, probably is the reason for the frequent inability in administrating the calculated dose.

In most studies discussed in this paper, tumor response was assessed using CT or MRI, in accordance with the so-called RECIST (Response Evaluation Criteria in Solid Tumors) criteria [188]. It would be advisable to add ^{18}F -FDG-PET to these imaging modalities, for the reason that this functional imaging technique is better suited in assessing residual tumor viability, since ^{18}F -FDG is obviously not taken up by necrotic (tumor) tissue. Furthermore, ^{18}F -FDG-PET has also been proven to be highly effective in detecting extrahepatic disease, hence is able to assist in improving accuracy of preoperative tumor staging [189].

It is our conviction that, in the near future, the ^{166}Ho microspheres will be able to take radioactive microsphere therapy to the next level, especially owing to the bimodal imaging possibilities (SPECT and MRI), which will allow for patient-individualized dosimetry. Moreover, this could be complemented by (selective) real-time MR-guided administration helping in further improving accuracy of dose delivery.

Encouraging results have been achieved with lipiodol and (particularly) microsphere based radioembolization techniques, as described in this chapter. Yet, apart from some exceptions (*e.g.*, well-differentiated thyroid cancer, testicular cancer), in the treatment of inoperable cancer there seems to be no such thing as a magic 'silver bullet'. Nonetheless, we consider substantial improvement in survival in the treatment of unresectable liver cancer feasible when locoregional radiation therapies are combined with the latest chemotherapy protocols, including angiogenesis inhibitors and other biological agents. In conclusion, next to improved dosimetry, combination of treatment modalities should result in improved clinical outcome and overall survival.

REFERENCES

1. Parkin DM, Bray F, Ferlay J, Pisani P. Global cancer statistics, 2002. *Ca Cancer J. Clin.* **2005**;55:74-108.
2. Russell AH, Tong D, Dawson LE, Wisbeck W. Adenocarcinoma of the proximal colon. Sites of initial dissemination and patterns of recurrence following surgery alone. *Cancer* **1984**;53:360-367.
3. Bengtsson G, Carlsson G, Hafstrom L, Jonsson PE. Natural history of patients with untreated liver metastases from colorectal cancer. *Am. J. Surg.* **1981**;141:586-589.
4. Giovannucci E, Rimm EB, Stampfer MJ, Colditz GA, Ascherio A, Willett WC. Intake of fat, meat, and fiber in relation to risk of colon cancer in men. *Cancer Res.* **1994**;54:2390-2397.
5. Le Marchand L, Wilkens LR, Kolonel LN, Hankin JH, Lyu LC. Associations of sedentary lifestyle, obesity, smoking, alcohol use, and diabetes with the risk of colorectal cancer. *Cancer Res.* **1997**;57:4787-4794.
6. Bennett JJ, Cao D, Posner MC. Determinants of unresectability and outcome of patients with occult colorectal hepatic metastases. *J. Surg. Oncol.* **2005**;92:64-69.
7. Scheele J, Altendorf-Hofmann A. Resection of colorectal liver metastases. *Langenbecks Arch. Surg.* **1999**;384:313-327.
8. Scheele J, Stang R, Altendorf-Hoffmann A, Paul M. Resection of colorectal liver metastases. *World J. Surg.* **1995**;19:59-71.
9. Llovet JM, Beaugrand M. Hepatocellular carcinoma: present status and future prospects. *J. Hepatol.* **2003**;38 Suppl 1:S136-S149.
10. Pawlik TM, Esnaola NF, Vauthey JN. Surgical treatment of hepatocellular carcinoma: similar long-term results despite geographic variations. *Liver Transpl.* **2004**;10:S74-S80.
11. Cormier JN, Thomas KT, Chari RS, Pinson CW. Management of hepatocellular carcinoma. *J. Gastrointest. Surg.* **2006**;10:761-780.
12. Okuda K, Ohtsuki T, Obata H, Tomimatsu M, *et al.* Natural history of hepatocellular carcinoma and prognosis in relation to treatment. Study of 850 patients. *Cancer* **1985**;56:918-928.
13. Llovet JM, Bustamante J, Castells A, Vilana R, *et al.* Natural history of untreated nonsurgical hepatocellular carcinoma: rationale for the design and evaluation of therapeutic trials. *Hepatology* **1999**;29:62-67.
14. Johnson PJ. Systemic chemotherapy of liver tumors. *Semin. Surg. Oncol.* **2000**;19:116-124.
15. Nowak AK, Stockler MR, Chow PK, Findlay M. Use of tamoxifen in advanced-stage hepatocellular carcinoma. A systematic review. *Cancer* **2005**;103:1408-1414.
16. Carr BI. Hepatocellular carcinoma: current management and future trends. *Gastroenterology* **2004**;127:S218-S224.
17. Advanced Colorectal Cancer Meta-Analysis Project. Modulation of fluorouracil by leucovorin in patients with advanced colorectal cancer: evidence in terms of response rate. Advanced Colorectal Cancer Meta-Analysis Project. *J. Clin. Oncol.* **1992**;10:896-903.

18. Simmonds PC. Palliative chemotherapy for advanced colorectal cancer: systematic review and meta-analysis. Colorectal Cancer Collaborative Group. *BMJ* **2000**;321:531-535.
19. Goldberg RM. Advances in the treatment of metastatic colorectal cancer. *Oncologist*. **2005**;10 Suppl 3:40-48.
20. Van Laarhoven HW, Punt CJ. Systemic treatment of advanced colorectal carcinoma. *Eur. J. Gastroenterol. Hepatol.* **2004**;16:283-289.
21. Van Cutsem E, Hoff PM, Harper P, Bukowski RM, *et al.* Oral capecitabine vs intravenous 5-fluorouracil and leucovorin: integrated efficacy data and novel analyses from two large, randomised, phase III trials. *Br. J. Cancer* **2004**;90:1190-1197.
22. Mayer RJ. Oral versus intravenous fluoropyrimidines for advanced colorectal cancer: by either route, it's all the same. *J. Clin. Oncol.* **2001**;19:4093-4096.
23. Cromheecke M, Konings AW, Szabo BG, Hoekstra HJ. Liver tissue tolerance for irradiation: experimental and clinical investigations. *Hepatogastroenterology* **2000**;47:1732-1740.
24. Ingold J, Reed G, Kaplan H, Bagshaw M. Radiation hepatitis. *Am. J. Roentgenol. Radium Ther. Nucl. Med* **1965**;93:200-208.
25. Lawrence TS, Robertson JM, Anscher MS, Jirtle RL, Ensminger WD, Fajardo LF. Hepatic toxicity resulting from cancer treatment. *Int. J. Radiat. Oncol. Biol. Phys.* **1995**;31:1237-1248.
26. Fajardo LF, Colby TV. Pathogenesis of veno-occlusive liver disease after radiation. *Arch. Pathol. Lab. Med.* **1980**;104:584-588.
27. Fuss M, Salter BJ, Herman TS, Thomas CR, Jr. External beam radiation therapy for hepatocellular carcinoma: potential of intensity-modulated and image-guided radiation therapy. *Gastroenterology* **2004**;127:S206-S217.
28. Dawson LA, McGinn CJ, Lawrence TS. Conformal chemoradiation for primary and metastatic liver malignancies. *Semin. Surg. Oncol.* **2003**;21:249-255.
29. Ten Haken RK, Lawrence TS, McShan DL, Tesser RJ, Fraass BA, Lichter AS. Technical considerations in the use of 3-D beam arrangements in the abdomen. *Radiother. Oncol.* **1991**;22:19-28.
30. Liu MT, Li SH, Chu TC, Hsieh CY, *et al.* Three-dimensional conformal radiation therapy for unresectable hepatocellular carcinoma patients who had failed with or were unsuited for transcatheter arterial chemoembolization. *Jpn. J. Clin. Oncol.* **2004**;34:532-539.
31. Ben-Josef E, Normolle D, Ensminger WD, Walker S, *et al.* Phase II trial of high-dose conformal radiation therapy with concurrent hepatic artery floxuridine for unresectable intrahepatic malignancies. *J. Clin. Oncol.* **2005**;23:8739-8747.
32. Lawrence TS, Tesser RJ, Ten Haken RK. An application of dose volume histograms to the treatment of intrahepatic malignancies with radiation therapy. *Int. J. Radiat. Oncol. Biol. Phys.* **1990**;19:1041-1047.
33. Fuss M, Thomas CR, Jr. Stereotactic body radiation therapy: an ablative treatment option for primary and secondary liver tumors. *Ann. Surg. Oncol.* **2004**;11:130-138.

34. Schefter TE, Kavanagh BD, Timmerman RD, Cardenes HR, Baron A, Gaspar LE. A phase I trial of stereotactic body radiation therapy (SBRT) for liver metastases. *Int. J. Radiat. Oncol. Biol. Phys.* **2005**;62:1371-1378.
35. Mazzaferro V, Regalia E, Doci R, Andreola S, *et al.* Liver transplantation for the treatment of small hepatocellular carcinomas in patients with cirrhosis. *N. Engl. J. Med.* **1996**;334:693-699.
36. Llovet JM, Schwartz M, Mazzaferro V. Resection and liver transplantation for hepatocellular carcinoma. *Semin. Liver Dis.* **2005**;25:181-200.
37. Yao FY, Ferrell L, Bass NM, Bacchetti P, Ascher NL, Roberts JP. Liver transplantation for hepatocellular carcinoma: comparison of the proposed UCSF criteria with the Milan criteria and the Pittsburgh modified TNM criteria. *Liver Transpl.* **2002**;8:765-774.
38. Yao FY, Ferrell L, Bass NM, Watson JJ, *et al.* Liver transplantation for hepatocellular carcinoma: expansion of the tumor size limits does not adversely impact survival. *Hepatology* **2001**;33:1394-1403.
39. Meyer CG, Penn I, James L. Liver transplantation for cholangiocarcinoma: results in 207 patients. *Transplantation* **2000**;69:1633-1637.
40. Olausson M, Friman S, Cahlin C, Nilsson O, *et al.* Indications and results of liver transplantation in patients with neuroendocrine tumors. *World J. Surg.* **2002**;26:998-1004.
41. Lehnert T. Liver transplantation for metastatic neuroendocrine carcinoma: an analysis of 103 patients. *Transplantation* **1998**;66:1307-1312.
42. Pichlmayr R, Weimann A, Oldhafer KJ, Schlitt HJ, *et al.* Role of liver transplantation in the treatment of unresectable liver cancer. *World J. Surg.* **1995**;19:807-813.
43. Frilling A, Rogiers X, Malago M, Liedke OM, Kaun M, Broelsch CE. Treatment of liver metastases in patients with neuroendocrine tumors. *Langenbecks Arch. Surg.* **1998**;383:62-70.
44. Frilling A, Rogiers X, Malago M, Liedke O, Kaun M, Broelsch CE. Liver transplantation in patients with liver metastases of neuroendocrine tumors. *Transplant. Proc.* **1998**;30:3298-3300.
45. Lencioni RA, Allgaier HP, Cioni D, Olschewski M, *et al.* Small hepatocellular carcinoma in cirrhosis: randomized comparison of radio-frequency thermal ablation versus percutaneous ethanol injection. *Radiology* **2003**;228:235-240.
46. Tranberg KG. Percutaneous ablation of liver tumours. *Best. Pract. Res. Clin. Gastroenterol.* **2004**;18:125-145.
47. Shibata T, Niinobu T, Ogata N, Takami M. Microwave coagulation therapy for multiple hepatic metastases from colorectal carcinoma. *Cancer* **2000**;89:276-284.
48. Illing RO, Kennedy JE, Wu F, Ter Haar GR, *et al.* The safety and feasibility of extracorporeal high-intensity focused ultrasound (HIFU) for the treatment of liver and kidney tumours in a Western population. *Br. J. Cancer* **2005**;93:890-895.
49. Solbiati L, Livraghi T, Goldberg SN, Ierace T, *et al.* Percutaneous radio-frequency ablation of hepatic metastases from colorectal cancer: long-term results in 117 patients. *Radiology* **2001**;221:159-166.

50. Curley SA. Radiofrequency ablation of malignant liver tumors. *Ann. Surg. Oncol.* **2003**;10:338-347.
51. Gannon CJ, Curley SA. The role of focal liver ablation in the treatment of unresectable primary and secondary malignant liver tumors. *Semin. Radiat. Oncol.* **2005**;15:265-272.
52. Machtens S, Baumann R, Hagemann J, Warszawski A, *et al.* Long-term results of interstitial brachytherapy (LDR-Brachytherapy) in the treatment of patients with prostate cancer. *World J. Urol.* **2006**.
53. Nag S, DeHaan M, Scruggs G, Mayr N, Martin EW. Long-term follow-up of patients of intrahepatic malignancies treated with iodine-125 brachytherapy. *Int. J. Radiat. Oncol. Biol. Phys.* **2006**;64:736-744.
54. Ricke J, Wust P, Wieners G, Beck A, *et al.* Liver malignancies: CT-guided interstitial brachytherapy in patients with unfavorable lesions for thermal ablation. *J. Vasc. Interv. Radiol.* **2004**;15:1279-1286.
55. Ricke J, Wust P, Stohlmann A, Beck A, *et al.* CT-guided interstitial brachytherapy of liver malignancies alone or in combination with thermal ablation: phase I-II results of a novel technique. *Int. J. Radiat. Oncol. Biol. Phys.* **2004**;58:1496-1505.
56. Bierman HR, Byron RL, Jr., Kelley KH, Grady A. Studies on the blood supply of tumors in man. III. Vascular patterns of the liver by hepatic arteriography in vivo. *J. Natl. Cancer Inst.* **1951**;12:107-131.
57. Mori W, Masuda M, Miyanaga T. Hepatic artery ligation and tumor necrosis in the liver. *Surgery* **1966**;59:359-363.
58. Nilsson LA. Therapeutic hepatic artery ligation in patients with secondary liver tumors. *Rev. Surg.* **1966**;23:374-376.
59. Ohlsson B, Lindell G, Lundstedt C, Jeppsson B, *et al.* Dearterialization of colorectal liver cancer: institutional experience. *Dig. Surg.* **1999**;16:229-235.
60. DeMatteo RP. The GIST of targeted cancer therapy: a tumor (gastrointestinal stromal tumor), a mutated gene (c-kit), and a molecular inhibitor (STI571). *Ann. Surg. Oncol.* **2002**;9:831-839.
61. Clancy TE, Dixon E, Perlis R, Sutherland FR, Zinner MJ. Hepatic arterial infusion after curative resection of colorectal cancer metastases: a meta-analysis of prospective clinical trials. *J. Gastrointest. Surg.* **2005**;9:198-206.
62. Grover A, Alexander HR, Jr. The past decade of experience with isolated hepatic perfusion. *Oncologist.* **2004**;9:653-664.
63. Rothbarth J, Tollenaar RA, Schellens JH, Nortier JW, *et al.* Isolated hepatic perfusion for the treatment of colorectal metastases confined to the liver: recent trends and perspectives. *Eur. J. Cancer* **2004**;40:1812-1824.
64. Llovet JM, Real MI, Montana X, Planas R, *et al.* Arterial embolisation or chemoembolisation versus symptomatic treatment in patients with unresectable hepatocellular carcinoma: a randomised controlled trial. *Lancet* **2002**;359:1734-1739.
65. Lo CM, Ngan H, Tso WK, Liu CL, *et al.* Randomized controlled trial of transarterial lipiodol chemoembolization for unresectable hepatocellular carcinoma. *Hepatology* **2002**;35:1164-1171.

66. Llovet JM, Bruix J. Systematic review of randomized trials for unresectable hepatocellular carcinoma: Chemoembolization improves survival. *Hepatology* **2003**;37:429-442.
67. Ramsey DE, Kernagis LY, Soulen MC, Geschwind JF. Chemoembolization of hepatocellular carcinoma. *J. Vasc. Interv. Radiol.* **2002**;13:S211-S221.
68. Lau WY, Yu SC, Lai EC, Leung TW. Transarterial chemoembolization for hepatocellular carcinoma. *J. Am. Coll. Surg.* **2006**;202:155-168.
69. Poon RT, Ngan H, Lo CM, Liu CL, Fan ST, Wong J. Transarterial chemoembolization for inoperable hepatocellular carcinoma and postresection intrahepatic recurrence. *J. Surg. Oncol.* **2000**;73:109-114.
70. Mocellin S, Rossi CR, Lise M, Nitti D. Colorectal cancer vaccines: principles, results, and perspectives. *Gastroenterology* **2004**;127:1821-1837.
71. Schuchmann M, Galle PR. Sensitizing to apoptosis--sharpening the medical sword. *J. Hepatol.* **2004**;40:335-336.
72. Alam JJ. Apoptosis: target for novel drugs. *Trends Biotechnol.* **2003**;21:479-483.
73. Ghobrial IM, Witzig TE, Adjei AA. Targeting apoptosis pathways in cancer therapy. *Ca Cancer J. Clin.* **2005**;55:178-194.
74. Debatin KM. Apoptosis pathways in cancer and cancer therapy. *Cancer Immunol. Immunother.* **2004**;53:153-159.
75. Aghi M, Martuza RL. Oncolytic viral therapies - the clinical experience. *Oncogene* **2005**;24:7802-7816.
76. Palmer DH, Chen MJ, Kerr DJ. Gene therapy for colorectal cancer. *Br. Med. Bull.* **2002**;64:201-225.
77. Rak JW, St Croix BD, Kerbel RS. Consequences of angiogenesis for tumor progression, metastasis and cancer therapy. *Anticancer Drugs* **1995**;6:3-18.
78. Folkman J, Cole P, Zimmerman S. Tumor behavior in isolated perfused organs: in vitro growth and metastases of biopsy material in rabbit thyroid and canine intestinal segment. *Ann. Surg.* **1966**;164:491-502.
79. Folkman J, Merler E, Abernathy C, Williams G. Isolation of a tumor factor responsible for angiogenesis. *J. Exp. Med.* **1971**;133:275-288.
80. Ribatti D, Vacca A, Presta M. The discovery of angiogenic factors: a historical review. *Gen. Pharmacol.* **2000**;35:227-231.
81. Shing Y, Folkman J, Sullivan R, Butterfield C, Murray J, Klagsbrun M. Heparin affinity: purification of a tumor-derived capillary endothelial cell growth factor. *Science* **1984**;223:1296-1299.
82. Hurwitz H, Fehrenbacher L, Novotny W, Cartwright T, *et al.* Bevacizumab plus irinotecan, fluorouracil, and leucovorin for metastatic colorectal cancer. *N. Engl. J. Med.* **2004**;350:2335-2342.
83. Carmeliet P. Angiogenesis in life, disease and medicine. *Nature* **2005**;438:932-936.
84. Rogers AB, Fox JG. Inflammation and Cancer. I. Rodent models of infectious gastrointestinal and liver cancer. *Am. J. Physiol Gastrointest. Liver Physiol* **2004**;286:G361-G366.

85. Heijstek MW, Kranenburg O, Borel Rinkes I. Mouse models of colorectal cancer and liver metastases. *Dig. Surg.* **2005**;22:16-25.
86. Perryman LE. Molecular pathology of severe combined immunodeficiency in mice, horses, and dogs. *Vet. Pathol.* **2004**;41:95-100.
87. Fu X, Herrera H, Kubota T, Hoffman RM. Extensive liver metastasis from human colon cancer in nude and scid mice after orthotopic onplantation of histologically-intact human colon carcinoma tissue. *Anticancer Res.* **1992**;12:1395-1397.
88. Bosma GC, Custer RP, Bosma MJ. A severe combined immunodeficiency mutation in the mouse. *Nature* **1983**;301:527-530.
89. Zhu Y, Richardson JA, Parada LF, Graff JM. Smad3 mutant mice develop metastatic colorectal cancer. *Cell* **1998**;94:703-714.
90. Dunnington DJ, Buscarino C, Gennaro D, Greig R, Poste G. Characterization of an animal model of metastatic colon carcinoma. *Int. J. Cancer* **1987**;39:248-254.
91. Hougen HP. The athymic nude rat. Immunobiological characteristics with special reference to establishment of non-antigen-specific T-cell reactivity and induction of antigen-specific immunity. *APMIS Suppl* **1991**;21:1-39.
92. Davies G, Duke D, Grant AG, Kelly SA, Hermon-Taylor J. Growth of human digestive-tumour xenografts in athymic nude rats. *Br. J. Cancer* **1981**;43:53-58.
93. Marchal F, Tran N, Marchal S, Leroux A, *et al.* Development of an HT29 liver metastases model in nude rats. *Oncol. Rep.* **2005**;14:1203-1207.
94. Nijssen JFW, Rook D, Brandt CJWM, Meijer R, *et al.* Targeting of liver tumour in rats by selective delivery of holmium-166 loaded microspheres: a biodistribution study. *Eur. J. Nucl. Med.* **2001**;28:743-749.
95. Rous P, Kidd JG, Smith WE. Experiments on the cause of the rabbit carcinomas derived from virus-induced papillomas: II. Loss by the Vx2 Carcinoma of the power to immunize host against the papilloma virus. *J. Exp. Med.* **1952**;96:159-174.
96. Smith WE, Kidd JG, Rous P. Experiments on the cause of the rabbit carcinomas derived from virus-induced papillomas: I. Propagation of several of the cancers in sucklings, with etiological tests. *J. Exp. Med.* **1952**;95:299-318.
97. Rous P, Beard JW. The progression to carcinoma of virus-induced rabbit papillomas (shope). *J. Exp. Med.* **1935**;62:523-548.
98. Shope RF, Weston Hurst E. Infectious papillomatosis of rabbits: with a note on the histopathology. *J. Exp. Med.* **1933**;58:607-624.
99. Berens ME, Giese A, Shapiro JR, Coons SW. Allogeneic astrocytoma in immune competent dogs. *Neoplasia.* **1999**;1:107-112.
100. Salcman M, Scott EW, Schepp RS, Knipp HC, Broadwell RD. Transplantable canine glioma model for use in experimental neuro-oncology. *Neurosurgery* **1982**;11:372-381.
101. Boomkens SY, Spee B, IJzer J, Kijes R, *et al.* The establishment and characterization of the first canine hepatocellular carcinoma cell line, which resembles human oncogenic expression patterns. *Comp. Hepatol.* **2004**;3:9.
102. McGuire TC, Poppie MJ. Hypogammaglobulinemia and thymic hypoplasia in horses: a primary combined immunodeficiency disorder. *Infect. Immun.* **1973**;8:272-277.

103. Jezyk PF, Felsburg PJ, Haskins ME, Patterson DF. X-linked severe combined immunodeficiency in the dog. *Clin. Immunol. Immunopathol.* **1989**;52:173-189.
104. Pullen RP, Somberg RL, Felsburg PJ, Henthorn PS. X-linked severe combined immunodeficiency in a family of Cardigan Welsh corgis. *J. Am. Anim Hosp. Assoc.* **1997**;33:494-499.
105. Somberg RL, Pullen RP, Casal ML, Patterson DF, Felsburg PJ, Henthorn PS. A single nucleotide insertion in the canine interleukin-2 receptor gamma chain results in X-linked severe combined immunodeficiency disease. *Vet. Immunol. Immunopathol.* **1995**;47:203-213.
106. Meek K, Kienker L, Dallas C, Wang W, *et al.* SCID in Jack Russell terriers: a new animal model of DNA-PKcs deficiency. *J. Immunol.* **2001**;167:2142-2150.
107. Cantor HM, Dumont AE. Hepatic suppression of sensitization to antigen absorbed into the portal system. *Nature* **1967**;215:744-745.
108. Rai R, Flecknell P, Richardson C, Manas DM. Creation of porcine liver tumor using human hepatoma cell lines: experimental study. *Cancer Biol. Ther.* **2005**;4:635-637.
109. Graw JJ, Berg H. Hepatocarcinogenetic effect of DENA in pigs. *Z. Krebsforsch. Klin. Onkol. Cancer Res. Clin. Oncol.* **1977**;89:137-143.
110. Li X, Zhou X, Guan Y, Wang YX, Scutt D, Gong QY. N-Nitrosodiethylamine-Induced Pig Liver Hepatocellular Carcinoma Model: Radiological and Histopathological Studies. *Cardiovasc. Intervent. Radiol.* **2006**;29:420-428.
111. LaFave JW, Grotenhuis I, Kim YS, MacLeaN LD, Perry JF, Jr. Y90-tagged microspheres in adjuvant tumor therapy. *Surgery* **1963**;53:778-783.
112. Blanchard RJ, Grotenhuis I, LaFave JW, Frye CW, Perry JF, Jr. Treatment of Experimental Tumors; Utilization of Radioactive Microspheres. *Arch. Surg.* **1964**;89:406-410.
113. Blanchard RJ, Grotenhuis I, LaFave JW, Perry JF, Jr. Blood supply to hepatic V2 carcinoma implants as measured by radioactive microspheres. *Proc. Soc. Exp. Biol. Med.* **1965**;118:465-468.
114. Blanchard RJ, LaFave JW, Kim YS, Frye CS, Ritchie WP, Perry JF, Jr. Treatment of patients with advanced cancer utilizing Y⁹⁰ microspheres. *Cancer* **1965**;18:375-380.
115. Ariel IM. Treatment of Inoperable Primary Pancreatic and Liver Cancer by the Intra-Arterial Administration of Radioactive Isotopes (Y⁹⁰ Radiating Microspheres). *Ann Surg* **1965**;267-278.
116. Mantravadi RV, Spigos DG, Tan WS, Felix EL. Intraarterial yttrium 90 in the treatment of hepatic malignancy. *Radiology* **1982**;142:783-786.
117. Grady ED. Internal radiation therapy of hepatic cancer. *Dis. Col. & Rect.* **1979**;22:371-375.
118. Blanchard RJ, Morrow IM, Sutherland JB. Treatment of liver tumors with yttrium-90 microspheres alone. *Can. Assoc. Radiol. J.* **1989**;40:206-210.
119. Wollner I, Knutsen C, Smith P, Prieskorn D, *et al.* Effects of hepatic arterial yttrium 90 glass microspheres in dogs. *Cancer* **1988**;61:1336-1344.
120. Murthy R, Nunez R, Szklaruk J, Erwin W, *et al.* Yttrium-90 microsphere therapy for hepatic malignancy: devices, indications, technical considerations, and potential

- complications. *Radiographics* **2005**;25 Suppl 1:S41-S55.
121. Kennedy AS, Nutting C, Coldwell D, Gaiser J, Drachenberg C. Pathologic response and microdosimetry of ⁹⁰Y microspheres in man: review of four explanted whole livers. *Int. J. Radiat. Oncol. Biol. Phys.* **2004**;60:1552-1563.
 122. Andrews JC, Walker SC, Ackermann RJ, Cotton LA, Ensminger WD, Shapiro B. Hepatic radioembolization with yttrium-90 containing glass microspheres: preliminary results and clinical follow-up. *J. Nucl. Med.* **1994**;35:1637-1644.
 123. Nijssen JFW, Van het Schip AD, Hennink WE, Rook DW, Van Rijk PP, De Klerk JMH. Advances in nuclear oncology: Microspheres for internal radionuclide therapy of liver metastases. *Current Medicinal Chemistry* **2002**;9:73-82.
 124. Houle S, Yip TK, Shepherd FA, Rotstein LE, *et al.* Hepatocellular carcinoma: pilot trial of treatment with Y-90 microspheres. *Radiology* **1989**;172:857-860.
 125. Van Hazel G, Blackwell A, Anderson J, Price D, *et al.* Randomised phase 2 trial of SIR-Spheres plus fluorouracil/leucovorin chemotherapy versus fluorouracil/leucovorin chemotherapy alone in advanced colorectal cancer. *J. Surg. Oncol.* **2004**;88:78-85.
 126. Van Hazel GA, Price D, Bower G, Sharma RA, Blanshard K, Stewart WP. Selective internal radiation therapy (SIRT) for liver metastases with concomitant systemic oxaliplatin, 5-fluorouracil and folonic acid: A phase I/II dose escalation study. *J. Clin. Oncol., 2005 ASCO Annual Meeting Proceedings* **2005**;23:3657.
 127. Goldstein D, Van Hazel G, Pavlakis N, Olver I. Selective Internal Radiation Therapy (SIRT) plus systemic chemotherapy with Irinotecan. A phase I dose escalation study. *J. Clin. Oncol., 2005 ASCO Annual Meeting Proceedings* **2005**;23:3701.
 128. Kennedy AS, Coldwell D, Nutting C, Murthy R, *et al.* Resin ⁹⁰Y-microsphere brachytherapy for unresectable colorectal liver metastases: Modern USA experience. *Int. J. Radiat. Oncol. Biol. Phys.* **2006**;65:412-425.
 129. Dancy JE, Shepherd FA, Paul K, Sniderman KW, *et al.* Treatment of Nonresectable Hepatocellular Carcinoma with Intrahepatic ⁹⁰Y-microspheres. *J. Nucl. Med.* **2000**;41:1673-1681.
 130. Leung TW, Lau WY, Ho SK, Ward SC, *et al.* Radiation pneumonitis after selective internal radiation treatment with intraarterial ⁹⁰yttrium-microspheres for inoperable hepatic tumors. *Int. J. Radiat. Oncol. Biol. Phys.* **1995**;33:919-924.
 131. Carr BI. Hepatic Arterial ⁹⁰Yttrium Glass Microspheres (Therasphere) for Unresectable Hepatocellular Carcinoma: Interim Safety and Survival Data on 65 Patients. *Liver Transpl.* **2004**;10:S107-S110.
 132. Yip D, Allen R, Ashton C, Jain S. Radiation-induced ulceration of the stomach secondary to hepatic embolization with radioactive yttrium microspheres in the treatment of metastatic colon cancer. *J. Gastroenterol. Hepatol.* **2004**;19:347-349.
 133. Herba MJ, Thirlwell MP. Radioembolization for hepatic metastases. *Semin. Oncol.* **2002**;29:152-159.
 134. Stubbs RS, Cannan RJ, Mitchell AW. Selective internal radiation therapy (SIRT) with ⁹⁰Yttrium microspheres for extensive colorectal liver metastases. *Hepatogastroenterology* **2001**;48:333-337.

135. Goin J, Dancey JE, Roberts C. Comparison of post-embolization syndrome in the treatment of patients with unresectable hepatocellular carcinoma: Trans-catheter arterial chemo-embolization versus yttrium glass microspheres. *World J. Nucl. Med.* **2004**;3:49-56.
136. Sato K, Lewandowski RJ, Bui JT, Omary R, *et al.* Treatment of Unresectable Primary and Metastatic Liver Cancer with Yttrium-90 Microspheres (TheraSphere®): Assessment of Hepatic Arterial Embolization. *Cardiovasc. Intervent. Radiol.* **2006**;29:522-529.
137. Ngan H, Peh WC. Arteriovenous shunting in hepatocellular carcinoma: its prevalence and clinical significance. *Clin. Radiol.* **1997**;52:36-40.
138. Salem R, Lewandowski R, Roberts C, Goin J, *et al.* Use of Yttrium-90 glass microspheres (TheraSphere) for the treatment of unresectable hepatocellular carcinoma in patients with portal vein thrombosis. *J. Vasc. Interv. Radiol.* **2004**;15:335-345.
139. Sandström M, Lubberink M, Lundquist H. Quantitative SPECT with Yttrium-90 for Radionuclide Therapy Dosimetry. *Eur. J. Nucl. Med. Mol. Imaging* **2007**;32:S260.
140. Mumper RJ, Jay M. Biodegradable Radiotherapeutic Polyester Microspheres: Optimization and in-vitro / in-vivo Evaluation. *J. Contr. Rel.* **1992**;18:193-204.
141. Mumper RJ, Ryo UY, Jay M. Neutron-activated holmium-166-poly (L-lactic acid) microspheres: a potential agent for the internal radiation therapy of hepatic tumors. *J. Nucl. Med.* **1991**;32:2139-2143.
142. Nijssen JFW, Zonnenberg BA, Woittiez JR, Rook DW, *et al.* Holmium-166 poly lactic acid microspheres applicable for intra-arterial radionuclide therapy of hepatic malignancies: effects of preparation and neutron activation techniques. *Eur. J. Nucl. Med.* **1999**;26:699-704.
143. Dale RG. Dose-rate effects in targeted radiotherapy. *Phys. Med. Biol.* **1996**;41:1871-1884.
144. Nijssen JFW, Van het Schip AD, Van Steenberg MJ, Zielhuis SW, *et al.* Influence of neutron irradiation on holmium acetylacetonate loaded poly(L-lactic acid) microspheres. *Biomaterials* **2002**;23:1831-1839.
145. Zielhuis SW, Nijssen JFW, De Roos R, Krijger GC, *et al.* Production of GMP-grade radioactive holmium loaded poly(L-lactic acid) microspheres for clinical application. *Int. J. Pharm.* **2006**;311:69-74.
146. Murthy R, Xiong H, Nunez R, Cohen AC, *et al.* Yttrium 90 resin microspheres for the treatment of unresectable colorectal hepatic metastases after failure of multiple chemotherapy regimens: preliminary results. *J. Vasc. Interv. Radiol.* **2005**;16:937-945.
147. Pöpperl G, Helmberger T, Munzing W, Schmid R, Jacobs TF, Tatsch K. Selective internal radiation therapy with SIR-Spheres in patients with nonresectable liver tumors. *Cancer Biother. Radiopharm.* **2005**;20:200-208.
148. Nijssen JFW. Radioactive holmium poly(L-lactic acid) microspheres for treatment of liver malignancies. PhD thesis, Utrecht University, The Netherlands. **2001**;109-122.
149. De Wit TC, Xiao J, Nijssen JF, Van het Schip FD, *et al.* Hybrid scatter correction applied to quantitative holmium-166 SPECT. *Phys. Med. Biol.* **2006**;51:4773-4787.
150. Nijssen JFW, Seppenwoolde JH, Havenith T, Bos C, Bakker CJG, Van het Schip AD.

- Liver tumors: MR imaging of radioactive holmium microspheres–phantom and rabbit study. *Radiology* **2004**;231:491-499.
151. Seppenwoolde JH, Nijsen JFW, Bartels LW, Zielhuis SW, Van het Schip AD, Bakker CJ. Internal radiation therapy of liver tumors: Qualitative and quantitative magnetic resonance imaging of the biodistribution of holmium-loaded microspheres in animal models. *Magn Reson. Med.* **2004**;53:76-84.
 152. Seppenwoolde JH, Bartels LW, Van der Weide R, Nijsen JFW, Van het Schip AD, Bakker CJ. Fully MR-guided hepatic artery catheterization for selective drug delivery: a feasibility study in pigs. *J. Magn Reson. Imaging* **2006**;23:123-129.
 153. Idezuki Y, Sugiura M, Hatano S, Kimoto S. Hepatography for detection of small tumor masses in liver: experiences with oily contrast medium. *Surgery* **1966**;60:566-572.
 154. Alfidi RJ, Laval-Jeantet M. AG 60.99: A promising contrast agent for computed tomography of the liver and spleen. *Radiology* **1976**;121:491.
 155. Iwai K, Maeda H, Konno T. Use of oily contrast medium for selective drug targeting to tumor: enhanced therapeutic effect and X-ray image. *Cancer Res.* **1984**;44:2115-2121.
 156. Konno T, Maeda H, Iwai K, Tashiro S, *et al.* Effect of arterial administration of high-molecular-weight anticancer agent SMANCS with lipid lymphographic agent on hepatoma: a preliminary report. *Eur. J. Cancer Clin. Oncol.* **1983**;19:1053-1065.
 157. Nakakuma K, Tashiro S, Hiraoka T, Uemura K, *et al.* Studies on anticancer treatment with an oily anticancer drug injected into the ligated feeding hepatic artery for liver cancer. *Cancer* **1983**;52:2193-2200.
 158. Ohishi H, Uchida H, Yoshimura H, Ohue S, *et al.* Hepatocellular carcinoma detected by iodized oil. Use of anticancer agents. *Radiology* **1985**;154:25-29.
 159. Miller DL, O'Leary TJ, Girton M. Distribution of iodized oil within the liver after hepatic arterial injection. *Radiology* **1987**;162:849-852.
 160. Kobayashi H, Inoue H, Shimada J, Yano T, *et al.* Intra-arterial injection of adriamycin/mitomycin C lipiodol suspension in liver metastases. *Acta Radiol.* **1987**;28:275-280.
 161. Bhattacharya S, Dhillon AP, Winslet MC, Davidson BR, *et al.* Human liver cancer cells and endothelial cells incorporate iodised oil. *Br. J. Cancer* **1996**;73:877-881.
 162. Miller DL, Vermess M, Doppman JL, Simon RM, *et al.* CT of the liver and spleen with EOE-13: review of 225 examinations. *AJR Am. J. Roentgenol.* **1984**;143:235-243.
 163. Nakakuma K, Tashiro S, Hiraoka T, Ogata K, Ootsuka K. Hepatocellular carcinoma and metastatic cancer detected by iodized oil. *Radiology* **1985**;154:15-17.
 164. Bizollon T, Rode A, Bancel B, Gueripel V, *et al.* Diagnostic value and tolerance of Lipiodol-computed tomography for the detection of small hepatocellular carcinoma: correlation with pathologic examination of explanted livers. *J. Hepatol.* **1998**;28:491-496.
 165. Bruix J, Sherman M, Llovet JM, Beaugrand M, *et al.* Clinical management of hepatocellular carcinoma. Conclusions of the Barcelona-2000 EASL conference. European Association for the Study of the Liver. *J. Hepatol.* **2001**;35:421-430.

166. Burrel M, Llovet JM, Ayuso C, Iglesias C, *et al.* MRI angiography is superior to helical CT for detection of HCC prior to liver transplantation: an explant correlation. *Hepatology* **2003**;38:1034-1042.
167. Kobayashi H, Hidaka H, Kajiya Y, Tanoue P, *et al.* Treatment of hepatocellular carcinoma by transarterial injection of anticancer agents in iodized oil suspension or of radioactive iodized oil solution. *Acta Radiol. Diagn. (Stockh)* **1986**;27:139-147.
168. Raoul JL, Bourguet P, Bretagne JF, Duvauferrier R, *et al.* Hepatic artery injection of I-131-labeled lipiodol. Part I. Biodistribution study results in patients with hepatocellular carcinoma and liver metastases. *Radiology* **1988**;168:541-545.
169. Bretagne JF, Raoul JL, Bourguet P, Duvauferrier R, *et al.* Hepatic artery injection of I-131-labeled lipiodol. Part II. Preliminary results of therapeutic use in patients with hepatocellular carcinoma and liver metastases. *Radiology* **1988**;168:547-550.
170. Brans B, Linden O, Giammarile F, Tennvall J, Punt C. Clinical applications of newer radionuclide therapies. *Eur. J. Cancer* **2006**;42:994-1003.
171. Lambert B, Van de Wiele C. Treatment of hepatocellular carcinoma by means of radiopharmaceuticals. *Eur. J. Nucl. Med. Mol. Imaging* **2005**;32:980-989.
172. Raoul JL, Guyader D, Bretagne JF, Heautot JF, *et al.* Prospective randomized trial of chemoembolization versus intra-arterial injection of ¹³¹I-labeled-iodized oil in the treatment of hepatocellular carcinoma. *Hepatology* **1997**;26:1156-1161.
173. WHO Press. *WHO Pharmaceuticals Newsletter* **2005**;No. 2:2.
174. Brans B, De Winter F, Defreyne L, Troisi R, *et al.* The anti-tumoral activity of neoadjuvant intra-arterial ¹³¹I-lipiodol treatment for hepatocellular carcinoma: a pilot study. *Cancer Biother. Radiopharm.* **2001**;16:333-338.
175. Raoul JL, Messner M, Boucher E, Bretagne JF, Campion JP, Boudjema K. Preoperative treatment of hepatocellular carcinoma with intra-arterial injection of ¹³¹I-labelled lipiodol. *Br. J. Surg.* **2003**;90:1379-1383.
176. Lambert B, Praet M, Vanlangenhove P, Troisi R, *et al.* Radiolabeled lipiodol therapy for hepatocellular carcinoma in patients awaiting liver transplantation: pathology of the explant livers and clinical outcome. *Cancer Biother. Radiopharm.* **2005**;20:209-214.
177. Chenoufi N, Raoul JL, Lescoat G, Brissot P, Bourguet P. In vitro demonstration of synergy between radionuclide and chemotherapy. *J. Nucl. Med.* **1998**;39:900-903.
178. Raoul JL, Boucher E, Olivie D, Guillygomarch A, Boudjema K, Garin E. Association of cisplatin and intra-arterial injection of ¹³¹I-lipiodol in treatment of hepatocellular carcinoma: results of phase II trial. *Int. J. Radiat. Oncol. Biol. Phys.* **2006**;64:745-750.
179. Madsen MT, Park CH, Thakur ML. Dosimetry of iodine-131 ethiodol in the treatment of hepatoma. *J. Nucl. Med.* **1988**;29:1038-1044.
180. Wang SJ, Lin WY, Chen MN, Shen LH, Tsai ZT, Ting G. Preparation and biodistribution of yttrium-90 Lipiodol in rats following hepatic arterial injection. *Eur. J. Nucl. Med.* **1995**;22:233-236.
181. Wang SJ, Lin WY, Chen MN, Hsieh BT, *et al.* Biodistribution of rhenium-188 Lipiodol infused via the hepatic artery of rats with hepatic tumours. *Eur. J. Nucl. Med.* **1996**;23:13-17.

182. Sundram FX, Jeong JM, Zanzonico P, Bernal P, *et al.* Trans-arterial rhenium-188 lipiodol in the treatment of inoperable hepatocellular carcinoma. An IAEA sponsored multi-centre phase 1 study. *World J. Nucl. Med.* **2002**;1:5-11.
183. Sundram F, Chau TC, Onkhuudai P, Bernal P, Padhy AK. Preliminary results of transarterial rhenium-188 HDD lipiodol in the treatment of inoperable primary hepatocellular carcinoma. *Eur. J. Nucl. Med. Mol. Imaging* **2004**;31:250-257.
184. Lambert B, Bacher K, Defreyne L, Gemmel F, *et al.* ¹⁸⁸Re-HDD/lipiodol therapy for hepatocellular carcinoma: a phase I clinical trial. *J. Nucl. Med.* **2005**;46:60-66.
185. Lambert B, Bacher K, De Keukeleire K, Smeets P, *et al.* ¹⁸⁸Re-HDD/lipiodol for treatment of hepatocellular carcinoma: a feasibility study in patients with advanced cirrhosis. *J. Nucl. Med.* **2005**;46:1326-1332.
186. Lambert B, Bacher K, Defreyne L, Van Vlierberghe H, *et al.* ¹⁸⁸Re-HDD/lipiodol therapy for hepatocellular carcinoma: an activity escalation study. *Eur. J. Nucl. Med. Mol. Imaging* **2006**;33:344-352.
187. Monsieurs MA, Bacher K, Brans B, Vral A, *et al.* Patient dosimetry for ¹³¹I-lipiodol therapy. *Eur. J. Nucl. Med. Mol. Imaging* **2003**;30:554-561.
188. Therasse P, Arbuuck SG, Eisenhauer EA, Wanders J, *et al.* New guidelines to evaluate the response to treatment in solid tumors. European Organization for Research and Treatment of Cancer, National Cancer Institute of the United States, National Cancer Institute of Canada. *J. Natl. Cancer Inst.* **2000**;92:205-216.
189. Bohm B, Voth M, Geoghegan J, Hellfritsch H, *et al.* Impact of positron emission tomography on strategy in liver resection for primary and secondary liver tumors. *J. Cancer Res. Clin. Oncol.* **2004**;130:266-272.

CHAPTER 3

Neutron activation of holmium poly(L-lactic acid) microspheres for hepatic arterial radioembolization: a validation study

Maarten A.D. Vente

Johannes F.W. Nijsen

Remmert de Roos

Mies J. van Steenbergen

Camiel Kaaijk

Maria J.J. Koster-Ammerlaan

Piet F.A. de Leege

Wim E. Hennink

Alfred D. van het Schip

Gerard C. Krijger

Biomedical Microdevices (accepted for publication)

ABSTRACT

Poly(L-lactic acid) microspheres loaded with holmium-166 acetylacetonate ($^{166}\text{Ho-PLLA-MS}$) are a novel microdevice for intra-arterial radioembolization in patients with unresectable liver malignancies. The neutron activation in a nuclear reactor, in particular the gamma heating, damages the $^{166}\text{Ho-PLLA-MS}$. The degree of damage is dependent on the irradiation characteristics and irradiation time in a particular reactor facility. The aim of this study was to standardize and objectively validate the activation procedure in a particular reactor. The methods included light- and scanning electron microscopy (SEM), particle size analysis, differential scanning calorimetry, viscometry, thermal neutron flux measurements, and energy deposition calculations. Seven-hours neutron irradiation results in sufficient specific activity of the $^{166}\text{Ho-PLLA-MS}$ while structural integrity is preserved. Neutron flux measurements and energy deposition calculations are required in the screening of other nuclear reactors. For the evaluation of microsphere quality, light microscopy, SEM, and particle size analysis are appropriate techniques.

1 INTRODUCTION

The global incidence of hepatocellular carcinoma (HCC), the most common type of primary liver cancer, is high (>600,000 new cases per year) and still increasing [1,2]. The only potentially curative treatment option in HCC is surgical resection. Unfortunately, most patients are presented with unresectable disease, and due to the lack of effective treatment alternatives, HCC is the 3rd cause of cancer related death [2]. The liver is also a very common organ for other cancers to spread to. This is especially the case for primary cancers of the gastrointestinal tract. Metastasis confined to the liver very often occurs in colorectal cancer, of which the global incidence is very high as well (ca. 1,000,000 new cases per year), particularly in the Western World. Colorectal cancer ranks as the 3rd most commonly diagnosed cancer type. The primary potentially curative treatment for colorectal liver metastases is surgical resection as well, yet only a minority of patients is eligible. The overall prognosis of colorectal cancer is rather good but, due to the high incidence and the reality that metastases in the liver are often unresectable, colorectal cancer is the 4th cause of cancer related death [2]. Therefore, the need exists for novel treatment options for patients with unresectable liver malignancies.

One emerging treatment option for patients with unresectable liver tumors is intra-arterial microbrachytherapy *via* radioactive microspheres, loaded with the high-energy beta-emitting radioisotope yttrium-90 (^{90}Y ; $E_{\beta\text{max}} = 2.28$ MeV, $I_{\beta} = 100\%$; $T_{1/2} = 64.1$ h), instilled into the hepatic artery [3,4]. The ^{90}Y microspheres are deposited into the liver tumors in much higher concentrations than into the non-tumorous liver as a consequence of the difference in blood supply between the normal liver and liver tumors. The normal liver is supplied by both the hepatic artery and (mainly) the portal vein, whereas liver tumors derive their blood uniquely from the hepatic artery [5].

Apart from these ^{90}Y microspheres, holmium-166 loaded poly(L-lactic acid) microspheres (^{166}Ho -PLLA-MS) are being developed for clinical application [6,7]. Whereas ^{90}Y is a pure beta emitter, ^{166}Ho is a combined beta-gamma emitter (^{166}Ho : $E_{\beta\text{max}} = 1.77$ and 1.85 MeV, $I_{\beta} = 48.7\%$ and 50.0%, respectively; $E_{\gamma} = 81$ keV, $I_{\gamma} = 6.7\%$; $T_{1/2} = 26.8$ h) and highly paramagnetic as well. It therefore offers medical imaging possibilities, through both single photon emission computed tomography (SPECT) and magnetic resonance imaging (MRI). Quantitative analysis of the

SPECT images and the MRI images has been demonstrated feasible [8-10]. ^{165}Ho -PLLA-MS are prepared through a straight-forward solvent evaporation method under Good Manufacturing Practice (GMP) conditions and are subsequently neutron activated in a nuclear reactor [6]. Extensive animal studies have been conducted which demonstrated that the toxicity profile of this microdevice is acceptable [11,12]. Also, the pharmaceutical quality has been investigated and found satisfactory [13,14].

Another issue to be addressed was assessment of the effects of the neutron irradiation on the microspheres' integrity. Especially the extent of the accompanying decomposition damage caused by gamma photons and fast neutrons, and possibly by the thermal neutron capture side reactions, needs to be investigated [15,16]. Gamma irradiation is accompanied by both heating resulting from absorption of gamma-photon energy and by the formation of free radicals [17]. The degree of damage that is inflicted upon the organic PLLA matrix is consequently dependent on the irradiation characteristics and the applied irradiation time in a particular reactor facility. It is paramount to know exactly how long a typical patient dosage of ^{165}Ho -PLLA-MS (600 mg) can be irradiated while remaining sufficiently intact for treatment of patients. In order to have sufficient time for transportation of the ^{166}Ho -PLLA-MS from the reactor to the hospital, the microspheres must be neutron irradiated for a certain period of time. The minimum irradiation time is therefore dependent on logistics and the required amount of radioactivity (5.0-15 GBq ^{166}Ho) to be instilled, consequently the thermal neutron flux. Conversely, the maximum irradiation time is set by the extent of irradiation damage that occurs. The aim of this research was to standardize and objectively validate the activation procedure in a particular reactor facility. Therefore, the maximum irradiation time of the ^{165}Ho -PLLA-MS in a particular reactor was determined, and techniques that are applicable for routine quality control testing were defined. Methods used include photon and neutron energy deposition calculations, measurement of the thermal neutron flux, light microscopy, scanning electron microscopy, particle size analysis, molecular weight assessment using viscometry, and thermal analysis through differential scanning calorimetry.

2 MATERIALS AND METHODS

2.1 Aim and study design

To assess the maximum irradiation time, samples of microspheres of 600 mg (typical patient dosage), consisting of ^{165}Ho -PLLA-MS or PLLA-MS, were neutron-irradiated for 0, 2, 4, 6, 7, 8, or 10 h;

To assess whether differences in microsphere characteristics are observed, when neutron irradiation is carried out in different time slots of the reactor cycle, 600 mg samples, consisting of ^{165}Ho -PLLA-MS, were neutron-irradiated for 6 or 7 h, at the first section, half-way, and at the last section of the reactor cycle. The variation in microsphere quality within a week was investigated as well in 6-h irradiated ^{166}Ho -PLLA-MS (600 mg);

To assess whether self-shielding is a significant factor in the neutron activation, the generated amount of radioactivity was measured in samples of 50, 100, 200, 400, 800, and 1000 mg of ^{166}Ho -PLLA-MS after neutron irradiation for 60 min.

2.2 Preparation of ^{165}Ho -PLLA-MS and of PLLA-MS

The preparation of GMP-grade ^{165}Ho -PLLA-MS has been described in detail in a previous paper [6]. In brief, holmium acetylacetonate (HoAcAc) and PLLA were dissolved in chloroform. This solution was subsequently emulsified in an aqueous solution of polyvinyl alcohol and, with the evaporation of the solvent, microspheres were formed. The microspheres were collected and fractionated according to size using stainless steel sieves. Except for deletion of the HoAcAc , the PLLA-MS were produced in the same manner. The microspheres were collected and packed in high-density polyethylene (HDPE) vials (type A; Posthumus Plastics, Beverwijk, The Netherlands).

2.3 Neutron irradiation procedure and neutron flux measurements

Neutron flux monitors were placed on both ends of the vials packing the ^{165}Ho -PLLA-MS or PLLA-MS. These neutron flux monitors were prepared from a certified chromium standard solution (NIST 3112a) and consisted of chromium (0.52 ± 0.03 mg) inside smaller HDPE vials (type V) [18]. The vials were then wrapped in thin poly-ethylene foil and placed in a HDPE 'rabbit'-irradiation container (type XY) (Fig. 1a). The samples were irradiated in a pneumatic rabbit

system facility of the nuclear reactor of the Delft University of Technology (Delft, The Netherlands) with a nominal thermal neutron flux of $5 \times 10^{16} \text{ m}^{-2} \text{ s}^{-1}$. The ^{166}Ho -PLLA-MS samples were allowed to decay for between four and eight weeks before analysis of the samples.

The amount of radioactivity (^{51}Cr) in the flux monitors was measured through gamma-ray spectrometry, using a germanium detector and a 92X-II spectrum analyzer which was linked to a PC equipped with GammaVision[®]-32 software, version 5.0 (EG & G ORTEC, Oak Ridge, TN, USA). Subsequently, the actual thermal neutron flux to which the flux monitors had been exposed was calculated using the following formula:

$$\varphi = \frac{\lambda \cdot A_{320} \cdot m_{Cr}}{N \cdot \sigma_{eff} \cdot m \cdot \varepsilon \cdot \theta \cdot \gamma \cdot (1 - e^{-\lambda \cdot t_{IRR}}) \cdot e^{-\lambda \cdot t_{WT}} \cdot (1 - e^{-\lambda \cdot t_{CT}}} \quad [m^{-2} \cdot s^{-1}]$$

where

- φ is the thermal neutron flux ($\text{m}^{-2} \text{ s}^{-1}$)
- λ is the decay constant ($\ln 2/T_{1/2}$) of ^{51}Cr : $2.896 \cdot 10^{-7} \text{ s}^{-1}$
- A_{320} is the 320 keV gamma peak area
- m_{Cr} is the average atomic mass of chromium : $51.9961 \text{ g mol}^{-1}$
- N is the number of nuclei/mol (equal to Avogadro's number) : $6.022 \cdot 10^{23}$
- σ_{eff} is the effective activation cross section of ^{50}Cr : $1.53 \cdot 10^{-27} \text{ m}^2$
- m is the weight of chromium in the vial (g)
- ε is the counting efficiency at 320 keV (cps/dps)
- θ is the isotopic abundance of ^{50}Cr (ratio $^{50}\text{Cr}/(^{50}\text{Cr} + ^{52}\text{Cr})$) : $4.35 \cdot 10^{-2}$
- γ is the abundance of the 320 keV gamma photon : $9.83 \cdot 10^{-2}$
- t_{IRR} is the neutron irradiation time (s)
- t_{WT} is the waiting time between neutron activation and spectrometry measurement (s)
- t_{CT} is the spectrometry measurement time (s)

Since the samples were located in the bottom half of the vials, the effective neutron flux to which a sample is exposed can be calculated, using linear interpolation, as follows:

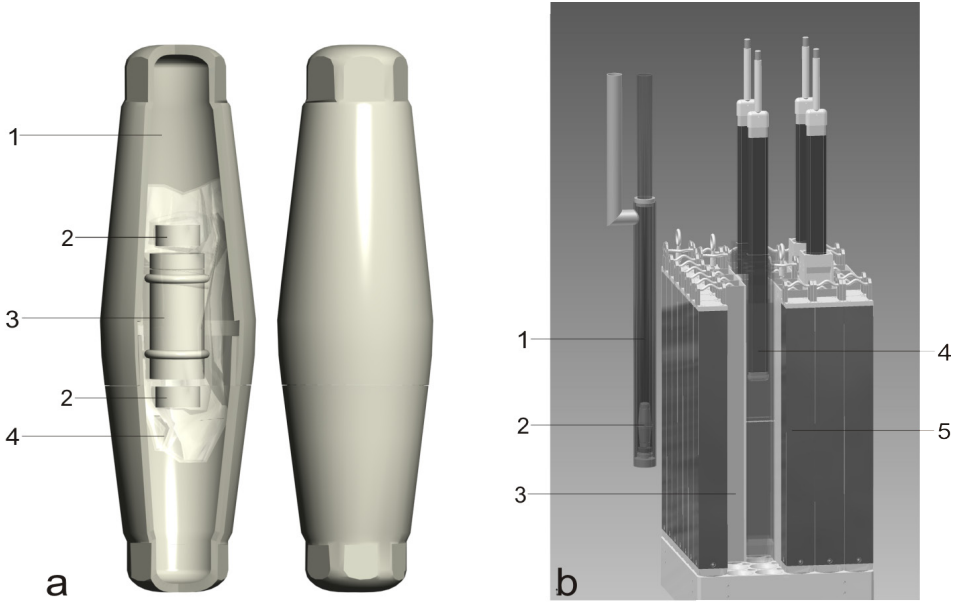


Figure 1 (a) Schematic representation of the HDPE 'rabbit' type irradiation container (1) containing the neutron flux monitors (2) on *top* and *bottom* of the vial that contains a sample of ^{165}Ho -PLLA-MS or PLLA-MS (3). The flux monitors and the vial containing the sample are wrapped in poly-ethylene foil (4); (b) Schematic representation of the pneumatic rabbit system (1) with the 'rabbit' at the distal end of the system (2), next to the reactor core of the Delft reactor, which is composed of fuel rods ($\text{U}_3\text{Si}_2\text{-Al}$) (3), borium-carbide control rods, 73.3% removed (4), and beryllium reflector elements (5).

$$\varphi_{\text{eff}} = \left(\frac{1}{3} \cdot \varphi_{\text{monitor } 1}\right) + \left(\frac{2}{3} \cdot \varphi_{\text{monitor } 2}\right) \quad [\text{m}^{-2} \cdot \text{s}^{-1}]$$

where

φ_{eff} is the effective neutron flux

$\varphi_{\text{monitor } 1}$ is the neutron flux measured by the monitor placed on top of the vial

$\varphi_{\text{monitor } 2}$ is the neutron flux measured by the monitor placed on the bottom of the vial

2.4 Energy deposition calculations

Energy spectra and energy depositions of neutrons and photons in the

irradiation facility were calculated using the stochastic transport Monte Carlo method-based code MCNP5 [19]. The code can be used in several transport modes: neutron only, photon only, or combined neutron/photon transport where the photons are produced by neutron interactions. In the calculations described here, the combined neutron/photon mode was used. The neutron energy regime was from 10^{-11} MeV to 20 MeV for all isotopes, and the photon energy regime was from 1 keV to 100 GeV.

The model describes the fuel assemblies in the Delft reactor by individual fuel plates and uses 15 axial regions along the height of the fuel. Each movable beryllium reflector element was modeled separately. All the existing beam tubes and irradiation facilities near the core were represented in the model. The material composition of the fuel was given per fuel assembly and per axial region. The burn-up dependent fuel composition was determined separately. The material composition was determined for 3 cases with full xenon equilibrium:

1. Begin of cycle, after 12 megawatt-days (MWD) at full power, with the control rods at 73.30% removed (Fig. 1b);
2. Half-way of cycle, after 68 MWD of full power, with the control rods at 81.30% removed;
3. End of cycle, after 130 MWD at full power, with the control rods at 97.03% removed.

The depletion of beryllium and the photo-neutron production in beryllium were neglected. For the calculations, the ENDF/B-VI data library was used as distributed with the MCNP5 package. The model has been validated on a recent Delft reactor configuration (2008) by comparing the reactivity and the measured axial distribution of $^{59}\text{Co}(n,\gamma)^{60}\text{Co}$ reaction rates. The average value of this Co activation measurement was used for power normalization, the ratio of the total power to fission power was assumed to be constant during the whole cycle. The aluminum tube of the pneumatic rabbit system and the HDPE rabbit vial were included in the calculations.

2.5 Particle size distribution, light microscopy and scanning electron microscopy (SEM)

The particle size distributions (volume percentage) of the non-irradiated samples (the control samples: ^{165}Ho -PLLA-MS and PLLA-MS) and the irradiated samples (^{166}Ho -PLLA-MS and PLLA-MS) were determined using a Coulter

Counter Multisizer 3 apparatus (Beckman Coulter Nederland, Mijdrecht, The Netherlands), equipped with a 100- μm aperture tube. The preset quality criteria were set at minimally 95 vol.-% between 15-60 μm , and 92 vol.-% between 20-50 μm . Microsphere morphology, *i.e.*, the extent of damage, was evaluated using light microscopy. The surface morphology was investigated by SEM using a Phenom[®] electron microscope (FEI Electron Optics, Eindhoven, The Netherlands). Samples were mounted on aluminum stubs and sputter-coated with a Pt layer of 6 nm.

2.6 Modulated differential scanning calorimetry (MDSC)

Thermal analysis was performed using a DSC Q1000 (TA Instruments Inc., New Castle, DE, USA). Samples of 6 mg of ¹⁶⁵Ho-PLLA-MS, ¹⁶⁶Ho-PLLA-MS, and non-irradiated and irradiated PLLA-MS were transferred into aluminum pans which were then hermetically sealed. The samples were heated from 20°C to 220°C at a rate of 2°C min⁻¹. The measurements were analyzed using Universal Analysis 2000 software (version 3.9A; TA Instruments Inc., New Castle, DE, USA).

2.7 Viscometry

The molecular weight was determined in the Ho-PLLA-MS samples (0, 2, 4, 6, 8, 10 h irradiated), PLLA-MS samples (0, 2, 4, 6, 7, 8, 10 h irradiated), and non-irradiated PLLA standards (obtained from PURAC biochem B.V., Gorinchem, The Netherlands) using dilute-solution viscometry. The samples were dissolved in chloroform, and the measurements were conducted at 25°C, using a Ubbelohde capillary viscometer, as described in the literature [20].

2.8 Sterility of the ¹⁶⁶Ho-PLLA-MS

To test the sterility of the microspheres, samples of 450 mg of ¹⁶⁵Ho-PLLA-MS, spiked with *Bacillus pumilis* spores as a biological indicator, were neutron irradiated for 6 h. Then, the samples were tested for bacterial contamination by a certified company (Bactimm B.V., Nijmegen, The Netherlands).

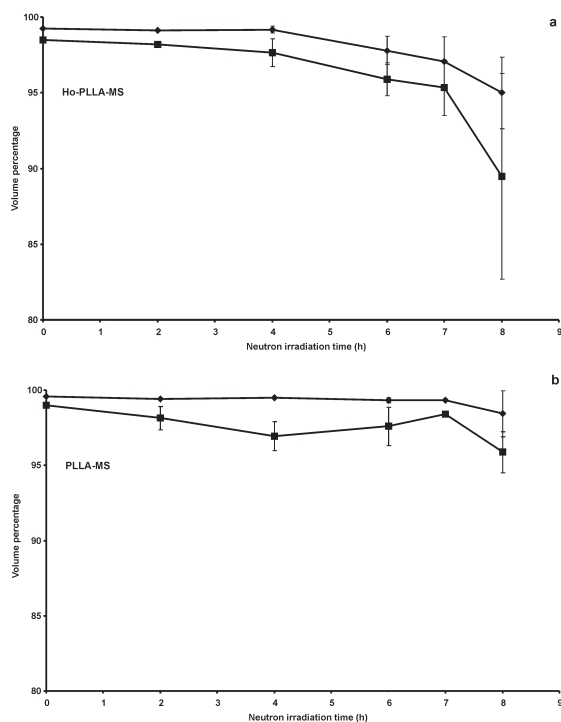


Figure 2 (a) Mean particle size (\pm SD) of the Ho-PLLA-MS, neutron-irradiated for 0, 2, 4, 6, 7, or 8 h; (b) Mean particle size (\pm SD) of the PLLA-MS, neutron-irradiated for 0, 2, 4, 6, 7, or 8 h (*diamond* 15-60 μ m; *square* 20-50 μ m)

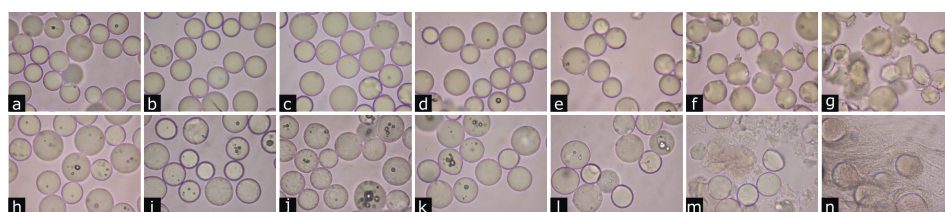


Figure 3 (a-g) Light micrographs of Ho-PLLA-MS, neutron-irradiated for 0, 2, 4, 6, 7, 8, or 10 h. In samples irradiated up to 7 h, damage is absent or minor (a-e). The damage observed in the 8-h irradiated microspheres and, in particular, in the 10-h irradiated microspheres is characterized by crumbles and breaking (f-g); (h-n) light micrographs of PLLA-MS, neutron-irradiated for 0, 2, 4, 6, 7, 8, or 10 h. In samples irradiated up to 7 h, damage is again absent or minor (h-l). The 8-hours irradiated microspheres reveal signs of melting, whereas in the 10-h irradiated samples most microspheres have melted and only sporadically some remnants of microspheres can be seen (m-n)

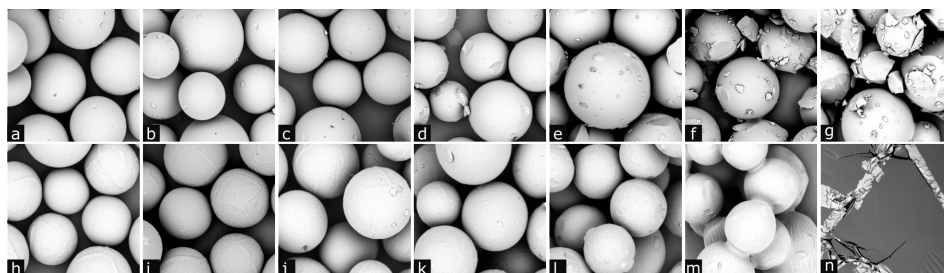


Figure 4 (a-g) Scanning electron micrographs of Ho-PLLA-MS, neutron-irradiated for 0, 2, 4, 6, 7, 8, or 10 h. In samples irradiated up to 7 h, damage is absent or minor (a-e). On the dented surface of the 8-h irradiated microspheres small microsphere fragments are seen (f). Disintegration has progressed in the 10-h irradiated microspheres with many microspheres actually having been broken into several large chunks, and many smaller fragments visible as well (g); (h-n) scanning electron micrographs of PLLA-MS, neutron-irradiated for 0, 2, 4, 6, 7, 8, or 10 h. In samples irradiated up to 6 h, damage is absent (h-k). In the 7-h irradiated samples, a tendency to interfusion is observed (l). Microsphere fusion is more frequently seen in the 8-h irradiated samples (m). In the 10-h irradiated samples, microspheres had completely melted, and no identifiable remnants of microspheres were found (n)

3 RESULTS AND DISCUSSION

3.1 Particle size distribution, light microscopy, and scanning electron microscopy (SEM)

Particle size analysis was performed on all samples (Fig. 2). For detailed information on microsphere morphology, light microscopy and SEM were employed (Figs. 3 and 4).

The particle size analyses of the ^{166}Ho -PLLA-MS showed that the required size distribution was guaranteed up to neutron irradiation for 7 h (Fig. 2a). Both light microscopic and SEM analysis showed that differences in morphology were hardly detectable between samples irradiated for 0, 2, and 4 h, with microspheres of these samples all exhibiting a smooth, intact surface (Figs. 3a-c and 4a-c). Although the surface of 6- and 7-h irradiated ^{166}Ho -PLLA-MS displayed some damage, the morphology of the microspheres was quite similar to that of the non-irradiated samples (Figs. 3d-e and 4d-e). Microsphere quality clearly decreased when exposed for an 8-hour irradiation period as small dents on the surface and a lot of fragments were visible (Figs. 3f and 4f). In addition, the particle size distribution was insufficient (Fig. 2a). Light microscopy and SEM of

the 10-h irradiated ^{166}Ho -PLLA-MS revealed extensively damaged microspheres, only barely spherical in shape (Figs. 3g and 4g). Particle size analysis of these samples proved impossible due to blockage of the apparatus' probe aperture as a consequence of the formation of particle agglomerates.

To assess the possible effects on microsphere quality after neutron irradiation in different slots of the reactor cycle, ^{165}Ho -PLLA-MS were irradiated for 6 or 7 h in the first, in the middle, and in the last section of the reactor cycle. These samples all met the preset particle size criteria (Fig. 5). The nuclear reactor explored in this study is a research reactor which is started up each Monday and shut off each Friday. Samples of ^{165}Ho -PLLA-MS were irradiated on Tuesdays, Wednesdays and Thursdays. No differences in quality were observed; they all met the required specifications.

For the PLLA-MS, particle size distribution was slightly better than for the ^{166}Ho -PLLA-MS (Fig. 2); the desired size distribution was maintained after 8 h of neutron irradiation. The PLLA-MS samples that were irradiated 0, 2, 4, and 6 h all remained completely spherical with an intact surface as observed by light microscopy and SEM (Figs. 3h-k and 4h-k). However, careful examination of the light micrographs and (especially) SEM images of the 7-h irradiated samples gave indications that the surfaces had partially liquefied (Fig. 4l). This 'melting' was more prominently visible on SEM images of the 8-h irradiated PLLA-MS samples which occasionally showed that microspheres had started to fuse (Fig. 4m). Ten-hour irradiation yielded PLLA-MS which had been destroyed (Figs. 3n and 4n). Particle size measurements of the latter samples were impossible since they had basically been turned into a solitary piece of an adhesive substance. In contrast to the light micrograph where a few sphere-like structures were still detectable, no spherical shape was found using SEM, which may be due to sample preparation for SEM.

3.2 Energy deposition and neutron flux

Irradiation-induced damage as a consequence of energy deposition can be a problem in the production of ^{166}Ho -PLLA-MS. Therefore, energy deposition was calculated for both neutrons and photons. The calculated total energy deposition showed a small decrease during the reactor cycle (Table 1). More than 93% of the total energy deposition came from the photons. This is in accordance with

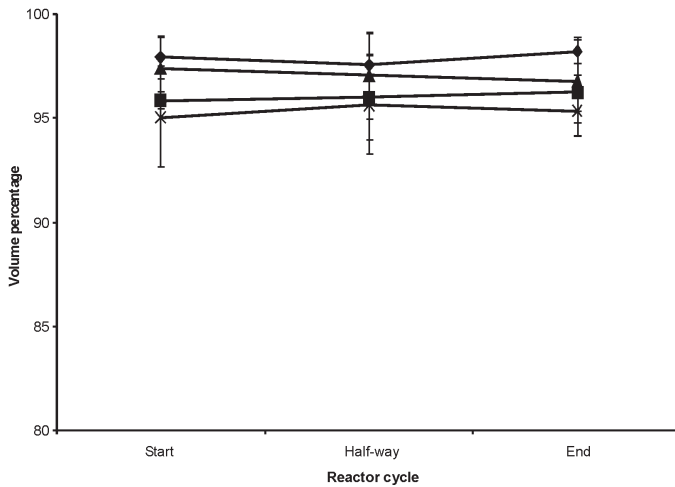


Figure 5 Mean particle size (\pm SD) of duplo samples of ^{166}Ho -PLLA-MS neutron-irradiated for 6 or 7 h at the first section, half-way, and at the last section of the reactor cycle. Particle size was invariably within the required specifications during the different time slots of the reactor cycle (*diamond* 15-60 μm , 6 h; *square* 20-50 μm , 6 h; *triangle* 15-60 μm , 7 h; *multiplication symbol* 20-50 μm , 7 h)

previous experimental findings, which indicated that damage to the ^{166}Ho -PLLA-MS is due mainly to gamma radiation [14].

Like the 'gamma heating' the thermal neutron flux measurements showed a slight decrease during the reactor cycle (Fig. 6). The thermal neutron flux measured using the Cr monitors on top of the vials was 6.8% higher than the flux measured by the monitors on the vial bottoms (5.21 ± 0.24 and $4.88 \pm 0.28 \times 10^{16} \text{ m}^{-2} \text{ s}^{-1}$ (mean \pm SD), respectively). The effective thermal neutron flux was $4.99 \pm 0.23 \times 10^{16} \text{ m}^{-2} \text{ s}^{-1}$ (mean \pm SD). Without any correction for the variation of flux during the reactor cycle, the above would implicate that for a requested patient dosage of 7.5 GBq ^{166}Ho the actually produced amount of radioactivity may vary between 6.8 and 8.2 GBq in 95% of cases. The consequence would be that a liver absorbed dose intended to be 80 Gy would vary between 73 and 87 Gy. This variation is accepted common practice in nuclear medicine.

To identify whether facilities in other nuclear reactors could be used for routine production of ^{166}Ho -PLLA-MS, the energy deposition by neutrons and, particularly, photons can be calculated and related to the thermal neutron flux.

3.3 Linearity of the activated fraction

In order to determine whether self-shielding occurs, *i.e.*, to assess the relation between the amount of microspheres irradiated and the amount of radioactivity produced, ascending amounts of ^{165}Ho -PLLA-MS (50-1,000 mg) were irradiated for 60 min. The specific activity (MBq/mg) was found to be linearly related to the amount of microspheres (Fig. 7). Coefficient of variance was only 2.6% (4.53 ± 0.12 MBq/mg). Neutron irradiation time does therefore not need to be adjusted for different amounts of ^{165}Ho -PLLA-MS.

3.4 Modulated differential scanning calorimetry

Both PLLA-MS and Ho-PLLA-MS, neutron irradiated for 0, 2, 4, 6, 7, 8, or 10 h, were analyzed by MDSC (Table 2). Irradiation of PLLA-MS resulted in a decrease

Table 1 Energy depositions delivered on microspheres during neutron irradiation

Reactor cycle time slot	Energy deposition (10^{13} MeV/g h)
	Neutrons
Begin	7.63 \pm 0.48
Mid	7.34 \pm 0.45
End	7.73 \pm 0.52
	Photons
Begin	112.0 \pm 4.7
Mid	111.4 \pm 6.8
End	106.2 \pm 5.0
	Neutrons + photons
Begin	119.7 \pm 5.2
Mid	118.7 \pm 7.0
End	113.9 \pm 5.5

Values are presented as mean \pm SD

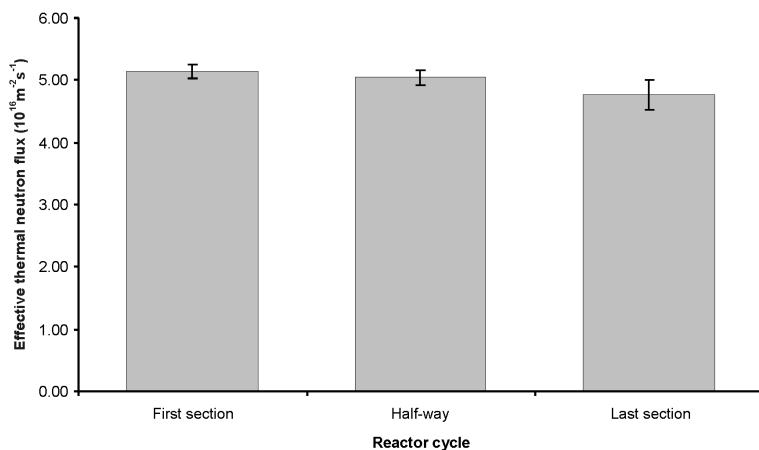


Figure 6 Effective thermal neutron flux measurements at the *first section*, *middle-section*, and at the *last section* of the reactor cycle (mean \pm SD, $n=12$ /section). A slight decline in flux is observed

in melting temperature (T_m) and decreased enthalpy of fusion (ΔH_m) with increasing irradiation time, indicating impairment of the crystalline phase of the PLLA matrix inflicted by the neutron irradiation. The T_m of non-irradiated PLLA-MS was $179\pm 0^\circ\text{C}$ and decreased to $113\pm 5^\circ\text{C}$ for 6-h irradiated samples. The ΔH_m for fully crystalline monodisperse lactic acid oligomers amounted to 93 J/g [21]. The ΔH_m for non-irradiated PLLA-MS was 57 ± 6 J/g and decreased to 14 ± 12 J/g after 6 h irradiation signifying that crystallinity decreased by roughly 75%. After 7 h of neutron irradiation and longer, no melting peak in the DSC thermogram was observed, indicating a complete loss of crystallinity. The glass transition temperature (T_g) decreased from 68°C to around 50°C after irradiation, and was non-detectable after irradiation for 7 h and longer, which is consistent with previously reported findings [14]. These findings indicate that after irradiation of 7 h structural changes of the polymer matrix occurred. This is consistent with light microscopy and SEM analysis, which revealed the onset of surface changes at 7 h irradiation (Fig. 4l). ^{165}Ho -PLLA-MS showed a lower T_m and ΔH_m compared to non-irradiated PLLA-MS ($148\pm 5^\circ\text{C}$ and 9 ± 4 J/g vs. $179\pm 0^\circ\text{C}$ and 57 ± 6 J/g). This is in accordance with previously reported findings and was ascribed to interaction of the carbonyl groups of PLLA with the holmium ion of the HoAcAc complex [16]. After neutron irradiation of 2 h and longer, no melting

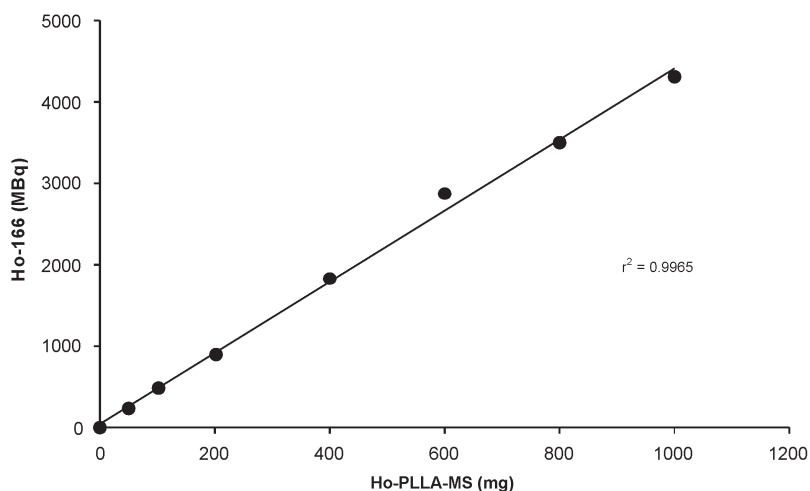


Figure 7 Generated amounts of radioactivity (end-of-bombardment) plotted against ascending amounts of ^{166}Ho -PLLA-MS following neutron activation for 60 min. A linear relation is observed demonstrating that no self-shielding occurs in higher amounts of microspheres

transitions were observed in the ^{166}Ho -PLLA-MS thermographs, indicating absence of crystallinity. Glass transition was present in the thermographs of the non-irradiated and all irradiated Ho-PLLA-MS samples, whereas in the PLLA-MS samples glass transition was absent after irradiation for 7 h and longer.

3.5 Viscometry

The molecular weight of PLLA-MS, neutron-irradiated for 0, 2, 4, 6, 7, 8, or 10 h, and Ho-PLLA-MS, irradiated for 0, 2, 4, or 6 h, was determined using dilute-solution viscometry (Table 3). ^{166}Ho -PLLA-MS irradiated for 7, 8, or 10 h were not included in this analysis, because these samples only partially dissolved in chloroform. A major difference in molecular weight was observed between the non-irradiated PLLA-MS and ^{165}Ho -PLLA-MS. The measured molecular weight of the PLLA in the ^{165}Ho -PLLA-MS was less than 40% that of the PLLA in the PLLA-MS. This apparent lower molecular weight of the PLLA is most likely due to the above mentioned interaction between PLLA and HoAcAc, and is in agreement with previously published results on gel permeation chromatography analysis of PLLA-MS and Ho-PLLA-MS samples [16]. After 2 h of irradiation, the molecular

Table 2 Transition temperatures of Ho-PLLA-MS and PLLA-MS ($n=4-8$)

Irradiation time (h)	Sample description	T_g (°C)	T_c (°C)	ΔH_c (J/g)	T_m (°C)	ΔH_m (J/g)
0	PLLA-MS	68±3	152±1	5±0	179±0	57±6
2	PLLA-MS	50±2	80±1	28±1	150±1	40±2
4	PLLA-MS	43±8	nd	nd	131±1	25±5
6	PLLA-MS	54±1	nd	nd	113±5	14±12
7	PLLA-MS	nd	nd	nd	nd	nd
8	PLLA-MS	nd	nd	nd	nd	nd
10	PLLA-MS	nd	nd	nd	nd	nd
0	Ho-PLLA-MS	65±2	123±14	9±6	148±5	9±4
2	Ho-PLLA-MS	52±3	nd	nd	nd	nd
4	Ho-PLLA-MS	55±3	nd	nd	nd	nd
6	Ho-PLLA-MS	54±5	nd	nd	nd	nd
7	Ho-PLLA-MS	55±3	nd	nd	nd	nd
8	Ho-PLLA-MS	58±5	nd	nd	nd	nd
10	Ho-PLLA-MS	58±2	nd	nd	nd	nd

nd not detectable, T_g glass transition temperature, T_c recrystallization temperature, ΔH_c enthalpy of the recrystallization, T_m melting temperature, ΔH_m enthalpy of fusion

weight in the samples of both categories had already decreased strongly (approximately 70%), as a consequence of radiation-induced chain scissions. After 6 h of irradiation and longer, the molecular weight had decreased by over 90%. In spite of this dramatic loss of PLLA chain length, the structural integrity was guaranteed up to 7 h (see Section 3.1). It was found in previous studies that providing that the microspheres had remained intact, a decrease in molecular weight is not associated with a clinically relevant release of radioactivity (<1%) [13,16,22].

3.6 Sterility of the ^{166}Ho -PLLA-MS

After neutron irradiation, samples spiked with spores of *B. pumilis* were tested for viable bacteria. Colony forming units were detected only in the spiked,

Table 3 Relative molecular weight of Ho-PLLA-MS and PLLA-MS after increasing neutron irradiation times

Irradiation time (h)	Sample description	Molecular weight (%)	Sample description	Molecular weight (%)
0	PLLA-MS	100	Ho-PLLA-MS	100
2		23		33
4		12		19
6		7		10
7		5		na
8		5		na
10		5		na

na not assessed

non-irradiated sample. The finding that no viable bacteria were present in the irradiated samples spiked with spores of *B. pumilis* was expected since the *D*-value (90% kill value) of *B. pumilis* spores is <2 kGy [23] and the gamma dose delivered on the sample was over 30 times higher than the dose used in routine gamma-radiation sterilization (840 kGy h⁻¹ and 25 kGy (minimum absorbed dose [24]), respectively). Since the samples had been irradiated for 6 h, the delivered gamma dose was in excess of 5,000 kGy.

3.7 Nuclear reactor testing strategy

The strategy consisted of several techniques and calculations to determine whether the Delft nuclear reactor is suitable for neutron activation of ¹⁶⁵Ho-PLLA-MS. Obviously, for reasons of logistics, upscaling and flexibility, it is important to explore whether other reactors in the world are available, and suitable, for this purpose.

In order to screen a reactor (facility) for its suitability for neutron activating ¹⁶⁵Ho-PLLA-MS, it is recommended to start with measurements of the thermal neutron flux and calculations of the total energy deposition. The thermal neutron flux (n/cm² h)/total energy deposition (MeV/g h) ratio can then be calculated. For the Delft reactor this ratio is 15. Thus, a ratio of 15 or higher implies that ¹⁶⁶Ho-PLLA-MS of acceptable quality can expectedly be produced. If the ratio is adequate, irradiations of a few 600-mg samples of ¹⁶⁵Ho-PLLA-MS are to be carried out to assess the maximum activation time. The quality

of the ^{166}Ho -PLLA-MS ought to be evaluated by light microscopy and particle size analysis. If the microspheres are of sufficient quality, SEM should be carried out. Subsequently, the reactor conditions and variations in time, *viz.* stability of the neutron flux, are to be investigated in more detail. PLLA-MS respond differently to neutron irradiation compared to ^{165}Ho -PLLA-MS, as was discussed in Section 3.1. However, the maximally tolerable irradiation time of the two types of microspheres was of the same order. It is therefore suggested that initial screening of a reactor (facility) is carried out with PLLA-MS since these particles do not become radioactive which permits carefree handling and analysis to be carried out immediately after neutron irradiation. Apart from reactor screening and validation, some of the methods discussed in this paper are also applicable for quality control, which is extremely important with regard to this highly radioactive microdevice. For instance, it is proposed that after irradiation a small sample is evaluated by light microscopy and/or particle size analysis.

4 CONCLUSIONS

It is concluded that ^{165}Ho -PLLA-MS can endure neutron activation in the Delft nuclear reactor up to 7 h and still maintain their structural integrity. After neutron activation for 7 h, the generated activity in a typical patient dosage of 600 mg of ^{166}Ho -PLLA-MS is high enough to allow for sufficient time for transportation to the hospital and also high enough to deliver liver absorbed doses in the tumoricidal range. Furthermore, in this particular reactor, the two most important reactor condition parameters, neutron flux and gamma heating, are relatively constant in time, allowing for the routine production of ^{166}Ho -PLLA-MS of a consistent quality.

Structural integrity was preserved after at least 7 h neutron irradiation even though the poly(L-lactic acid) matrix of this microdevice is in fact relatively sensitive to neutron irradiation, specifically the accompanying gamma heating. DSC measurements showed that the crystalline structure was lost completely between 0 and 2 h of irradiation. Viscometry analysis also showed that chain length decreases rapidly during neutron irradiation, yet microscopically the microspheres' surface remained virtually intact and particle size distribution was acceptable after irradiation of 7 h.

The activated fraction was independent of the amount of ^{165}Ho -PLLA-MS

that was neutron activated, meaning no self-shielding had occurred, at least up to the maximum patient dosage of 1,000 mg. As expected, both spiked and unspiked samples of ^{166}Ho -PLLA-MS were sterile after neutron irradiation.

Neutron flux measurements and energy deposition calculations are required in the screening of other nuclear reactors. For the evaluation of microsphere quality, not only in reactor screening but also in routine quality control, light microscopy, SEM, and particle size analysis are appropriate techniques.

Acknowledgements

Financial support by the Dutch Technology Foundation STW under grant 06069 is gratefully acknowledged.

REFERENCES

1. Gomaa AI, Khan SA, Toledano MB, Waked I, Taylor-Robinson SD. Hepatocellular carcinoma: epidemiology, risk factors and pathogenesis. *World J. Gastroenterol.* **2008**;14:4300-4308.
2. Parkin DM, Bray F, Ferlay J, Pisani P. Global cancer statistics, 2002. *Ca Cancer J. Clin.* **2005**;55:74-108.
3. Gulec SA, Fong Y. Yttrium 90 microsphere selective internal radiation treatment of hepatic colorectal metastases. *Arch. Surg.* **2007**;142:675-682.
4. Vente MAD, Hobbelink MGG, Van het Schip AD, Zonnenberg BA, Nijsen JFW. Radionuclide liver cancer therapies: from concept to current clinical status. *Anticancer Agents Med. Chem.* **2007**;7:441-459.
5. Bierman HR, Byron RL, Jr., Kelley KH, Grady A. Studies on the blood supply of tumors in man. III. Vascular patterns of the liver by hepatic arteriography in vivo. *J. Natl. Cancer Inst.* **1951**;12:107-131.
6. Zielhuis SW, Nijsen JFW, De Roos R, Krijger GC, *et al.* Production of GMP-grade radioactive holmium loaded poly(L-lactic acid) microspheres for clinical application. *Int. J. Pharm.* **2006**;311:69-74.
7. Nijsen JFW, Van Steenbergen MJ, Kooijman H, Talsma H, *et al.* Characterization of poly(L-lactic acid) microspheres loaded with holmium acetylacetonate. *Biomaterials* **2001**;22:3073-3081.
8. De Wit TC, Xiao J, Nijsen JF, Van het Schip FD, *et al.* Hybrid scatter correction applied to quantitative holmium-166 SPECT. *Phys. Med. Biol.* **2006**;51:4773-4787.
9. Nijsen JFW, Seppenwoolde JH, Havenith T, Bos C, *et al.* Liver tumors: MR imaging of radioactive holmium microspheres—phantom and rabbit study. *Radiology* **2004**;231:491-499.
10. Seppenwoolde JH, Nijsen JFW, Bartels LW, Zielhuis SW, *et al.* Internal radiation therapy of liver tumors: Qualitative and quantitative magnetic resonance imaging of the biodistribution of holmium-loaded microspheres in animal models. *Magn Reson. Med.* **2004**;53:76-84.
11. Vente MAD, Nijsen JFW, De Wit TC, Seppenwoolde JH, *et al.* Clinical effects of transcatheter hepatic arterial embolization with holmium-166 poly(L-lactic acid) microspheres in healthy pigs. *Eur. J. Nucl. Med. Mol. Imaging* **2008**;35:1259-1271.
12. Zielhuis SW, Nijsen JFW, Seppenwoolde JH, Bakker CJG, *et al.* Long-term toxicity of holmium-loaded poly(L-lactic acid) microspheres in rats. *Biomaterials* **2007**;28:4591-4599.
13. Zielhuis SW, Nijsen JFW, Krijger GC, Van het Schip AD, Hennink WE. Holmium-loaded poly(L-lactic acid) microspheres: In vitro degradation study. *Biomacromolecules* **2006**;7:2217-2223.
14. Zielhuis SW, Nijsen JFW, Dorland L, Krijger GC, *et al.* Removal of chloroform from biodegradable therapeutic microspheres by radiolysis. *Int. J. Pharm.* **2006**;315:67-74.
15. Yamaguchi H, Waker AJ. A model for the induction of DNA damages by fast neutrons and their evolution into cell clonogenic inactivation. *J. Radiat. Res. (Tokyo)* **2007**;48:289-303.

16. Nijsen JFW, Van het Schip AD, Van Steenberghe MJ, Zielhuis SW, *et al.* Influence of neutron irradiation on holmium acetylacetonate loaded poly(L-lactic acid) microspheres. *Biomaterials* **2002**;23:1831-1839.
17. Mader K, Domb A, Swartz HM. Gamma-sterilization-induced radicals in biodegradable drug delivery systems. *Appl. Radiat. Isot.* **1996**;47:1669-1674.
18. Koster-Ammerlaan MJ, Bacchi MA, Bode P, De Nadai Fernandes EA. A new monitor for routine thermal and epithermal neutron fluence rate monitoring in k0 INAA. *Appl. Radiat. Isot.* **2008**;66:1964-1969.
19. X-5 Monte Carlo Team. MCNP- a general monte carlo n-particle transport code, version 5. LA-UR-03-1987, LA-CP-03-0245, LA-CP-03-0284. *Los Alamos National Laboratory* **2003**.
20. Omelczuk MO, McGinity JW. The influence of polymer glass transition temperature and molecular weight on drug release from tablets containing poly(DL-lactic acid). *Pharm. Res.* **1992**;9:26-32.
21. De Jong S, Van Dijk-Wolthuis WNE, Kettenes-Van den Bosch JJ, Schuyl PJW, Hennink WE. Monodisperse enantiometric lactic acid oligomers: Preparation, characterization, and stereocomplex formation. *Macromolecules* **1998**;31:6397-6402.
22. Van Es RJ, Nijsen JFW, Van het Schip AD, Dullens HFJ, *et al.* Intra-arterial embolization of head-and-neck cancer with radioactive holmium-166 poly(L-lactic acid) microspheres: an experimental study in rabbits. *Int. J. Oral Maxillofac. Surg.* **2001**;30:407-413.
23. Prince HN. D-values of *Bacillus pumilus* spores on irradiated devices (inoculated product). *Appl. Environ. Microbiol.* **1978**;36:392-393.
24. European Directorate for the Quality of Medicines & HealthCare. *European Pharmacopoeia*. **2008**;6th edn., Suppl. 6.3:Par. 5.1.1.

CHAPTER 4

Clinical effects of transcatheter hepatic arterial embolization with holmium-166 poly(L-lactic acid) microspheres in healthy pigs

Maarten A.D. Vente

Johannes F.W. Nijssen

Tim C. de Wit

Jan H. Seppenwoolde

Gerard C. Krijger

Peter R. Seevinck

Albert Huisman

Bernard A. Zonnenberg

Ted S.G.A.M. van den Ingh

Alfred D. van het Schip

European Journal of Nuclear Medicine and Molecular Imaging 2008;35:1259-71.

ABSTRACT

Aim: To evaluate the toxicity of holmium-166 poly(L-lactic acid) microspheres administered into the hepatic artery in pigs.

Methods: Healthy pigs (20-30 kg) were injected into the hepatic artery with holmium-165 loaded microspheres ($^{165}\text{Ho-PLLA-MS}$; $n=5$) or with holmium-166 loaded microspheres ($^{166}\text{Ho-PLLA-MS}$; $n=13$). The microspheres' biodistribution was assessed by gamma scintigraphy and/or magnetic resonance imaging (MRI). The animals were monitored clinically, biochemically, and ($^{166}\text{Ho-PLLA-MS}$ group only) hematologically over a period of one month ($^{165}\text{Ho-PLLA-MS}$ group), or over one or two months ($^{166}\text{Ho-PLLA-MS}$ group). Finally, a pathological examination was undertaken.

Results: Following microsphere administration, some animals exhibited a slightly diminished level of consciousness and a dip in appetite, both of which were transient. Four lethal adverse events occurred in the $^{166}\text{Ho-PLLA-MS}$ group, due either to incorrect administration or comorbidity: inadvertent delivery of microspheres into the gastric wall ($n=2$), preexisting gastric ulceration ($n=1$), and endocarditis ($n=1$). Aspartate aminotransferase levels were transiently elevated post- $^{166}\text{Ho-PLLA-MS}$ administration. In the other blood parameters no abnormalities were observed. Nuclear images were acquired from all animals from the $^{166}\text{Ho-PLLA-MS}$ group, and MRI was performed, if available. In pigs from the $^{166}\text{Ho-PLLA-MS}$ group, atrophy of one or more liver lobes was frequently observed. The actual radioactivity distribution was assessed through *ex vivo* $^{166\text{m}}\text{Ho}$ measurements.

Conclusion: It can be concluded that the toxicity profile of Ho-PLLA-MS is low. In pigs, hepatic arterial embolization with $^{166}\text{Ho-PLLA-MS}$ in amounts corresponding with liver absorbed doses of over 100 Gy, if correctly administered, is not associated with clinically relevant side effects. This result offers a good perspective for upcoming patient trials.

INTRODUCTION

Internal radiation therapy with yttrium-90 (^{90}Y) loaded microspheres, injected into the hepatic artery, has demonstrated to be an effective treatment option in the management of patients with unresectable intrahepatic malignancies [1-5]. Two ^{90}Y microsphere products are currently commercially available and in clinical use: TheraSphere[®] (MDS Nordion Inc., Kanata, Ontario, Canada) and SIR-Spheres[®] (SIRTeX Medical Ltd., Sydney, New South Wales, Australia). These two devices differ considerably in physical characteristics, particularly with regard to density and specific activity (Table 1); TheraSphere[®] microspheres are glass microspheres, consequently not biodegradable and, more importantly, of a high density compared to plasma [6]. This may increase the risk of proximal intravascular settling [7]. SIR-Spheres[®] are resin-based microspheres of near-plasma density [8]. A disadvantage of SIR-Spheres[®] is the relatively low specific activity [9], which necessitates the administration of relatively high amounts of these microspheres. This has been reported to frequently lead to retrograde flow and/or failure to deliver the intended dose [10,11].

For tumor dosimetry calculations, quantitative imaging is essential, which would also allow assessment of the radiation dose delivered to the non-tumorous liver tissue. As ^{90}Y is a pure beta emitter, the only way to (quantitatively) assess the biodistribution of the SIR-Spheres[®] and TheraSphere[®] microspheres would be by means of Bremsstrahlung scintigraphy of which the image quality has unfortunately been demonstrated to be insufficient for this purpose [12]. At the nuclear medicine department of the University Medical Center Utrecht (Utrecht, The Netherlands), holmium-166 poly(L-lactic acid) microspheres (^{166}Ho -PLLA-MS) have been developed which have several advantageous properties when compared with the available ^{90}Y microspheres. The most important advantage of the use of holmium is in medical imaging and therefore also in dosimetry. Since ^{166}Ho is a combined beta-gamma emitter (Table 1), these microspheres allow for quantitative nuclear imaging [13]; this allows that, instead of using technetium-99m labeled albumin macroaggregates to predict the biodistribution of the microspheres [14], a small scout dose of ^{166}Ho -PLLA-MS can be applied. Secondly, following administration of the therapeutic dose, its distribution can be accurately assessed. In addition, as holmium is a highly paramagnetic element it is suitable for (quantitative) magnetic resonance imaging (MRI) [15,16],

especially useful for medium- and long-term monitoring of the intrahepatic behavior of the holmium microspheres. This property also allows for real-time visualization of the deposition of microspheres during a (fully) MRI-guided selective administration [17]. Other advantageous features of holmium are its higher dose-rate, and its higher neutron-absorption cross section (Table 1), as a consequence of which considerably shorter reactor time is needed.

The pharmaceutical quality of the ^{166}Ho -PLLA-MS has been extensively investigated and proven to be satisfactory [18-20]. Furthermore, it must have been demonstrated, with aid of adequate animal studies, that the device is expected to be efficacious. Therefore, a non-survival biodistribution study in rats was performed in which it was demonstrated that the microsphere deposition was restricted to the tumor-bearing liver lobe, and that in the tumorous tissue the radioactivity concentration was six times higher than in the non-target liver tissue [21]. In order to definitely demonstrate that ^{166}Ho -PLLA-MS injected into the hepatic artery have a tumoricidal effect, an efficacy study in Vx2-carcinoma-bearing rabbits was performed [22]. In all animals treated with ^{166}Ho -PLLA-MS, tumour growth was arrested and necrosis had set in. Finally, before initiation of a phase I clinical trial, it must be ascertained that the toxicity profile of the device will be acceptable. An extensive toxicity study in (non-tumor-bearing) pigs has therefore been conducted. The porcine model was chosen mainly for its body size, since a catheterization procedure is involved in the treatment, for which the smaller laboratory animal species are unsuitable [23]. The aim of this study was to investigate the acute and medium-term toxicity of the ^{166}Ho -PLLA-MS, and to ascertain potential complications associated with the catheterization-administration procedure.

METHODS AND MATERIALS

Study design

The study was divided into two substudies: the aim of the first substudy, which consisted of five pig experiments, was to evaluate the clinical effects of transcatheter hepatic arterial administration of escalating amounts of (non-radioactive) ^{165}Ho -PLLA-MS (7.5-37.5 mg/kg in steps of 7.5 mg/kg); the second substudy consisted of 13 pigs which were administered ^{166}Ho -PLLA-MS (200-300 mg) with the aim of assessing the clinical effects of increasing amounts of

Table 1 Microsphere characteristics

Microsphere	TheraSphere®	SIR-Spheres®	Holmium microspheres
Radionuclide	yttrium-90		holmium-166
Radionuclide properties			
$T_{1/2}$ (h)	64.1		26.8
Max. β^- -energy (MeV)	2.28 (100%)		1.77 (48.7%), 1.85 (50.0%)
γ -energy (keV)	no γ -emission		80.6 (6.7%)
Neutron cross-section (barn)	^{89}Y : 1.3		^{165}Ho : 64
Matrix material	glass	resin	poly(L-lactic acid)
Density (g/ml)	3.3	1.6	1.4
Diameter (μm)	25 \pm 10	32 \pm 10	30 \pm 5
Activity/microsphere (Bq)	1,250*-2,500	50*	450*
Number of microspheres per dose	4,000,000	50,000,000	33,000,000

* Calculated values

radioactivity, starting at 3.15 MBq ^{166}Ho /g liver tissue. Escalation of administered activity was implemented in increments of 3.15 MBq/g up to 9.45 MBq ^{166}Ho /g liver tissue, corresponding with a liver absorbed dose of 50, 100, and 150 Gy, respectively. Each group was intended to consist of 2 to 4 animals, depending on the encountered side effects. Animals in the ^{165}Ho -PLLA-MS group were sacrificed one month after microsphere administration, and the animals in the ^{166}Ho -PLLA-MS group randomized to termination one or two months post-administration.

Animals

Eighteen healthy female pigs, 3-4 months old, weighing 20-30 kg, and specified pathogen-free, were obtained from the Animal Sciences Group, Wageningen University and Research Center, Lelystad, The Netherlands. A 2-week acclimatization period was allowed. The animals were kept under conventional conditions with *ad libitum* access to tap water, and given standard pelleted feed twice a day. The experiments were conducted in agreement with the local

applicable Dutch law, “Wet op de dierproeven” (art. 9) (1977), and the European Convention for the Protection of Vertebrate Animals used for Experimental and Other Scientific Purposes (1986), and approved by the ethical committee for animal experimentation of the University Medical Center Utrecht, Utrecht, The Netherlands (DEC-GNK no. 03.03.032).

Microsphere preparation

Good manufacturing practice (GMP) grade ^{165}Ho -PLLA-MS were prepared as previously described [19,24]. In the case of the radioactive substudy, the microspheres were packed in high-density polyethylene vials (Posthumus Plastics, Beverwijk, The Netherlands) and neutron activated via the $^{165}\text{Ho}(n,\gamma)^{166}\text{Ho}$ reaction in the nuclear reactor of the Delft University of Technology (Delft, The Netherlands) with a thermal neutron flux of $5 \times 10^{12} \text{ cm}^{-2} \text{ s}^{-1}$ for a predetermined length of time (1.5-7.5 h). After arrival at the hospital, the microspheres were suspended in 1 ml of a Pluronic[®] solution [25], and transferred into a glass V-bottom vial. The amount of radioactivity was then measured in a dose calibrator (VDC-404, Veenstra Instrumenten B.V., Joure, The Netherlands).

Anesthesia and analgesia

Premedication for general anesthesia consisted of azaperon (4 mg/kg), ketamine hydrochloride (10 mg/kg), and atropine (0.1 mg/10 kg) IM. Induction of general anesthesia consisted of thiopental (5-10 mg/kg or propofol (2.5-3.5 mg/kg) IV. General anesthesia was maintained by continuous intravenous infusion of 8-9 mg/kg/h propofol or by inhalation of isoflurane (1.5-2.0%) in O_2 /air (1:1), in combination with midazolam hydrochloride (0.2 mg/kg) IV. Peri-operative analgesia was provided by sufentanil (loading dose: 5 $\mu\text{g}/\text{kg}$, maintenance dose: 10 $\mu\text{g}/\text{kg}/\text{h}$) IV. Peri-operative antibiotic prophylaxis consisted of a pre-operative dose of amoxicillin with clavulanic acid (10 mg/kg) IV.

Postoperative medication consisted of buprenorphine (0.015 mg/kg) and carprofen (4 mg/kg) IV, and ampicillin (7.5 mg/kg) IM. The animals were terminated by an overdose of sodium pentobarbitone (100-200 mg/kg) IV, after ketamine sedation.

Chronic intravascular catheter

For convenient withdrawal of blood samples and administration of medication, a 7F silicone catheter (Instech Solomon, Plymouth Meeting, PA, USA) was inserted into the external jugular vein and immobilized, and then subcutaneously tunneled to exit dorsally between the scapulas. The postoperative protocol consisted of daily flushing with saline and injection of a heparin saline solution into the catheter, and topical antibacterial prophylaxis (procaine benzylpenicillin 200,000 IE/ml + dihydrostreptomycin 200 mg/ml) on the exit site for two weeks.

Catheterization and microsphere administration

An Avanti®+ catheter sheath introducer (5F, Cordis Europe N.V., Roden, The Netherlands) was inserted into the right femoral artery. The catheters deployed in the experiments were Performa® Modified Hook Flush, Softouch® Osborn 2 and Softouch® Straight Flush, in combination with double-ended (J-tip and straight tip) and straight fixed core (super stiff) guide wires (Merit Medical Europe, Maastricht-Airport, The Netherlands). The tip of the catheter was positioned in *A. hepatica propria*, i.e., in the hepatic artery, distally to where the gastroduodenal artery branches off. The microspheres were flushed out of the vial and into the catheter by injecting 15-20 ml of saline solution into the vial at a rate of 0.5-1.0 ml s⁻¹.

Imaging protocols

Microsphere distribution was assessed by single photon emission computed tomography (SPECT), planar nuclear imaging, and (if available) MRI, three days post-administration. Immobilization was obtained by propofol, after premedication with ketamine. SPECT and MRI were acquired according to previously described protocols [13,15].

Dosimetry

The liver absorbed doses were calculated as follows. For ¹⁶⁶Ho, the calculated absorbed energy is 15.87 mJ MBq⁻¹ (based on S values, as calculated by Dr. M.W. Konijnenberg (Mallinckrodt Medical B.V., Covidien, Petten, The Netherlands), through the use of the Monte-Carlo MCNPX code (Los Alamos National Laboratory, Los Alamos, NM, USA)). Assuming that all energy is absorbed in the

liver, the cumulative dose (mGy MBq^{-1}) may be calculated to be $15.87 \text{ mJ MBq}^{-1} / \text{liver weight (kg)}$. The weight of the porcine liver equates to 1.97% of the body weight [26]. Thus, for example, in a pig of 25 kg with a liver of approximately 490 g in which $4,500 \text{ MBq } ^{166}\text{Ho}$ is administered, the organ absorbed dose is: $15.87 \cdot 10^{-3} \text{ J MBq}^{-1} \times 4,500 \text{ MBq} / 0.490 \text{ kg} = 146 \text{ Gy}$.

Clinical follow-up

The animals were monitored for clinical side effects on a daily basis. Clinical parameters monitored included demeanor, consciousness level/alertness, posture and gait, food intake, and growth (the animals were weighed twice a week).

Blood samples were taken before microsphere administration (baseline values), 10 min after delivery of the microspheres, and twice a week until termination. Hemoglobin (Hb), leukocyte count, and platelet count were determined within 4 hours of sampling, using a Cell-Dyn[®] 4000 hematology analyser (Abbott Laboratories, Santa Clara, CA, USA). Prothrombin time (PT) was determined within 4 hours of sampling, using a STA[®] coagulation analyzer (Diagnostica Stago, Asnières, France). Plasma samples for chemical analyses were stored after centrifugation and kept frozen at -20°C until analysis. Gamma-glutamyltransferase (GGT), alkaline phosphatase (ALP), alanine aminotransferase (ALT), aspartate aminotransferase (AST) and bilirubin were analyzed, using a Vitros[®] 950 chemistry system (Ortho Clinical Diagnostics, Rochester, NY, USA).

Postmortem examination

After termination, a gross pathological examination was performed, during which the liver and gallbladder, spleen, lungs, and stomach were collected and processed for histological examination. Tissue sections ($4\text{-}\mu\text{m}$ thick) were routinely prepared and stained with hematoxylin and eosin, and evaluated by light microscopy.

Ex vivo radioactivity distribution assessment

The liver and gallbladder, spleen, lungs, and stomach of the animals, which had been administered with $^{166}\text{Ho-PLLA-MS}$, were processed into a homogeneous

suspension, using a kitchen blender and chemical destruction (sodium hydroxide 8.25 mmol/l). For every organ suspension the content of holmium-166 metastable (^{166m}Ho , $T_{1/2} \approx 1,200$ years) was measured directly using a low-background gamma-counter (Tobor, Nuclear Chicago, Chicago, IL, USA). During neutron activation, both ^{166}Ho and ^{166m}Ho are formed ($^{166}\text{Ho}/^{166m}\text{Ho} \approx 1,000,000:1$). Since the ^{166m}Ho interorgan distribution is linear to the ^{166}Ho distribution, the interorgan radioactivity distribution of the ^{166}Ho -PLLA-MS could then be calculated accurately.

RESULTS

Clinical follow-up

In the non-radioactive experiments, the amount of ^{165}Ho -PLLA-MS was escalated up to 700 mg, which on a bodyweight basis corresponds to three times the amount that will be administered to patients. Whether the entire dosage was selectively deposited in the liver, and whether or not a significant part of the injected microspheres had ended up in organs other than the liver could not be quantitatively assessed. In the radioactive experiments, between 1.4 and 6.5 GBq ^{166}Ho was administered, which (when corrected for extrahepatic deposition) equates to attained whole-liver nominal absorbed doses of between 59 and 162 Gy; Table 2 gives an overview of the amounts of microspheres actually administered, and, where appropriate, the real amounts of radioactivity that were delivered and, accordingly, the estimated liver absorbed doses.

Following the catheterization-administration procedure, inappetence and a slightly diminished state of consciousness, both of which were transient, was observed in some animals in both substudies. Typically, in a couple of days, consciousness level and appetite returned to pretreatment levels. However, daily contact (for at least 20 min) between researcher and pig, beginning two weeks prior to the start of the experiment, clearly advanced the return of appetite within two days in most of the animals.

In total, five serious adverse events were observed (Table 3). Complications that occurred were either due to erroneous microsphere delivery, *i.e.*, extrahepatic deposition, or due to comorbidity, with the exception of pig 3. This animal was administered ^{165}Ho -PLLA-MS and experienced a paraparesis, probably attributable to a catheterization-related spinal cord infarction, that spontaneously

Table 2 Overview of the pig experiments

Pig no.	Body weight (kg) ^a	Administered dosage of HoMS			Imaging modalities			Termination time (days post administration)
		(mg) ^b	(MBq)	Specific activity (MBq/mg) ^c	(MBq/g liver) ^d	Absorbed liver dose (Gy) ^e	MRI	
1	21.8	159	-	-	-	-	-	30
2	18.0	320	-	-	-	-	-	30
3	18.7	430	-	-	-	-	-	30
4	18.0	599	-	-	-	-	-	30
5	19.4	700	-	-	-	-	-	30
6	21.9	294	1,786	6.1	4.1	66 (50)	+	30
7	19.0	240	2,439	10.2	6.5	103 (100)	+	60
8	18.2	281	4,409	15.7	6.3	101 (150)	-	6
9	19.3	221	1,410	6.4	3.7	59 (50)	+	60
10	20.0	244	3,133	12.8	3.8	60 (100)	+	5
11	20.1	297	2,657	8.9	6.7	107 (100)	+	60
12	19.1	278	2,846	10.2	7.6	120 (150)	-	20
13	24.5	157	2,954	18.8	6.1	97 (150)	+	60
14	26.4	138	3,371	24.4	6.5	103 (150)	+	30
15	29.7	170	5,825	34.3	8.3	132 (150)	+	53
16	28.8	191	5,874	30.8	6.7	106 (150)	+	30
17	28.2	192	6,485	33.8	10.2	162 (150)	-	30
18	29.3	223	5,895	26.4	7.4	118 (150)	-	60

^a Body weight at time of administration.

^b Regarding the administered amount of microspheres in the non-radioactive experiments (pig no. 1-5), it was assumed that the entire administered dose was selectively deposited in the liver.

^c In the last six experiments, specific activity was higher (hence number of microspheres lower) to reduce the risk of backflow.

^d According to literature [26], the weight of the porcine liver equates to 1.97% of its body weight. The portion of the administered amount of radioactivity actually delivered into the liver was calculated by measuring the ^{166m}Ho contents in the *ex vivo* organs.

^e The organ dose was calculated as follows: $[15.87 \text{ m}] \cdot \text{MBq}^{-1} \cdot A \text{ (MBq)} / LW \text{ (kg)}] \times 10^{-3}$ (where *A* is administered amount of radioactivity and *LW* is liver weight). Intended liver dose is given between parentheses.

Table 3 Adverse events

Pig no.	Adverse event	Comment	Clinical outcome
3	Transient paraparesis	Ascribed to a spinal cord infarction	Resolved within 24 hours
8	Acute peritonitis, necrosis of the stomach wall and full-thickness gastric wall rupture	Due to inadvertent administration of ¹⁶⁶ Ho-PLLA-MS into <i>A. gastroduodenalis</i>	Found dead at day 6
10	Multifocal ulceration of the stomach, one large perforating ulcer	As a consequence of backflow of ¹⁶⁶ Ho-PLLA-MS into <i>A. gastroduodenalis</i>	Euthanized at day 5
12	Chronic anemia due to persistently bleeding ulcer	Pepsinogen serum levels revealed that the peptic ulcer was present before ¹⁶⁶ Ho-PLLA-MS had been administered	Demise from heart failure at day 20
15	Endocarditis of the tricuspid valve, chronic anemia due to persistently bleeding ulcer	The endocarditis was most probably associated with unhygienic blood withdrawal from the chronic intravascular catheter	Euthanized at day 53

resolved within 24 h. In pigs 8 and 10, treated with radioactive microspheres, clinically significant backflow into the gastroduodenal artery occurred. This artery conveys blood to the stomach, duodenum, and the pancreas, and arises from the common hepatic artery, close to the origin of the right and left hepatic artery (Fig. 1) [27]. Pig 8 expired from multifocal perforating gastric ulceration and peritonitis six days post administration, and pig 10 was euthanized when excessive deposition of radioactivity in the stomach was observed on the nuclear images. Pig 12 was diagnosed with severe persistent anemia (Hb<2.5 mmol/l) one week post-operation, and died from heart failure on day 20. During the postmortem examination, the animal was found to have suffered from multiple

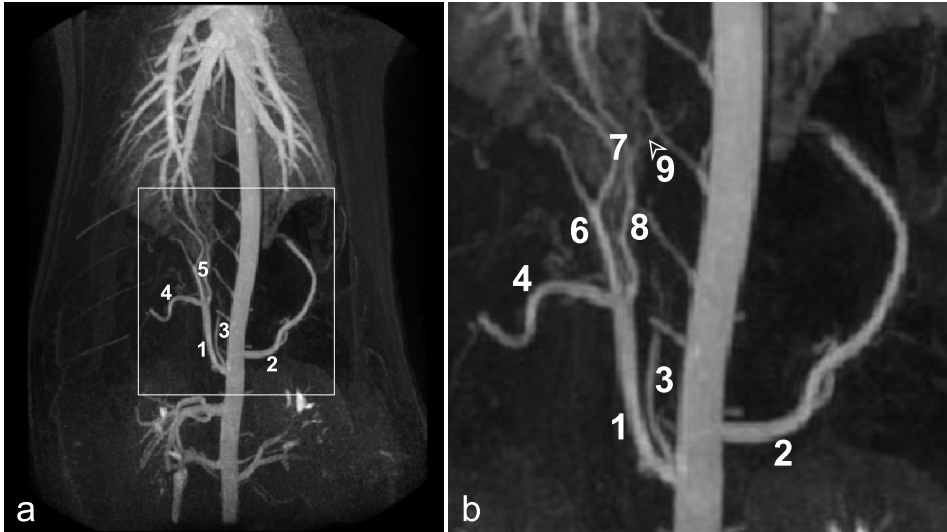


Figure 1 MR arteriography of the thorax and abdomen of a pig, anteroposterior projection (a); Excerpt of a (b): Common hepatic artery (1), splenic artery (2), caudal phrenic artery (3), gastroduodenal artery (4), (branches of the) proper hepatic artery (5), right hepatic artery (6), medial hepatic arteries (7), left hepatic artery (8), right gastric artery (9)

perforating gastric ulcers, which were not confined to the esophageal region. A bleeding ulcer was most probably already present when the animal underwent ^{166}Ho -PLLA-MS administration, as was demonstrated by the (difference in pre- and post-treatment) pepsinogen serum levels (data not shown). Pig 15 had to be euthanized prematurely because of its poor clinical condition; seven weeks after ^{166}Ho -PLLA-MS administration, it was found in a lethargic state, feverish, and unwilling to eat. It was also very anemic ($\text{Hb} < 3.0 \text{ mmol/l}$) and exhibited signs of consumption coagulopathy. Despite antibacterial and antipyretic treatment, and supportive care, its condition continued to deteriorate and required euthanization at day 53. At necropsy, an endocarditis, most probably infective, was found, almost certainly associated with unhygienic blood withdrawal from the chronic intravascular catheter. Deep gastric ulcers were also found, the largest one being in the *pars oesophagea* of the stomach.

Laboratory evaluation

Hematological and (especially) hematochemical reference values of healthy pigs

vary considerably between sources [28-30]. This is because different analysis methods had been used, and because the measured values of some parameters are highly age-dependent (*e.g.*, ALP, of which the serum levels are higher in growing animals). Most blood reference values from literature could therefore not be used in this study. Instead, it was decided to compare the mean values of the samples obtained post-treatment with the mean of the baseline values for each parameter.

The serum activities of GGT, ALP, and ALT exhibited no clinically relevant changes (Fig. 2a-c). In the ALP serum levels, a trivial difference was observed between the ^{165}Ho -PLLA-MS group and the ^{166}Ho -PLLA-MS group, which was already present in the baseline values. After radioactive microsphere administration, a moderate and transient elevation of AST levels was observed (Fig. 2d). In most samples, bilirubin was not detectable, and in the few in which it was detectable, levels did not surpass $4.0 \mu\text{mol/l}$ (data not shown). Mean hemoglobin levels were all higher than the mean of the hemoglobin baseline levels (Fig. 3a), even though the two animals diagnosed with severe persistent anemia were also included in the analysis. Similarly, platelet counts in the initial post-procedural samples were low, compared to those in samples collected later (Fig. 3b). The platelet counts varied considerably, both intra- and interindividually, but remained in the normal range. The mean total leukocyte count also remained within normal limits (Fig. 3c) [28]. Prothrombin time was not prolonged in any of the samples (Fig. 3d).

Post-mortem examinations

The main pathological findings of the animals are summarized in Table 4. In the pigs which had been administered non-radioactive holmium microspheres, no gross abnormalities were seen, except for the liver of pig 3 ($22.5 \text{ mg } ^{165}\text{Ho}$ -PLLA-MS/kg) in which the right lobes showed moderate atrophy and the left lobes slight (compensatory) hypertrophy. In one animal in this group, ulceration of the esophageal region of the stomach was seen. Moderate to marked atrophy of one or more liver lobes with compensatory hyperplasia of the other lobes was frequently observed in the animals treated with radioactive holmium microspheres (Table 4). In five animals (all from the ^{166}Ho -PLLA-MS substudy), moderate to extensive, often perforating, ulceration of the cardiac, fundic, and/

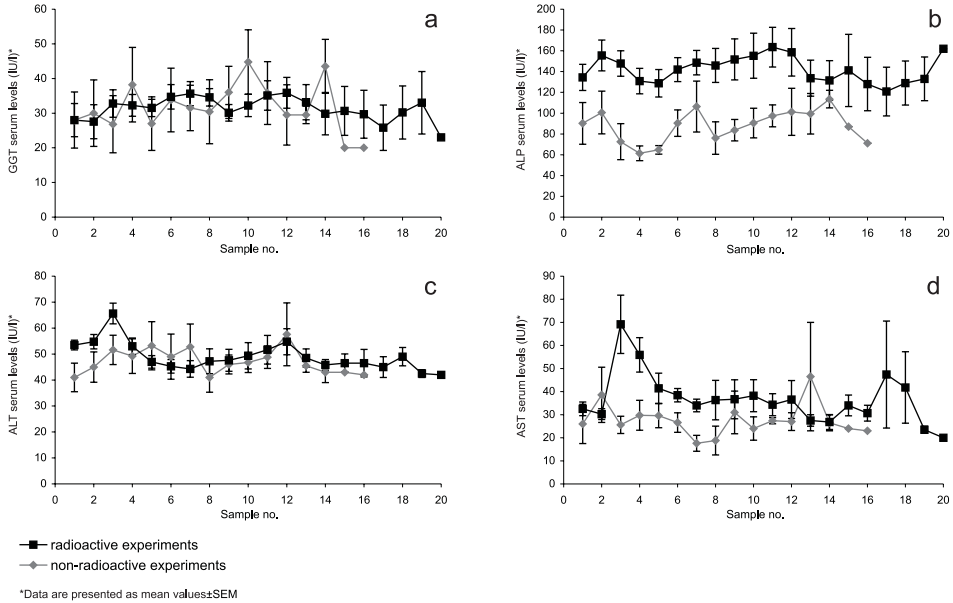


Figure 2 Liver enzymes serum activities. Time in between samples was 3 or 4 days, and value 1 was derived from samples taken prior to microsphere administration: serum activities of GGT (a); serum activities of ALP (b); serum activities of ALT (c); serum activities of AST (d)

or antral regions of the stomach was observed. In five animals, ulceration of the esophageal region of the stomach was seen (Table 4). In two animals, infarction of the gallbladder was observed (Table 4).

Histological examinations of pigs of the ¹⁶⁵Ho-PLLA-MS group regularly showed small and sometimes larger aggregates of microspheres in arteries of the liver, as well as some solitary intra-arteriolar microspheres in the stomach and gallbladder. Larger aggregates in the livers were associated with fibrosis and sometimes multinucleated giant cells surrounding individual spheres (Fig. 4a). In pig 3, in the right lateral liver lobe, a large portal area was seen with coagulative necrosis, surrounded by multinucleated giant cells, many pigmented macrophages and a fibrous capsule. In this capsule, some large aggregates of spheres were present (Fig. 4b). In the surrounding atrophic parenchyma, moderately broadened interlobular septa with fibrosis and arteriolar and ductular proliferation were seen; within these septa, small aggregates of microspheres

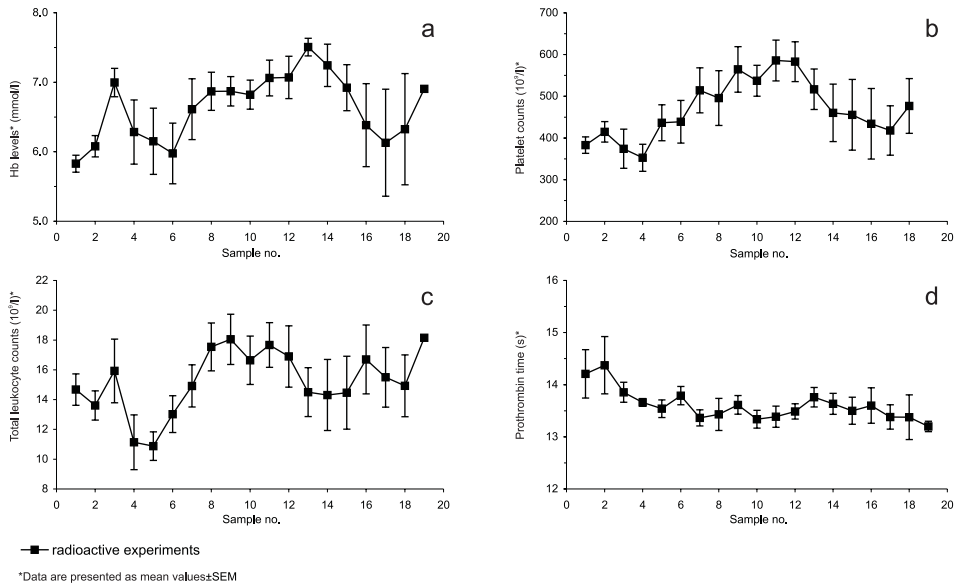


Figure 3 Hematological values. Time in between samples was 3 or 4 days, and value 1 was derived from samples taken prior to microsphere administration: hemoglobin concentrations (a); platelet counts (b); leukocyte counts (c); prothrombin time (d).

were present. Histological examinations of pigs 8 and 10 (¹⁶⁶Ho-PLLA-MS group), which died spontaneously at day 6 and was euthanized *in extremis* at day 5, respectively, showed multifocal aggregates in the hepatic arteries in the portal tracts. These aggregates were associated with complete necrosis of the portal area and the adjacent parenchyma (Fig. 4c). In the stomach of these animals, intra-arteriolar aggregates were sometimes seen, associated with thrombosis and necrosis of the arteriolar wall (Fig. 4d). In the other pigs in this group, which survived for 30 or 60 days, in the atrophic liver lobes large aggregates of microspheres were frequently seen, associated with large areas of coagulative necrosis (often with yellow discoloration by bile imbibition) and surrounded by multinucleated giant cells, pigmented macrophages, and a fibrous capsule (Fig. 4e). In the two animals with infarction of the gallbladder, there was necrosis of the wall of the gallbladder with fibrous encapsulation. In the lumen of the gallbladder necrotic debris, inspissated bile, and bile containing macrophages

were present. An intra-arteriolar aggregate was sometimes observed within the fibrous capsule (Fig. 4f). Histological examinations of the spleen in both groups showed only very rarely a solitary microsphere without additional histological changes. In none of the animals were microspheres seen in the lungs.

Imaging and microsphere biodistribution

Nuclear imaging (planar and SPECT) was performed in all thirteen radioactive experiments. The distribution of radioactivity was assessed by *ex vivo* ^{166}mHo measurements. Figure 5a shows a planar nuclear image in which highly selective hepatic accumulation of the radioactivity is demonstrated, as was the case in seven animals in which, according to the ^{166}mHo measurements, more than 95% of the injected dose was deposited in the liver. On the nuclear images of six animals, accumulation of ^{166}Ho -PLLA-MS in the stomach was observed; although clinically inconsequential, on the images of four pigs, a low to moderate amount of radioactivity (<20%) was shown to be present in the stomach (Fig. 5b). In two other animals (pigs 8 and 10), the images revealed excessive deposition of radioactivity in the gastric wall (48% and 53% of injected activity, respectively; Fig. 5c). In none of the experiments was ^{166}Ho detected to be present in the lungs. This was in accordance with the histological examinations. In two animals, a portion of the radioactivity was delivered into the spleen (ca. 10%). The nuclear images revealed that the intrahepatic microsphere distribution was distinctly heterogeneous.

MRI was performed in one non-radioactive experiment (pig 5) and in nine radioactive experiments (Table 2; Figs. 6a-f). While the intrahepatic distribution of the microspheres could be accurately assessed, demonstration of either presence or absence of microspheres in the lungs proved to be unfeasible, as the holmium-based artifacts on T_2^* -weighted images are black, as is the air in the lungs. The presence of stomach gas and other contents also made it very difficult to assess whether microspheres had been deposited into the gastric wall.

DISCUSSION

The clinical effects of (non-radioactive) ^{165}Ho and (radioactive) ^{166}Ho poly(L-lactic acid) microspheres when injected into the proper hepatic artery using a catheter were investigated in non-tumor-bearing pigs. With regard to the

Table 4 Main pathological findings

Pig no.	Liver atrophy	Liver necrosis	Gallbladder infarction	Gastric ulcers	
				Antrum, corpus and/or fundus	Esophageal region
1	-	-	-	-	+
2	-	-	-	-	-
3	+(RL, RM)	+(RL)	-	-	-
4	-	-	-	-	-
5	-	-	-	-	-
6	-	-	-	-	-
7	-	-	-	-	-
8	-	+(RL)	-	+	-
9	+(RL)	-	-	-	-
10	-	+(RM)	-	+	-
11	+(RM, LM)	+(RM)	-	-	-
12	+(LL, LM)	+(RL, RM, LM, LL)	-	+	+
13	+(LL, LM)	-	-	-	-
14	-	+(HR, RL, LM)	+	-	-
15	+(LM, LL)	+(RL, LM, LL)	-	+	+
16	+(RL, RM)	+(RM)	+	-	+
17	+(LM, LL)	+(LM, LL)	-	+	-
18	+(RM, LM, LL)	+(RL, RM)	-	-	+

HR hilar region, *LM* left medial lobe, *LL* left lateral lobe, *RL* right lateral lobe, *RM* right medial lobe

¹⁶⁵Ho-PLLA-MS, it was investigated whether the administration of increasing amounts of microspheres would lead to signs of toxicity. The aim of the ¹⁶⁶Ho-PLLA-MS substudy was to evaluate the effects of escalating liver absorbed doses (from 50 up to 150 Gy). All animals were extensively monitored, both clinically, hematologically, and biochemically. After termination, a postmortem examination was undertaken. As quantitative ¹⁶⁶Ho SPECT for clinical application is still in development, (the extent of) extrahepatic microsphere deposition was quantified through measuring the relative ^{166m}Ho content in organ homogenates.

Gastric ulcers have been a frequently encountered pathological finding in this study, located both in the esophageal region and in other parts of the stomach. Although gastric ulceration in the esophageal region is a very common

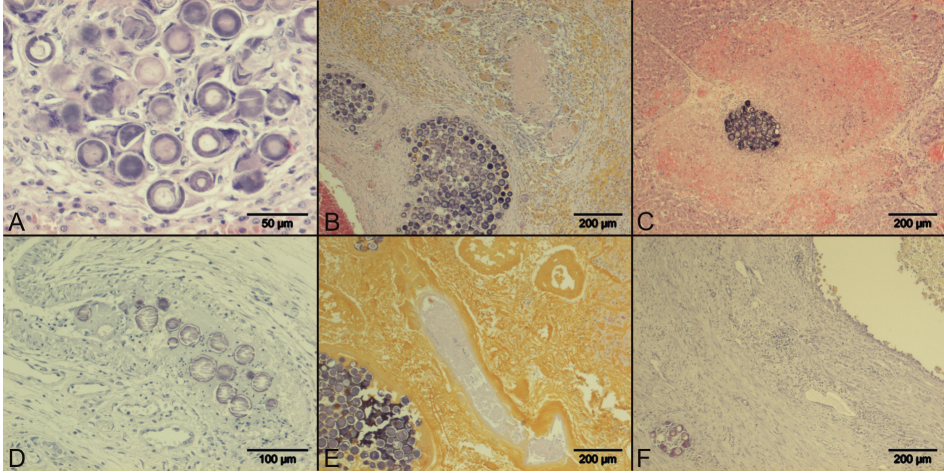


Figure 4 (a) Liver of pig 3 ($^{166}\text{Ho-PLLA-MS}$): Aggregate of microspheres within a hepatic artery with fibrosis and multinucleated giant cells. (b) Liver of pig 3 ($^{166}\text{Ho-PLLA-MS}$): large portal area with necrosis surrounded by macrophages and multinucleated giant cells and a fibrous capsule with large aggregates of microspheres. (c) Liver of pig 8 ($^{166}\text{Ho-PLLA-MS}$): a confined moderate-sized aggregate, probably within a hepatic artery, surrounded by hepatic necrosis and hemorrhage of the surrounding parenchyma and partial necrosis of the portal structures. (d) Stomach of pig 10 ($^{166}\text{Ho-PLLA-MS}$): submucosal artery with microspheres associated with fibrinoid deposition and necrosis of the arterial wall. (e) Liver of pig 11 ($^{166}\text{Ho-PLLA-MS}$): large area with yellow coloured necrosis and a large aggregate of microspheres within a necrotic hepatic artery. (f) Gallbladder of pig 16 ($^{166}\text{Ho-PLLA-MS}$): lumen filled with necrotic debris, macrophages and some neutrophils. Marked fibrosis of the wall with an aggregate of microspheres within an artery

abnormality in pigs and considered a mainly husbandry-related phenomenon [31], it nonetheless can have a fatal outcome (due to persistent hemorrhage). One animal in this study (pig 12) died as a consequence of very severe persistent gastric bleeding, and although the gastric ulcers found at gross pathological examination were not confined to the esophageal region, a bleeding ulcer was most probably already present when the animal underwent $^{166}\text{Ho-PLLA-MS}$ administration, as was demonstrated by the (difference in pre- and post-treatment) pepsinogen serum levels [32,33]. After this event, the animals to be used in all remaining experiments were transported from the supplier under mild sedation with azaperon to help reduce stress and given antacid medication (sucralfate suspension). The pigs were visited by the researcher on a daily basis,

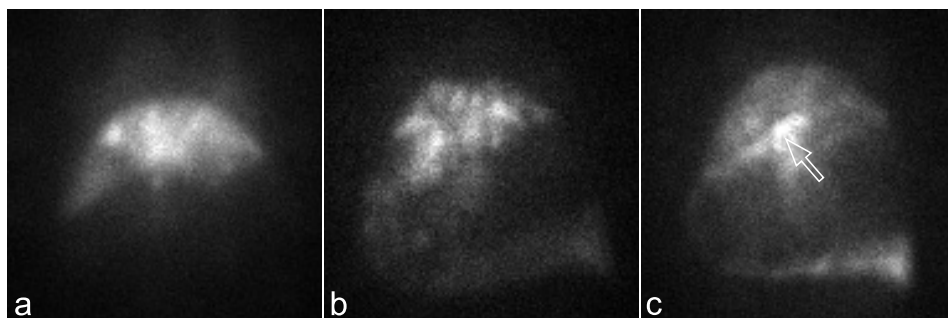


Figure 5 Nuclear images of pigs administered ^{166}Ho -PLLA-MS. Planar nuclear image of pig 15, demonstrating highly selective deposition of ^{166}Ho -PLLA-MS microspheres in the liver (a); planar nuclear image of pig 18, on which a substantial amount of ^{166}Ho (17.4%) is revealed to be present in the gastric wall (b); planar nuclear image of pig 10, demonstrating excessive amounts of radioactivity (52.5% of injected dose) present in the stomach. An intense hotspot in the lesser curvature of the stomach is depicted by the arrow (c)

starting in the acclimatization period, both to help them get acquainted with the researcher and to provide a diversion from daily routine. Pig 15 also developed a severe anemia due to bleeding ulcers, but because the onset was more than six weeks post-treatment, it was certainly not related to the microsphere treatment. Since this animal also suffered from a septic endocarditis, which will have brought about distress and anorexia, it is more likely that the ulcers, hence the persistent blood loss, were associated with this comorbidity. During the course of the experiments, the use of chronic intravascular catheters has proved to be ideal, both for the administration of intravenous medication and for obtaining blood samples. However, it must be stressed that, to minimize the risk of catheter-related infections or even sepsis, these devices should be operated in a strictly sterile manner.

The key component of a toxicity study is usually the pharmaceutical compound that is administered to the animal. In this radioembolization study, as well as the pharmaceutical quality of the microspheres, a very important factor was the manner in which the catheterization-microsphere administration procedure was carried out. The most important (lethal) complication that has occurred was inadvertent deposition of an excessive amount of ^{166}Ho -PLLA-MS in the gastric wall (pigs 8 and 10), as a consequence of which perforating ulcers

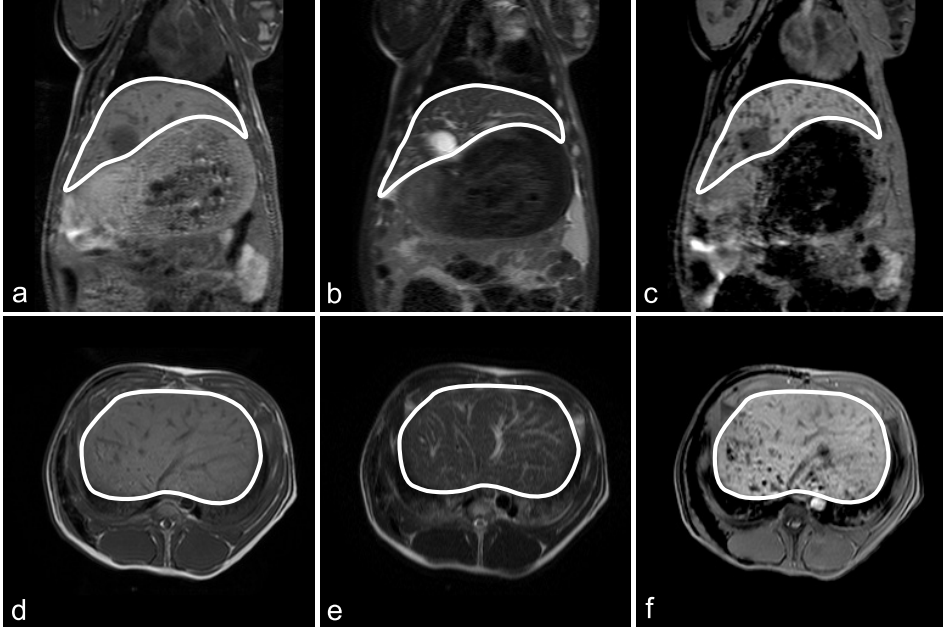


Figure 6 *In vivo* coronal (a-c) and transverse (d-f) MR images of pig 17. The anatomical images are found in a and d (T_1 -weighted SE), and panels b and e (T_2 -weighted SE images). c and f The holmium-sensitive T_2^* -weighted GE images. In the T_1 -weighted SE images the vessels and gallbladder show up as hypo-intense structures and as hyperintense structures in the T_2 -weighted SE images. In the T_2^* -weighted GE images, the clusters of microspheres are visualized as additional focal regions of signal loss, especially in the dorsal region

were induced. The cause of this radioembolization of the stomach was most probably unintentional injection of microspheres into the gastroduodenal artery, as a result of inaccurate catheter positioning and/or too high a force applied to flush the microspheres into the proper hepatic artery, thus resulting in retrograde flow. Catheter manipulation can also lead to vasospasm, for which pigs are predisposed, further increasing the risk of backflow. In the last six experiments, the specific activity of the ^{166}Ho -PLLA-MS was increased (from ca. 10 to ca. 25 MBq/mg); hence the amount of microspheres to be administered significantly decreased (Table 2). Until these experiments, a hockey-stick-shaped catheter was used, both to pass the celiac axis and to administer the microspheres. To reduce the risk of backflow, in the subsequent experiments, the microspheres

were administered using a straight-tip catheter. Furthermore, in the last eight experiments an iodine contrast agent (Telebrix® 35) was added to the flushing fluid (50:50) in order to be able to monitor for backflow using X-ray C-arm imaging. In the remaining experiments, deposition of excessive amounts of ^{166}Ho -PLLA-MS into the gastric wall did not occur, although, in four cases, there was still some radioactivity (<20% of injected dose) present in the stomach wall. Backflow into *A. gastroduodenalis* still cannot be fully excluded, but it is more likely that a portion of the microspheres ended up in *A. gastrica dextra* (Fig. 1), which branches off the hepatic artery distally from the site of the catheter tip positioning during administration. It has been reported in the literature (on human patients) that both *A. gastroduodenalis* and *A. gastrica dextra* are able to be prophylactically occluded, usually by coiling [34,35]. As the aim was for the whole liver to be exposed to the treatment, superselective microsphere administration was not performed.

As the focus of this study was not on imaging but on potential toxic side-effects of these microspheres, and because quantitative SPECT analysis will only be available in the near future, this was refrained from and the SPECT images merely analyzed in a semi-quantitative fashion. It was opted instead to quantify the actual biodistribution by measuring the $^{166\text{m}}\text{Ho}$ content in the *ex vivo* organs. The nuclear imaging did prove very useful for the detection of radioactivity deposition into the lungs. As mentioned earlier, MRI could not exclude holmium microsphere presence in lungs or (hardly) in the stomach wall. However, it could be used to detect shunting to the lungs by measuring the holmium content in blood passing through the *Vena cava caudalis*, as was proposed in a previous paper [16].

In this study, it was demonstrated that pigs can cope with extremely high liver absorbed doses, up to over 100 Gy in nine experiments. The maximum organ dose to the (human) liver from external beam radiation is approximately 30-35 Gy [36,37] or well below the range where tumoricidal effects can be expected. Apart from biological effective dose considerations like differences in dose rate, one explanation for this phenomenon is the distinctly inhomogeneous intrahepatic distribution of radioactivity, as was visualized by the scintigraphic images and the MR images.

Despite the overall lack of clinical signs in the pigs or, more specifically,

symptoms of liver disease, postmortem examinations did reveal abnormalities in most of the animals. The extent and severity of the abnormalities differed considerably between the two groups. In the animals which had been injected with ^{165}Ho -PLLA-MS, only very mild liver changes were observed, whereas the livers that had been exposed to ^{166}Ho -PLLA-MS showed blatant changes, *i.e.*, gross atrophy (accompanied with compensatory hypertrophy) and (microscopic) coagulative necrosis of parts of the livers. In itself, this is what can be expected following embolization of the hepatic artery with microspheres loaded with high amounts of a high-energy beta-emitting radionuclide.

In the monitored hematological parameters, no alterations were seen (except in the animals that suffered from persistently bleeding ulcers). The absence of myelosuppression was as expected because, in previously conducted *in vitro* and *in vivo* studies, it was demonstrated that only a very small fraction of the ^{166}Ho is released from the microspheres [38-40]. Overall, hematochemical abnormalities were absent, with the exception of the AST levels in the ^{166}Ho group; a transient rise in which these levels roughly doubled from sample 2 to 3 (Fig. 2d) was seen, which is in accordance with the postmortem findings, specifically the presence of ischemic/necrotic tissue for which AST is an indicator in the pig [41], and this accords also with the literature on ^{90}Y microsphere treatment, in which a transient rise in the liver enzymes serum levels is usually reported [35,42].

After chemoembolization, the incidence of the so-called 'post embolization syndrome', which includes fatigue, nausea, emesis, and/or right upper quadrant pain, is very high [43,44]. These symptoms have been reported following ^{90}Y microsphere infusion as well but the incidence is low [2,45]. Therefore, as expected, in this pig study, no vomiting was seen as well even if appetite was usually temporarily decreased. The animals exhibited no signs of abdominal pain.

Despite the fact that the cystic artery, which conveys blood to the gallbladder, branches off the right medial hepatic artery distally, similarly to *A. gastrica dextra*, gallbladder pathology was observed in only two animals. It can be postulated that the reason for the absence of pathological findings in the gallbladders of the other pigs is that premedication consisted of atropine, which blocks parasympathetic activity, resulting in a decreased blood flow in this feeble artery during the microsphere administration. Gallbladder pathology

("radiation cholecystitis") subsequent to ^{90}Y microsphere treatment is a potential complication reported in the literature [9,46]. Nevertheless, in most centers, a cholecystectomy preceding ^{90}Y microsphere radioembolization is not standard procedure.

Before patients undergo treatment with ^{90}Y microspheres, SPECT and planar nuclear images are acquired after hepatic arterial injection with technetium-99m-labeled macroaggregates. One of the reasons for this is to monitor for and/or quantify hepatopulmonary shunting, as excessive delivery of microspheres into the lungs can obviously lead to pulmonary failure. Whereas in (primary) liver cancer patients all kinds of anomalous arteriovenous connections commonly exist [35], this is not usually the case in healthy humans or in healthy pigs. Therefore, as could be expected, no radioactivity was detected in the lungs in any of the experiments, neither on any of the nuclear images nor on histological slides.

In this study, the critical factor has been demonstrated to be the administration technique. In summary, the catheter should be positioned correctly, *i.e.*, the tip distally from where *A. gastroduodenalis* branches off the common hepatic artery, and the flushing force/rate kept low. In addition, the specific activity of the microspheres should be sufficiently high, and backflow should be monitored or altogether inhibited by coiling.

It can be concluded that the toxicity profile of the holmium poly(L-lactic acid) microspheres is low. If the microspheres were administered in a correct manner, *viz.* deposited selectively into the liver, hepatic arterial embolization in pigs, with ^{166}Ho -PLLA-MS in high doses, was well tolerated and the clinical side-effects notably mild. Owing to the favorable outcome of this animal study, a phase I clinical trial is being planned for the near future.

Acknowledgments

This research was financially supported by the Dutch Technology Foundation STW (grant 06069). The authors would also like to thank Dr. M.W. Konijnenberg (Mallinckrodt Medical B.V., Covidien, Petten, The Netherlands) for supplying us with the *S* values for ^{166}Ho , and Miss Rosanne Varkevisser, B.Sc., for conducting the *ex vivo* radioactivity measurements.

REFERENCES

1. Garrean S, Muhs A, Bui JT, Blend MJ, *et al.* Complete eradication of hepatic metastasis from colorectal cancer by Yttrium-90 SIRT. *World J. Gastroenterol.* **2007**;13:3016-3019.
2. Sato K, Lewandowski RJ, Bui JT, Omary R, *et al.* Treatment of unresectable primary and metastatic liver cancer with yttrium-90 microspheres (TheraSphere®): assessment of Hepatic Arterial Embolization. *Cardiovasc. Intervent. Radiol.* **2006**;29:522-529.
3. Sangro B, Bilbao JI, Boan J, Martinez-Cuesta A, *et al.* Radioembolization using ⁹⁰Y-resin microspheres for patients with advanced hepatocellular carcinoma. *Int. J. Radiat. Oncol. Biol. Phys.* **2006**;66:522-529.
4. Kennedy AS, Coldwell D, Nutting C, Murthy R, *et al.* Resin ⁹⁰Y-microsphere brachytherapy for unresectable colorectal liver metastases: modern USA experience. *Int. J. Radiat. Oncol. Biol. Phys.* **2006**;65:412-425.
5. Van Hazel G, Blackwell A, Anderson J, Price D, *et al.* Randomised phase 2 trial of SIR-Spheres plus fluorouracil/leucovorin chemotherapy versus fluorouracil/leucovorin chemotherapy alone in advanced colorectal cancer. *J. Surg. Oncol.* **2004**;88:78-85.
6. Andrews JC, Walker SC, Ackermann RJ, Cotton LA, *et al.* Hepatic radioembolization with yttrium-90 containing glass microspheres: preliminary results and clinical follow-up. *J. Nucl. Med.* **1994**;35:1637-1644.
7. Nijsen JFW, Van het Schip AD, Hennink WE, Rook DW, *et al.* Advances in nuclear oncology: Microspheres for internal radionuclide therapy of liver metastases. *Curr. Med. Chem.* **2002**;9:73-82.
8. Ho S, Lau JW, Leung TW. Intrahepatic ⁹⁰Y-microspheres for hepatocellular carcinoma. *J. Nucl. Med.* **2001**;42:1587-1589.
9. Murthy R, Nunez R, Szklaruk J, Erwin W, *et al.* Yttrium-90 microsphere therapy for hepatic malignancy: devices, indications, technical considerations, and potential complications. *Radiographics* **2005**;25 Suppl 1:S41-S55.
10. Murthy R, Xiong H, Nunez R, Cohen AC, *et al.* Yttrium 90 resin microspheres for the treatment of unresectable colorectal hepatic metastases after failure of multiple chemotherapy regimens: preliminary results. *J. Vasc. Interv. Radiol.* **2005**;16:937-945.
11. Pöpperl G, Helmberger T, Munzing W, Schmid R, *et al.* Selective internal radiation therapy with SIR-Spheres in patients with nonresectable liver tumors. *Cancer Biother. Radiopharm.* **2005**;20:200-208.
12. Sandström M, Lubberink M, Lundquist H. Quantitative SPECT with Yttrium-90 for Radionuclide Therapy Dosimetry. *Eur. J. Nucl. Med. Mol. Imaging* **2007**;32:S260.
13. De Wit TC, Xiao J, Nijsen JF, Van het Schip FD, *et al.* Hybrid scatter correction applied to quantitative holmium-166 SPECT. *Phys. Med. Biol.* **2006**;51:4773-4787.
14. Ho S, Lau WY, Leung TW, Chan M, *et al.* Tumour-to-normal uptake ratio of ⁹⁰Y microspheres in hepatic cancer assessed with ⁹⁹Tc^m macroaggregated albumin. *Br. J. Radiol.* **1997**;70:823-828.
15. Seppenwoolde JH, Nijsen JFW, Bartels LW, Zielhuis SW, *et al.* Internal radiation therapy of liver tumors: qualitative and quantitative magnetic resonance imaging of the biodistribution of holmium-loaded microspheres in animal models. *Magn. Reson. Med.* **2004**;53:76-84.

16. Nijsen JFW, Seppenwoolde JH, Havenith T, Bos C, *et al.* Liver tumors: MR imaging of radioactive holmium microspheres—phantom and rabbit study. *Radiology* **2004**;231:491-499.
17. Seppenwoolde JH, Bartels LW, Van der Weide R, Nijsen JFW, *et al.* Fully MR-guided hepatic artery catheterization for selective drug delivery: a feasibility study in pigs. *J. Magn. Reson. Imaging* **2006**;23:123-129.
18. Zielhuis SW, Nijsen JFW, Dorland L, Krijger GC, *et al.* Removal of chloroform from biodegradable therapeutic microspheres by radiolysis. *Int. J. Pharm.* **2006**;315:67-74.
19. Zielhuis SW, Nijsen JFW, De Roos R, Krijger GC, *et al.* Production of GMP-grade radioactive holmium loaded poly(L-lactic acid) microspheres for clinical application. *Int. J. Pharm.* **2006**;311:69-74.
20. Nijsen JFW, Van het Schip AD, Van Steenberg MJ, Zielhuis SW, *et al.* Influence of neutron irradiation on holmium acetylacetonate loaded poly(L-lactic acid) microspheres. *Biomaterials* **2002**;23:1831-1839.
21. Nijsen JFW, Rook D, Brandt CJWM, Meijer R, *et al.* Targeting of liver tumour in rats by selective delivery of holmium-166 loaded microspheres: a biodistribution study. *Eur. J. Nucl. Med.* **2001**;28:743-749.
22. Nijsen JFW. Radioactive holmium poly(L-lactic acid) microspheres for treatment of liver malignancies. PhD thesis, Utrecht University, The Netherlands. **2001**;109-122.
23. Vente MAD, Hobbelink MGG, Van het Schip AD, Zonnenberg BA, Nijsen JFW. Radionuclide liver cancer therapies: from concept to current clinical status. *Anticancer Agents Med. Chem.* **2007**;7:441-459.
24. Nijsen JFW, Zonnenberg BA, Woittiez JR, Rook DW, *et al.* Holmium-166 poly lactic acid microspheres applicable for intra-arterial radionuclide therapy of hepatic malignancies: effects of preparation and neutron activation techniques. *Eur. J. Nucl. Med.* **1999**;26:699-704.
25. Zielhuis SW, Nijsen JFW, Figueiredo R, Feddes B, *et al.* Surface characteristics of holmium-loaded poly(l-lactic acid) microspheres. *Biomaterials* **2005**;26:925-932.
26. Boxenbaum H. Interspecies variation in liver weight, hepatic blood flow, and antipyrine intrinsic clearance: extrapolation of data to benzodiazepines and phenytoin. *J. Pharmacokinet. Biopharm.* **1980**;8:165-176.
27. Dondelinger RF, Ghysels MP, Brisbois D, Donkers E, *et al.* Relevant radiological anatomy of the pig as a training model in interventional radiology. *Eur. Radiol.* **1998**;8:1254-1273.
28. Faustini M, Munari E, Colombani C, Russo V, *et al.* Haematology and plasma biochemistry of Stamboek pre-pubertal gilts in Italy: reference values. *J. Vet. Med. A Physiol Pathol. Clin. Med.* **2000**;47:525-532.
29. Hannon JP, Bossone CA, Wade CE. Normal physiological values for conscious pigs used in biomedical research. *Lab Anim Sci.* **1990**;40:293-298.
30. Odink J, Smeets JF, Visser IJ, Sandman H, Sniijders JM. Hematological and clinicochemical profiles of healthy swine and swine with inflammatory processes. *J. Anim Sci.* **1990**;68:163-170.

31. Guise HJ, Carlyle WW, Penny RH, Abbott TA, *et al.* Gastric ulcers in finishing pigs: their prevalence and failure to influence growth rate. *Vet. Rec.* **1997**;141:563-566.
32. Sidikou DI, Banga-Mboko H, Tamboura HH, Hornick JL, *et al.* Correlation between a proteolytic method and a radioimmunoassay for porcine serum pepsinogen concentrations. *Res. Vet. Sci.* **2006**;80:260-266.
33. Banga-Mboko H, Tamboura H, Maes D, Traore H, *et al.* Survey of gastric lesions and blood pepsinogen levels in pigs in Burkina Faso. *Vet. Res. Commun.* **2003**;27:595-602.
34. Murthy R, Brown DB, Salem R, Meranze SG, *et al.* Gastrointestinal complications associated with hepatic arterial yttrium-90 microsphere therapy. *J. Vasc. Interv. Radiol.* **2007**;18:553-561.
35. Salem R, Thurston KG, Carr BI, Goin JE, Geschwind JF. Yttrium-90 microspheres: radiation therapy for unresectable liver cancer. *J. Vasc. Interv. Radiol.* **2002**;13:S223-S229.
36. Cromheecke M, Konings AW, Szabo BG, Hoekstra HJ. Liver tissue tolerance for irradiation: experimental and clinical investigations. *Hepatogastroenterology* **2000**;47:1732-1740.
37. Ingold J, Reed G, Kaplan H, Bagshaw M. Radiation hepatitis. *Am. J. Roentgenol. Radium Ther. Nucl. Med* **1965**;93:200-208.
38. Zielhuis SW, Nijssen JFW, Seppenwoolde JH, Bakker CJG, *et al.* Long-term toxicity of holmium-loaded poly(L-lactic acid) microspheres in rats. *Biomaterials* **2007**;28:4591-4599.
39. Zielhuis SW, Nijssen JFW, Krijger GC, Van het Schip AD, Hennink WE. Holmium-loaded poly(L-lactic acid) microspheres: In vitro degradation study. *Biomacromolecules* **2006**;7:2217-2223.
40. Van Es RJ, Nijssen JFW, Van het Schip AD, Dullens HF, *et al.* Intra-arterial embolization of head-and-neck cancer with radioactive holmium-166 poly(L-lactic acid) microspheres: an experimental study in rabbits. *Int. J. Oral Maxillofac. Surg.* **2001**;30:407-413.
41. Jeppsson B, Dahl EP, Fredlund PE, Stenram U, Bengmark S. Hepatic necrosis in the pig produced by transient arterial occlusion. *Eur. Surg. Res.* **1979**;11:243-253.
42. Garrean S, Joseph EN. Yttrium-90 internal radiation therapy for hepatic malignancy. *Surg. Oncol.* **2005**;14:179-193.
43. Ramsey DE, Kernagis LY, Soulen MC, Geschwind JF. Chemoembolization of hepatocellular carcinoma. *J. Vasc. Interv. Radiol.* **2002**;13:S211-S221.
44. Leung DA, Goin JE, Sickles C, Raskay BJ, Soulen MC. Determinants of postembolization syndrome after hepatic chemoembolization. *J. Vasc. Interv. Radiol.* **2001**;12:321-326.
45. Salem R, Lewandowski R, Roberts C, Goin J, *et al.* Use of yttrium-90 glass microspheres (TheraSphere) for the treatment of unresectable hepatocellular carcinoma in patients with portal vein thrombosis. *J. Vasc. Interv. Radiol.* **2004**;15:335-345.
46. Miller FH, Keppke AL, Reddy D, Huang J, *et al.* Response of liver metastases after treatment with yttrium-90 microspheres: role of size, necrosis, and PET. *AJR Am. J. Roentgenol.* **2007**;188:776-783.

CHAPTER 5

Holmium-166 poly(L-lactic acid) microsphere radioembolization of the liver: technical aspects studied in a large-animal model

Maarten A.D. Vente

Tim C. de Wit

Maurice A.A.J. van den Bosch

Wouter Bult

Peter R. Seevinck

Bernard A. Zonnenberg

Hugo W.A.M. de Jong

Gerard C. Krijger

Chris J.G. Bakker

Alfred D. van het Schip

Johannes F.W. Nijssen

Submitted

ABSTRACT

The accuracy of a small scout dose of holmium-166 loaded poly(L-lactic acid) microspheres ($^{166}\text{Ho-PLLA-MS}$) in predicting the distribution of a treatment dose of $^{166}\text{Ho-PLLA-MS}$ was assessed in the porcine model, using single photon emission tomography (SPECT). The applicability of multimodal medical imaging was also investigated. Five pigs (weighing 70-75 kg) were transcatheter hepatic arterially injected with a scout dose (60 mg) and SPECT was acquired. Subsequently, a 'treatment dose' was administered (540 mg) and SPECT, X-ray computed tomography (CT), and magnetic resonance imaging (MRI) of the total dose performed. The two SPECT studies of each animal were compared. For validation of quantitative SPECT in an inhomogeneous distribution, an *ex vivo* liver was instilled with $^{166}\text{Ho-PLLA-MS}$ and SPECT acquired. The liver was cut into 6-mm slices and planar images were acquired, which were registered to the SPECT image. Qualitatively, the scout dose and total dose images were similar in all animals, except for one animal because of catheter displacement. Quantitative analysis, feasible in two animals, confirmed this poor similarity ($r^2 = 0.34$). In the other animal the relation was significantly better ($r^2 = 0.66$). The relation between the SPECT and planar images acquired from the *ex vivo* liver was strong ($r^2 = 0.90$). In healthy pigs, a scout dose of $^{166}\text{Ho-PLLA-MS}$ can accurately predict the biodistribution of a treatment dose. The sensitivity of CT is too low for this purpose. MRI can accurately visualize low concentrations of $^{166}\text{Ho-PLLA-MS}$. Quantitative ^{166}Ho SPECT was validated for clinical application.

INTRODUCTION

Intra-arterial radioembolization with yttrium-90 microspheres (^{90}Y -MS), either resin-based (SIR-Spheres[®], SIRTech Medical Ltd., Sydney, New South Wales, Australia) or with a glass matrix (TheraSphere[®], MDS Nordion Inc., Kanata, Ontario, Canada), is an increasingly applied treatment for patients with unresectable liver malignancies, with over 10,000 patients having been treated to date [1,2]. Efficacy of ^{90}Y radioembolization relies on the difference in blood supply between liver malignancies and the normal liver parenchyma, which is exclusively arterial and mainly portal, respectively [3,4]. This allows for the ^{90}Y -MS, when instilled into the hepatic artery, to passively target the tumors, consequently delivering high tumor absorbed doses whilst largely sparing the non-tumorous liver tissue [1]. A critical component is the pretreatment procedure, which consists of meticulous celiac and superior mesenteric angiography and selective coiling of arteries supplying non-target organs such as the gastroduodenal artery and the right gastric artery. This is performed to ensure that the dose of ^{90}Y -MS is implanted exclusively into the liver, hence to prevent deposition of these high-energy beta-emitting microspheres in other visceral organs, particularly the stomach, duodenum and pancreas. To assess whether the coiling has been performed appropriately, technetium-99m albumin macroaggregates ($^{99\text{m}}\text{Tc}$ -MAA) are injected through the catheter placed in the proper hepatic artery. Subsequently, single photon emission computed tomography (SPECT) and planar images are acquired. The planar images are used to determine whether extrahepatic deposition of the ^{90}Y -MS should be expected and to calculate the lung-shunt fraction [5-7]. The $^{99\text{m}}\text{Tc}$ -MAA SPECT image is used to predict the intrahepatic distribution of the ^{90}Y -MS or, more specifically, the tumor-to-normal tissue ratio [8-10]. The $^{99\text{m}}\text{Tc}$ -MAA are thus deployed as full surrogates for the ^{90}Y -MS. However, there are indications that this assumption is not justified, as the reality is that the $^{99\text{m}}\text{Tc}$ -MAA image does not in all cases accurately correspond with the post- ^{90}Y -MS infusion Bremsstrahlung image. This is caused by differences in resolution between the $^{99\text{m}}\text{Tc}$ image and the ^{90}Y Bremsstrahlung image, and is also due to the overt differences in physical characteristics and in numbers of particles infused between the $^{99\text{m}}\text{Tc}$ -MAA and the ^{90}Y -MS [11,12]. Furthermore, it has been demonstrated clinically that the intrahepatic uptake pattern of $^{99\text{m}}\text{Tc}$ -MAA is not a strong predictor of tumor response after ^{90}Y radioembolization [13].

Post-administration visualization of the ^{90}Y -MS is thus possible through Bremsstrahlung SPECT imaging, but the quality is poor and reliable quantitative analysis is not feasible [14,15]. Largely for this lack of adequate visualization, poly(L-lactic acid) microspheres loaded with the isotope holmium-166 (^{166}Ho -PLLA-MS) have been developed [16-19]. Like ^{90}Y , ^{166}Ho is a high-energy beta-emitter, but it emits low-energy gamma photons as well (Table 1), allowing for gamma scintigraphy, suitable for quantitative analysis [20]. Quantitative SPECT, and consequently dosimetric analysis, would be useful in trying to predict efficacy and toxicity. Because holmium is also a highly paramagnetic element, the (intrahepatic) distribution of the ^{166}Ho -PLLA-MS can be assessed through magnetic resonance imaging (MRI) as well [21,22]. In addition, instead of $^{99\text{m}}\text{Tc}$ -MAA, a small scout dose of ^{166}Ho -PLLA-MS could be utilized to predict the biodistribution of the treatment dose of ^{166}Ho -PLLA-MS.

In this article, several technical aspects of intra-arterial radioembolization of the liver with ^{166}Ho -PLLA-MS are addressed. The concept of a small scout dose of ^{166}Ho -PLLA-MS employed to predict the biodistribution of the therapeutic dose of ^{166}Ho -PLLA-MS is investigated in the porcine model, by comparing the respective SPECT studies. The applicability of a dedicated administration system and of multimodal imaging (gamma scintigraphy, X-ray computed tomography (CT), and MRI) are also investigated. The accuracy of quantitative ^{166}Ho SPECT analysis for an inhomogeneous distribution is also assessed.

MATERIALS AND METHODS

Animals

Five healthy female pigs, approximately 8-9 months old and weighing 70-75 kg, were acquired from the Animal Sciences Group, Wageningen University and Research Center, Lelystad, The Netherlands. A 2-week acclimatization period was allowed. The experiments were conducted in agreement with the local applicable Dutch law, "Wet op de dierproeven" (art. 9) (1977), and the European Convention for the Protection of Vertebrate Animals used for Experimental and Other Scientific Purposes (1986), and approved by the ethical committee for animal experimentation of the University Medical Center Utrecht, Utrecht, The Netherlands (DEC-ABC-no. 2007.III.07.092).

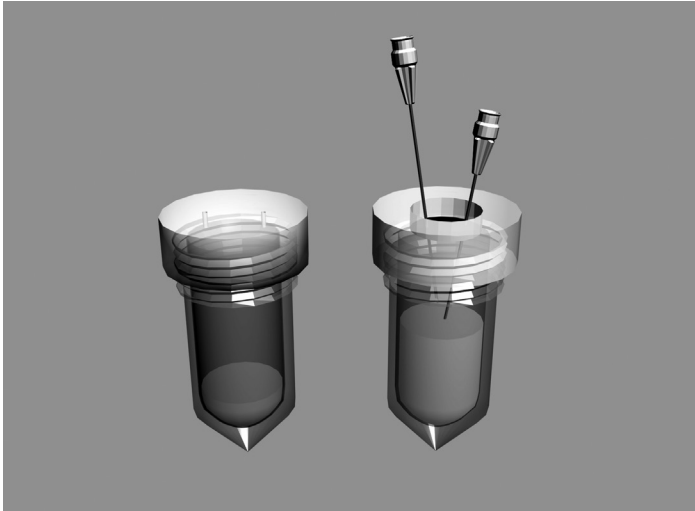


Figure 1 Schematic drawing of the custom-made HDPE neutron-activation/administration vial, fitted with a cover, as used during neutron activation (at the left), and equipped with a cover holding a septum, as used during administration of the ^{166}Ho -PLLA-MS (at the right)

Microsphere preparation

Good manufacturing practice (GMP) grade ^{165}Ho -PLLA-MS were prepared as previously described [17]. The ^{165}Ho -PLLA-MS (scout dose: 60 mg; ‘treatment dose’: 540 mg) were packed in custom-made high-density polyethylene (HDPE) vials (Fig. 1) and neutron activated via the $^{165}\text{Ho}(n,\gamma)^{166}\text{Ho}$ reaction in the nuclear reactor of the Delft University of Technology (Delft, The Netherlands) in a facility with a thermal neutron flux of $5 \times 10^{12} \text{ cm}^{-2} \text{ s}^{-1}$. Upon delivery at the hospital, two incompletely predrilled holes of the vial cover were perforated by needles (19G \times 50 mm), and the microspheres were suspended in 2 ml of water for injection containing 2% Pluronic[®] F-68 (Sigma-Aldrich Chemie B.V., Zwijndrecht, The Netherlands) and 10% ethanol abs. (Merck B.V., Amsterdam, The Netherlands). The cover of the vial was then removed and a tiny amount (ca. 1 mg) of ^{166}Ho -PLLA-MS was taken out for quality control (light microscopy) [23]. Next, a vial cover fitted with a PTFE/silicone septum (Sigma-Aldrich Chemie B.V., Zwijndrecht, The Netherlands) was screwed on top of the vial (Fig. 1). The septum was punctured by two needles (19G \times 50 mm). The amounts of radioactivity were measured

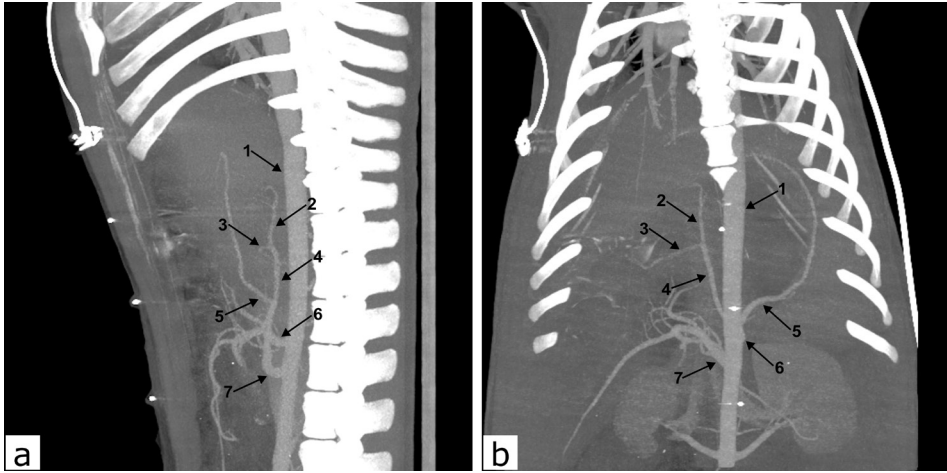


Figure 2 CT arteriography (maximum intensity projections). Lateral projections (a) and ventrodorsal projections (b): abdominal aorta (1), proper hepatic artery (2), gastroduodenal artery (3), common hepatic artery (4), splenic artery (5), celiac axis (6), and cranial mesenteric artery (7). The radiopaque objects on the abdominal wall are CT markers

in a dose calibrator that was calibrated for this geometric configuration (VDC-404, Veenstra Instrumenten B.V., Joure, The Netherlands). In order to prevent pile up and dead-time effects in the gamma camera, both the scout dose and the treatment dose consisted of 250 MBq ^{166}Ho at the time of injection.

Anesthesia and analgesia

Premedication for general anesthesia consisted of azaperone (4 mg/kg), ketamine hydrochloride (10 mg/kg), and atropine (0.1 mg/10 kg) IM. Induction of general anesthesia consisted of propofol (2.5-3.5 mg/kg) IV. General anesthesia was maintained by propofol (8-9 mg/kg/h) IV or inhalation of isoflurane (1.5-2.0%) in O_2/air (1:1), in combination with midazolam hydrochloride (0.2 mg/kg) IV. Peri-operative analgesia was provided by sufentanil (loading dose: 5 $\mu\text{g}/\text{kg}$, maintenance dose: 10 $\mu\text{g}/\text{kg}/\text{h}$) IV.

Computed tomography angiography (CTA)

In order to gather information in advance on the exact vascular anatomy of the celiac axis and the hepatic artery of each animal, a CTA of the abdominal aorta

was obtained about 10 days prior to the interventional procedure. The procedure was conducted under propofol anesthesia after ketamine premedication. CT angiograms were obtained using a 64-slice CT system (Brilliance®, Philips Healthcare, Best, The Netherlands). The tube voltage was set at 120 kVp with a tube current of 300 mAs/rotation. The central ear vein was cannulated with a 18-G Abbocath-T® catheter (Abbott Ireland Ltd., Sligo, Republic of Ireland) and a nonionic iodinated contrast agent (Ultravist® 300, Bayer B.V., Mijdrecht, The Netherlands) was injected at a rate of 4 ml/s, using a dual-head contrast injector system (Stellant®, Medrad Europe B.V., Beek, The Netherlands), with a post-threshold delay of 5 s, using bolus tracking. The image covered the area from the aortic arch to the renal arteries. Axial image series with a slice thickness of 0.9 mm and an increment of 0.7 mm were reconstructed. Maximum intensity projections (MIPs) were rendered using the default bone removal algorithm (Fig. 2).

Administration system

A custom-made administration system was used (Fig. 3), that consisted of polyethylene tube lines equipped with one-way valves (Medisize B.V., Hillegom, The Netherlands) preventing inflow of blood into the system and thus inhibiting backflow of microspheres in the lines. The lines were interconnected using a Y-connector (World Precision Instruments Inc., Sarasota, FL, USA). The polyethylene lines were connected to the Softouch® Straight Selective catheter, to the vial containing the ¹⁶⁶Ho-PLLA-MS, and to three-stopcock manifolds (3-way) to which 20-ml syringes, containing the saline-contrast agent mixture were connected. To reduce the radiation dose on personnel, the vial containing the ¹⁶⁶Ho-PLLA-MS was placed in a high-density lead-glass vial shield.

Angiography and microsphere administration procedure

A right femoral artery puncture was made and an Avanti®+ sheath (7F, Cordis Europe N.V., Roden, The Netherlands) was introduced. Under C-arm fluoroscopic guidance (Arcadis® Orbic 3D, Siemens Nederland N.V., The Hague, The Netherlands), a 4F pigtail catheter was advanced into the abdominal aorta and, in order to locate the origin of the celiac axis, an abdominal aortogram was obtained by injecting a bolus (25 ml/s during 3 s) of an iodine contrast agent (Telebrix® 35, Guerbet Nederland B.V., Gorinchem, The Netherlands), using an angiography

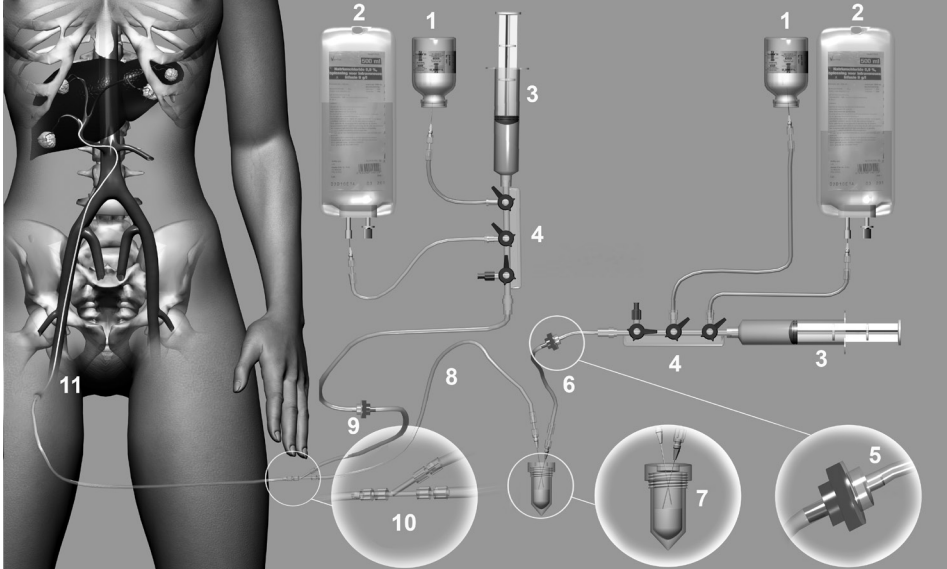


Figure 3 Schematic drawing of the custom-made ^{166}Ho -PLLA-MS administration system, which consists of the following components: iodine contrast agent (1), saline solution (2), 20-ml syringe (Luer-Lock) (3), three-stopcock manifold (3-way) (4), one-way valve (5), inlet line (6), administration vial containing the ^{166}Ho -PLLA-MS (7), outlet line (8), flushing line (9), Y-connector (10), and catheter (11). Not shown in this diagram is the lead-glass vial shield in which the HDPE vial is placed to limit the radiation dose to which the personnel is exposed

injector (Mark V ProVis[®], Medrad Europe B.V., Beek, The Netherlands). Then, the common hepatic artery was catheterized and the exact anatomy of its branches was mapped out. The catheters (4F) used in this study were Performa[®] Cardiac Pigtail, Softouch[®] Osborn 2, Softouch[®] Berenstein 1, and Softouch[®] Straight Selective, in combination with double-ended (J-tip and straight tip) and straight fixed core (super stiff, Bentson) guide wires (Merit Medical Europe, Maastricht-Airport, The Netherlands). The scout dose and treatment dose of ^{166}Ho -PLLA-MS were flushed out of the vial and into the (straight tip) catheter, positioned in the proper hepatic artery, by injecting 40-60 ml of a 50/50 mixture of saline and iodine contrast agent into the vial, under fluoroscopy guidance, at a rate of 0.5-1.0 ml/s.

Medical imaging protocols

For registration purposes, multimodality markers (MM3005 Radiology/Radiation Therapy Marker, IZI Medical Products Inc., Baltimore, MD, USA), filled with 2 MBq ^{99m}Tc each, were attached to the skin just cranially and caudally from the liver. *In vivo* planar nuclear imaging and SPECT imaging were performed directly after administration of the scout dose, and repeated after administration of the treatment dose. The nuclear medicine studies were acquired using a dual-headed gamma camera equipped with medium-energy, general-purpose, parallel-hole collimators (Vertex MCD, Philips Healthcare, Best, The Netherlands). Gadolinium-153 scanning line sources (5.5 GBq) were used for attenuation correction (energy window: 100 keV \pm 10%). The ^{166}Ho photo peak window was set to 81 keV \pm 7.5%. A window centered at 118 keV \pm 6% was used to obtain an estimate for the down-scatter in both the emission and transmission window. The 360° SPECT study consisted of 120 projections for 30 s/angle (128x128 matrix). SPECT reconstruction was performed according to a previously described protocol [20]. CT was performed after the treatment dose was administered. CT images were acquired on a 64-slice CT system (Brilliance®, Philips Healthcare, Best, The Netherlands), with a tube voltage of 120 kVp at a current of 400 mAs. Subsequent to termination with an overdose of sodium pentobarbitone (100-200 mg/kg) IV, MRI was performed, including T_1 , T_2 , and T_2^* protocols, using a 1.5-T clinical scanner (Achieva®, Philips Healthcare, Best, The Netherlands), according to previously described protocols [22].

SPECT analysis

The distribution of the scout dose was compared to the distribution of the 'total dose' (scout dose + treatment dose). After rigid registration of both SPECT studies and downsampling to a 32x32x32 matrix (18.9 mm voxel size), scatter plots were generated of which regression analysis was done. The accuracy of quantitative SPECT was assessed in a realistic model (inhomogeneous radioactivity distribution), by comparing the distribution of a SPECT image with the planar images of a pig's liver, in which ^{166}Ho -PLLA-MS had been injected *ex vivo*. The liver was taken out and placed in a metal box, in which also five 16-mm diameter tubes were placed. The box was filled with carboxymethyl cellulose

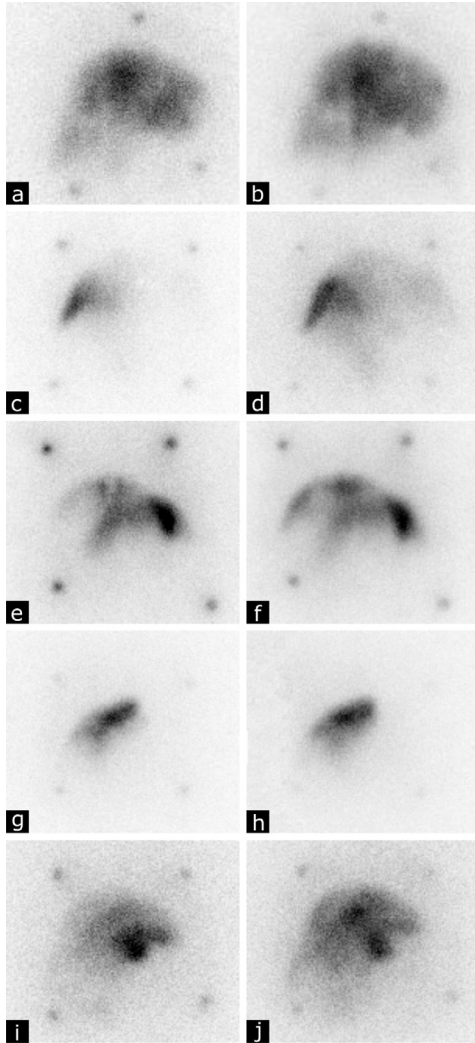


Figure 4 Planar nuclear images (ventro-dorsal view) of the pigs acquired after hepatic arterial administration of the scout dose of ^{166}Ho -PLLA-MS (60 mg, 250 MBq) (**a, c, e, g, i**), and planar nuclear images acquired from the total dose, which constitutes the scout dose and the subsequently administered ‘treatment dose’ of ^{166}Ho -PLLA-MS (540 mg, 250 MBq) (**b, d, f, h, j**)

(CMC) (2.5%) and subsequently frozen at -20°C . Twenty-four hours later the tubes were removed and the remaining cylindrical holes were filled with a ^{166}Ho /CMC chloride solution as radioactive markers. The box was again placed in the freezer. After SPECT acquisition, the embedded liver was cut into eight 6-mm thick slices with a floor-model band saw (C.-E. Reich GmbH, Geradstetten, Remshalden, Germany) and planar nuclear images were acquired of each slice.

The planar images were combined into a 3-D volume. This volume was registered to the SPECT image and resampled to the same (isotropic) voxel size, after which scatter plot analysis was performed. The markers were used for registration and normalization of the slices.

RESULTS

Angiography and microsphere administration procedure

Selective catheterization of the hepatic artery was successfully performed in all five pigs, and no procedure-related complications occurred. All animals received both a ^{166}Ho -PLLA-MS scout dose and treatment dose, using the custom-made administration system. The ^{166}Ho -PLLA-MS were gradually flushed out of the administration vial, in a controlled manner. Y-connectors of a diameter matching that of the tube lines were used which prevented lodging of the ^{166}Ho -PLLA-MS in the system. It was measured that <1% of the radioactivity had remained in the administration systems used in any of these experiments.

SPECT analysis

Qualitative visual analysis of the SPECT images revealed that, in all five animals, the ^{166}Ho -PLLA-MS had been deposited into the liver exclusively. Qualitatively, the intrahepatic radioactivity distributions according to the respective scout dose and 'total dose' images of four out of five animals seemed similar (Fig. 4a-h). This was not the case for the images of the fifth animal, which was caused by unintended catheter displacement between the administration of the scout dose and the treatment dose (Fig. 4i-j). Rigid registration of the SPECT images of the scout dose and total dose was feasible in two out of five animals. In one of these animals (the one in which the catheter was displaced between administrations), the relation between the scout dose distribution and total dose distribution was rather poor ($r^2 = 0.34$), whereas in the other animal, the relation was significantly better ($r^2 = 0.66$) (Fig. 5).

In order to validate quantitative SPECT analysis, an *ex vivo* pig liver was injected with ^{166}Ho -PLLA-MS and a SPECT study acquired. Planar nuclear images of slices of this liver were combined into a 3-D volume and compared with the SPECT image by scatter plot analysis. This revealed a strong correlation between the SPECT and the planar images ($r^2 = 0.90$) (Fig. 6).

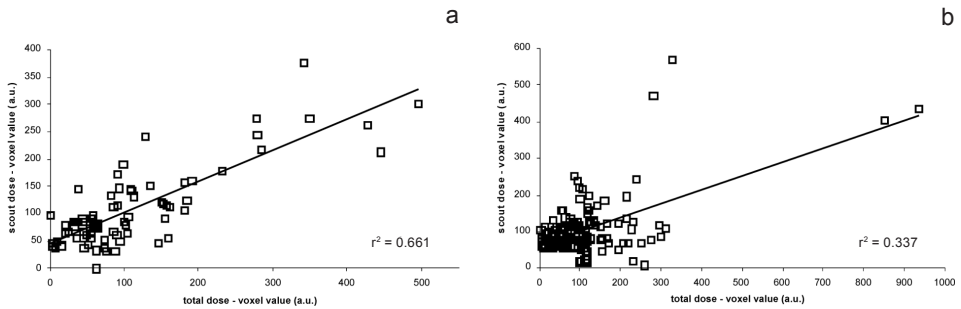


Figure 5 Scatter plots obtained from the SPECT images of two pigs, in which the distribution of the respective scout dose and total dose were compared. In one animal, the relation between the scout dose and the total dose was quite strong (a), whereas in the other animal the relation between the scout dose and the total dose was rather poor (b)

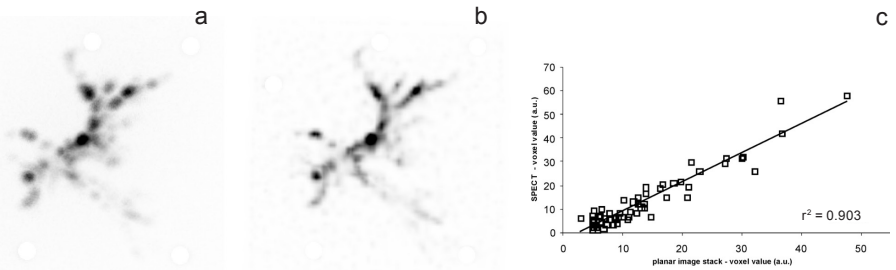


Figure 6 Maximum intensity projections of the stacked planar nuclear images acquired from an *ex vivo* pig liver (a) and of the SPECT image of this liver (b). Quantification of the SPECT images using hybrid scatter correction demonstrated that the radioactivity distribution according to the SPECT images was highly similar to the distribution based on the planar images (c)

CT and MRI

Relatively high concentrations of ¹⁶⁶Ho-PLLA-MS present in hepatic arteries could be visualized by CT, notably when maximum intensity projections were acquired (Fig. 7a). Holmium-based artifacts could be observed on the T₂*-weighted MRI images (Fig. 7b). The distribution patterns in liver parts with relatively high concentrations of ¹⁶⁶Ho-PLLA-MS observed on the MRI images were quite similar to the distribution patterns in these parts as visualized by CT. A discrepancy was seen between the performance of these two modalities with respect to liver regions containing lower concentrations of ¹⁶⁶Ho-PLLA-

Table 1 Characteristics of the microparticles

	SIR-Spheres (SIRTeX Medical Ltd.)	TheraSphere (MDS Nordion Inc.)	^{99m} Tc-MAA (Technescan® LyoMAA, Mallinckrodt Medical Inc.)	¹⁶⁶ Ho-PLLA- MS (UMC Utrecht)
Radionuclide	⁹⁰ Y		^{99m} Tc	¹⁶⁶ Ho
β-emission (MeV)	2.28 (100%)		no β-emission	1.77 (49%) 1.85 (50%)
γ-emission (keV)	no γ-emission		141 keV (89%)	80.6 (6.7%)
Matrix material	resin	glass	aggregated human serum albumin	PLLA
Density (g/ml)	1.6 [30]	3.2 [30]	1.1 [31]	1.4
Diameter (μm)	32±10 [30]	25±10 [30]	10-60 [11]	30±5
Administered number of particles	50,000,000 [6]	4,000,000 [6]	150,000 [11]	33,000,000

MS. Relatively low concentrations still detectable by MRI were absent on the CT images. Therefore, qualitatively assessed, the CT and MRI images of the livers *in toto* were not fully comparable with each other.

DISCUSSION

In intra-arterial ⁹⁰Y-MS radioembolization, ^{99m}Tc-MAA scintigraphy is performed following pretreatment angiography and coiling, one to two weeks before treatment, in order to detect lung shunting and to predict the intrahepatic distribution of the ⁹⁰Y-MS and possible deposition into extrahepatic organs. Various studies have reported that the intrahepatic ^{99m}Tc-MAA image does not in all cases accurately reflect the intrahepatic distribution of the ⁹⁰Y-MS [11,12]. This is due to differences in resolution between the ^{99m}Tc and the ⁹⁰Y images, and

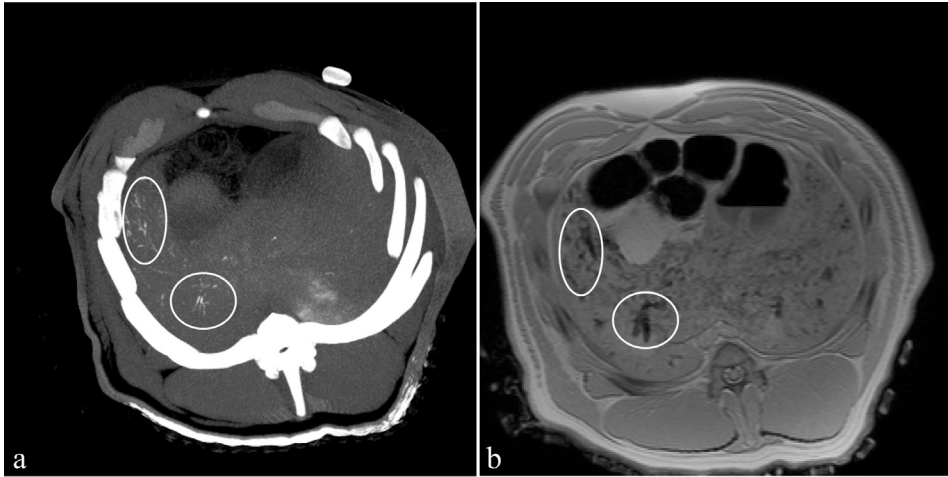


Figure 7 ^{166}Ho -PLLA-MS visualized by CT maximum intensity projection (a), and by T_2 -weighted MRI (8-mm slice) (b). High concentrations are encircled

dissimilarities in partitioning owing to differences in physical characteristics and numbers of particles infused (Table 1).

The characteristics of ^{166}Ho -PLLA-MS enable the use of a scout dose of ^{166}Ho -PLLA-MS to predict the distribution of the therapeutic dose of ^{166}Ho -PLLA-MS. In this study, this concept has been tested in a relatively anthropomorphic animal model, namely the domestic pig. Five pigs were successfully catheterized and hepatic arterially injected with both a scout dose and a treatment dose. The use of the dedicated neutron activation/administration vial with two separate vial covers resulted in a successful and safe administration procedure. Use of this vial made pretreatment quality control of the ^{166}Ho -PLLA-MS possible and prevented the need to transfer radioactivity from a neutron activation vial to an administration vial. The internal volume of the vial used in this study was almost six times larger than the volume of the glass vial used in a previous toxicity study in pigs (6.0 vs. 1.1 ml) [16]. Compared with the glass vial, the ^{166}Ho -PLLA-MS were flushed out more gradually. The internal diameter of the tube lines was also larger than the diameter of the lines used in the previous study (3.0 mm vs. 1.0 mm), which aided a controlled instillation of microspheres as well. The tube lines in the systems supplied by the manufacturers of the glass and resin

microspheres are connected using standard three-way stopcocks. It is reported in the literature on ^{90}Y -MS that microspheres tend to be retained in and just before the stopcock [24]. Loosening up the jammed microspheres requires tapping and/or gently shaking of the stopcock. In the presently used system, this lodging of microspheres did not occur for, instead of stopcocks, Y-connectors of a diameter matching that of the tube lines were used. Administration of the ^{166}Ho -PLLA-MS suspended in a mixture of saline and iodine contrast permitted immediate observation of stasis and/or backflow and timely interruption of the procedure.

Based on qualitative visual analysis of the five pairs of nuclear medicine studies, it was concluded that in all five animals the ^{166}Ho -PLLA-MS had been selectively deposited into the liver, and that the respective intrahepatic biodistributions (scout and total dose) were very comparable in four pigs. In one animal in which the catheter had been displaced between administrations they were not. Quantitative scatter plot analysis of the SPECT images obtained from this animal confirmed that the biodistributions were indeed quite dissimilar. This finding emphasizes that proper position of the catheter tip has to be checked carefully between administrations of the scout dose and the treatment dose.

Preclinical research has also been conducted by other groups on the development of microspheres that mimic ^{90}Y -MS better than the $^{99\text{m}}\text{Tc}$ -MAA, and which, like ^{166}Ho -PLLA-MS, possess high-quality imaging possibilities. Recently proposed substitutes for the glass ^{90}Y -MS were iron-labeled glass-ceramic microspheres [12]. In a feasibility study, it was demonstrated that transcatheter delivery of these iron-labeled microspheres in Vx2-carcinoma-bearing rabbits could be visualized in real-time by MRI. Resin microspheres labeled with fluorine-18 (^{18}F), allowing for positron emission tomography, were proposed to serve as surrogates for the resin ^{90}Y -MS [25,26]. These ^{18}F microspheres were not only meant to replace the $^{99\text{m}}\text{Tc}$ -MAA, but also to enable accurate assessment of the biodistribution of the treatment dose when co-injected with the resin ^{90}Y -MS. Regarding both the iron-labeled glass-ceramic microspheres and the ^{18}F resin microspheres, extensive preclinical research is warranted before clinical application will be allowed.

^{166}Ho is a true multimodal agent, allowing for visualization by gamma scintigraphy, MRI, and CT. The sensitivity of CT for holmium is relatively low; compared with SPECT its sensitivity is 2-3 orders of magnitude lower, and

approximately 20 times lower than that of MRI [27]. In agreement with this, only relatively high concentrations of ^{166}Ho -PLLA-MS could be visualized by CT in this study. It is therefore expected that CT is too insensitive to allow reliable biodistribution assessment of a scout dose of 60 mg of ^{166}Ho -PLLA-MS. MRI was able to detect at lower concentrations than CT ^{166}Ho -PLLA-MS. This observation, supported by previously reported results [27,28], implies that MRI can accurately visualize a scout dose of ^{166}Ho -PLLA-MS. As MRI provides detailed anatomic imaging as well, this modality is thought to be especially useful in dynamic imaging of ^{166}Ho -PLLA-MS accumulating in and around tumors, and could provide real-time monitored (supra)selective administration of ^{166}Ho -PLLA-MS [29]. For its high sensitivity, SPECT is currently the best suited imaging modality for visualization of both the scout dose and the treatment dose of ^{166}Ho -PLLA-MS. For safety and efficacy purposes, individualized dose calculation is required. To this end, pretreatment tumor and liver dosimetry is a prerequisite. Dosimetry entails quantitative SPECT analysis which was validated for a distinctly inhomogeneous distribution of ^{166}Ho -PLLA-MS in this study. Dosimetric analysis of the scout dose can be performed directly post administration.

The methodology described in this paper is aimed at improving clinical results of radioembolization in patients with unresectable liver tumors. Confirmation of the clinical applicability of this concept has to be established in upcoming patient studies.

CONCLUSIONS

In non-tumor-bearing pigs, a scout dose of ^{166}Ho -PLLA-MS can accurately predict the biodistribution of a treatment dose of ^{166}Ho -PLLA-MS, as assessed by qualitative and quantitative SPECT. The sensitivity of CT is considered insufficient for this purpose. MRI can accurately visualize low concentrations of ^{166}Ho -PLLA-MS. Quantitative ^{166}Ho SPECT, necessary for dosimetric analysis, was validated in a realistic model. The custom-made administration system and neutron-activation/administration vial was tested as well and found satisfactory in the administration of ^{166}Ho -PLLA-MS.

Acknowledgments

Financial support by the Dutch Technology Foundation STW under grant 06069 is gratefully acknowledged. The authors would also like to thank Mr. Simon Plomp for his assistance in the preparation of the liver slices, and Mr. Remmert de Roos for his assistance in the preparation of the microspheres.

REFERENCES

1. Gulec SA, Fong Y. Yttrium 90 microsphere selective internal radiation treatment of hepatic colorectal metastases. *Arch. Surg.* **2007**;142:675-682.
2. Salem R, Thurston KG. Radioembolization with yttrium-90 microspheres: a state-of-the-art brachytherapy treatment for primary and secondary liver malignancies: part 3: comprehensive literature review and future direction. *J. Vasc. Interv. Radiol.* **2006**;17:1571-1593.
3. Breedis C, Young G. The blood supply of neoplasms in the liver. *Am. J. Pathol.* **1954**;30:969-977.
4. Bierman HR, Byron RL, Jr., Kelley KH, Grady A. Studies on the blood supply of tumors in man. III. Vascular patterns of the liver by hepatic arteriography in vivo. *J. Natl. Cancer Inst.* **1951**;12:107-131.
5. Salem R, Thurston KG. Radioembolization with ⁹⁰Yttrium microspheres: a state-of-the-art brachytherapy treatment for primary and secondary liver malignancies. Part 1: Technical and methodologic considerations. *J. Vasc. Interv. Radiol.* **2006**;17:1251-1278.
6. Murthy R, Nunez R, Szklaruk J, Erwin W, *et al.* Yttrium-90 microsphere therapy for hepatic malignancy: devices, indications, technical considerations, and potential complications. *Radiographics* **2005**;25 Suppl 1:S41-S55.
7. Leung WT, Lau WY, Ho SK, Chan M, *et al.* Measuring lung shunting in hepatocellular carcinoma with intrahepatic-arterial technetium-99m macroaggregated albumin. *J. Nucl. Med.* **1994**;35:70-73.
8. Ho S, Lau WY, Leung TW, Johnson PJ. Internal radiation therapy for patients with primary or metastatic hepatic cancer: a review. *Cancer* **1998**;83:1894-1907.
9. Ho S, Lau WY, Leung TW, Chan M, *et al.* Partition model for estimating radiation doses from yttrium-90 microspheres in treating hepatic tumours. *Eur. J. Nucl. Med.* **1996**;23:947-952.
10. Leung TW, Lau WY, Ho SK, Chan M, *et al.* Determination of tumour vascularity using selective hepatic angiography as compared with intrahepatic-arterial technetium-99m macroaggregated albumin scan in hepatocellular carcinoma. *Cancer Chemother. Pharmacol.* **1994**;33 Suppl:S33-36.
11. Koch W, Tatsch K. Nuclear medicine procedures for treatment evaluation. In: Bilbao JI, Reiser MF (eds.) *Liver Radioembolization with ⁹⁰Y Microspheres*, 1st edn. Springer, Heidelberg **2008**;75-91.
12. Gupta T, Virmani S, Neidt TM, Szolc-Kowalska B, *et al.* MR Tracking of iron-labeled glass radioembolization microspheres during transcatheter delivery to rabbit VX2 liver tumors: feasibility study. *Radiology* **2008**;249:845-854.
13. Dhabuwala A, Lamerton P, Stubbs RS. Relationship of ^{99m}technetium labelled macroaggregated albumin (^{99m}Tc-MAA) uptake by colorectal liver metastases to response following selective internal radiation therapy (SIRT). *BMC Nucl. Med.* **2005**;5:7.
14. Sarfaraz M, Kennedy AS, Lodge MA, Li XA, *et al.* Radiation absorbed dose distribution in a patient treated with yttrium-90 microspheres for hepatocellular carcinoma. *Med. Phys.* **2004**;31:2449-2453.

15. Sandström M, Lubberink M, Lundquist H. Quantitative SPECT with yttrium-90 for radionuclide therapy dosimetry. *Eur. J. Nucl. Med. Mol. Imaging* **2007**;32:S260.
16. Vente MAD, Nijsen JFW, De Wit TC, Seppenwoolde JH, *et al.* Clinical effects of transcatheter hepatic arterial embolization with holmium-166 poly(L-lactic acid) microspheres in healthy pigs. *Eur. J. Nucl. Med. Mol. Imaging* **2008**;35:1259-1271.
17. Zielhuis SW, Nijsen JFW, De Roos R, Krijger GC, *et al.* Production of GMP-grade radioactive holmium loaded poly(l-lactic acid) microspheres for clinical application. *Int. J. Pharm.* **2006**;311:69-74.
18. Nijsen JFW, Van Steenberg MJ, Kooijman H, Talsma H, *et al.* Characterization of poly(L-lactic acid) microspheres loaded with holmium acetylacetonate. *Biomaterials* **2001**;22:3073-3081.
19. Nijsen JFW, Zonnenberg BA, Woittiez JR, Rook DW, *et al.* Holmium-166 poly lactic acid microspheres applicable for intra-arterial radionuclide therapy of hepatic malignancies: effects of preparation and neutron activation techniques. *Eur. J. Nucl. Med.* **1999**;26:699-704.
20. De Wit TC, Xiao J, Nijsen JF, Van het Schip FD, *et al.* Hybrid scatter correction applied to quantitative holmium-166 SPECT. *Phys. Med. Biol.* **2006**;51:4773-4787.
21. Seppenwoolde JH, Nijsen JFW, Bartels LW, Zielhuis SW, *et al.* Internal radiation therapy of liver tumors: Qualitative and quantitative magnetic resonance imaging of the biodistribution of holmium-loaded microspheres in animal models. *Magn Reson. Med.* **2004**;53:76-84.
22. Nijsen JFW, Seppenwoolde JH, Havenith T, Bos C, *et al.* Liver tumors: MR imaging of radioactive holmium microspheres—phantom and rabbit study. *Radiology* **2004**;231:491-499.
23. Vente MAD, Nijsen JFW, De Roos R, Van Steenberg MJ, *et al.* Neutron activation of holmium poly(L-lactic acid) microspheres for hepatic arterial radioembolization: a validation study. *Biomed Microdevices* **2009**.
24. Salem R, Thurston KG, Carr BI, Goin JE, Geschwind JF. Yttrium-90 microspheres: radiation therapy for unresectable liver cancer. *J. Vasc. Interv. Radiol.* **2002**;13:S223-S229.
25. Selwyn RG, Avila-Rodriguez MA, Converse AK, Hampel JA, *et al.* ¹⁸F-labeled resin microspheres as surrogates for ⁹⁰Y resin microspheres used in the treatment of hepatic tumors: a radiolabeling and PET validation study. *Phys. Med. Biol.* **2007**;52:7397-7408.
26. Avila-Rodriguez MA, Selwyn RG, Hampel JA, Thomadsen BR, *et al.* Positron-emitting resin microspheres as surrogates of ⁹⁰Y SIR-Spheres: a radiolabeling and stability study. *Nucl. Med. Biol.* **2007**;34:585-590.
27. Seevinck PR, Seppenwoolde JH, De Wit TC, Nijsen JF, *et al.* Factors affecting the sensitivity and detection limits of MRI, CT, and SPECT for multimodal diagnostic and therapeutic agents. *Anticancer Agents Med. Chem.* **2007**;7:317-334.
28. Seevinck PR, Bult W, Nijsen JFW, Vente MAD, *et al.* Highly-loaded holmium microspheres for test dose detection and biodistribution prediction in internal radiation therapy of liver tumors. *International Society for Magnetic Resonance in Medicine* **2008**;274.
29. Seppenwoolde JH, Bartels LW, Van der Weide R, Nijsen JFW, *et al.* Fully MR-guided

- hepatic artery catheterization for selective drug delivery: a feasibility study in pigs. *J. Magn Reson. Imaging* **2006**;23:123-129.
30. Kennedy AS, Nutting C, Coldwell D, Gaiser J, Drachenberg C. Pathologic response and microdosimetry of ⁹⁰Y microspheres in man: review of four explanted whole livers. *Int. J. Radiat. Oncol. Biol. Phys.* **2004**;60:1552-1563.
 31. Rao SN, Basu SP, Sanny CG, Manley RV, Hartsuck JA. Preliminary x-ray investigation of an orthorhombic crystal form of human plasma albumin. *J. Biol. Chem.* **1976**;251:3191-3193.

CHAPTER 6

Hepatic dosimetry for holmium-166 and yttrium-90 radioembolization: comparison of MIRD, dose-point kernel, and MCNP

**Mark W. Konijnenberg
Maarten A.D. Vente
Tim C. de Wit
Hugo W.A.M. de Jong
Alfred D. van het Schip
Johannes F.W. Nijssen**

Submitted

ABSTRACT

Aim: The applicability of the Medical Internal Radiation Dose (MIRD) dose estimation scheme, Monte Carlo simulation (MCNP), and the dose-point kernel convolution (PK) method for holmium-166 (^{166}Ho) and yttrium-90 (^{90}Y) radioembolization dosimetry was assessed and the methods compared in an inhomogeneous radioactivity distribution.

Methods: ^{166}Ho loaded poly(L-lactic acid) microspheres were hepatic arterially instilled into a pig. After termination, its liver was excised and cut into 6-mm slices. The slices were placed on a storage phosphor screen for autoradiography. A 3-D radioactivity distribution was obtained by stacking the autoradiographs. The measured optical densities were used as input for absorbed dose calculations with MCNP for both ^{166}Ho and ^{90}Y . The same 3-D dose distributions were also calculated with dose-point kernels generated by MCNP and from MIRD pamphlet 17. Additionally, MCNP calculations were performed using a MIRD humanoid stylized model assuming a homogeneous activity distribution inside the liver. Dose-volume histogram (DVH) analysis was performed on the respective absorbed-dose distributions. For all methods, the mean absorbed dose was compared with the S value from the internal dose calculation code Olinda/EXM.

Results: The isodose curves for ^{166}Ho and ^{90}Y were similar. For both radionuclides, the absorbed-dose distribution as calculated by MCNP was almost identical to the corresponding PK result, both the DVHs and the isodose representations.

Conclusion: In microsphere radioembolization the radioactivity distribution is inherently heterogeneous. Since the MIRD method for calculating mean organ doses assumes a homogeneous distribution, it is insufficient for this application. The PK method provides a quick and acceptable alternative to MCNP for liver radioembolization dosimetry. The dose distribution was comparable between ^{166}Ho and ^{90}Y .

INTRODUCTION

Intra-arterial radioembolization with microspheres is increasingly used for treatment of patients with unresectable liver malignancies [1,2]. The currently clinically applied microspheres are loaded with the high-energy beta-emitter yttrium-90 (^{90}Y : $E_{\beta\text{max}} = 2.28$ MeV, $I_{\beta} = 100\%$; $T_{1/2} = 64.1$ h) and have either a glass matrix (TheraSphere[®], MDS Nordion Inc., Kanata, Ontario, Canada) or are resin-based (SIR-Spheres[®], SIRTeX Medical Ltd., Sydney, New South Wales, Australia). Tumor selectivity is based on the difference in blood supply between liver tumors and the non-tumorous liver parenchyma, which is exclusively arterial and mainly portal, respectively [3,4]. These ^{90}Y microspheres are instilled into the hepatic artery using a catheter and predominantly accumulate peri- and endotumorally. In this way, a relatively high tumor absorbed radiation dose (hereafter referred to as “dose”) is delivered, whereas the non-tumorous liver parenchyma is largely spared. High response rates have been reported in the literature and a survival advantage is suggested [5-7]. A major drawback of the use of the radioisotope ^{90}Y is the lack of gamma emission, limiting imaging options of the microspheres’ distribution. Bremsstrahlung single photon emission tomography (SPECT) or whole body scintigraphy can be acquired but quantitative analysis (*i.e.*, revealing exact dose information) of these images is not possible due to the intrinsically low spatial resolution, significant noise, and difficulties with attenuation and scatter correction [8,9]. As direct dosimetry of these ^{90}Y microspheres is not possible, technetium-99m labeled albumin aggregates ($^{99\text{m}}\text{Tc-MAA}$) are used as surrogates to predict the distribution of the ^{90}Y microspheres. It is assumed that the distribution of the $^{99\text{m}}\text{Tc-MAA}$ accurately mimics that of the ^{90}Y microspheres, which may not necessarily be the case [10,11]. Apart from ^{90}Y microspheres, poly(L-lactic acid) microspheres have been developed, loaded with the combined beta-gamma emitter holmium-166 ($^{166}\text{Ho-PLLA-MS}$) (^{166}Ho : $E_{\beta\text{max}} = 1.77$ and 1.85 MeV, $I_{\beta} = 48.7$ and 50.0% , respectively; $E_{\gamma} = 80.6$ keV, $I_{\gamma} = 6.71\%$; $T_{1/2} = 26.8$ h), which are thought to have some favorable characteristics, particularly on the part of visualization options [12-14]. The low-energy gamma emission allows that, instead of using $^{99\text{m}}\text{Tc-MAA}$, a small scout dose of the $^{166}\text{Ho-PLLA-MS}$ can be administered to predict the distribution of the therapeutic dose. This scout dose is essential to evaluate the effectiveness of the pretreatment coiling of relevant vasculature which is done to ensure only intrahepatic distribution

of the therapeutic dose will take place. Furthermore, the scout dose could be used to calculate the doses that would be delivered on the liver tumors and the liver parenchyma by the therapeutic amount of activity of ^{166}Ho -PLLA-MS. Accordingly, based on the relative dose distribution of the scout dose, the correct amount of radioactivity that ought be instilled could be determined. Several methods are available to perform dose calculations. The most commonly used method is the MIRD schema (Medical Internal Radiation Dose Committee) [15]. The MIRD schema uses precalculated S values, where S values are defined as the mean dose to a target organ per total disintegrations of a particular radionuclide in a source organ. The Olinda/EXM software [16] provides a user-friendly code to calculate the patient dosimetry for a radiopharmaceutical, based on quantitative measurements of activity uptake in physiologically active organs at relevant time-points. However, in MIRD a uniform organ-activity distribution is assumed as well as complete intrahepatic absorption of the emitted beta-energy, and, as a rule, in radionuclide therapy, both assumptions are not in agreement with reality. Furthermore, instead of the real anatomy of the patient, the method is based on specific phantoms. A method that corresponds better with the factual, habitually erratic distribution of the radioactivity is voxelized Monte Carlo (MC) simulation, based on quantitative SPECT reconstruction. However, MC simulation is a relatively time-consuming undertaking. In this paper, a dose-point kernel convolution (PK) method was therefore investigated which may be a real-time alternative with acceptable accuracy. the applicability of the above-mentioned methods (MIRD, MC simulation, and PK based dosimetry) for both ^{166}Ho and ^{90}Y hepatic dosimetry was investigated in a non-tumorous pig liver using autoradiography.

MATERIALS & METHODS

Aim

Existing radiation dose calculation models capable of creating 3-D dose distributions need to be evaluated for applicability in hepatic dosimetry for ^{166}Ho -PLLA-MS therapy. A MC model was used to assess the intrahepatic 3-D dose distribution based on ^{166}Ho autoradiography. These results were compared with the liver dose according to the MIRD dosimetry and by PK dosimetry. All three dosimetry methods were used to evaluate differences between ^{166}Ho and ^{90}Y dose distributions.

Autoradiography

An about 8-month old female pig with a body weight of 75 kg was hepatic arterially injected with ^{166}Ho -PLLA-MS (500 MBq, 600 mg) and then terminated. The liver was taken out, weighed (1,478 g), and embedded in a carboxymethyl cellulose (CMC) (2.5%) solution, and subsequently frozen at -20°C . In the CMC solution around the liver five 16-mm \varnothing tubes were placed which were removed after freezing, resulting in five empty cylindrical holes, which were filled with a $^{166}\text{HoCl}_3$ /CMC solution as radioactive markers and frozen. The embedded liver was cut into eight 6-mm thick slices with a floor-model band saw (C.-E. Reich GmbH, Geradstetten, Remshalden, Germany) and both sides of the slices were placed on a storage phosphor screen for autoradiography (8 min exposure time/slice) and scanned using a Storm[®] imaging system (GE Healthcare Life Sciences, Diegem, Belgium; 200 μm pixel size). The markers were used for transformation and to normalize the slices. The autoradiograph of a central slice with the five markers included is shown in Figure 1. The experiment was conducted in agreement with the local applicable Dutch law, "Wet op de dierproeven" (art. 9) (1977), and the European Convention for the Protection of Vertebrate Animals used for Experimental and Other Scientific Purposes (1986), and approved by the ethical committee for animal experimentation of the University Medical Center Utrecht, Utrecht, The Netherlands (DEC-ABC-no. 2007.III.07.092).

Activity distribution

The optical densities in the autoradiographs were used as source distribution for both the MC and the PK radiation transport calculations. Each slice was

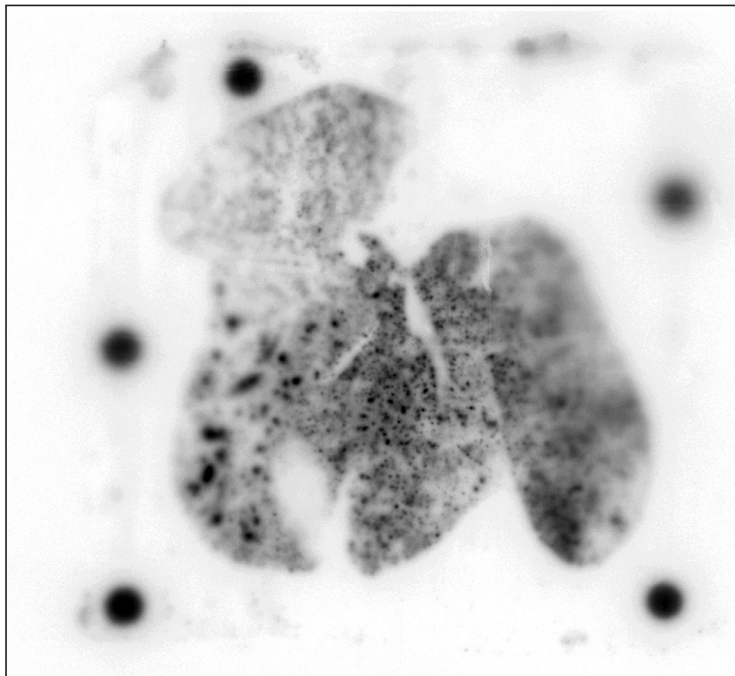


Figure 1 Autoradiograph of a central 6-mm thick slice of a pig's liver, acquired 3 days after infusion with 500 MBq ¹⁶⁶Ho-PLLA-MS. The five ¹⁶⁶Ho markers outside of the liver section are visible as large dots

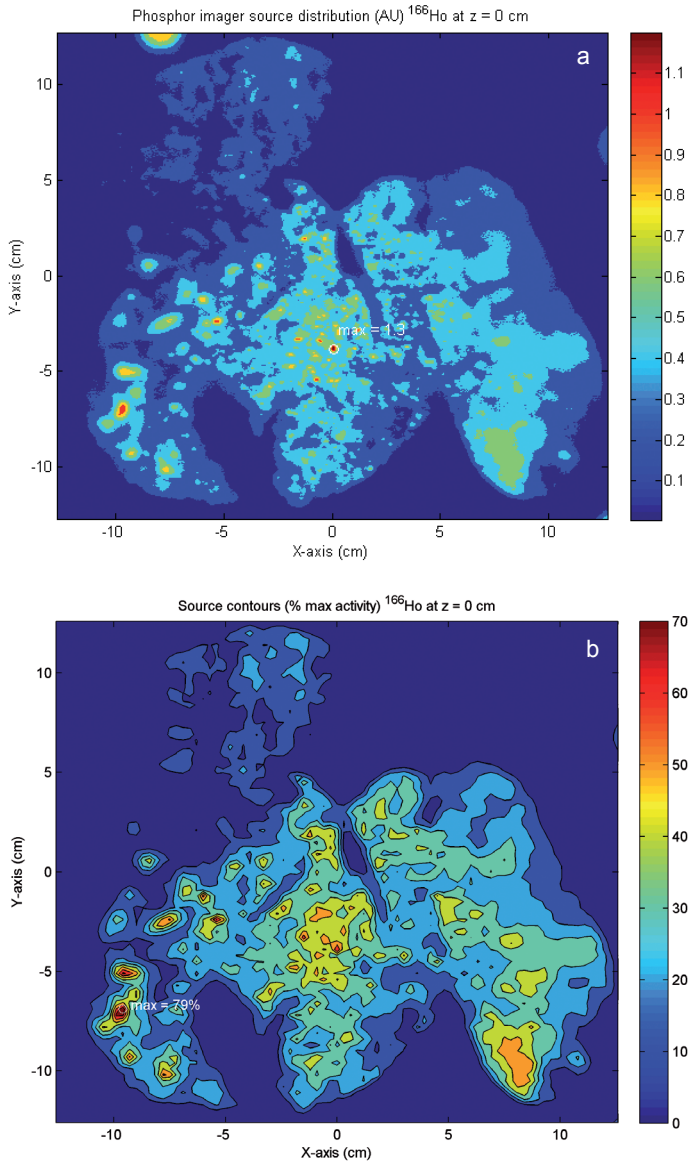


Figure 2 (a) Central slice of the digitized source distribution (voxel size $0.2 \times 0.2 \times 3 \text{ mm}^3$). The marker at the top left corner is shown deliberately to indicate its intensity. Source data from the markers were excluded from the dosimetry distributions. The colour bar shows the source intensities. (b) The central slice-distribution resampled to a $3 \times 3 \times 3 \text{ mm}^3$ voxel grid. The colour bar shows the source intensity normalized to the maximum voxel value in the 3-D volume

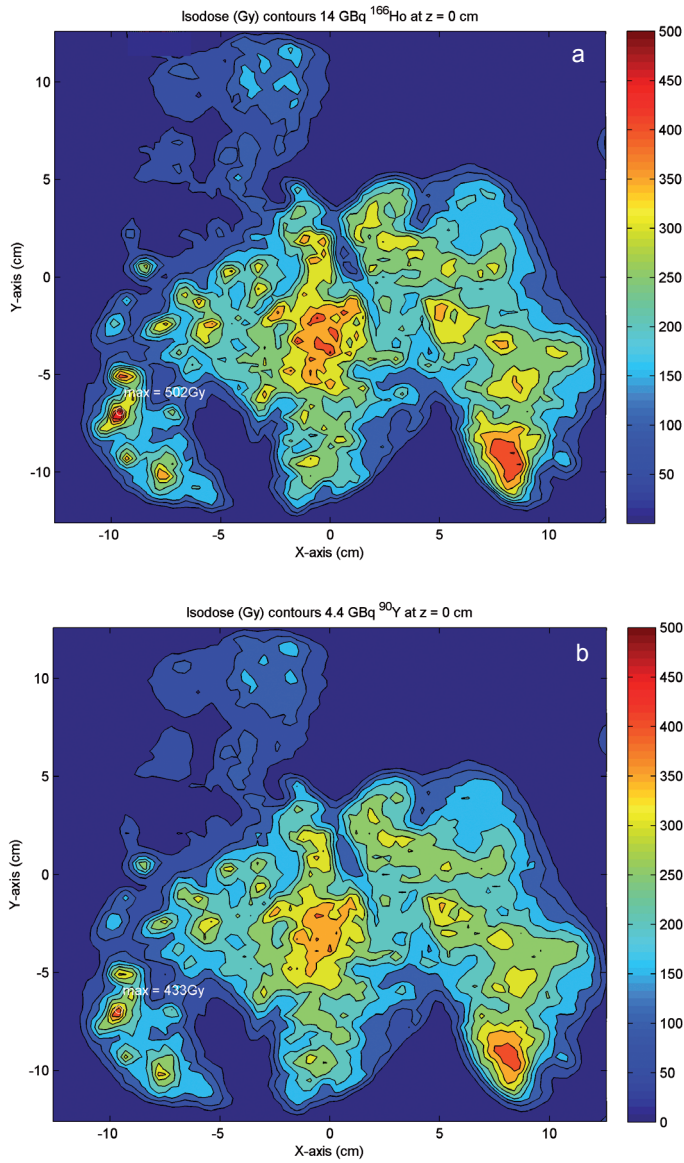


Figure 3 (a) Isodose curves calculated with MCNP5, using the source distribution shown in Figure 2b, for the ^{166}Ho dose distribution through the central liver slice, normalized to a total injected activity of 14.2 GBq. (b) Isodose curves for 4.4 GBq ^{90}Y . The maximum dose values for ^{166}Ho and ^{90}Y are depicted by white circles, and amount to 502 and 433 Gy, respectively. Both activities correspond to a mean liver dose of 150 Gy

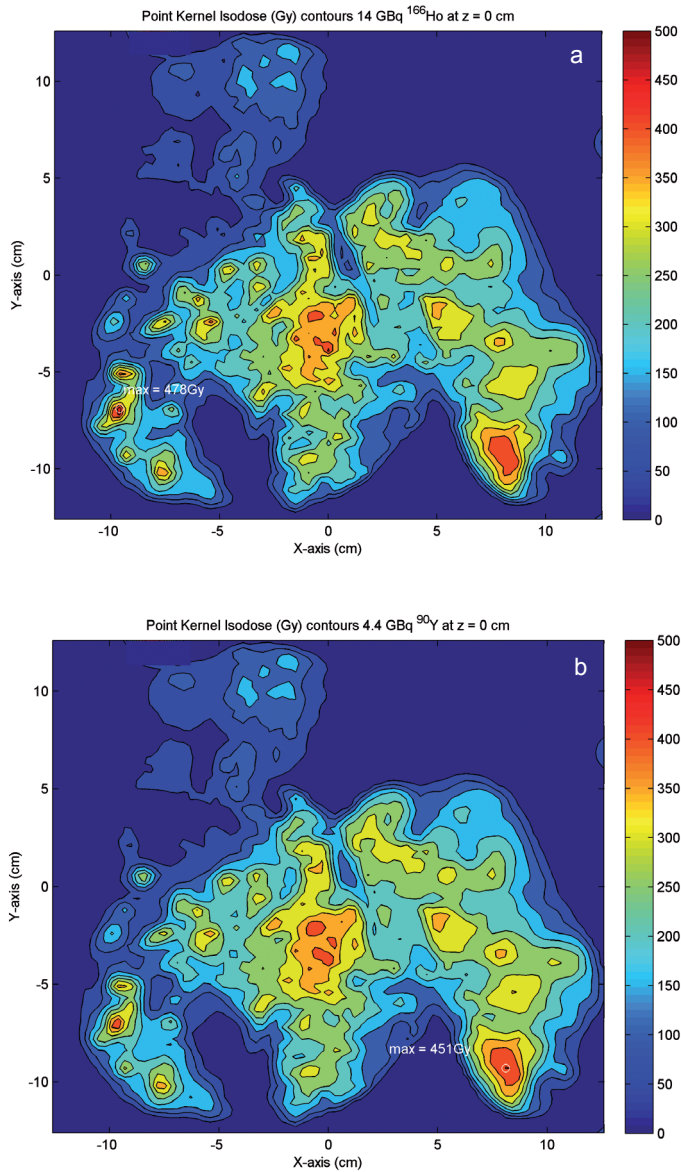


Figure 4 Isodose curves on the dose map of the central liver slice, calculated with the PK method, using the source distribution shown in Figure 2b, for (a) 14.2 GBq ¹⁶⁶Ho, and for (b) 4.4 GBq ⁹⁰Y. The maximum dose values for ¹⁶⁶Ho and ⁹⁰Y are depicted by white circles, and amount to 478 and 451 Gy, respectively. Both activities correspond to a mean liver dose of 150 Gy

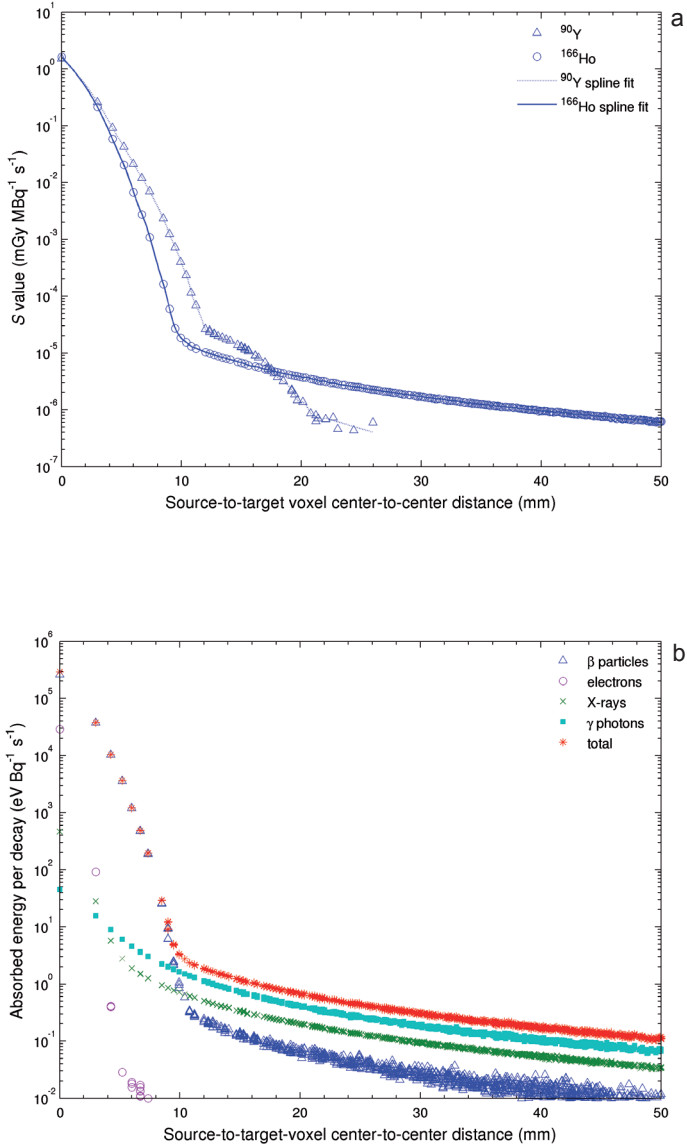


Figure 5 (a) Radionuclide S values for ¹⁶⁶Ho and ⁹⁰Y within 3-mm voxels. The S values for ¹⁶⁶Ho were determined with MCNP inside 1.06 g/cm³ liver tissue voxels and the S values for ⁹⁰Y for unit density 3-mm tissue voxels were taken from MIRD pamphlet 17, rescaled to the density of 1.06 g/cm³. The lines through the data show the spline fits used in the PK convolution. **(b)** Absorbed energy in 3-mm size voxels per decay for the emission spectrum of ¹⁶⁶Ho as a function of distance between the voxels

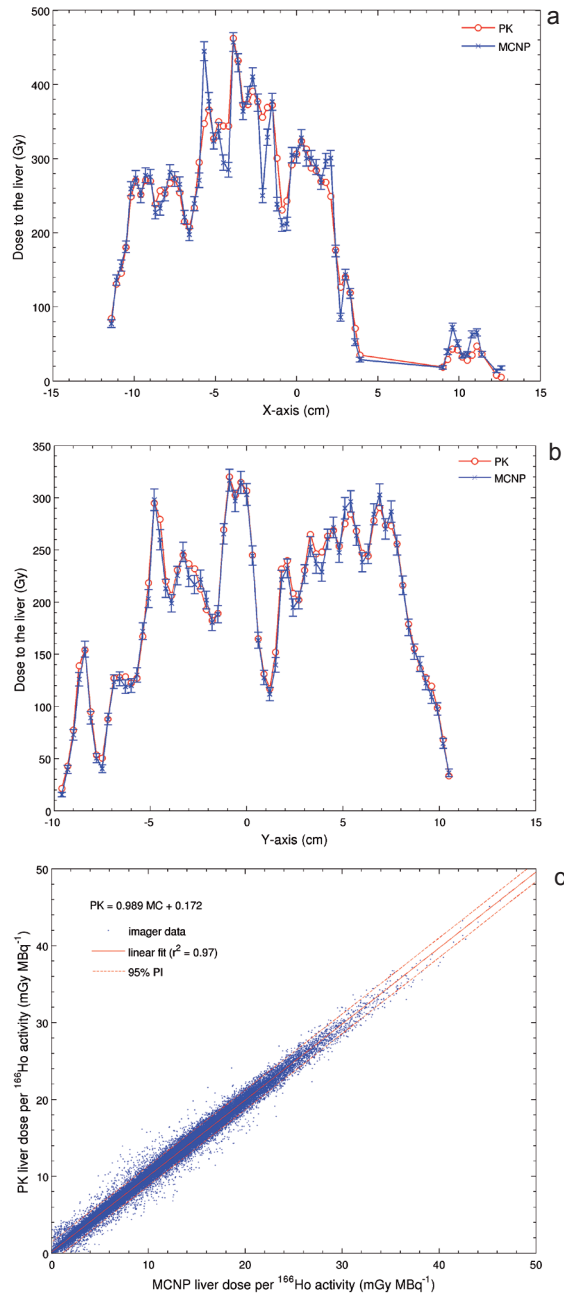


Figure 6 Comparisons between MCNP and PK dose distributions in the pig's liver, by profiles of the MCNP (with error bars, showing the statistical errors) and PK doses along $Y=0$ (a) and along $X=0$ (b) in the central plane ($Z=0$). (c) Scatter-plot of the MC voxel dose results versus the PK voxel doses for ^{166}Ho , with the least-squares linear fit through the data (solid red line) and the 95% prediction interval (dashed red lines)

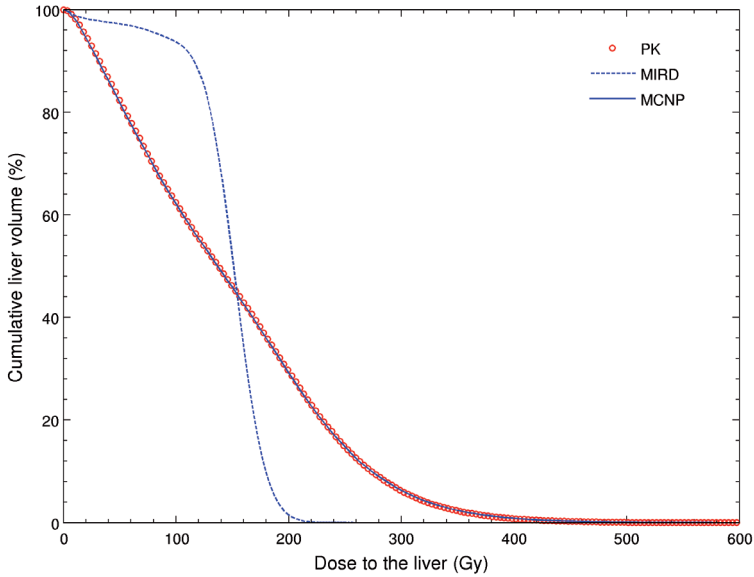


Figure 7 Cumulative Dose Volume Histogram for liver cancer therapy with 14.2 GBq ^{166}Ho based on the activity distribution measured in a pig’s liver of 1,478 g (MCNP and PK) and for a homogeneous activity distribution in the 1,400-g liver of a 15-year-old humanoid phantom (MIRD), rescaled to 1,478 g analogous to the pig’s liver

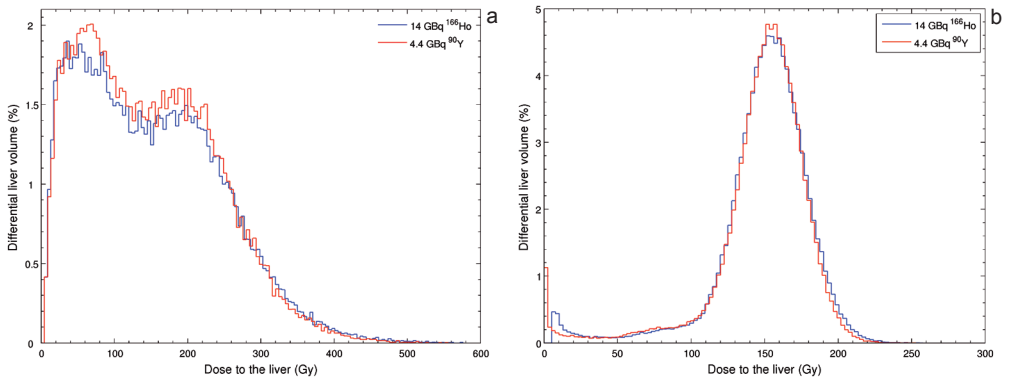


Figure 8 (a) Differential DVH for 150-Gy mean liver dose for 14.2 GBq ^{166}Ho (solid line) and for 4.4 GBq ^{90}Y (dashed line). (b) Differential DVH for homogeneous activity distributions of 4.4 GBq ^{90}Y and 14.2 GBq ^{166}Ho in the liver of the 15-year-old MIRD phantom

Table 1 Elemental composition (% by mass) and density (g/cm³) of normal tissue (ORNL Report TM-8381) and liver tissue (ICRU Report 44)

<i>Element composition</i>	<i>Normal tissue</i>	<i>Liver tissue</i>
Hydrogen	10.45	10.2
Carbon	22.66	13.9
Nitrogen	2.49	3.0
Oxygen	63.53	71.6
Sodium	0.11	0.2
Phosphor	0.13	0.3
Sulphur	0.20	0.3
Chloride	0.13	0.2
Potassium	0.21	0.3
Density (g/cm³)	1.04	1.06

normalized by using the mean counts in the ROIs drawn around the 5 markers in each slice, using the software package ImageJ (National Inst. of Health, U.S.; <http://rsb.info.nih.gov/ij/>). Alignment of the autoradiographs was achieved by rigid transformation based on the marker positions. The autoradiographs of the bottom and top of each slice were combined into a 3-D volume with a slice thickness of 3 mm. The resulting 1275 x 1275 x 17 matrix was downsampled to a 85 x 85 x 17 matrix, yielding isotropic 3-mm voxels (Fig. 2). No correction was made for the electron transport contribution from activity deposits lying deeper in the liver slice. The liver was segmented by setting the threshold for the source distribution such to obtain the true liver weight. This lower threshold value was also used for gamma-ray background subtraction. The liver composition (shown in Table 1) and its density (1.06 g/cm³) were taken from ICRU¹ report 44 [17]. The total number of 51,655 voxels within the segmented liver volume yielded a volume of 1,395 cm³ and a weight of 1,478 g.

¹ International Commission on Radiation Units and Measurements

Table 2 Beta-ray, low-energy electron, X-ray and gamma-ray spectrum from the 26.8-h half-life radionuclide ^{166}Ho used in the calculations (RADAR web-site). The beta-spectrum (100% beta's per decay; $E_{\text{mean}} = 0.665$ MeV and $E_{\text{max}} = 1.857$ MeV) was obtained from the same reference

<i>Radiation</i>	<i>Energy (MeV)</i>	<i>Intensity per decay (%)</i>
β	0.0519	0.31
β	0.1149	0.95
β	0.6509	48.70
β	0.6936	50.00
Auger electron L	0.0055	27.80
Conversion electron K	0.0231	11.50
Auger electron K	0.0397	0.63
Conversion electron L	0.0708	26.50
Conversion electron M	0.0784	6.44
Conversion electron N+	0.0801	1.76
L – X-Ray	0.0070	8.30
$K\alpha_2$ – X-Ray	0.0482	3.10
$K\alpha_1$ – X-Ray	0.0491	5.50
$K\beta$ – X-Ray	0.0557	2.25
γ	0.0806	6.71
γ	1.3794	0.93
γ	1.5819	0.19
γ	1.6625	0.12

MC calculations

The source distribution from the voxelized autoradiographs was used as input within the Monte Carlo code MCNP (MCNP5 vs. 1.20; LANL, Los Alamos, NM). The default particle physics setting for MCNP was used (energy cut-off at 1 keV, photo-electric effect and coherent photon scattering turned on, Bremsstrahlung and X-ray production by electrons). All calculations were performed on a 2.6

GHz dual-core Pentium PC with 2 GB RAM. Inside a homogeneous 18.5-cm radius sphere of normal tissue, a 25.5 x 25.5 x 5.4 cm box was used to represent the liver, discretized on a 3-mm size voxel grid. The ¹⁶⁶Ho beta-, gamma- and X-ray energy spectra were taken from the RADAR (RAAdiation Dose Assessment Resource) web-site [18] and used as sources in separate input files (see Table 2). The dose distribution was also calculated for the beta spectrum of ⁹⁰Y. The source voxel distribution was randomly sampled, and the sample points were randomly positioned inside each source voxel. The absorbed energy in all voxels inside the liver box was recorded. The numbers of particle histories (15 million beta particles (¹⁶⁶Ho and ⁹⁰Y) and 500,000 gamma photons) were chosen to obtain a statistical error below 5% in each liver voxel. The particle transport of the low-energy conversion- and Auger-electrons was not calculated as the range for these particles in tissue is well below the 3-mm voxel size; the total electron energy (27 keV/decay) can be considered to be locally deposited in each source voxel. The outputs from the MC calculations were handled in Matlab (Version 2008a, The MathWorks, Inc., Natick, MA, US) to calculate dose distributions and dose volume histograms (DVH). The dose per voxel was calculated with the assumption of complete trapping of activity in the liver using equation 1.

$$D = \frac{k\tilde{A}\sum_i n_i E_i \phi}{m} = \frac{k IA/\lambda \sum_i n_i E_i \phi}{m} \Rightarrow D/IA = \frac{k \sum_i n_i E_i \phi}{\lambda m} \quad (1)$$

With D the dose [mGy], IA the injected amount of activity [MBq], k the proportionality constant ($0.1602 \frac{mGy}{MBq} / \frac{MeV}{Bq.g}$), λ the radionuclide decay constant [s^{-1}], m the voxel mass [g], and $\sum_i n_i E_i \phi$ the absorbed energy per decay in each voxel [$MeV Bq^{-1} s^{-1}$].

PK calculations

The PK calculations were performed in Matlab by summing over all possible source-target distances using equation 2 to calculate the dose D_i in each voxel i , with $A(j)$ the activity in each source voxel j and $|r_j - r_i|$ the distance between the source and target voxel.

Table 3 Absorbed fractions of energy ϕ for the ^{166}Ho emissions and the S values calculated with MCNP, with the PK method, and according to the Olinda/EXM code. The MIRD model based S values were corrected for the pig's liver weight of 1,478 g instead of 1,400 g

<i>Dose model</i> <i>^{166}Ho spectrum</i>	β -particles ϕ (%)	γ -photons ϕ (%)	S value (mGy MBq⁻¹ s⁻¹)
MCNP phosphor image	97.1	14.0	7.40 E-5
PK phosphor image	97.9	10.7	7.43 E-5
MCNP MIRD 15-yr	97.9	18.0	7.54 E-5
MIRD 15-year-old	96	16	7.58 E-5

$$D_i = \sum_{j \in \text{liver}} A(j) \cdot PK(r_j - r_i) \quad (2)$$

The PK dose function was calculated by using MC in a 3-mm voxel structure similar to MIRD pamphlet 17 [19]. The tissue composition of the voxels was the same as in the MC model (ICRU44 liver tissue). A 15 × 15 × 15 cubical voxel grid was chosen to calculate the doses in each voxel when the activity was homogeneously distributed in a corner voxel. The numbers of particle histories were chosen to obtain statistical errors for the beta particles below 5% within 15-mm range of the source voxel (100 million beta particles), and for the gamma photons below 5% everywhere (40 million gamma photons). Besides beta particles and gamma photons, also the transport of the low-energy electrons and the X-rays was calculated, separately (40 million histories, each). In each voxel the absorbed energies of all radiation components were summed, weighed by their abundance according to Table 2. The absorbed energies were converted to dose per activity with equation 1. The voxel doses were sorted according to the mid-point distance between the source and target voxels; multiple entries for the same distance were averaged, weighted by its MC accuracy. The voxel-based point kernel for ^{90}Y from the MIRD pamphlet 17 [19] could be used to calculate the ^{90}Y dose distributions inside the liver. As the density of the tissue used in MIRD pamphlet 17 is 1.00 g/cm³, the ^{90}Y PK was rescaled to the ICRU liver density of 1.06 g/cm³. The PK convolution was calculated for the same segmentation volume as was used in the MC calculation.

Table 4 Absorbed fractions of energy ϕ for the ^{90}Y beta-spectrum and the S values calculated with MCNP, with the PK method (from MIRD pamphlet 17), and according to the Olinda/EXM code. The MIRD-model based S values were corrected for the pig's liver weight of 1,478 g instead of 1,400 g

<i>Dose model</i> ^{90}Y spectrum	β -particles ϕ (%)	S value (mGy MBq $^{-1}$ s $^{-1}$)
MCNP phosphor image	95.8	9.72 E-5
PK phosphor image	96.5	9.75 E-5
MCNP MIRD 15-yr	96.4	9.77 E-5
MIRD 15-year-old	100	1.01 E-4

MIRD-liver phantom calculation

The 1400-g liver of a 15-year-old according to the MIRD family of stylized models [20] was modeled in MCNP to verify the voxelization step. The liver was superimposed on a 3-mm voxel grid and the activity, for both ^{90}Y and ^{166}Ho , was assumed to be homogeneously distributed over the whole liver. The number of particle histories used was lower than in the autoradiography calculations (5 million beta particles and 1 million gamma-ray events), as only the mean dose and the dose volume histogram were of interest and not the exact isodose distributions per slice. The statistical error of the results in each voxel was still below 10%. The mean dose to the liver was compared with the S value (or dose conversion factor) from the internal dose calculation code Olinda/EXM [16].

RESULTS

Dose distributions were calculated with MCNP in 3-mm size voxels for activity distributions according to the liver autoradiography data. Results for the MC calculations of the autoradiography source model took long in order to obtain sufficiently high accuracy. With the PK method there is a clear advantage in that these calculations are performed much quicker. The absorbed fractions of energy and resulting S values are shown in Tables 3 and 4, as are the Olinda/EXM values. The results for the 15-year-old MIRD phantom's liver are valid for a 1400-g liver;

the dose values are adjusted for the actual liver weight. The isodose curves for the central liver slice for ^{166}Ho (Fig. 3a) calculated with MCNP agree very well with the ^{90}Y isodose curves (Fig. 3b). The PK method results were almost identical to the MCNP results (Fig. 4).

PK results

The resulting *S* values for the 3 mm-size voxels are shown in Figure 5a. In comparison to the voxel-based ^{90}Y point kernel given in MIRD pamphlet 17, the ^{166}Ho PK falls off more sharply, due to its lower beta-energy. The gamma-spectrum component of ^{166}Ho dominates at distances beyond 10 mm (Fig. 5b). The good correlations of the PK voxel doses with the MC results are shown in Figure 6; on average, the PK dose is $0.59\% \pm 0.03\%$ (mean \pm SEM) higher than the MCNP dose.

Dose Volume Histograms

The cumulative dose volume histograms in Figure 7 show again that overall the PK method results compare very well with the MCNP results. The MIRD result for a homogeneous activity distribution inside the liver of the 15-year-old child phantom shows a completely different distribution. The dose volume distribution in the MIRD model is Gaussian shaped, with only a small volume receiving a low dose. In contrast, the MCNP and PK results show that 10% of the liver volume receives a dose lower than 34 Gy and a minimum dose of 3 Gy. The mean dose to the liver is comparable between MCNP and PK. 146.5 Gy and 147.0 Gy, respectively ($p=0.35$). The differential dose volume histograms, as calculated by MCNP, for a mean liver dose of 150 Gy by ^{166}Ho and ^{90}Y are shown in Figure 8a. The ^{166}Ho and the ^{90}Y results both show a much broader dose distribution than assumed in the MIRD model (Fig. 8b). The DVH data can be fitted with a summed Gaussian curve ($r^2 = 0.97$), with one peak at a low dose of 46 Gy (34 Gy FWHM²) and a second peak at 173 Gy (89 Gy FWHM). There is no significant difference between the peaks found for ^{90}Y and ^{166}Ho . The MIRD-based DVH can be fitted with a single Gaussian ($r^2 = 0.99$) with a FWHM of 21 Gy.

² Full width at half maximum

DISCUSSION

The dose to the liver delivered in hepatic arterial radioembolization with high-energy beta-emitting microspheres is not homogeneously distributed. In fact, the distinctly inhomogeneous intrahepatic dose distribution is exactly the explanation for the liver to be able to tolerate the instillation of high amounts of radioactivity. The common practice of reporting mean doses to the liver in ^{90}Y radioembolization using the MIRD schema [12,21] should therefore be considered with care. In radioembolization using ^{166}Ho -PLLA-MS, which is to be clinically introduced soon, the distribution of the radioactivity in the normal liver and in the liver tumors, can conceivably be predicted using a small scout dose of the same microspheres. For accurate tumor and normal-liver tissue dosimetry, both to assess the probability of tumor response and to calculate the percentage of the normal liver that will be at risk of an excessive radiation dose, average dose estimation is not sufficient. Dosimetry through MC simulations would be the superior method but, due to time constraints, it is not the most practical method. The voxel-based PK convolution method, faster by several orders of magnitude and requiring less specific expertise, would be the preferred method. The dose distributions calculated with MCNP and PK do not differ significantly. This might not be the case if the liver's density map is taken into account. Boundary effects have not been studied and it is on pragmatic grounds that PK is considered a quick alternative for MC inside homogenous tissue.

In this paper, the usefulness of MIRD, MCNP, and the PK convolution method for intra-arterial radioembolization using ^{166}Ho -PLLA-MS has been explored in a non-tumor bearing pig liver *via* phosphor imaging. The present calculation of the dose distribution inside the liver of a healthy pig for ^{166}Ho -PLLA-MS, based on autoradiography data, shows a broad distribution, which is not represented by a normal distribution. Although it has been demonstrated that healthy pigs can clinically tolerate very high liver doses, the presence of tumors in the liver, especially in case of considerable tumor burden, and tumor neovascularization, could have (positive) consequences for the dose delivered on the normal liver, and perhaps also on the dose distribution in the normal liver. Follow-up studies in tumor-bearing livers of human origin are planned that will address this issue.

Based on MCNP and PK analysis of the dose distribution according to

the autoradiography of the 6-mm liver slices, a significant percentage of the liver would be liable to receive a dose higher than 30-35 Gy, classically the limiting dose for the normal liver [22,23]. However, this generally accepted dose limit is derived from the experiences in patients that had received external beam radiation therapy to the liver, of which the dose rate is much higher. It is plausible that the tolerable dose of the normal liver parenchyma in internal radiation therapy is of another order of magnitude. Nevertheless, if 9.62 MBq/g liver tissue, in the form of ^{166}Ho -PLLA-MS, would have been injected, which corresponds to an average (MIRD) dose of 150 Gy, 98%, 90%, and 91% of the liver would receive a dose higher than 30 Gy according to the MIRD, MCNP, and PK methods, respectively. Aside from the absence of tumors which would reduce the dose to the normal liver, these results are primarily associated with the model that was used. The liver slices had a thickness of 6 mm because thinner slices could not be handled without breaking the CMC-embedded slices. The implication of this is that the measured radioactivity distribution was blurred (beta and gamma contributions from deeper layers), resulting in a decreased heterogeneity, causing an overestimation in the low-dose regions and an underestimation in the high-dose regions. This was partly corrected for by gamma-background subtraction. An additional loss of heterogeneity is introduced by post-processing, *i.e.*, down-sampling and thresholding. By down-sampling the autoradiographs to a 3-mm size voxel grid, effectively a large part of the beta transport was averaged out. The influence of the threshold value used both for segmentation of the liver slices and background correction was considerable. As can be observed in Figure 2a, the digitized source distribution of the liver does not exactly match the liver contour of Figure 1. This is inherent to the threshold value approach, which excludes tissue with low activity and includes parts outside the liver where optical densities in the autoradiographs were measured due to resolution effects. This last phenomenon is observed for activity depositions near the boundary of liver tissue and embedding material. Again, this will decrease the heterogeneity in this approach and, more importantly, decrease the volume receiving a dose under 30 Gy. In the DVH corresponding to the non-background corrected activity distribution, the two peaks of the double Gaussian fit shifted nearer to each other around the mean of 150 Gy.

The FWHM of the PK's is much smaller than the resolution of clinical SPECT (>1 cm) which, in general, will result in dose overestimation in low-

dose areas. The establishment of new dose limits might be required if relatively low-resolution SPECT images have to be used to predict tumor response and liver-tissue toxicity, as is the case for internal radionuclide therapy. Other issues raised here, in particular the effect of blurring, must be taken into account in individualized dosimetry. Additional research needs to be performed, especially on the influence of the relatively low clinical SPECT resolution on the dose distribution.

CONCLUSION

MIRD is insufficient for realistic dosimetry calculations as required in hepatic arterial radioembolization, due to the inherently inhomogeneous distribution of microspheres. An alternative and very effective method is MCNP, which unfortunately is relatively time-consuming. Therefore, the accuracy of the PK method was investigated in an *ex vivo* pig liver. The PK results were very similar to the MCNP results and were obtained several orders of magnitude faster. PK is therefore an attractive method to calculate dose distributions in the liver, making it feasible to calculate the amount of activity required for an effective treatment, based on the distribution of a small scout activity of ^{166}Ho -PLLA-MS. The overestimations in the low-dose regions and the underestimations in the high-dose regions, as observed in both the MCNP and PK results, were not related to these methods, but rather to inaccuracies in the underlying source distribution. This resulted in a dose distribution less heterogeneous than the true dose distribution. Especially the overestimation in the low dose regions could pose a problem in the pretreatment assessment in which a 30-Gy dose is usually applied as the limit above which liver toxicity is expected to occur. This dose limit should be reassessed on its correctness, not just because of this overestimation but also because higher doses may be tolerated by the liver in this type of radiation therapy.

Acknowledgments

Financial support by the Dutch Technology Foundation STW under grant 06069 is gratefully acknowledged. The authors would also like to thank Mr. Willem van Wolferen for his assistance in the preparation of the liver slices.

REFERENCES

1. Gulec SA, Fong Y. Yttrium 90 microsphere selective internal radiation treatment of hepatic colorectal metastases. *Arch. Surg.* **2007**;142:675-682.
2. Salem R, Thurston KG. Radioembolization with yttrium-90 microspheres: a state-of-the-art brachytherapy treatment for primary and secondary liver malignancies: part 3: comprehensive literature review and future direction. *J. Vasc. Interv. Radiol.* **2006**;17:1571-1593.
3. Breedis C, Young G. The Blood Supply of Neoplasms in The Liver. *Am. J. Pathol.* **1954**;30:969-977.
4. Bierman HR, Byron RL, Jr., Kelley KH, Grady A. Studies on the blood supply of tumors in man. III. Vascular patterns of the liver by hepatic arteriography in vivo. *J. Natl. Cancer Inst.* **1951**;12:107-131.
5. Vente MAD, Wondergem M, Van der Tweel I, Van den Bosch MAAJ, *et al.* Yttrium-90 microsphere radioembolization for the treatment of liver malignancies: a structured meta-analysis. *Eur. Radiol.* **2008**;19:951-959.
6. Salem R, Lewandowski RJ, Atassi B, Gordon SC, *et al.* Treatment of unresectable hepatocellular carcinoma with use of ⁹⁰Y microspheres (TheraSphere): safety, tumor response, and survival. *J. Vasc. Interv. Radiol.* **2005**;16:1627-1639.
7. Van Hazel G, Blackwell A, Anderson J, Price D, *et al.* Randomised phase 2 trial of SIR-Spheres plus fluorouracil/leucovorin chemotherapy versus fluorouracil/leucovorin chemotherapy alone in advanced colorectal cancer. *J. Surg. Oncol.* **2004**;88:78-85.
8. Sarfaraz M, Kennedy AS, Lodge MA, Li XA, *et al.* Radiation absorbed dose distribution in a patient treated with yttrium-90 microspheres for hepatocellular carcinoma. *Med. Phys.* **2004**;31:2449-2453.
9. Sandström M, Lubberink M, Lundquist H. Quantitative SPECT with Yttrium-90 for Radionuclide Therapy Dosimetry. *Eur. J. Nucl. Med. Mol. Imaging* **2007**;32:S260.
10. Koch W, Tatsch K. Nuclear medicine procedures for treatment evaluation. In: Bilbao JJ, Reiser M F (eds.) *Liver Radioembolization with ⁹⁰Y Microspheres*, 1st edn. Springer, Heidelberg **2008**;75-91.
11. Gupta T, Virmani S, Neidt TM, Szolc-Kowalska B, *et al.* MR tracking of iron-labeled glass radioembolization microspheres during transcatheter delivery to rabbit VX2 Liver Tumors: Feasibility Study. *Radiology* **2008**;249:845-854.
12. Vente MAD, Nijssen JFW, De Wit TC, Seppenwoolde JH, *et al.* Clinical effects of transcatheter hepatic arterial embolization with holmium-166 poly(L-lactic acid) microspheres in healthy pigs. *Eur. J. Nucl. Med. Mol. Imaging* **2008**;35:1259-1271.
13. Zielhuis SW, Nijssen JFW, De Roos R, Krijger GC, *et al.* Production of GMP-grade radioactive holmium loaded poly(l-lactic acid) microspheres for clinical application. *Int. J. Pharm.* **2006**;311:69-74.
14. Nijssen JFW, Zonnenberg BA, Woittiez JR, Rook DW, *et al.* Holmium-166 poly lactic acid microspheres applicable for intra-arterial radionuclide therapy of hepatic malignancies: effects of preparation and neutron activation techniques. *Eur. J. Nucl. Med.* **1999**;26:699-704.

15. Loevinger R, Budinger T, Watson E. MIRD Primer for absorbed dose calculations. **1988**.
16. Stabin MG, Sparks RB, Crowe E. OLINDA/EXM: the second-generation personal computer software for internal dose assessment in nuclear medicine. *J. Nucl. Med.* **2005**;46:1023-1027.
17. International Commission on Radiation Units and Measurements. Tissue substitutes in radiation dosimetry and measurement, ICRU Report 44. Bethesda, MD **1989**.
18. Stabin MG, Siegel JA. Physical models and dose factors for use in internal dose assessment. *Health Phys.* **2003**;85:294-310.
19. Bolch WE, Bouchet LG, Robertson JS, Wessels BW, *et al.* MIRD pamphlet No. 17: the dosimetry of nonuniform activity distributions—radionuclide S values at the voxel level. Medical Internal Radiation Dose Committee. *J. Nucl. Med.* **1999**;40:11S-36S.
20. Cristy M, Eckerman K. Specific absorbed fractions of energy at various ages from internal photon sources. Oak Ridge National Laboratory. Oakridge, TN **1987**.
21. Gulec SA, Mesoloras G, Stabin M. Dosimetric techniques in ⁹⁰Y-microsphere therapy of liver cancer: The MIRD equations for dose calculations. *J. Nucl. Med.* **2006**;47:1209-1211.
22. Cromheecke M, Konings AW, Szabo BG, Hoekstra HJ. Liver tissue tolerance for irradiation: experimental and clinical investigations. *Hepatogastroenterology* **2000**;47:1732-1740.
23. Ingold J, Reed G, Kaplan H, Bagshaw M. Radiation hepatitis. *Am. J. Roentgenol. Radium Ther. Nucl. Med* **1965**;93:200-208.

CHAPTER 7

Yttrium-90 microsphere radioembolization for the treatment of liver malignancies: A structured meta-analysis

**Maarten A.D. Vente
Maurits Wondergem
Ingeborg van der Tweel
Maurice A.A.J. van den Bosch
Bernard A. Zonnenberg
Marnix G.E.H. Lam
Alfred D. van het Schip
Johannes F.W. Nijsen**

European Radiology, 2009;19:951-959

ABSTRACT

Radioembolization with yttrium-90 microspheres (^{90}Y -RE), either glass- or resin-based, is increasingly applied in patients with unresectable liver malignancies. Clinical results are promising but overall response and survival are not yet known. Therefore, a meta-analysis on tumor response and survival in patients who underwent ^{90}Y -RE was conducted. Based on an extensive literature search, six groups were formed. Determinants were cancer type, microsphere type, chemotherapy protocol used, and stage (deployment in firstline or as salvage therapy). For colorectal liver metastases (mCRC), in a salvage setting, response was 79% for ^{90}Y -RE combined with 5-fluorouracil/leucovorin (5-FU/LV), and 79% when combined with 5-FU/LV/oxaliplatin or 5-FU/LV/irinotecan, and in a first-line setting 91% and 91%, respectively. For hepatocellular carcinoma (HCC), response was 89% for resin microspheres and 78% for glass microspheres. No statistical method is available to assess median survival based on data presented in the literature. In mCRC, ^{90}Y -RE delivers high response rates, especially if used neoadjuvant to chemotherapy. In HCC, ^{90}Y -RE with resin microspheres is significantly more effective than ^{90}Y -RE with glass microspheres. The impact on survival will become known only when the results of phase III studies are published.

INTRODUCTION

Internal radiation therapy through transarterial delivery of beta-emitting yttrium-90 (^{90}Y)-loaded microspheres, often referred to as ^{90}Y radioembolization (^{90}Y -RE), is an emerging technique for the treatment of patients with unresectable primary or metastatic liver tumors [1,2]. The efficacy of this radioembolization technique is based on the fact that intrahepatic malignancies derive their blood supply almost entirely from the hepatic artery, as opposed to the normal liver, which mainly depends on the portal vein for its blood supply [3]. The microspheres are injected selectively into the proper hepatic artery and subsequently become lodged in the microvasculature surrounding the tumor. Very high irradiation doses are delivered to the tumors, whereas the surrounding liver parenchyma is largely spared [4].

Two FDA-approved ^{90}Y microsphere products are in clinical use at present: TheraSphere[®] (MDS Nordion Inc., Kanata, Ontario, Canada), which are glass microspheres, and the resin-based SIR-Spheres[®] (SIRTeX Medical Ltd., Sydney, New South Wales, Australia) (Table 1). The glass microspheres are approved for use in radiation treatment or as a neoadjuvant to surgery or transplantation in patients with hepatocellular carcinoma (HCC). The resin microspheres have FDA premarket approval for the treatment of hepatic metastatic colorectal cancer (mCRC), with adjuvant hepatic arterial infusion of floxuridine. However, patients suffering from other liver dominant cancers have also undergone therapy with these ^{90}Y microspheres. These include, among others, liver metastases of breast cancer, pancreatic cancer, and neuroendocrine tumors [5,6]. Since in most studies that have been published the majority of patients underwent ^{90}Y -RE in a salvage setting, and most of the literature comprised phase I and II studies with small patient numbers, the overall response and real impact on survival are not known. In order to assess the effect of ^{90}Y -RE for primary and secondary liver malignancies, a systematic meta-analysis has been performed of the available literature.

Table 1 Yttrium-90 microsphere products characteristics

Microsphere product	Yttrium-90 characteristics		Matrix material	Density (g/ml)	Diameter (μm)	Administered amount of particles (mg)	Administered number of particles	Standard dose (MBq)	Activity per microsphere (Bq)		
	$T_{1/2}$ (h)	Cross section ^a (barn)								β -energy (keV)	Mean tissue range (mm)
TheraSphere [®] (MDS Nordion Inc.)	64.0	1.3	2,280 (100%)	3.9	glass	3.3	25 \pm 10	110 ^b	4,000,000	5,000	1,250 ^b -2,500
SIR-Spheres [®] (SIRTeX Ltd.)					resin	1.6	32 \pm 10	1,370 ^b	50,000,000	3,000	50 ^b

^a Thermal neutron cross section of yttrium-89

^b Calculated values

METHODS

Identification of studies

A comprehensive search was carried out, using several databases from 1986 onwards, in order to identify relevant studies. The following search strategy was used to search the MEDLINE database with PubMed: (“yttrium” [MeSH Terms] OR yttrium [Text Word]) AND (“liver” [MeSH Terms] OR liver [Text Word]). The limit “humans” was used. The EMBASE database was searched with the limit “human” using: (“yttrium”/exp OR “yttrium”) AND (“liver”/exp OR “liver”). The Cochrane library database was searched with the keywords “yttrium” and “liver”. The search was completed by screening the reference lists and related articles of all relevant articles found. In addition, the presentations given at a workshop held in Chicago 4-5 May 2007 (“Emerging Trends in Radioembolization Using Microspheres: A Clinical Workshop”) and the list of publications in the clinicians’ section of the webpage of SIRTeX Medical Ltd. [7] and the Resource Library on the webpage of MDS Nordion Inc. [8] were screened.

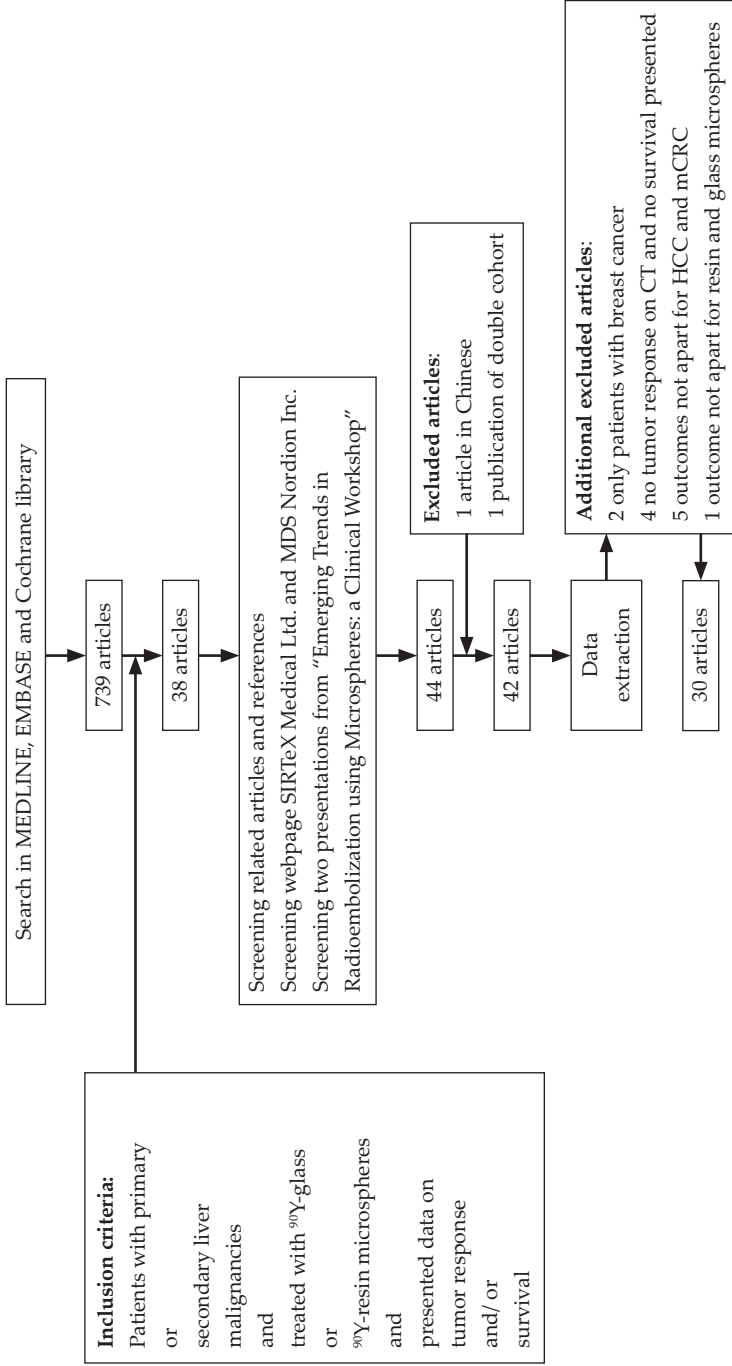
Inclusion and exclusion criteria

All abstracts of relevant studies were reviewed with a set of predefined inclusion and exclusion criteria. All articles from 1986 onwards which presented data concerning tumor response or survival of patients with primary or secondary liver malignancies after treatment with ⁹⁰Y glass or ⁹⁰Y resin microspheres were included for further data extraction. This resulted in 44 articles (Fig. 1). Articles written in a language other than English or German were excluded; articles that presented data that was thought to have been presented previously were used once. Consequently, one article was excluded because it was written in Chinese, and another was excluded since it was thought to present data that were also presented in an article on another, larger trial. This resulted in 42 articles from which data were extracted.

Data extraction

After the initial assessment for inclusion, the following data were extracted from the 42 articles selected: study design, number, and demographic data of patients; minor extrahepatic disease included/excluded, previous therapies targeted on the liver tumor, administered dosage, site of microsphere delivery, use of angiotensin

Figure 1 Flowchart



II, number of microsphere treatments, (neo)adjuvant therapies, tumor response measured by CT, MRI, and/or ^{18}F -FDG-PET, serum markers measurements (CEA, AFP), time to progression, and survival.

After initial data extraction, the exclusion criteria were reassessed. It became clear that most studies presented adequate data on patients with HCC or with mCRC, and that response was usually measured by CT. The meta-analysis was therefore limited to these two tumor types. In order to perform a meta-analysis, additional exclusion criteria were incorporated. Articles that did not present data about HCC and/or mCRC and articles only presenting data on groups with mixed primary disease were excluded from the meta-analysis. Articles that did not present tumor response measured by CT-scans or that did not present data on median survival times were also excluded. Following the additional exclusion criteria, an additional 12 articles were excluded from the meta-analysis.

Data structuring

The 30 remaining articles were divided into two groups, according to tumor type, *i.e.*, mCRC or HCC. The pathology of these two types of liver tumors is very different. Colorectal carcinoma initially metastasizes to one or a few focal parts of the liver, whereas HCC usually spreads diffusely throughout the liver. Response to chemotherapy is also very different in these tumor types. This resulted in the formation of two groups (mCRC and HCC), for which the studies were compared on design and patient population, in order to assess the comparability of the results.

In the group of patients with mCRC, after data extraction the use of different (generations of) chemotherapy regimens was identified as a major source of heterogeneity. Two covariates were therefore included in the meta-regression model: (1) whether the older generation of cytostatic agents (5-FU/LV or floxuridine) or the newer generation (5-FU/LV + oxaliplatin (FOLFOX) or 5-FU/LV + irinotecan (FOLFIRI)) was used, and (2) whether ^{90}Y -RE was given as a salvage therapy or as a first-line treatment with adjuvant chemotherapy. No separation was made between the microsphere product that was used (glass or resin) because of the small number of patients with mCRC treated with the glass microspheres (ca. 8%).

In view of the chemoresistant nature of HCC [9], previously given therapy was not observed as a source of heterogeneity. Therefore, the main source of heterogeneity observed in this group was the microsphere product used, either glass or resin. This resulted in the formation of two subgroups.

To allow comparability of results with regard to tumor response, the category of 'any response' (AR) was introduced. The AR category comprises all patients originally from the categories complete response, partial response, and stable disease.

Meta-analysis

The study of Andrews *et al.* [10] included just one HCC patient. This patient was therefore not included in the analysis. The proportions of patients with AR were modeled by a meta-regression analysis according to Hamza *et al.* [11]. This method uses the exact binomial likelihood approach instead of an approximate method based on the normal distribution of within-study variability. A random effects model was applied since considerable heterogeneity was observed between the studies. The meta-regression analysis was performed using PROC NL MIXED in SAS version 9.1, as described by Hamza *et al.*

RESULTS

Thirty articles were included in the meta-analysis. In 999 out of 1,217 patients, tumor response was assessed by CT. The proportion of AR for HCC and mCRC combined varied between 0.29 and 1.00 with a median value of 0.82. Treatment with glass microspheres showed a lower response (AR=0.77) than treatment with resin microspheres (AR=0.85) ($p=0.07$), with an estimated odds ratio of 0.56 (95%-CI 0.29-1.06).

Colorectal liver metastases

In a total of 19 eligible studies, 792 patients with mCRC had undergone $^{90}\text{Y-RE}$ [5,10,12-28]. In 18 studies, tumor response was assessed in a total of 681 patients. Of these patients, 486/681 had received $^{90}\text{Y-RE}$ in a salvage setting, of which 124/486 had been previously treated and/or co-treated with 5-FU/LV or floxuridine, and 362/486 had been given the newer-generation cytostatic agents. One hundred

ninety-five patients had received ^{90}Y -RE as a first-line treatment, of which 175/195 were treated with adjuvant 5-FU/LV or floxuridine and 20/195 with FOLFOX.

The specific cytostatic agent(s) (“old” versus “new”) that were used did not affect response ($p=0.96$). Whether ^{90}Y -RE was offered in a salvage setting or as a first-line therapy affected tumor response significantly ($p=0.07$). The estimated proportions of AR, based on the regression model, were 0.79 and 0.79 in salvage setting and 0.91 and 0.91 in the first-line, for the older and newer chemotherapy, respectively.

Median survival after ^{90}Y -RE, irrespective of differences in determinants (microsphere type, chemotherapy protocol, and stage: salvage or first-line), varied from 6.7 to 17.0 months. The reported median survival from diagnosis of mCRC ranged from 10.8 to 29.4 months (Table 2).

Two randomized controlled trials were performed in patients with unresectable mCRC. In 2001, Gray *et al.* [13] presented the results for 76 patients who had been randomized to either ^{90}Y -RE (resin) as neoadjuvant to hepatic arterial infusion (HAI) of floxuridine or to HAI alone. Patients in the combination arm showed a significantly greater response when measured by tumor volume, and a significantly increased time to progression. AR was 78% and 59% ($p=0.03$) for the combination arm and the HAI-alone arm, respectively, and time to progression, based on tumor area measurements, was 15.9 months vs. 9.7 months ($p=0.001$), respectively. In 2004, Van Hazel *et al.* [14] reported on the outcome in 21 previously untreated patients with mCRC in a similar study, in which it was demonstrated that the addition of a single administration of resin microspheres prior to 5-FU/LV significantly increased response, time to progression, and survival. In this phase II trial, AR was 100% in the combination arm vs. 60% in the chemotherapy-alone arm ($p<0.001$), time to progression 18.6 and 3.6 months ($p<0.0005$), respectively, and survival 29.4 and 12.8 months ($p=0.02$). Thirty-six months post-randomization, 36% of patients in the combination arm were still alive whereas no patients from the 5-FU/LV-alone arm were alive at that time.

Hepatocellular carcinoma

In 14 articles, clinical data were presented on tumor response and survival for 425 patients with HCC who had received ^{90}Y -RE [10,17,23,29-39]. Twelve studies

Table 2 Tumor responses and median survivals after ⁹⁰Y-RE in mCRC

Study	Number (n)	Results		Tumor response on CT										Median survival (months)	
		CT performed in	Response measured at (months post ⁹⁰ Y-RE)	RECIST ^a (%)	CR (%)	PR (%)	SD (%)	AR (%)	PD (%)	From diagnosis	From ⁹⁰ Y-RE				
Resin microspheres															
Gray <i>et al.</i> (1992) [13]	29	22	3	-	0	45	37	82	18	NR	NR	NR	NR	NR	
Stubbs <i>et al.</i> (1999) [29]	30	27	3	-	0	70	19	89	11	10.8 (range 1.9-41.0)	6.7 (range 1.0-15.8)				
Gray <i>et al.</i> (2000) [28]	71	51	3	-	0	75	12	86	14	17.3	9.9				
Gray <i>et al.</i> (2001) ^b [14]	36	36 ^c	3	-	6	44	28	78	14	NR	17.0				
Stubbs <i>et al.</i> (2001) [16]	50	44	3	-	0	73	18	91	9	14.5 (range 1.9-91.4)	9.8 (range 1.0-30.3)				
Van Hazel <i>et al.</i> (2004) ^b [15]	11	11	3	yes	0	91	9	100	0	29.4	NR				
Lim <i>et al.</i> (2005a) [18]	30	30	2	yes	0	33	27	60	40	NR	NR				
Lim <i>et al.</i> (2005b) [19]	32	32	2	yes	0	31	28	59	41	NR	NR				
Murthy <i>et al.</i> (2005) [17]	12	9	NR	yes	0	0	56	56	44	24.6	4.5				
Mancini <i>et al.</i> (2006) [20]	35	35	1.5	yes	0	12	76	88	13	NR	NR				
Kennedy <i>et al.</i> (2006) [21]	208	208	3	-	0	36	55	91	10	NR	NR			Responders 10.5 Non-responders 4.5	
Stubbs <i>et al.</i> (2006) [22]	100	80	3	-	1	73	20	94	6	16.2 (range 1.1-101.6)	11 (range 0.1-76.6)				
Jakobs <i>et al.</i> (2007) [24]	18	18	2-3	-	0	NS	NS	76	24	NR	NR				
Sharma <i>et al.</i> (2007) [23]	20	20	3	yes	0	90	10	100	0	NR	NR				
Glass microspheres															
Anderson <i>et al.</i> (1992) [25]	7	7	2	-	0	0	86	86	14	NR	11 (range 5-25+)				
Andrews <i>et al.</i> (1994) [11]	17	17	2	-	0	29	29	59	41	NR	13.8				
Wong <i>et al.</i> (2002) [26]	8	8	3	-	12	12	38	63	38	NR	NR				
Lewandowski <i>et al.</i> (2005) [27]	27	26	3	-	0	35	52	87	13	NR	9.3 (95%-CI 7.2-13.3)				
Sato <i>et al.</i> (2008) [6]	51	51	5.3	-	NR	NR	NR	NR	NR	NR	15.2				

CR complete response, PR partial response, SD stable disease, AR any response (= CR + PR + SD), PD progressive disease, NR not reported, NS not specified

^a Response measured and presented according to RECIST criteria [40]

^b Response and survival for ⁹⁰Y-RE arm alone

^c CT of 3 out of 36 patients not assessable

presented data of tumor response for a total of 318 patients. Treatment with resin microspheres was associated with a significantly higher proportion of AR than glass microsphere treatment (0.89 vs. 0.78 ($p=0.02$)).

Median survival was reported in 7 studies, in which survival time was defined as survival from treatment or from diagnosis or recurrence. Median survival from microsphere treatment varied between 7.1 and 21.0 months, and median survival from diagnosis or recurrence was 9.4-24.0 months (Table 3).

DISCUSSION

This meta-analysis showed that in patients with mCRC the tumor response of $^{90}\text{Y-RE}$ is high, with AR rates of approximately 80% in a salvage setting, and over 90% when used as first-line treatment, as neoadjuvant to chemotherapy. The response rates reported for studies, in which 5FU/LV was combined with irinotecan or oxaliplatin, were similar to those of studies in which only 5FU/LV was used. This can probably be explained by differences in the criteria for tumor response that were used (WHO versus RECIST criteria [40]).

Regarding the question which microsphere is most effective in the treatment of mCRC – glass or resin – no conclusions can be reached since only 8% of the patients with mCRC were treated with the glass microspheres. Furthermore, the meta-analysis showed that resin microspheres were significantly more effective in treating HCC than the glass microspheres (AR 89% vs. 78% ($p=0.02$)). This is a rather unexpected finding because it is the glass microspheres which are FDA approved for treating HCC, whereas the resin microspheres are approved for mCRC, not HCC. It may be postulated that this outcome is the consequence of the substantial difference in numbers of microspheres that are infused: a dose of glass microspheres consists of 4 million microspheres, whereas a dose of resin microspheres usually contains 50 million microspheres [41]. It has been reported in the literature that administration of resin microspheres had to be prematurely halted, before the predetermined amount of radioactivity was instilled, due to macroscopic embolization [42]. In contrast, the relatively very low number of glass microspheres per dose is associated with microscopic embolization [38]. However, the low number of particles infused in the case of the glass microspheres may be a disadvantage when targeting a tumor type that is often diffusely spread throughout the liver at time of diagnosis [43]; the radiation dose

Table 3 Tumor responses and median survivals after ⁹⁰Y-RE in HCC

Study	Number		Results													From ⁹⁰ Y-RE				
	(n)	CT performed in	Tumor response on CT			RECIST ^a			SD (%)			AR (%)			PD (%)			Median survival (months)		
			Response measured at (months post ⁹⁰ Y-RE)	CR (%)	PR (%)	SD (%)	AR (%)	PD (%)	From diagnosis (or recurrence)											
Resin microspheres																				
Lau <i>et al.</i> (1994) [31]	18	18	2	-	0	44	89	11												7.1
Lau <i>et al.</i> (1998) [32]	71	71	2	-	0	27	92	8												NR
Lim <i>et al.</i> (2005b) [19]	5	4	2	yes	0	25	75	25												NR
Sangro <i>et al.</i> (2006) [33]	24	21	2	-	NS	NS	88	12												7.1 (95%-CI 2.1-12)
Jakobs <i>et al.</i> (2007) [24]	5	5	2-3	yes	0	NS	100	0												NR
Glass microspheres																				
Houle <i>et al.</i> (1989) [34]	7	7	NR	-	0	0	29	71												NR
Andrews <i>et al.</i> (1994) [11]	1	1	2	-	0	0	0	100												NR
Dancey <i>et al.</i> (2000) [35]	22	19	2-3	-	5	16	58	21												12 (range 2-42)
Carr <i>et al.</i> (2004) [36]	65	65	3	-	3	28	40	71												NR
Geschwind <i>et al.</i> (2004) [30]	100	NR	NR	NR	NR	NR	NR	NR												Okuda I 12 (95%-CI 2-42) Okuda II 10 (95%-CI 6-20)
Liu <i>et al.</i> (2004) [37]	11	11	1-1.5	-	9	72	0	82												NR
Salem <i>et al.</i> (2005) [38]	43	43	varying	-	NS	NS	NS	79												Okuda I 24 (95%-CI 18-28) Okuda II 12 (95%-CI 9-17)
Kulik <i>et al.</i> (2006) [40]	35	34	6 (0.8-16)	-	NS	NS	NS	88												NR
Sato <i>et al.</i> (2006) [39]	19	19	5 (1.5-14)	-	NS	NS	NS	79												NR

CR complete response, PR partial response, SD stable disease, AR any response (= CR + PR + SD), PD progressive disease, NR not reported, NS not specified
^a response measured and presented according to RECIST criteria [40]

would be distributed in and around the tumors too heterogeneously to be able to deliver a tumoricidal dose to the entire lesion, even if the total amount of radioactivity of a dose of glass microspheres is at least 50% higher than is the case in the resin microspheres (Table 1). Another (theoretical) consideration is that the macroembolic effect of the resin microspheres is accompanied by a greater lack of oxygen resulting in ischemia and therefore enhanced efficacy. On the other hand, shortage of oxygen might also diminish the tumoricidal effect of ionizing radiation due to a lack of oxygen radicals that is produced in this environment.

However, this macroembolic effect can be associated with clinical signs, the so-called post-embolization syndrome (PES), which is reported to frequently occur after resin microspheres infusion, but not often subsequent to administration of the minimally embolic glass microspheres. PES is characterized by fatigue, nausea, fever, right upper quadrant pain, and/or vomitus, all of which are transitory and can be effectively controlled by outpatient medication [20,38,44-46].

Serious complications have been reported if microspheres were inadvertently deposited in excessive amounts in organs other than the liver. Conditions that have been reported include gastrointestinal ulceration/bleeding, gastritis/duodenitis, cholecystitis, pancreatitis, and radiation pneumonitis [41,44,47-51]. Training, careful patient selection, meticulous pre-treatment assessment, and coiling of relevant vasculature reduce complication rates massively [52]. Radiation-induced liver disease following ^{90}Y -RE has been reported sporadically [14,53]. Careful patient selection and individualized dose calculation minimize the risk of this complication. Profound and persistent lymphopenia, with rapid onset and in some cases lasting over 12 months, though without clinical consequences, has been reported in patients with HCC following ^{90}Y -RE with glass microspheres [35,37]. This complication has not been observed subsequent to ^{90}Y -RE with resin microspheres (as monotherapy). The underlying mechanism is not clear but myelosuppression is not probable since leaching of radioactivity from the glass microspheres does not take place [54]. However, following ^{90}Y -RE, in addition to the liver tumors and to some extent the liver parenchyma, a radiation dose is delivered to the blood each time it passes the liver, which might explain this laboratory adverse event.

Unfortunately, in this meta-analysis, overall tumor response could only

be assessed as 'any response', which is caused by the reality that response categories were not uniformly defined in the analyzed studies. It is expected that this problem of being able to compare tumor response will disappear in the near future, since the RECIST criteria, published in 2001 [40], are evermore applied. In accordance with the RECIST criteria, tumor response in malignant liver disease is assessed using cross-sectional anatomic imaging (CT, MRI), by measuring tumor size. However, lesion size reduction does not always occur, even if treatment is effective. This is associated with different peri- and endotumoral processes that can occur post $^{90}\text{Y-RE}$, *e.g.*, peritumoral edema and hemorrhage, and ring enhancement [55]. Therefore, actual tumor response may often be better than is reported, based on CT measurements alone. In a significant number of cases 'stable disease' could actually be minor, partial, or even complete response. In order to improve sensitivity in assessing tumor response, it is therefore strongly recommended that $^{18}\text{F-FDG-PET}$ or functional MRI (diffusion-weighted MRI) is added to post-treatment response assessment protocols [55-58].

Only two randomized controlled trials were found in the literature, both on resin microspheres and mCRC. The results were encouraging, showing a major survival benefit for the $^{90}\text{Y-RE}$ + chemo arm. However, since then larger controlled trials have commenced, in which more effective chemotherapeutics were used [59].

In this paper, the emphasis was placed on $^{90}\text{Y-RE}$ in patients with unresectable HCC and mCRC. Nonetheless, patients with liver metastases from primaries other than mCRC have been treated with $^{90}\text{Y-RE}$. This is particularly the case for liver metastasized breast cancer, of which response rates of over 90% are reported [60,61]. $^{90}\text{Y-RE}$ has been applied in patients with neuroendocrine liver metastases, too, albeit in small numbers [10,62]. Reported response rates were 100%, and it would therefore be worthwhile to further explore the use of $^{90}\text{Y-RE}$ for this indication.

Fortunately, $^{90}\text{Y-RE}$ is not the only novel and effective treatment option offered to patients with unresectable HCC. Recently, a breakthrough has been reported in the field of biological agents. For sorafenib (Nexavar®, Bayer Healthcare AG, Leverkusen, Germany), an oral multikinase inhibitor, a statistically significant and clinically meaningful improvement in survival has been shown in HCC patients with advanced disease: 10.7 months in the sorafenib group

versus 7.9 months in the placebo group ($p=0.0006$) [63]. Recently, a phase I/II trial has started in which patients with unresectable HCC are treated with the resin microspheres plus sorafenib [59].

The clinical efficacy of other promising molecular agents, *e.g.*, bevacizumab, erlotinib, is currently investigated as well. When added to FOLFOX or XELOX (capecitabine + oxaliplatin), the angiogenesis inhibitor bevacizumab (Avastin®, Genentech Inc., South San Francisco, CA, USA) has been proven to prolong survival of patients with colorectal cancer by approximately six months compared with FOLFOX or XELOX alone [64,65]. In fact, in an ongoing multicenter study, the “FAST” trial, patients with unresectable colorectal liver metastases are treated concurrently with FOLFOX or FOLFIRI, bevacizumab, and ⁹⁰Y-RE (resin microspheres) [66].

In conclusion, ⁹⁰Y-RE is associated with high response rates, both in a salvage and in a first-line setting. The true impact on survival will only become known after publication of several ongoing and/or to be initiated phase III studies. The results of trials in which ⁹⁰Y-RE and modern chemotherapy agents are combined with novel biological agents are awaited with interest as well.

Acknowledgments

Financial support by the Dutch Technology Foundation STW (grant 06069) is gratefully acknowledged.

REFERENCES

1. Salem R, Thurston KG. Radioembolization with yttrium-90 microspheres: a state-of-the-art brachytherapy treatment for primary and secondary liver malignancies: part 3: comprehensive literature review and future direction. *J. Vasc. Interv. Radiol.* **2006**;17:1571-1593.
2. Vente MAD, Hobbelink MGG, Van het Schip AD, Zonnenberg BA, Nijsen JFW. Radionuclide liver cancer therapies: from concept to current clinical status. *Anticancer Agents Med. Chem.* **2007**;7:441-459.
3. Bierman HR, Byron RL, Jr., Kelley KH, Grady A. Studies on the blood supply of tumors in man. III. Vascular patterns of the liver by hepatic arteriography in vivo. *J. Natl. Cancer Inst.* **1951**;12:107-131.
4. Gulec SA, Fong Y. Yttrium 90 microsphere selective internal radiation treatment of hepatic colorectal metastases. *Arch. Surg.* **2007**;142:675-682.
5. Sato KT, Lewandowski RJ, Mulcahy MF, Atassi B, *et al.* Unresectable chemorefractory liver metastases: radioembolization with 90Y microspheres—safety, efficacy, and survival. *Radiology* **2008**;247:507-515.
6. Murthy R, Kamat P, Nunez R, Madoff DC, *et al.* Yttrium-90 microsphere radioembolotherapy of hepatic metastatic neuroendocrine carcinomas after hepatic arterial embolization. *J. Vasc. Interv. Radiol.* **2008**;19:145-151.
7. SIRTex Medical Ltd. Publications (international). Available via <http://www.sirtex.com/content.cfm?sec=usa&MenuID=1120&ID=F4CC0AB7>. Accessed 1 May 2008.
8. MDS Nordion Inc. Publications. Available via <http://www.nordion.com/therasphere/physicians-publications-eu.asp>. Accessed 1 May 2008.
9. Carr BI. Hepatocellular carcinoma: current management and future trends. *Gastroenterology* **2004**;127:S218-S224.
10. Andrews JC, Walker SC, Ackermann RJ, Cotton LA, *et al.* Hepatic radioembolization with yttrium-90 containing glass microspheres: preliminary results and clinical follow-up. *J. Nucl. Med.* **1994**;35:1637-1644.
11. Hamza TH, Van Houwelingen HC, Stijnen T. The binomial distribution of meta-analysis was preferred to model within-study variability. *J. Clin. Epidemiol.* **2008**;61:41-51.
12. Gray BN, Anderson JE, Burton MA, Van Hazel G, *et al.* Regression of liver metastases following treatment with yttrium-90 microspheres. *Aust. N. Z. J. Surg.* **1992**;62:105-110.
13. Gray B, Van Hazel G, Hope M, Burton M, *et al.* Randomised trial of SIR-Spheres plus chemotherapy vs. chemotherapy. *Ann. Oncol.* **2001**;12:1711-1720.
14. Van Hazel G, Blackwell A, Anderson J, Price D, *et al.* Randomised phase 2 trial of SIR-Spheres plus fluorouracil/leucovorin chemotherapy versus fluorouracil/leucovorin chemotherapy alone in advanced colorectal cancer. *J. Surg. Oncol.* **2004**;88:78-85.
15. Stubbs RS, Cannan RJ, Mitchell AW. Selective internal radiation therapy with

- ⁹⁰yttrium microspheres for extensive colorectal liver metastases. *J. Gastrointest. Surg.* **2001**;5:294-302.
16. Murthy R, Xiong H, Nunez R, Cohen AC, *et al.* Yttrium 90 resin microspheres for the treatment of unresectable colorectal hepatic metastases after failure of multiple chemotherapy regimens: preliminary results. *J. Vasc. Interv. Radiol.* **2005**;16:937-945.
 17. Lim L, Gibbs P, Yip D, Shapiro JD, *et al.* Prospective study of treatment with selective internal radiation therapy spheres in patients with unresectable primary or secondary hepatic malignancies. *Intern. Med. J.* **2005**;35:222-227.
 18. Lim L, Gibbs P, Yip D, Shapiro JD, *et al.* A prospective evaluation of treatment with Selective Internal Radiation Therapy (SIR-spheres) in patients with unresectable liver metastases from colorectal cancer previously treated with 5-FU based chemotherapy. *BMC. Cancer* **2005**;5:132.
 19. Mancini R, Carpanese L, Sciuto R, Pizzi G, *et al.* A multicentric phase II clinical trial on intra-arterial hepatic radiotherapy with ⁹⁰yttrium SIR-spheres in unresectable, colorectal liver metastases refractory to i.v. chemotherapy: preliminary results on toxicity and response rates. *In Vivo* **2006**;20:711-714.
 20. Kennedy AS, Coldwell D, Nutting C, Murthy R, *et al.* Resin ⁹⁰Y-microsphere brachytherapy for unresectable colorectal liver metastases: Modern USA experience. *Int. J. Radiat. Oncol. Biol. Phys.* **2006**;65:412-425.
 21. Stubbs RS, O'Brien I, Correia MM. Selective internal radiation therapy with ⁹⁰Y microspheres for colorectal liver metastases: single-centre experience with 100 patients. *ANZ. J. Surg.* **2006**;76:696-703.
 22. Sharma RA, Van Hazel GA, Morgan B, Berry DP, *et al.* Radioembolization of liver metastases from colorectal cancer using yttrium-90 microspheres with concomitant systemic oxaliplatin, fluorouracil, and leucovorin chemotherapy. *J. Clin. Oncol.* **2007**;25:1099-1106.
 23. Jakobs TF, Hoffmann RT, Poepperl G, Schmitz A, *et al.* Mid-term results in otherwise treatment refractory primary or secondary liver confined tumours treated with selective internal radiation therapy (SIRT) using ⁹⁰Yttrium resin-microspheres. *Eur. Radiol.* **2007**;17:1320-1330.
 24. Anderson JH, Goldberg JA, Bessent RG, Kerr DJ, *et al.* Glass yttrium-90 microspheres for patients with colorectal liver metastases. *Radiother. Oncol.* **1992**;25:137-139.
 25. Wong CY, Salem R, Raman S, Gates VL, Dworkin HJ. Evaluating ⁹⁰Y-glass microsphere treatment response of unresectable colorectal liver metastases by [¹⁸F]FDG PET: a comparison with CT or MRI. *Eur. J. Nucl. Med. Mol. Imaging* **2002**;29:815-820.
 26. Lewandowski RJ, Thurston KG, Goin JE, Wong CY, *et al.* ⁹⁰Y microsphere (TheraSphere) treatment for unresectable colorectal cancer metastases of the liver: response to treatment at targeted doses of 135-150 Gy as measured by [¹⁸F]fluorodeoxyglucose positron emission tomography and computed tomographic imaging. *J. Vasc. Interv. Radiol.* **2005**;16:1641-1651.
 27. Gray B, Van Hazel G, Buck M, Paton G, *et al.* Treatment of colorectal liver metastases with SIR-Spheres plus chemotherapy. *GI Cancer* **2000**;3:249-257.

28. Stubbs RS, Cannan RJ, Mitchell AW, Alwan MH. An initial experience with selective internal radiation therapy (SIRT) for non-resectable colorectal liver metastases. *GI Cancer* **1999**;3:135-143.
29. Geschwind JF, Salem R, Carr BI, Soulen MC, *et al.* Yttrium-90 microspheres for the treatment of hepatocellular carcinoma. *Gastroenterology* **2004**;127:S194-S205.
30. Lau WY, Leung WT, Ho S, Leung NW, *et al.* Treatment of inoperable hepatocellular carcinoma with intrahepatic arterial yttrium-90 microspheres: a phase I and II study. *Br. J. Cancer* **1994**;70:994-999.
31. Lau WY, Ho S, Leung TW, Chan M, *et al.* Selective internal radiation therapy for nonresectable hepatocellular carcinoma with intraarterial infusion of ⁹⁰yttrium microspheres. *Int. J. Radiat. Oncol. Biol. Phys.* **1998**;40:583-592.
32. Sangro B, Bilbao JI, Boan J, Martinez-Cuesta A, *et al.* Radioembolization using ⁹⁰Y-resin microspheres for patients with advanced hepatocellular carcinoma. *Int. J. Radiat. Oncol. Biol. Phys.* **2006**;66:792-800.
33. Houle S, Yip TK, Sheperd FA, Rotstein LE, *et al.* Hepatocellular Carcinoma: Pilot Trial of Treatment with Y-90 Microspheres. *Radiology* **1989**;172:857-860.
34. Dancy JE, Shepherd FA, Paul K, Sniderman KW, *et al.* Treatment of nonresectable hepatocellular carcinoma with intrahepatic ⁹⁰Y-microspheres. *J. Nucl. Med.* **2000**;41:1673-1681.
35. Carr BI. Hepatic arterial ⁹⁰Yttrium glass microspheres (Therasphere) for unresectable hepatocellular carcinoma: Interim safety and survival data on 65 patients. *Liver Transpl.* **2004**;10 Suppl 2:S107-S110.
36. Liu MD, Uaje MB, Al Ghazi MS, Fields D, *et al.* Use of Yttrium-90 TheraSphere for the treatment of unresectable hepatocellular carcinoma. *Am. Surg.* **2004**;70:947-953.
37. Salem R, Lewandowski RJ, Atassi B, Gordon SC, *et al.* Treatment of unresectable hepatocellular carcinoma with use of ⁹⁰Y microspheres (TheraSphere): safety, tumor response, and survival. *J. Vasc. Interv. Radiol.* **2005**;16:1627-1639.
38. Sato K, Lewandowski RJ, Bui JT, Omary R, *et al.* Treatment of Unresectable Primary and Metastatic Liver Cancer with Yttrium-90 Microspheres (TheraSphere®): Assessment of Hepatic Arterial Embolization. *Cardiovasc. Intervent. Radiol.* **2006**;29:522-529.
39. Kulik LM, Atassi B, Van Holsbeeck L, Souman T, *et al.* Yttrium-90 microspheres (TheraSphere) treatment of unresectable hepatocellular carcinoma: downstaging to resection, RFA and bridge to transplantation. *J. Surg. Oncol.* **2006**;94:572-586.
40. Therasse P, Arbuck SG, Eisenhauer EA, Wanders J, *et al.* New guidelines to evaluate the response to treatment in solid tumors. European Organization for Research and Treatment of Cancer, National Cancer Institute of the United States, National Cancer Institute of Canada. *J. Natl. Cancer Inst.* **2000**;92:205-216.
41. Murthy R, Nunez R, Szklaruk J, Erwin W, *et al.* Yttrium-90 microsphere therapy for hepatic malignancy: devices, indications, technical considerations, and potential complications. *Radiographics* **2005**;25 Suppl 1:S41-S55.
42. Pöpperl G, Helmberger T, Munzing W, Schmid R, *et al.* Selective internal radiation therapy with SIR-Spheres in patients with nonresectable liver tumors. *Cancer Biother.*

- Radiopharm.* **2005**;20:200-208.
43. Saar B, Kellner-Weldon F. Radiological diagnosis of hepatocellular carcinoma. *Liver Int.* **2008**;28:189-199.
 44. Salem R, Thurston KG. Radioembolization with ⁹⁰yttrium microspheres: a state-of-the-art brachytherapy treatment for primary and secondary liver malignancies. Part 2: special topics. *J. Vasc. Interv. Radiol.* **2006**;17:1425-1439.
 45. Coldwell D, Kennedy A. Treatment of hepatic metastases from breast cancer with Yttrium-90 SIR-Spheres radioembolization. *Society of Interventional Radiology 2005 annual meeting*, New Orleans, LA, USA.
 46. Goin J, Dancey JE, Roberts C. Comparison of post-embolization syndrome in the treatment of patients with unresectable hepatocellular carcinoma: Trans-catheter arterial chemo-embolization versus yttrium glass microspheres. *World J. Nucl. Med.* **2004**;3:49-56.
 47. Murthy R, Brown DB, Salem R, Meranze SG, *et al.* Gastrointestinal complications associated with hepatic arterial yttrium-90 microsphere therapy. *J. Vasc. Interv. Radiol.* **2007**;18:553-561.
 48. Carretero C, Munoz-Navas M, Betes M, Angos R, *et al.* Gastroduodenal injury after radioembolization of hepatic tumors. *Am. J. Gastroenterol.* **2007**;102:1216-1220.
 49. Salem R, Thurston KG. Radioembolization with ⁹⁰Yttrium microspheres: a state-of-the-art brachytherapy treatment for primary and secondary liver malignancies. Part 1: Technical and methodologic considerations. *J. Vasc. Interv. Radiol.* **2006**;17:1251-1278.
 50. Lewandowski R, Salem R. Incidence of radiation cholecystitis in patients receiving Y-90 treatment for unresectable liver malignancies. *J. Vasc. Interv. Radiol.* **2004**;15:S162.
 51. Leung TW, Lau WY, Ho SK, Ward SC, *et al.* Radiation pneumonitis after selective internal radiation treatment with intraarterial ⁹⁰yttrium-microspheres for inoperable hepatic tumors. *Int. J. Radiat. Oncol. Biol. Phys.* **1995**;33:919-924.
 52. Salem R, Lewandowski RJ, Sato KT, Atassi B, *et al.* Technical aspects of radioembolization with ⁹⁰Y microspheres. *Tech. Vasc Interv Radiol* **2007**;10:12-29.
 53. Neff R, Abdel-Misih R, Khatri J, Dignazio M, *et al.* The toxicity of liver directed yttrium-90 microspheres in primary and metastatic liver tumors. *Cancer Invest* **2008**;26:173-177.
 54. Wollner IS, Knutsen CA, Ullrich KA, Chrisp CE, *et al.* Effects of hepatic arterial yttrium-90 microsphere administration alone and combined with regional bromodeoxyuridine infusion in dogs. *Cancer Res.* **1987**;47:3285-3290.
 55. Atassi B, Bangash AK, Bahrani A, Pizzi G, *et al.* Multimodality imaging following ⁹⁰Y radioembolization: a comprehensive review and pictorial essay. *Radiographics* **2008**;28:81-99.
 56. Bienert M, McCook B, Carr BI, Geller DA, *et al.* ⁹⁰Y microsphere treatment of unresectable liver metastases: changes in ¹⁸F-FDG uptake and tumour size on PET/CT. *Eur. J. Nucl. Med. Mol. Imaging* **2005**;32:778-787.
 57. Wong CY, Qing F, Savin M, Campbell J, *et al.* Reduction of metastatic load to

- liver after intraarterial hepatic yttrium-90 radioembolization as evaluated by [¹⁸F] fluorodeoxyglucose positron emission tomographic imaging. *J. Vasc. Interv. Radiol.* **2005**;16:1101-1106.
58. Kwee TC, Takahara T, Ochiai R, Nievelstein RA, Luijten PR. Diffusion-weighted whole-body imaging with background body signal suppression (DWIBS): features and potential applications in oncology. *Eur. Radiol* **2008**;18:1937-1952.
 59. U.S. National Institutes of Health (NIH): Medical Research Center. <http://clinicalresearch.nih.gov/> Accessed 1 May 2008.
 60. Bangash AK, Atassi B, Kaklamani V, Rhee TK, *et al.* ⁹⁰Y radioembolization of metastatic breast cancer to the liver: toxicity, imaging response, survival. *J. Vasc. Interv. Radiol.* **2007**;18:621-628.
 61. Coldwell DM, Kennedy AS, Nutting CW. Use of yttrium-90 microspheres in the treatment of unresectable hepatic metastases from breast cancer. *Int. J. Radiat. Oncol. Biol. Phys.* **2007**;69:800-804.
 62. Gulec SA, Mesoloras G, Dezarn WA, McNeillie P, Kennedy AS. Safety and efficacy of Y-90 microsphere treatment in patients with primary and metastatic liver cancer: The tumor selectivity of the treatment as a function of tumor to liver flow ratio. *J. Transl. Med.* **2007**;5:15.
 63. Llovet S, Ricci V, Mazzaferro P, Hilgard P, *et al.* Sorafenib improves survival in advanced hepatocellular carcinoma (HCC): Results of a Phase III randomized placebo-controlled trial (SHARP trial). *J. Clin. Oncol.* **2007**;25:18S.
 64. Hochster HS, Hart LL, Ramanathan RK, Hainsworth JD, *et al.* Safety and efficacy of oxaliplatin/fluoropyrimidine regimens with or without bevacizumab as first-line treatment of metastatic colorectal cancer (mCRC): Final analysis of the TREE-study. *J. Clin. Oncol.* **2006**;24:148S.
 65. Hochster HS, Welles L, Hart L, Ramanathan K, *et al.* Safety and efficacy of bevacizumab (Bev) when added to oxaliplatin/fluoropyrimidine (O/F) regimens as first-line treatment of metastatic colorectal cancer (mCRC): TREE 1 & 2 Studies [Abstract]. *J. Clin. Oncol.* **2005**;23:249S.
 66. Kennedy A. ⁹⁰Y Microspheres + chemoTx first line patients with mCRC. Presented at "Emerging Trends in Radioembolization using Microspheres, a Clinical Workshop", Chicago, IL, 4-5 May **2007**.

CHAPTER 8

Interstitial microbrachytherapy using small holmium-166 acetylacetonate microspheres for radioablation of intrahepatic malignancies

Maarten A.D. Vente
Wouter Bult
Kathelijne Peremans
Hendrik Haers
Eva Vandermeulen
Peter R. Seevinck
Alfred D. van het Schip
Remmert de Roos
Chris J.G. Bakker
Gerard C. Krijger
Johannes F.W. Nijssen

Submitted

ABSTRACT

In this paper, interstitial microbrachytherapy of liver malignancies using ^{166}Ho acetylacetonate microspheres ($^{166}\text{HoAcAcMS}$), $<10\ \mu\text{m}$ in diameter, is presented as a complementary technique to radiofrequency ablation. The radioisotope ^{166}Ho was chosen for its multimodal imaging characteristics. A feasibility study in a cat with liver cancer was performed.

Materials & methods: Microspheres were prepared by solvent evaporation, using holmium acetylacetonate crystals as the sole ingredient. Microspheres were characterized using scanning electron microscopy, coulter counter analysis, and titrimetry. The microspheres were neutron activated in a nuclear reactor. A feline patient was treated twice. *In vivo* nuclear imaging was performed. Magnetic resonance imaging and X-ray computed tomography of the *ex vivo* liver was performed.

Results: The holmium loading was 45% (w/w) and the microspheres remained intact after neutron irradiation. The treatments were well tolerated and the clinical condition of the cat improved markedly. Six months after the first treatment the animal was euthanized due to disease progression.

Conclusions: $^{166}\text{HoAcAcMS}$ $<10\ \mu\text{m}$ with a high ^{166}Ho content were produced. Treatment of a cat with liver cancer was associated with a 6-months extension of survival in a relatively good condition. $^{166}\text{HoAcAcMS}$ appear to be an optimal device for microbrachytherapy. Additional preclinical studies are warranted.

INTRODUCTION

Primary liver cancer (hepatocellular carcinoma (HCC), cholangiocarcinoma) is the fifth most common cancer, worldwide. The incidence rate is over 600,000 new cases each year and the mortality rate is almost as high. Five-year survival rates are only 3-5% because the majority of patients is not eligible for surgical resection (partial hepatectomy or orthotopic liver transplantation) [1,2]. Systemic chemotherapy has proven ineffective in HCC. However, the recently introduced oral multikinase inhibitor sorafenib offers a survival benefit of several months [3]. The liver is also the most common site of metastatic spread. As many as 50% of all patients with a primary malignancy will in due course develop hepatic metastases. Metastasis confined to the liver most commonly, but not exclusively, occurs from colorectal carcinoma, of which the incidence is very high as well [4]. Globally, colorectal carcinoma ranks as the third most common cancer with approximately one million new cases every year and a mortality about half the incidence rate. Five-year survival in the developed world is about 55% [1,4]. Main prognostic factors for survival in colorectal cancer include, next to the extent of lymph node metastases, the extent of liver metastases and resectability of these lesions [5]. Lately, survival has improved owing to new first-line systemic chemotherapy protocols, consisting of 5-fluorouracil/leucovorin, combined with oxaliplatin or irinotecan, with the addition of bevacizumab, a monoclonal antibody against vascular endothelial growth factor. Currently, median survival in patients with unresectable disease is nearly two years [6,7].

Several techniques have been developed to improve resectability rates. One approach is the application of heat. It has been known for a long time that malignant tumor cells are relatively sensitive to heat [8]. Based on this knowledge, several techniques have been developed which employ hyperthermia for the selective destruction of malignant tumor cells [9]. These include, among others, the local thermoablative techniques: radiofrequency ablation (RFA), microwave coagulation therapy and laser-induced thermotherapy. The most widely used thermoablative technique is RFA, during which a needle electrode is inserted into the center of the tumor. This enables the delivery of radiofrequency waves (460-500 kHz) which are converted into frictional heat (>50°C) by ionic agitation, resulting in coagulation necrosis of neoplastic tissue [10,11]. RFA can be performed percutaneously, laparoscopically, or *via* laparotomy, under ultrasound, X-ray

computed tomography (CT), or magnetic resonance imaging (MRI) guidance [12]. RFA is an effective technique but certainly has its limitations, especially with regard to tumor size and localization [13-15]. The latter not only as in tumor (in)accessibility or adjacency to delicate structures (biliary vessels) but also because of the so-called 'heat-sink phenomenon', *i.e.*, tissue cooling by blood flow from adjacent vessels that causes thermal loss, hence incomplete tumor ablation and consequently tumor recurrence [10,16,17].

In this paper, we present a local ablation technique using small (<10 μm) holmium-166 acetylacetonate microspheres ($^{166}\text{HoAcAcMS}$) with a very high holmium-load, to be injected intratumorally, in which tumor necrosis is to be induced by beta irradiation. ^{166}Ho not only emits high-energy beta particles but gamma rays as well, which allows for nuclear imaging. This could be helpful in predicting efficacy through calculating the delivered tumor absorbed dose. Due to the paramagnetic properties of holmium, HoAcAcMS can also be visualized by MRI. The attenuation coefficient of holmium is high because of its high density [18]. Consequently, when using higher concentrations, it can function as a CT contrast agent. In addition, since the tumor destructive effect is not delivered by lesion heating but through ionization the heat-sink phenomenon should be non-existent. These $^{166}\text{HoAcAcMS}$ are therefore proposed as a complementary technique, to be deployed in the ablation of lesions that are in close vicinity of large vessels. In this article we describe the preparation and physical characteristics of the $^{166}\text{HoAcAcMS}$ and also present the results of the treatment of a feline patient with HCC with intratumoral injections of these particles.

MATERIALS AND METHODS

Microspheres preparation

The holmium acetylacetonate complex (HoAcAc) was prepared as described previously [19]. In summary, the pH of an aqueous acetylacetonate solution (1,400 ml; 16.6% w/w) was adjusted to pH 8.5 with ammoniumhydroxide. Holmium chloride (12.5 g) was dissolved in water and added to the aqueous acetylacetonate solution. Holmium acetylacetonate crystals were formed at room temperature in 24 hours. The crystals were collected and washed three times with water, and dried over Sicapent[®] (Merck Nederland B.V., Amsterdam, The Netherlands) under a constant flow (12 l min^{-1}) of nitrogen for 48 hours. The holmium acetylacetonate

microspheres were prepared using solvent evaporation; ten grams of holmium acetylacetonate crystals were dissolved in 186 g of chloroform and added to an aqueous PVA solution (2% w/w). The solution was continuously stirred at a preset stirring speed of 500 rpm. To increase the evaporation of chloroform, the solutions were thermostated at 25°C and a constant flow of nitrogen (12 l min⁻¹) was applied. After 40 hours of evaporation, the formed microspheres were collected by centrifugation and washed five times with water. The washed microspheres were sieved using a wet sieving system (Electronic Sieve Vibrator, EMS 755 and ultrasonic processor UDS 751; Topaz GmbH, Dresden, Germany) as described by Zielhuis *et al* [20]. The microspheres were dried at room temperature overnight, followed by drying at 50°C for 48 hours.

Microsphere characterization, neutron activation and dose preparation

The size distribution was determined using a Coulter counter (Multisizer 3; Beckman Coulter, Mijdrecht, The Netherlands), equipped with an orifice of 100 µm. In order to investigate surface morphology, scanning electron microscopy (SEM) was performed (Phenom; FEI Co., Eindhoven, The Netherlands). Samples were mounted on aluminum stubs and, if applicable, dried under a continuous flow of nitrogen. A 6-nm platinum layer was applied. The holmium content of the microspheres was determined by a complexometric titration with EDTA [21]. The microspheres were packed in high-density poly-ethylene (HDPE) vials (type A; Posthumus Plastics, Beverwijk, The Netherlands) and neutron activated *via* the ¹⁶⁵Ho(n,γ)¹⁶⁶Ho reaction in a nuclear reactor facility with a nominal thermal neutron flux of 5 × 10¹² cm⁻² s⁻¹ (Delft Reactor Institute, The Netherlands). After delivery at the nuclear medicine division of the Faculty of Veterinary Medicine of Ghent University (Merelbeke, Belgium), the ¹⁶⁶HoAcAcMS were suspended in 1.1 ml of distilled water containing 2% Pluronic® F-68 (Sigma-Aldrich Chemie B.V., Zwijndrecht, The Netherlands) and 10% ethanol abs. (Merck B.V., Amsterdam, The Netherlands), and subsequently transferred into ten (first treatment) or 15 (second treatment) 1-ml Luer Lock syringes prefilled with 0.2 ml of the same solution. The suspension was then mixed with 0.1 ml of air. The amount of radioactivity present in each syringe was measured in a dose calibrator (VDC-404, Veenstra Instrumenten B.V., Joure, The Netherlands). The first and second dosages were planned to consist of 1,000 MBq (100 mg) and 1,500 MBq (150 mg),

respectively. The syringe was placed into an acrylic glass cylinder (inner and outer diameter 9 and 25 mm, respectively) to limit the radiation dose to the hands during manipulation.

Patient characteristics

The patient characteristics were as follows: 14 year-old neutered male cat (European Short Hair) with biopsy-proven HCC. Findings during physical examination included impaired alertness, ataxia, emaciation (2.3 kg bodyweight) and muscle weakness, mydriasis, a dull coat, and a large palpable mass in the epigastric and mesogastric regions. The liver was extensively nodularly enlarged and, as was assessed by ultrasound examination, about 95% of its volume consisted of neoplastic tissue. Hematological and biochemical abnormalities consisted of lymphocytosis, neutropenia, prolonged PT and APTT, elevated urea, decreased total protein, elevated bilirubin, and elevated AST and ALT (Table 1). The clinical condition of this animal was very poor and the single alternative to euthanasia was decided to be an experimental palliative treatment, in this case intratumoral injections of $^{166}\text{HoAcAcMS}$.

The owner gave informed consent prior to treatment and agreed – knowing that the treatment would be of a palliative nature – that eventually the remains would be made available for further examination.

Anesthesia and analgesia

Premedication for general anesthesia consisted of midazolam (0.2 mg/kg IV). General anesthesia was induced by propofol (6 mg/kg IV) and maintained by inhalation of 1.5-2.0% isoflurane in O_2 /air (1:1). Peri- and postoperative analgesia consisted of buprenorphine (4dd 0.06 mg IV or IM) and antibacterial prophylaxis was provided by amoxicillin/clavulanic acid (4dd 0.5 ml IV or, after discharge, 2dd 37.5 mg PO). Additional medication consisted of metoclopramid (4dd 0.1 mg IV or, after discharge, 4dd 0.15 mg PO) and prednisolone (2dd 2.5 mg PO).

Administration procedure of the microspheres

Prior to the treatment procedure, an ultrasound examination was performed, including a baseline and contrast-enhanced (SonoVue[®], Bracco International, Inc., Switzerland) ultrasonographic examination, to aid in distinguishing

between normal liver parenchyma, (viable) tumors, and necrotic tissue. The $^{166}\text{HoAcAcMS}$ were injected intratumorally under ultrasound guidance. The needles that were used were 22G x 40 mm and 22G x 50 mm. The first treatment was performed during laparotomy, whereas the second treatment was carried out percutaneously.

Multimodality imaging

The *in vivo* $^{166}\text{HoAcAcMS}$ distribution was assessed by planar nuclear imaging and single photon emission computed tomography (SPECT), using a three-head gamma camera (Triad[®], Trionix Research Laboratory, Twinsburg, OH, USA), equipped with a low-energy, ultrahigh resolution parallel hole collimator. Acquisition mode: step-and-shoot, 120 views over 360°, 10 s/view, 128x128 matrix. Reconstruction: Butterworth filter, cut-off 1.2, order 5. CT of the *ex vivo* liver was performed using a 64-slice CT system (Brilliance[®], Philips Medical Systems, Best, The Netherlands). Settings: tube voltage: 120 kV; tube current: 269 mAs. MR imaging of the *ex vivo* liver was performed using a 1.5-T clinical MR scanner (Intera[®], Philips Medical Systems, Best, The Netherlands). MRI was acquired according to previously described protocols [22].

Ex vivo neutron activation analysis

If holmium, a calcium analogue, would elude the microspheres and subsequently diffuse into the bloodstream, it would expectedly be integrated in the bone matrix [23]. Therefore, in order to determine whether any release of holmium had occurred, neutron activation analysis of a piece (ca. 1.5 g) of the femur of this cat was performed. A piece of the femur of an untreated cat was used as a control. The analysis was undertaken at the Delft Reactor Institute of the Delft University of Technology, Delft, The Netherlands, as described previously [24,25].

RESULTS

Microspheres characterization

The particle size was determined, before and after neutron irradiation, using a coulter counter. Since the amount of radioactivity is linear to particle volume, not diameter, it was opted to display the distribution in volume percentage. The

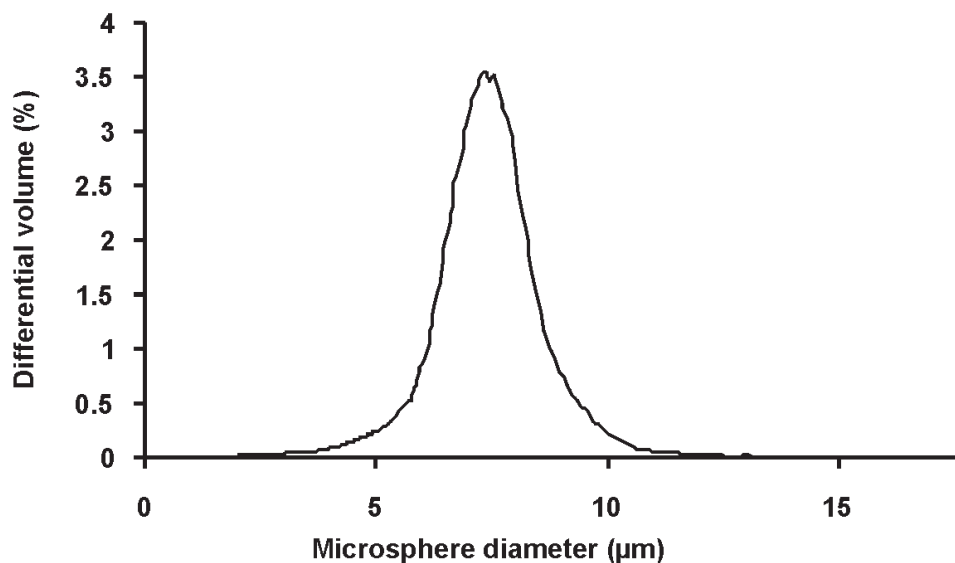


Figure 1 Particle size distribution of the HoAcAcMS. Mean diameter = 7.3 μm (SD = 1.7 μm)

particle size measurements showed a Gaussian distribution (Fig. 1). The mean diameter of the microspheres was 7.3 μm (SD = 1.7 μm). Neutron irradiation for two hours in a nuclear reactor had not affected the size distribution, signifying that no damage was inflicted to the microspheres. SEM of (non-irradiated) $^{165}\text{HoAcAcMS}$ showed perfectly spherical particles with a smooth surface (Fig. 2a and c). After neutron irradiation for 120 minutes and suspending in the Pluronic®/ethanol solution (and after the radioactivity had decayed), SEM revealed changes to the surface of the $^{166}\text{HoAcAcMS}$. The surface had become rougher (Fig. 2b and d). The holmium content of the $^{165}\text{HoAcAcMS}$, as determined by complexometric titration, was 45% (w/w).

Feasibility study in a cat with liver cancer

We explored the feasibility, tolerability and efficacy of intratumoral injections with the $^{166}\text{HoAcAcMS}$ in, essentially, a spontaneous animal model, namely a housecat with primary liver cancer.

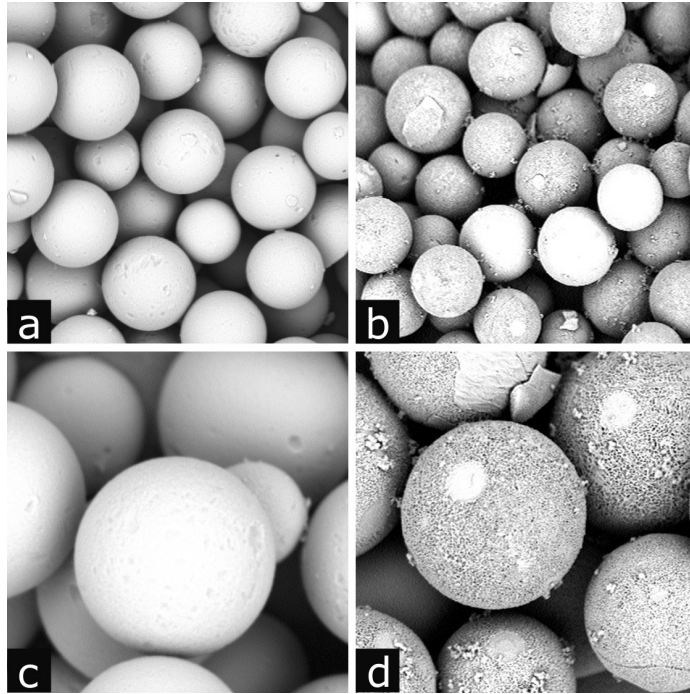


Figure 2 SEM images of the HoAcAcMS. Before neutron activation (a, c) and after neutron activation (b, d). Neutron irradiation induced minor surface changes. The spherical shape remained intact

Treatment and clinical result

The first treatment consisted of intratumoral injections with $^{166}\text{HoAcAcMS}$, $<10\ \mu\text{m}$ in mean diameter, during laparotomy. Ultrasonography was used to distinguish between tumorous tissue and normal hepatic parenchyma, and also to avoid inadvertent injection of microspheres into large vessels, in particular hepatic veins, which may result in radioembolization of the lung. A dosage of 100 mg of $^{166}\text{HoAcAcMS}$ (1,000 MBq) was divided over ten syringes and the content of each syringe was deposited intratumorally, divided over three positions per syringe. The $^{166}\text{HoAcAcMS}$ suspension was injected carefully and slowly, under real-time ultrasound monitoring, which aided in avoiding deposition of $^{166}\text{HoAcAcMS}$ outside the lesion. It was measured that 550 MBq had been administered. Subsequently, the biodistribution of the $^{166}\text{HoAcAcMS}$

Table 1 Biochemical and haematological blood parameters

Parameter	Reference values	Treatment	Day 4 post-treatment	Day 14	Day 40	Day 56	Day 85	Day 112/2 nd treatment	Day 4	Day 27	Day 69/ euthanasia
leukocytes (μ l)	5000-15000	NM	28150	NM	29650	15650	21290	19410	19140	15320	16800
neutrophils (%)	50.0-75.0	30.2	91.1	92	94.4	78.4	84.4	91.9	96	72.6	87.7
lymphocytes (%)	15-45	67	5.8	2	1.4	15.4	7.1	4	0.7	24.3	6.9
prothrombin time (s)	5.0-11.0	21.3	7.6	6.9	NM	9.8	7.2	8.8	8.2	NM	NM
activated partial thromboplastin time (s)	10.0-20.0	67.7	17	15.8	NM	15	10.4	17	15.9	NM	NM
urea (mg/dl)	40-70	222	170	98	129	98	158	80	116	84	103
total protein (g/dl)	5.6-7.8	5.5	5.3	6.3	7	7.3	7.8	7.5	6	6.6	6.8
albumin (g/dl)	2.50-4.50	2.45	2.36	2.88	3.11	3.36	3.62	3.5	2.81	3.19	3.34
bilirubin (mg/dl)	<0.40	0.42	0.37	0.24	0.21	0.23	0.3	0.34	0.34	0.34	0.41
AST (U/l)	<46	4417	917	289	465	453	653	565	1292	625	496
ALT (U/l)	<43	3183	1415	395	618	587	927	900	2022	693	659
ALP (U/l)	<58	NM	NM	289	386	495	NM	NM	354	478	512
body weight (kg)		2.3	2.7	NM	2.9	3.0	NM	3.0	NM	3.0	NM

Note: only parameters with (initially) distinctly altered values are displayed

NM not measured

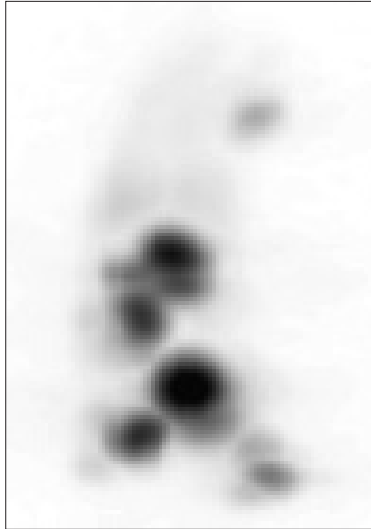


Figure 3 Nuclear image (maximum intensity projection), acquired directly after the first treatment, which demonstrated that the radioactivity distribution was confined to the liver

was (qualitatively) assessed by nuclear imaging (planar and SPECT) (Fig. 3). The distribution of the deposits of $^{166}\text{HoAcAcMS}$ was confined to the liver (tumors). Four days post-treatment, at which time the coagulation times and bilirubin had normalized (Table 1), the cat was taken home by the owner. At discharge, the exposure rate measured at a distance of 1 m from the animal was $0.23 \mu\text{Sv h}^{-1}$. Clinically, the cat rapidly improved (improved appetite, weight gain, improved alertness and mobility, improved condition of coat), but during a follow-up visit five weeks post-treatment wound dehiscence of the celiotomy incision was noticed. This event was probably associated with the prednisolone medication that was therefore immediately halted. The disrupted abdominal incision was surgically reclosed. During this procedure, it was observed that the liver lobes were grossly enlarged with multiple necrotic areas. The animal recovered from surgery without complications. However, about 100 days after the first treatment, its clinical condition started to deteriorate and the liver was significantly enlarged. It was decided to retreat the animal and this was performed at day 112. Pre-treatment assessment consisted of ultrasound examination, including baseline and contrast-enhanced ultrasound, to help in distinguishing between



Figure 4 Contrast-enhanced ultrasonography, which was used to aid in differentiating between non-tumorous liver parenchyma (*asterisk*), viable tumorous tissue (*arrow point*), and necrotic tissue (*arrow*). Contrast is retained longer in the liver parenchyma than in the neoplastic tissue, whereas no uptake occurs in necrotic tissue

liver parenchyma, (viable) tumours, and necrotic tissue (Fig. 4). This time, the procedure was performed percutaneously under ultrasound guidance. The planned dose consisted of 1,500 MBq of $^{166}\text{HoAcAcMS}$ (150 mg), and the radioactivity was divided over fifteen syringes. The amount of activity that was actually administered was 950 MBq. Post-procedural nuclear imaging confirmed that the $^{166}\text{HoAcAcMS}$ had once more been deposited exclusively into the liver. The cat was taken home in a relatively good condition. Although the animal's clinical condition and relevant blood parameters remained constant for some time, about two months after the second treatment the presence of the very large, partially necrotic, partially hypertrophic and still tumor-infiltrated liver, was presenting a source of persistent and aggravating discomfort. For this reason, it was decided, 69 days after the second treatment or six months after the first procedure, to humanely euthanize the animal.

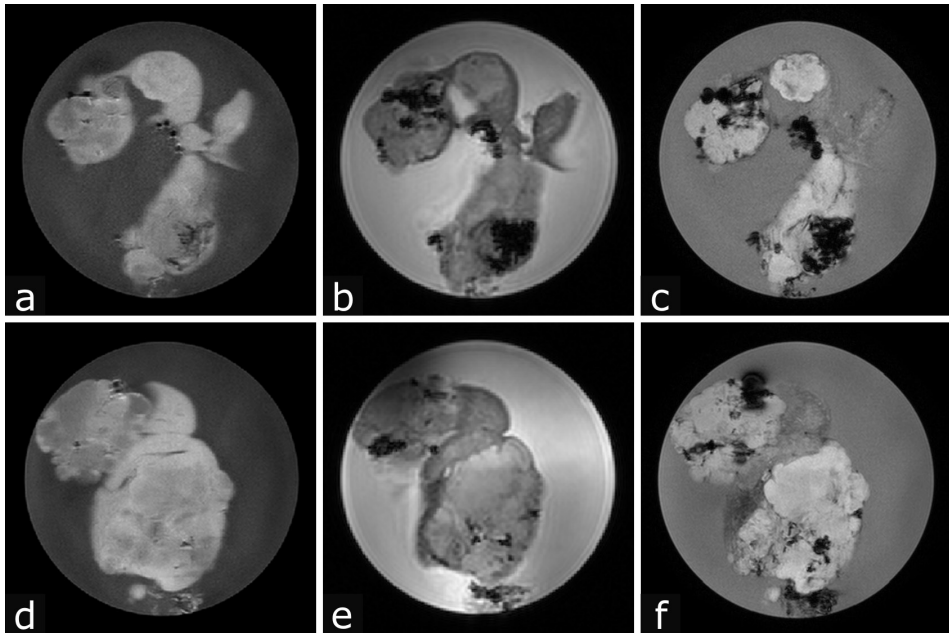


Figure 5 MR images of the *ex-vivo* liver. T_1 -weighted TSE, insensitive for holmium (a, d), 3D FFE (b, e), and T_2 -weighted mFFE (c, f), both of which are holmium-sensitive sequences, on which the holmium cluster of HoAcAcMS are visible as black artifacts

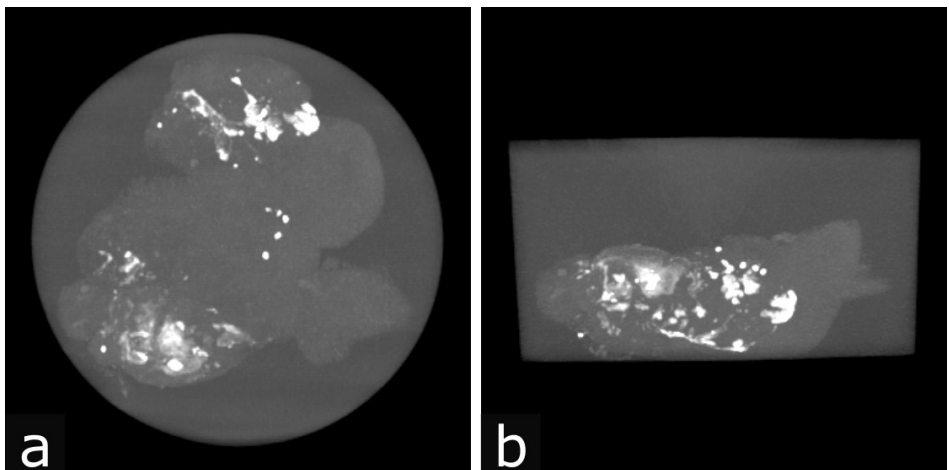


Figure 6 CT images (maximum-intensity projections) of the *ex-vivo* liver; top view (a) and side view (b). The radiopaque structures correspond with the HoAcAcMS depots

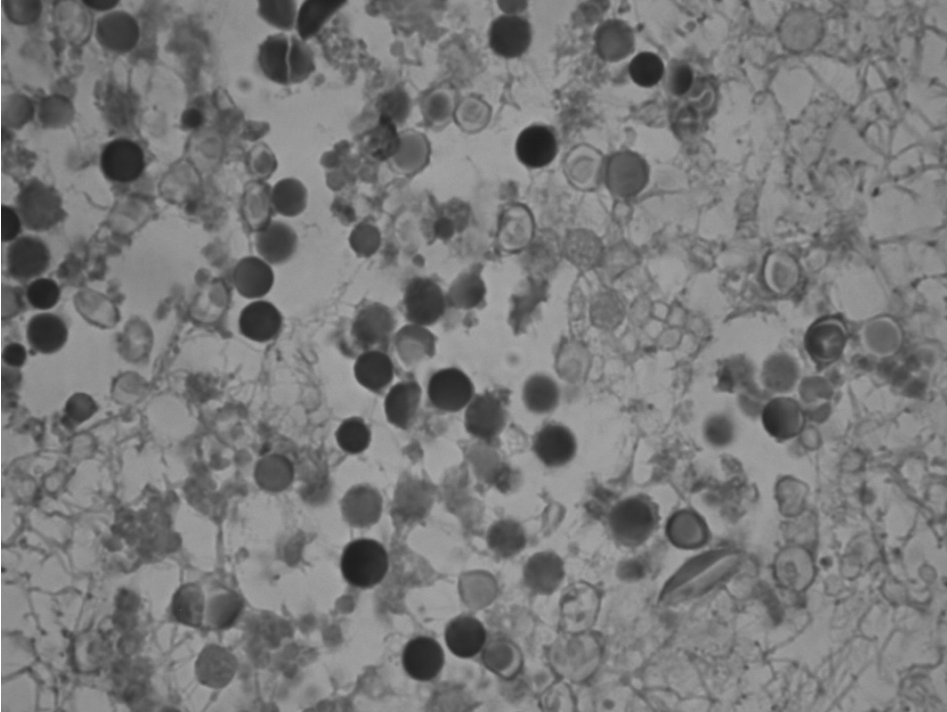


Figure 7 Histological (hematoxylin eosin stained) images revealing intact HoAcAcMS amidst necrotic tumorous tissue

Postmortem examination

The feline patient was subjected to a complete necropsy. Gross examination revealed an emaciated physical condition and a very large liver with a very heterogeneous, nodular outer surface. No macroscopic abnormalities were observed in any of the other organs, and there were no signs of metastatic disease. Prior to processing it for histological examination, the liver was flushed with a formaldehyde solution (4%) and then placed in a plastic bucket containing the same solution. Subsequently, MRI and CT of the liver were performed. The deposits of $^{166}\text{HoAcAcMS}$ were clearly visualized by both modalities (Figs. 5 and 6), indicating that the microspheres had remained at the site of injection. During histological examination of the liver, clusters of intact $^{166}\text{HoAcAcMS}$ were seen, surrounded by necrotic (tumorous) tissue (Fig. 7). This means that the microspheres had retained their structural integrity, at least for a period of

over two months, the period between the second administration and euthanasia. In order to detect if a (measurable) part of the holmium had escaped from the $^{166}\text{HoAcAcMS}$, neutron activation analysis of a piece of bone was performed. In both the sample of the treated cat and that of the control animal, the signal was below the detection limit.

DISCUSSION

The application of high-energy beta-emitting microspheres or complexes for radioablation of solid malignancies is not a recently developed technique. Already back in the 1940s, 50s, and 60s, radioactive particles were proposed for the treatment of unresectable tumors, either through intra-arterial or interstitial microbrachytherapy techniques. Colloids were the radioactive materials typically used for intratumoral injections. A major problem was safety since these colloids often rapidly degraded resulting in systemic radiation effects [26].

More recently, Tian *et al.* [27] reported on the treatment of 33 patients with unresectable liver tumors with ultrasound-guided intratumoral injections of yttrium-90 (^{90}Y) loaded glass microspheres. Most tumors that were treated were smaller than 5 cm in diameter (1-6 sessions/patient) and the total dose varied between 370-4,440 MBq ^{90}Y . In the 27 patients that were still alive between twelve to 32 months post-treatment, ultrasound examination revealed that 90.6% of the 32 foci treated had signs of tumor shrinkage. Despite the rather good clinical results, since then, the use of ^{90}Y microspheres as an intratumorally injected radioablation device has not been reported upon in the literature.

The microspheres that we presented in this paper were labeled with ^{166}Ho , which has several advantages over ^{90}Y , in particular its multimodal medical imaging possibilities. ^{166}Ho has already been clinically applied as an intratumoral radioablation device, though not integrated in microspheres but complexed to chitosan [28]. Chitosan is a linear biopolymer and forms a chelate complex with heavy metals, including holmium. Under acidic conditions, chitosan is soluble (pKa 6.3-6.7), but when injected into tissue (pH \approx 7.6) it turns into a gel [29,30]. The included forty patients with solitary HCC (<3 cm in diameter) were treated with ^{166}Ho -chitosan, percutaneously injected, under ultrasound guidance. Injected dose varied between 1,110 and 2,220 MBq. For long-term response assessment, the

31 patients with complete tumor necrosis (based on CT) were followed (median follow-up: 26.5 months, range: 9-36 months). Eleven of 31 patients maintained a complete response status, whereas the remainder developed local and/or other intrahepatic recurrences. The 1-year, 2-year, and 3-year survival rates were 87.2%, 71.8%, and 65.3%, respectively. Overall side effects were mild, but hematological toxicity was observed in a significant portion of the patients, including grade 3 and grade 4 events. According to the authors, these events were associated with radioactivity that had leached to the blood. Although chitosan is said to turn into a gel in tissue due to the (near) neutral pH of the interstitial fluid in normal tissue, it could be theorized that in the relatively acidic tumorous tissue chitosan is only partially present as a gel [30]; hence, in tumorous tissue the ^{166}Ho -chitosan might be partially present as a fluid, therefore able to diffuse out of the tumors and into the blood. It is therefore our opinion that, due to the excessive leaching of radioactivity, ^{166}Ho -chitosan is not the optimal device for interstitial microbrachytherapy.

For this reason, we have opted for microspheres as the carrier device, and conducted an initial feasibility study in a feline oncological patient. This cat, suffering from extensive HCC, was intratumorally injected with $^{166}\text{HoAcAcMS}$. Ultrasound guidance proved a vital part of the administration procedure, not only with regard to correct needle placement but also for monitoring the actual intratumoral administration of the $^{166}\text{HoAcAcMS}$. Due to inclusion of air in the suspension, which was expelled simultaneously with the $^{166}\text{HoAcAcMS}$ and acted as a contrast agent, visualization of their deposition was allowed on real-time ultrasonography. Due to the multimodal imaging possibilities (SPECT, MRI, and CT), the distribution of the $^{166}\text{HoAcAcMS}$ could be visualized. Histological analysis showed that they remained intact for an extended length of time *in vivo*. Further studies in a laboratory animal model will have to be carried out on this issue. Post-treatment there were no signs of myelosuppression, indicating that no release of significant amounts of radioactivity had taken place. This was confirmed by neutron activation analysis. Although the cat was treated *in extremis*, the treatment was undoubtedly beneficial, *i.e.*, clinically the animal rapidly improved. The treatment was well tolerated and repeated once when overt tumor recurrence was observed. Its lifespan was extended by six months, which was associated with a relatively good quality of life.

CONCLUSION

In this paper, we reported on the feasibility of producing small microspheres with a high holmium content, relative to the holmium loaded poly(L-lactic acid) microspheres (Ho-PLLA-MS) which have been developed in our group for intra-arterial radioembolization. We were able to produce HoAcAcMS with a diameter less than 10 μm . Furthermore, we demonstrated its resistance against neutron irradiation, using SEM and particle size analysis. The irradiated HoAcAcMS remained spherical and the size distribution had not changed. Compared to the Ho-PLLA-MS, the HoAcAcMS, intended for dedicated use as an intratumoral radioablation agent, have a high Ho content (45% w/w versus 17% w/w). Obviously, concerning the HoAcAcMS several issues need to be addressed, pharmaceutical and otherwise, including the *in vivo* stability behavior of these particles, the maximally tolerated neutron irradiation duration, toxicity, and efficacy.

The treatment of a feline patient with excessive hepatic tumor burden also proved feasible. This study gave indications that the $^{166}\text{HoAcAcMS}$ remain intact long-time once intratumorally deposited, but this must be confirmed in well designed laboratory animal studies. We therefore conclude that the $^{166}\text{HoAcAcMS}$ may be a useful RFA-complementary device, for the radioablation of intrahepatic malignancies, and potentially also applicable in the treatment of inoperable tumors in other organs, *e.g.*, brain, kidney, but that several preclinical studies are warranted before a phase-I patient study will be allowed to be commenced.

Acknowledgments

Financial support by the Dutch Technology Foundation STW (grant 06069) is gratefully acknowledged.

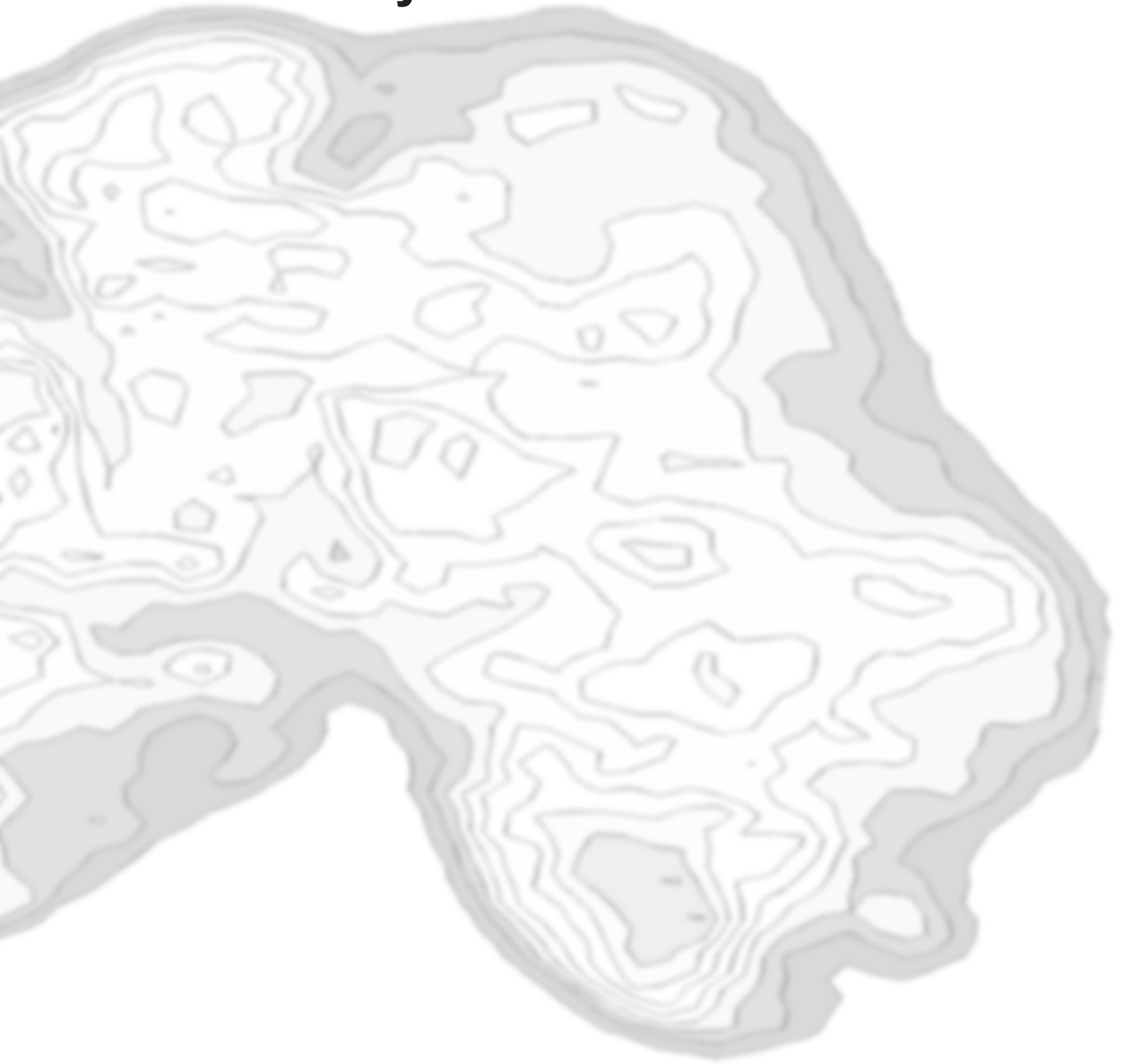
REFERENCES

1. Parkin DM, Bray F, Ferlay J, Pisani P. Global cancer statistics, 2002. *Ca Cancer J. Clin.* **2005**;55:74-108.
2. Kamangar F, Dores GM, Anderson WF. Patterns of cancer incidence, mortality, and prevalence across five continents: defining priorities to reduce cancer disparities in different geographic regions of the world. *J. Clin. Oncol.* **2006**;24:2137-2150.
3. Llovet JM, Bruix J. Molecular targeted therapies in hepatocellular carcinoma. *Hepatology* **2008**;48:1312-1327.
4. Choti MA, Bulkley GB. Management of hepatic metastases. *Liver Transpl. Surg.* **1999**;5:65-80.
5. Yamamura T, Tsukikawa S, Akaiishi O, Tanaka K, *et al.* Multivariate analysis of the prognostic factors of patients with unresectable synchronous liver metastases from colorectal cancer. *Dis. Colon Rectum* **1997**;40:1425-1429.
6. Hochster HS, Hart LL, Ramanathan RK, Childs BH, *et al.* Safety and efficacy of oxaliplatin and fluoropyrimidine regimens with or without bevacizumab as first-line treatment of metastatic colorectal cancer: results of the TREE Study. *J. Clin. Oncol.* **2008**;26:3523-3529.
7. Zuckerman DS, Clark JW. Systemic therapy for metastatic colorectal cancer: current questions. *Cancer* **2008**;112:1879-1891.
8. Cavaliere R, Ciocatto EC, Giovanella BC, Heidelberger C, *et al.* Selective heat sensitivity of cancer cells. Biochemical and clinical studies. *Cancer* **1967**;20:1351-1381.
9. Christophi C, Winkworth A, Muraliharan V, Evans P. The treatment of malignancy by hyperthermia. *Surg. Oncol.* **1998**;7:83-90.
10. Liapi E, Geschwind JF. Transcatheter and ablative therapeutic approaches for solid malignancies. *J. Clin. Oncol.* **2007**;25:978-986.
11. Goldberg SN, Gazelle GS, Mueller PR. Thermal ablation therapy for focal malignancy: a unified approach to underlying principles, techniques, and diagnostic imaging guidance. *AJR Am. J. Roentgenol.* **2000**;174:323-331.
12. Joosten J, Ruers T. Local radiofrequency ablation techniques for liver metastases of colorectal cancer. *Crit Rev. Oncol. Hematol.* **2007**;62:153-163.
13. Gillams AR, Lees WR. Five-year survival following radiofrequency ablation of small, solitary, hepatic colorectal metastases. *J. Vasc. Interv. Radiol.* **2008**;19:712-717.
14. Lencioni R, Crocetti L. Radiofrequency ablation of liver cancer. *Tech. Vasc. Interv. Radiol.* **2007**;10:38-46.
15. Abitabile P, Hartl U, Lange J, Maurer CA. Radiofrequency ablation permits an effective treatment for colorectal liver metastasis. *Eur. J. Surg. Oncol.* **2007**;33:67-71.
16. Goldberg SN, Hahn PF, Tanabe KK, Mueller PR, *et al.* Percutaneous radiofrequency tissue ablation: does perfusion-mediated tissue cooling limit coagulation necrosis? *J. Vasc. Interv. Radiol.* **1998**;9:101-111.
17. Patterson EJ, Scudamore CH, Owen DA, Nagy AG, Buczkowski AK. Radiofrequency ablation of porcine liver in vivo: effects of blood flow and treatment time on lesion size. *Ann. Surg.* **1998**;227:559-565.

18. Seevinck PR, Seppenwoolde JH, De Wit TC, Nijsen JF, *et al.* Factors affecting the sensitivity and detection limits of MRI, CT, and SPECT for multimodal diagnostic and therapeutic agents. *Anticancer Agents Med. Chem.* **2007**;7:317-334.
19. Nijsen JFW, Zonnenberg BA, Woittiez JR, Rook DW, *et al.* Holmium-166 poly lactic acid microspheres applicable for intra-arterial radionuclide therapy of hepatic malignancies: effects of preparation and neutron activation techniques. *Eur. J. Nucl. Med.* **1999**;26:699-704.
20. Zielhuis SW, Nijsen JFW, De Roos R, Krijger GC, *et al.* Production of GMP-grade radioactive holmium loaded poly(l-lactic acid) microspheres for clinical application. *Int. J. Pharm.* **2006**;311:69-74.
21. Zielhuis SW, Nijsen JFW, Figueiredo R, Feddes B, *et al.* Surface characteristics of holmium-loaded poly(l-lactic acid) microspheres. *Biomaterials* **2005**;26:925-932.
22. Seppenwoolde JH, Nijsen JFW, Bartels LW, Zielhuis SW, *et al.* Internal radiation therapy of liver tumors: Qualitative and quantitative magnetic resonance imaging of the biodistribution of holmium-loaded microspheres in animal models. *Magn Reson. Med.* **2004**;53:76-84.
23. Durbin PW. Metabolic characteristics within a chemical family. *Health Phys.* **1960**;2:225-238.
24. Bode P. Automation and quality assurance in the NAA facilities in Delft. *J. Radioanal. Nucl. Chem.* **2008**;245:127-132.
25. Zielhuis SW, Nijsen JFW, Seppenwoolde JH, Bakker CJG, *et al.* Long-term toxicity of holmium-loaded poly(L-lactic acid) microspheres in rats. *Biomaterials* **2007**;28:4591-4599.
26. Nakhgevary KB, Mobini J, Bassett JG, Miller E. Nonabsorbable radioactive material in the treatment of carcinomas by local injections. *Cancer* **1988**;61:931-940.
27. Tian JH, Xu BX, Zhang JM, Dong BW, *et al.* Ultrasound-guided internal radiotherapy using yttrium-90-glass microspheres for liver malignancies. *J. Nucl. Med.* **1996**;37:958-963.
28. Kim JK, Han KH, Lee JT, Paik YH, *et al.* Long-term clinical outcome of phase IIb clinical trial of percutaneous injection with holmium-166/chitosan complex (Milican) for the treatment of small hepatocellular carcinoma. *Clin. Cancer Res.* **2006**;12:543-548.
29. Chen MC, Yeh GHC, Chiang BH. Antimicrobial and physicochemical properties of methylcellulose and chitosan films containing a preservative. *J. Food Process. Pres.* **1996**;20:379-390.
30. Van den Berg AP, Wike-Hooley JL, Van den Berg-Blok AE, Van der Zee J, Reinhold HS. Tumour pH in human mammary carcinoma. *Eur. J. Cancer Clin. Oncol.* **1982**;18:457-462.

CHAPTER 9

Summary and future directions



SUMMARY

At the nuclear medicine department of the University Medical Center Utrecht, on holmium-166 poly(L-lactic acid) microspheres ($^{166}\text{Ho-PLLA-MS}$) – intended as an intra-arterial microdevice for internal radiation therapy of patients with unresectable liver malignancies – research has been conducted already since the mid-nineties. The aim of this thesis is to bring the concept of radioembolization with $^{166}\text{Ho-PLLA-MS}$ to clinical application. To this end, several important aspects pertaining to the $^{166}\text{Ho-PLLA-MS}$ are addressed.

Chapter 2 comprises a comprehensive review of the literature on the lipiodol- and microsphere-based radioembolization techniques that have been developed for treatment of patients with unresectable intrahepatic malignancies. Lipiodol radioembolization consists of instillation into the hepatic artery of either iodine-131 (^{131}I) or rhenium-188 (^{188}Re) labeled lipiodol (iodinated poppyseed oil). After transcatheter administration, the radiolabeled lipiodol is taken up by both the normal hepatocytes and the tumor cells. In comparison with the hepatocytes, the uptake of lipiodol by the tumor cells is slow but associated with ultimately much higher intracellular lipiodol concentrations and a considerably longer retention time. ^{131}I - and ^{188}Re -lipiodol are applied exclusively for the treatment of hepatocellular carcinoma (HCC), mostly as a palliative treatment option. With respect to efficacy, ^{188}Re -lipiodol is at least equivalent to chemoembolization but significantly better tolerated. In order to properly evaluate the role of radiolabeled lipiodol as a neo-adjuvant treatment option, randomized studies are required.

Tumor specificity of radioactive microspheres is based exclusively on the entirely arterial dependency of intrahepatic malignancies. Glass and resin microspheres, loaded with the radioisotope ^{90}Y , have been increasingly applied in the last decade. Compared to lipiodol-radioembolization, the pretreatment assessment procedure for microsphere radioembolization is more critical and complex, in particular because the ^{90}Y microspheres must be deposited strictly intrahepatically. ^{90}Y radioembolization has demonstrated to be effective in both HCC and metastatic liver cancer, especially when used in conjunction with systemic chemotherapy. Poly(L-lactic acid) microspheres loaded with holmium-166 ($^{166}\text{Ho-PLLA-MS}$) constitute a new development in microsphere radioembolization. Because this isotope emits both gamma rays and beta

particles, and is a highly paramagnetic element as well, it permits quantitative *in vivo* visualization of the ^{166}Ho -PLLA-MS with both nuclear imaging (gamma scintigraphy) and magnetic resonance imaging (MRI), which could allow for patient-individualized dosimetry.

Animal models that are potentially useful in preclinical research on novel treatment options for liver malignancies are discussed in this chapter as well.

Chapter 3 describes the validation and standardization of the neutron activation of the ^{165}Ho -PLLA-MS in a specific reactor. This is a delicate procedure because the neutron activation in a nuclear reactor is accompanied by gamma radiation which may inflict damage to the microspheres. Differential scanning calorimetry revealed that the crystalline phase of the PLLA matrix was already severely impaired after 2 hours of irradiation. Viscometry showed that the molecular weight of the PLLA in the 2-hours irradiated samples had already decreased by approximately 70%. Nonetheless, using particle size analysis, light microscopy, and scanning electron microscopy, it was found that, even after 7 hours of neutron irradiation, the structural integrity of the ^{166}Ho -PLLA-MS was guaranteed. The most important conclusion was that the ratio between the measured thermal neutron flux and the calculated total energy deposition determines whether a reactor facility might be suitable for neutron activation of the ^{165}Ho -PLLA-MS.

In **Chapter 4**, the results of a toxicity study in non-tumor-bearing pigs, which had been hepatic arterially injected with either ^{165}Ho -PLLA-MS or ^{166}Ho -PLLA-MS, are presented. It was found that the administration of amounts of radioactivity equating to liver absorbed doses in excess of 120 Gy was associated with merely mild side effects. However, inadvertent deposition of an excessive amount of ^{166}Ho -PLLA-MS into the gastric wall, as was confirmed by gamma scintigraphy, occurred in two animals and resulted in perforating gastric ulcerations. No myelosuppression was observed, and the only biochemical side effect of ^{166}Ho -PLLA-MS radioembolization was a moderate and transient elevation in the serum levels of the enzyme aspartate aminotransferase, indicating the presence of necrotic liver tissue. The animals were terminated at one or two months post-administration. The main finding during necropsy was moderate to marked atrophy of one or more liver lobes with compensatory hyperplasia of the other

lobes, especially in the ^{166}Ho -PLLA-MS group. It was concluded that the toxicity profile of the ^{166}Ho -PLLA-MS in pigs is favorable provided that the ^{166}Ho -PLLA-MS are deposited exclusively into the liver.

Chapter 5 reports on a pig study in which several technical aspects pertaining to hepatic arterial radioembolization with ^{166}Ho -PLLA-MS are investigated. The main aim was to assess whether the distribution of the treatment dose could be predicted using a small scout dose of ^{166}Ho -PLLA-MS. Scintigraphic images were acquired from the scout dose and from the total dose, and were compared both visually and quantitatively. With the exception of one animal (of five) in which the catheter was displaced between the two administrations, the respective distributions were similar. During these experiments, a dedicated administration system and neutron-activation/administration vial were used which was found to perform satisfactorily. The applicability of X-ray computed tomography (CT) and MRI was also investigated. It was concluded that the sensitivity of CT is too low to consistently and completely visualize a scout dose of ^{166}Ho -PLLA-MS. MRI, however, can accurately visualize relatively low concentrations of ^{166}Ho -PLLA-MS. Quantitative analysis of ^{166}Ho SPECT (single photon emission computed tomography; three-dimensional scintigraphic imaging) images was validated for an inhomogeneous background. SPECT images were acquired from an *ex vivo* pig liver in which ^{166}Ho -PLLA-MS had been injected as were planar images of slices of this liver as well. The SPECT images were quantitatively compared with the planar images and a strong relation was found.

In **Chapter 6**, several dosimetric methods, potentially applicable in microsphere radioembolization with ^{166}Ho and ^{90}Y , were compared. The applicability and value of the “Medical Internal Radiation Dose” (MIRD) dose estimation scheme, of Monte Carlo simulation (MCNP), and of the dose point-kernel convolution (PK) method were investigated in a heterogeneous radioactivity distribution, *viz.* an *ex vivo* pig liver containing ^{166}Ho -PLLA-MS. The liver was cut into slices and autoradiography was performed, and the acquired images were reconstructed into a 3-dimensional source distribution, to be used for the absorbed dose calculations. The results of the PK method were almost identical to the MCNP results yet were obtained much faster. It was confirmed that MIRD is an

insufficient method since it assumes a homogeneous radioactivity distribution. The dose distributions for ^{166}Ho and ^{90}Y were also shown to be similar.

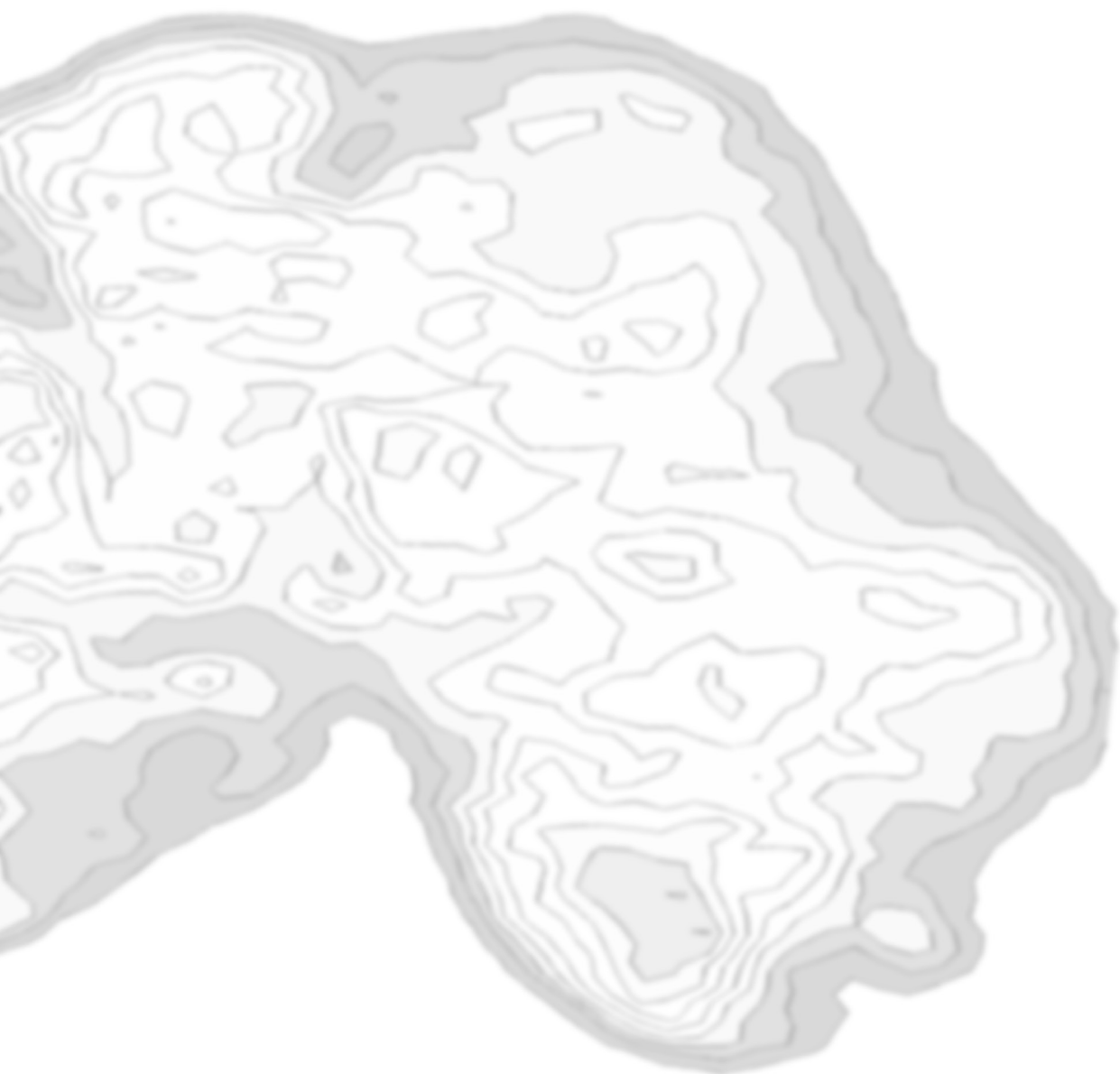
The aim of **Chapter 7** is to determine the mean tumor response (*i.e.*, degree of tumor regression) after radioembolization with the currently clinically applied ^{90}Y microspheres and its effect on survival in patients with unresectable liver malignancies. A structured meta-analysis of the available literature was therefore performed. Determinants were cancer type (HCC or colorectal liver metastases (mCRC)), microsphere type (glass- or resin-based), the chemotherapy protocol that was used, and whether ^{90}Y radioembolization was used as a salvage treatment or in the first-line. To allow comparability of results with respect to tumor response, the category 'any response' (AR) was introduced, comprising all patients from the categories complete response, partial response, and stable disease. The AR rates were high: AR for mCRC and HCC combined was 77% for the glass microspheres and 85% for the resin microspheres. For mCRC, response (glass and resin microspheres) in a salvage setting was 79%, and 91% in a first-line setting, regardless of the type of chemotherapy that was used. For HCC, response was 89% for the resin microspheres versus 78% for the glass microspheres. Based on the available data, the impact on overall survival could not be assessed. Randomized studies are therefore warranted.

In **Chapter 8**, dedicated ^{166}Ho acetylacetonate microspheres ($^{166}\text{HoAcAcMS}$) are proposed as a local ablation device. These $^{166}\text{HoAcAcMS}$ are smaller than the $^{166}\text{Ho-PLLA-MS}$ (mean diameter 7.3 μm and 30 μm , respectively) and the holmium content is significantly higher (45% and 17% (w/w), respectively). Neutron irradiation did not affect the microspheres' structural integrity. A feasibility study in a house cat with inoperable HCC was conducted. $^{166}\text{HoAcAcMS}$ were intratumorally injected, under ultrasound guidance. SPECT confirmed that the distribution of the $^{166}\text{HoAcAcMS}$ was confined to the liver. The treatment was well tolerated and the feline patient's clinical condition rapidly improved. Three months after the first treatment, when tumor recurrence was detected, the treatment was repeated. This treatment once more proved effective but of a palliative nature, and six months after the first treatment, the animal was euthanized. *Ex vivo* MRI and CT revealed that the $^{166}\text{HoAcAcMS}$ were still present in the liver, which was confirmed by histological examination.

FUTURE DIRECTION

A phase I clinical trial on ^{166}Ho -PLLA-MS is currently being prepared in which dose cohorts of 3-6 patients each, with unresectable liver malignancies of various origin, will undergo hepatic arterial radioembolization with ascending amounts of radioactivity, equating to liver absorbed doses of 20, 40, 60, or 80 Gy. In this study, as is customary in ^{90}Y radioembolization, in the pretreatment procedure, $^{99\text{m}}\text{Tc}$ albumin macroaggregates will be used to determine whether the biodistribution of the ^{166}Ho -PLLA-MS will expectedly be favorable, and also to calculate the lung-shunt fraction. Additionally, at the day of treatment, patients will first have instilled a scout dose of ^{166}Ho -PLLA-MS (250 MBq). Next to toxicity assessment which is the primary aim of this study, it will be investigated whether this scout dose will accurately correlate with the distribution of the treatment dose (1.3-5.0 GBq/kg). Retrospective quantitative SPECT analysis will be performed on the SPECT images of these patients. Tumor and liver absorbed doses will be calculated using the dose point-kernel method, and these data will be related to the liver toxicity and tumor response observed in these cohorts. The knowledge, *i.e.*, dosimetric data, that will be acquired in this manner can than be made use of in phase II and III studies to optimize clinical outcome. In these upcoming patient studies, the ^{166}Ho -PLLA-MS will be instilled bilobarly or unilobarly, under fluoroscopy guidance to monitor for retrograde flow. In the meantime, research on administration under real-time MRI guidance will continue. Since the ^{166}Ho -PLLA-MS can be visualized by MRI, this approach would enable for tumors to be highly-selectively targeted and receive a very high and precise dose, whereas the absorbed dose on the normal liver tissue ought be inconsequential. Finally, further improvements in holmium quantification with MRI will enable dose planning and dose calculations using a non-radioactive scout dose of ^{165}Ho -PLLA-MS.

Samenvatting in het Nederlands



Onderzoek aan holmium-166 poly(L-melkzuur) microsferen ($^{166}\text{Ho-PLLA-MS}$) – beoogd als een intra-arterieel microdevice voor interne radiotherapie bij patiënten met niet-reseceerbare levermaligniteiten – is op de afdeling Nucleaire Geneeskunde van het Universitair Medisch Centrum Utrecht reeds gaande sinds het midden van de jaren negentig. Het doel van dit promotieonderzoek is om het concept van de radioembolisatie met $^{166}\text{Ho-PLLA-MS}$ tot klinische toepassing te brengen. Hiertoe zijn meerdere belangrijke aspecten met betrekking tot de $^{166}\text{Ho-PLLA-MS}$ onderzocht.

Hoofdstuk 2 omvat een uitgebreid overzicht van de literatuur over lipiodol- en microsfeergebaseerde radioembolisatietechnieken, die zijn ontwikkeld voor de behandeling van patiënten met niet-reseceerbare levermaligniteiten. Lipiodol-radioembolisatie behelst het in de leverslagader inspuiten van hetzij jodium-131 (^{131}I) dan wel rhenium-188 (^{188}Re) gelabeld lipiodol (gejodeerd papaverzaadolie). Na de toediening met behulp van een catheter wordt het radioactieve lipiodol opgenomen door zowel de normale hepatocyten als de tumorcellen. In vergelijking met de hepatocyten is de opname van lipiodol door de tumorcellen traag, maar is de intracellulaire concentratie uiteindelijk veel hoger en de retentietijd aanmerkelijk langer. ^{131}I - en ^{188}Re -lipiodol worden uitsluitend toegepast voor behandeling van het hepatocellulair carcinoom (HCC), doorgaans als een palliatieve behandelingsoptie. Wat de werkzaamheid betreft is ^{188}Re -lipiodol minstens equivalent aan chemoembolisatie, maar wordt het aanzienlijk beter verdragen. Teneinde de waarde van radioactief lipiodol als een neo-adjuvante behandelingsoptie te kunnen bepalen, zijn gerandomiseerde studies vereist.

Tumorselectiviteit van radioactieve microsferen is uitsluitend het gevolg van de exclusief arteriële afhankelijkheid van levermaligniteiten. Glas- en harsmicrosferen, beladen met het radio-isotoop yttrium-90 (^{90}Y), zijn in het afgelopen decennium in toenemende mate toegepast. In vergelijking met lipiodol-radioembolisatie is de voorbereidende procedure voor microsfeer-radioembolisatie kritischer en complexer, vooral omdat de depositie van de ^{90}Y microsferen strikt intrahepatisch moet zijn. Van ^{90}Y -radioembolisatie is aangetoond dat het zowel werkzaam is bij HCC als bij naar de lever gemetastaseerde kanker, in het bijzonder indien toegepast in combinatie met systemische chemotherapie.

Een nieuwe ontwikkeling in microsfeer-radioembolisatie vormen poly(L-melkzuur) microsferen, beladen met holmium-166 ($^{166}\text{Ho-PLLA-MS}$). Omdat dit isotoop zowel gammastraling als bètadeeltjes uitzendt en het bovendien een zeer paramagnetisch element betreft, is kwantitatieve *in vivo* visualisatie van de $^{166}\text{Ho-PLLA-MS}$ mogelijk met zowel nucleaire beeldvorming (gamma scintigrafie) als magnetische resonantiebeeldvorming, 'magnetic resonance imaging' (MRI), wat individuele patiëntendosimetrie mogelijk maakt.

Diermodellen die mogelijk bruikbaar zijn voor preklinisch onderzoek aan nieuwe behandelingsopties voor levermaligniteiten worden ook besproken in dit hoofdstuk.

Hoofdstuk 3 beschrijft de validatie en standaardisatie van de neutronenactivering van de $^{165}\text{Ho-PLLA-MS}$ in een specifieke reactor. Dit is een delicate procedure, omdat de neutronenactivering in een kernreactor gepaard gaat met gammabestraling die schade aan de microsferen kan berokkenen. Differentiële scanning calorimetrie toonde aan dat de kristallijne fase van de PLLA-matrix al na 2 uur bestraling ernstig was aangetast. Viscometrie liet zien dat het molecuulgewicht van het PLLA in de 2-uur bestraalde monsters al met ongeveer 70% was gedaald. Nochtans werd met deeltjesgrootte-analyse, lichtmicroscopie en rasterelectronenmicroscopie gevonden dat de structurele integriteit zelfs na 7 uur neutronenbestraling was gewaarborgd. De belangrijkste conclusie was dat de ratio tussen de gemeten flux van de thermische neutronen en de berekende totale-energiedepositie bepaalt of een reactorfaciliteit geschikt zou kunnen zijn voor neutronenactivering van de $^{165}\text{Ho-PLLA-MS}$.

In **Hoofdstuk 4** worden de resultaten gepresenteerd van een toxiciteitsstudie, uitgevoerd bij niet-tumordragende varkens, die in de leverslagader $^{165}\text{Ho-PLLA-MS}$ of $^{166}\text{Ho-PLLA-MS}$ toegediend gekregen hadden. De toediening van hoeveelheden radioactiviteit, overeenkomend met geabsorbeerde leverdoses van meer dan 120 Gy, bleek tot slechts milde neveneffecten te leiden. Echter, onbedoelde depositie van een overmatige hoeveelheid $^{166}\text{Ho-PLLA-MS}$ in de maagwand, zoals bevestigd werd met gamma scintigrafie, wat plaatsvond bij twee dieren, resulteerde in perforerende ulcera in de maag. Er werd geen beenmergtoxiciteit gezien, en het enige biochemische bijverschijnsel van

radioembolisatie met ^{166}Ho -PLLA-MS was een matige en tijdelijke stijging in de serumspiegels van het enzym aspartaataminotransferase, duidend op aanwezigheid van necrotisch leverweefsel. De dieren werden een of twee maanden na de toediening geëuthanaseerd. De belangrijkste sectiebevinding was een matige tot uitgesproken atrofie van een of meerdere leverlobben met compensatoire hyperplasie van de andere lobben, vooral bij dieren uit de ^{166}Ho -PLLA-MS groep. Geconcludeerd werd dat het toxiciteitsprofiel van de ^{166}Ho -PLLA-MS gunstig is, mits de ^{166}Ho -PLLA-MS uitsluitend in de lever worden gedeponereerd.

Hoofdstuk 5 rapporteert over een varkensstudie waarin meerdere technische aspecten met betrekking tot radioembolisatie van de leverslagader met ^{166}Ho -PLLA-MS werden onderzocht. Hoofddoel was te testen of de verdeling van de therapeutische dosis kan worden voorspeld op basis van een kleine testdosis van ^{166}Ho -PLLA-MS. Scintigrafische beelden werden vervaardigd van de testdosis en van de totale dosis, en vervolgens zowel visueel als kwantitatief beoordeeld. Op één dier (van de vijf) na, waarbij de catheterpositie was veranderd tussen de twee toedieningen, waren de respectievelijke distributies vergelijkbaar. Tijdens deze experimenten werden een speciaal ontwikkeld toediensysteem en activerings-/toedienvaatje gebruikt die adequaat bleken te functioneren. De toepasbaarheid van computertomografie (CT) en van MRI werden eveneens onderzocht. Er werd geconcludeerd dat de gevoeligheid van CT te laag is om een testdosis ^{166}Ho -PLLA-MS consistent en volledig in beeld te kunnen brengen. Daarentegen kan MRI ook relatief lage concentraties ^{166}Ho -PLLA-MS visualiseren. Kwantitatieve analyse van ^{166}Ho SPECT ('single photon emission computed tomography'; driedimensionale scintigrafische beeldvorming)-beelden werd gevalideerd voor een inhomogene achtergrond. SPECT-beelden werden verkregen van een *ex vivo* varkenslever waarin ^{166}Ho -PLLA-MS waren geïnjecteerd, alsmede planaire beelden van plakken van deze lever. De SPECT-beelden werden kwantitatief vergeleken met de planaire beelden en een sterke relatie werd gevonden.

In **Hoofdstuk 6** worden verschillende, mogelijkerwijs bruikbare methoden voor dosimetrie voor ^{166}Ho en ^{90}Y radioembolisatie met elkaar vergeleken. De toepasbaarheid en waarde van de methode voor dosisschatting van de "Medical

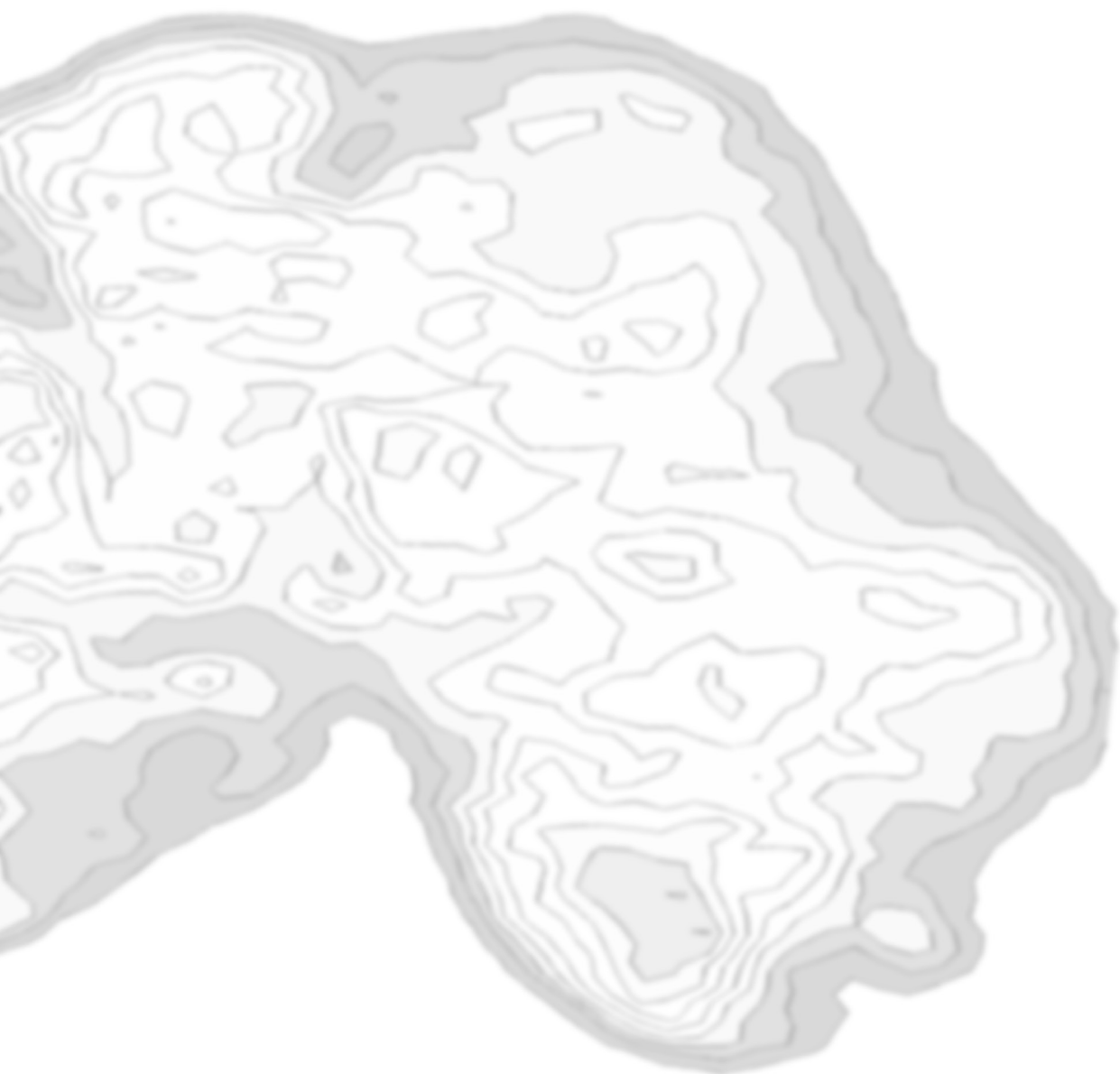
Internal Radiation Dose" (MIRD)-commissie, van Monte Carlo simulaties (MCNP), en van de dosiskernmethode werden onderzocht in een heterogene radioactiviteitsverdeling, te weten een *ex vivo* varkenslever, met daarin ¹⁶⁶Ho-PLLA-MS. Deze lever werd in plakken gesneden waarvan autoradiografie werd uitgevoerd, waarna de verkregen beelden werden gereconstrueerd naar een driedimensionaal volume, dat werd gebruikt voor de geabsorbeerde-dosisberekeningen. De resultaten van de dosiskernmethode waren bijna identiek aan de MCNP-resultaten, maar werden veel sneller verkregen. Bevestigd werd dat MIRD een niet-toereikende methode is, omdat het uitgaat van een homogene radioactiviteitsdistributie. De dosisverdelingen van ¹⁶⁶Ho en ⁹⁰Y waren sterk vergelijkbaar.

Het doel van **Hoofdstuk 7** is het bepalen van de gemiddelde tumorrespons (*i.e.* mate van tumorregressie) bij patiënten met levermaligniteiten op radioembolisatie met de momenteel klinisch toegepaste ⁹⁰Y microsferen en het effect op de overleving. Een gestructureerde meta-analyse van de beschikbare literatuur werd hiertoe verricht. Determinanten waren tumortype (HCC of colorectale metastasen (mCRC)), microsfeertype (glas of hars), het gebruikte chemotherapieprotocol, en of ⁹⁰Y radioembolisatie werd ingezet als 'salvage' therapie dan wel als primaire therapie. Om de verzamelde resultaten qua tumorrespons te kunnen vergelijken werd de categorie 'enige respons' ('any response' (AR)) geïntroduceerd, bestaande uit alle patiënten uit de categorieën 'complete respons', 'partiële respons' en 'stabiele ziekte'. De AR-cijfers waren hoog: AR voor mCRC en HCC gecombineerd was 77% voor de glasmicrosferen en 85% voor de harsmicrosferen. Voor mCRC was de respons (glas- en harsmicrosferen) 79% indien toegepast als 'salvage' therapie, en 91% indien ingezet in de eerste lijn. Voor HCC was de respons 89% voor de harsmicrosferen versus 78% voor de glasmicrosferen. Op basis van de beschikbare gegevens kon het effect op de overleving niet worden bepaald. Hiervoor zijn gerandomiseerde studies vereist.

In **Hoofdstuk 8** worden ¹⁶⁶Ho-acetylacetaat microsferen (¹⁶⁶HoAcAcMS) voorgesteld voor lokale tumorablatie. Deze ¹⁶⁶HoAcAcMS zijn kleiner dan de ¹⁶⁶Ho-PLLA-MS (gemiddelde diameter respectievelijk 7,3 en 30 μm) en het holmiumgehalte is aanmerkelijk hoger (respectievelijk 45% en 17% (w/w)).

Neutronenactivering had geen gevolgen voor de structurele integriteit van de microsferen. Een haalbaarheidsstudie werd uitgevoerd bij een huiskat met inoperabele HCC. $^{166}\text{HoAcAcMS}$ werden intratumoraal, onder echogeleide, geïnjecteerd. SPECT bevestigde dat de distributie van de $^{166}\text{HoAcAcMS}$ was begrensd tot de lever. De behandeling werd goed doorstaan en de klinische toestand van de feline patiënt verbeterde snel. Nadat drie maanden na de eerste behandeling tumorrecidief werd geconstateerd, werd de behandeling herhaald. Ook deze behandeling bleek effectief maar palliatief van aard, en zes maanden na de eerste behandeling werd het dier geëuthanaseerd. *Ex vivo* MRI en CT onthulden dat de $^{166}\text{HoAcAcMS}$ nog steeds in de lever aanwezig waren, hetgeen werd bevestigd door histologisch onderzoek.

Dankwoord



Zoals gangbaar is, volgt er nu een reeks dankzeggingen aan en loftuitingen op alle mensen met wie ik de afgelopen vijf jaren doorgaans zo plezierig heb mogen samenwerken. Het betreft een, zo mag ik het wel omschrijven, bonte verzameling van persoonlijkheden van diverse pluimage en achtergrond, zonder wier ondersteuning en inbreng dit promotieonderzoek niet succesvol had kunnen worden afgerond.

Prof. dr. P.P. van Rijk, beste promotor, beste Peter, hartelijk dank voor het vertrouwen dat je in me hebt gesteld. Uiteraard is het wel jammer dat je vrij vlug na mijn aanstelling als aio met emeritaat bent gegaan, waardoor je de aanstaande klinische introductie van de holmium microsferen niet in functie zult meemaken, maar ik weet dat je je niet verveelt met de vele hobby's die je hebt.

Dr. A.D. van het Schip, beste co-promotor, beste Fred, als een promotieonderzoek (althans in mijn beleving) een sport zou zijn, dan zou het wielrennen zijn, en de aio zou een wielrenner zijn, en dan geen baanrenner of tijdritspecialist, maar een tourrenner, en jij zou diens coach zijn, eentje die weet hoe een renner een succesvolle tour kan rijden, omdat je weet dat het niet iedere etappe supersnel hoeft en kan gaan, maar die een doordachte tactiek en een goed uithoudingsvermogen als devies heeft, wel altijd met de eindstreep indachtig, ook als deze nog heel ver weg moge zijn, wetende dat er bergen gaan komen die bedwongen moeten worden, maar die van steile beklimmingen allang niet meer onder de indruk is. Ja, ongeveer zoals het voorgaande zou ik je willen typeren (dat was overigens een zin van 120 woorden, Fred). Bedankt voor je inzet!

Dr. J.F.W. Nijsen, beste co-promotor, beste Frank, je vormde samen met Fred de dagelijkse supervisie, maar toch heb ik dat niet echt als zodanig ervaren, althans niet in de zin van een autoritaire 'baas'. Het was eerder een kwestie – en dit geldt evengoed voor Fred – van een goede ondersteuning en samenwerking. Je was te allen tijde bereid om resultaten te bespreken, plannings door te nemen en, indien nodig, om de helpende hand te bieden, bijvoorbeeld bij het uitvoeren van de complexe dierexperimenten. Je wordt de laatste tijd helaas erg beziggehouden door allerlei vervelende niet-werkgerelateerde zaken en ik hoop dat die binnenkort allemaal achter de rug zijn. Bedankt voor alles!

Dr. B.A. Zonnenberg, beste Bernard, helaas mag een promovendus maximaal twee co-promotoren hebben, anders was je zeker gevraagd de derde te zijn. Ondanks

je drukke werkzaamheden in de kliniek was je negen van de tien keer aanwezig bij het wekelijkse overleg van de holmiumgroep, en je inbreng hierin, die zowel deskundig als creatief was en altijd positief, werd algemeen gewaardeerd.

Prof. dr. P.R. Luijten, beste Peter, het was helaas te laat om je nog als tweede promotor toe te voegen, want dat had je zeker verdiend. Onze maandelijkse overleggen, het laatste anderhalf jaar, hebben dat beetje extra structuur opgeleverd dat nodig was om de laatste experimenten en papers simultaan en nog tamelijk vlot te hebben kunnen afronden.

Prof. dr. W.P.Th.M. Mali, dank dat u mij de financiële ademruimte heeft verleend, die het mogelijk maakte om mijn onderzoek in blessuretijd af te ronden. Voorts ben ik zeer verheugd door uw enthousiasme voor interventioneel radiologische technieken in de strijd tegen kanker. Ik deel uw geloof in een grote toekomst voor deze minmaal invasieve methoden.

Prof. dr. ir. M.A. Viergever, beste Max, toen je ons indertijd verzocht om ons, dat wil zeggen de onderzoekers van het holmiumproject, te voegen bij het Image Sciences Institute en de wekelijkse meetings te gaan bezoeken, had ik niet kunnen bevroeden dat ik drie jaar later inderdaad zou begrijpen wat termen als 'iteratieve reconstructies', 'rigide en elastische registratie' en 'segmentatiealgoritmen' daadwerkelijk inhouden (nou ja, ongeveer dan).

Dr. G.C. Krijger, beste Gerard, onze samenwerking heb ik als een groot genoegen ervaren. Je hebt namelijk een uitermate ontstressend effect op anderen. Met name de bestralingen voor de zogenaamde 'Delftstudie' hebben je veel tijd gekost, en uiteindelijk heeft dit stuk pas na drie jaar daglicht gezien, maar... het manuscript werd wel binnen drie (!) dagen na indienen geaccepteerd! Je (ex)collega's Camiel Kaaijk, Anneke Koster-Ammerlaan en Piet de Leege dank ik voor hun input bij deze studie.

Dr. T.C. de Wit, beste Tim, fysicus extraordinaire, ik wil je graag bedanken omdat je mij op zoveel verschillende vlakken altijd uitermate behulpzaam bent geweest, niet alleen op fysisch-mathematisch vlak, maar ook als ik weer eens problemen kreeg met computerprogramma's, omloop nodig had voor dierexperimenten, of met wat dan ook. Over enkele weken ga je als klinisch fysicus aan de slag in het AMC en ik wens je daar veel succes!

Dr. M.A.A.J. van den Bosch, beste Maurice, het is goed te zien dat een radioloog in het UMC Utrecht zich bereid heeft gevonden c.q. het lef heeft gehad om zich het deelvakgebied van de intra-arteriële radioembolisatie eigen te maken. De eerste behandelingen met de yttrium microsferen in het UMC zijn inmiddels achter de rug en met goede resultaten. Naar verwachting zal nog dit jaar de fase I studie met de holmium microsferen starten en ik verwacht er, mede dankzij de inmiddels door jou opgebouwde expertise, goede resultaten van.

Wouter Bult, mijn kamergenoot en collega-aio gedurende de afgelopen drieënehalf jaar, dat we het vanaf dag één uitermate goed met elkaar hebben kunnen vinden, is grotendeels te danken aan het gevoel voor volstrekt niet-subtiele humor dat we delen. Ofschoon je een harde werker bent met een goed stel hersenen, verliep je onderzoek soms wat stroef. Gelukkig gaat het momenteel met je project de goede kant op, en ga je het absoluut tot een succesvol einde brengen, maar het zal nog een pittige laatste periode worden. Vanwege je huwelijksreis kun je helaas niet aanwezig zijn bij mijn verdediging. Ik wens jou en Roos een gelukkig huwelijk toe!

Remmert de Roos, mijn trouwe rechterhand (en daarom paranimf) tijdens mijn onderzoek, als het ging om het praktische labwerk en het voorbereiden van experimenten. We waren niet het snelste team in het lab, maar wellicht wel het gezelligste. Bewonderenswaardig is de omvang van je netwerk binnen het UMC Utrecht als ook daarbuiten. Op korte termijn een bepaalde chemische stof nodig? Een set injectienaalden van een afwijkende maat? Of er moest snel een perspex afscherming gemaakt worden? Jij wist altijd wel even iets of iemand te regelen, en vooral ook heel vlug.

Prof. dr. ir. W.E. Hennink, beste Wim, polymeerprof par excellence, bedankt voor je deskundige inbreng als het ging om moeilijk te interpreteren differentiële scanning calorimetrie (DSC) of gelpermeatiechromatografie (GPC) data.

Mies van Steenbergen, dankzij jouw SOP's en goede uitleg – altijd in een gemoeidelijke en humorvolle sfeer – wist zelfs ik in de voor mij voorheen onbekende wereld van de DSC en GPC te overleven. In plaats van 'researchanalist' zou ik je overigens eerder als 'laboratoriummanager' willen betitelen.

Dr. S.W. Zielhuis, beste Sander, mijn vorige kamergenoot en de vorige 'Wouter', dank voor je hulp en de gezelligheid gedurende onze tijd samen op de afdeling. Binnenkort zul je de opleiding tot ziekenhuisapotheker afronden en in het AMC, op, jawel, de afdeling Nucleaire Geneeskunde, je carrière voortzetten. De cirkel is rond, zou je kunnen zeggen.

Peter Seevinck, je bent verantwoordelijk voor veel van de (niet-nucleaire) beeldvorming binnen mijn project, en hebt ook op andere wijze bijgedragen, waarvoor dank. Voor jou nadert het einde van je bestaan als aio ook op korte termijn, en ik wens je sterkte met de laatste loodjes. Als je manuscript naar de commissie is gestuurd, moet er maar weer eens een kroegavondje worden afgesproken, want de laatste keer is ook alweer veel te lang geleden.

Dr. C.J.G. Bakker, beste Chris, je hebt je samen met je aio's, Peter S., Gerrit van de Maat en Hendrik de Leeuw driftig op de kwantitatieve beeldvorming van holmium met behulp van MRI gestort. Ik ben benieuwd welke sequentie of manier van scannen uiteindelijk de winnaar zal worden!

Dr. ir. J.H. Seppenwoolde, beste Jan-Henry, van 'het roer omgooien' gesproken: zijnde een gewaardeerd MRI-fysicus toch maar te besluiten om jezelf en je gezin te transplanteren naar Ecuador, om daar voor minimaal vijf jaar zendelingswerk te gaan doen. Ik vond het nogal wat. Naar verluid maken jullie het goed. Hopelijk heb je mijn boekje ontvangen.

Dr. K. Peremans, beste Kathelijne, de enige echte 'nucleaire diergeneeskundige' die ik ken, en de rest van het team in Merelbeke, met name je collega-dierenartsen Eva Vandermeulen, Simon Vermeire, Sara Janssens en Hendrik Haers, hartelijk dank voor de gastvrijheid en de uiterst flexibele samenwerking! De behandelingen bij de honden bleken erg lastig uit te voeren, maar de resultaten bij de katten mochten er zeker zijn. Ik hoop dat de samenwerking tussen jullie en de holmiumgroep nog lang zal voortduren. En Eva en Simon, sterkte met het afronden van jullie promotieonderzoeken.

Dr. M.G.E.H. Lam, beste Marnix, je bent een nucleair geneeskundige die oncologische therapie duidelijk hoog in het vaandel heeft staan. Naast dat je een specialist bent op het gebied van botzoekende radiofarmaca voor de behandeling van pijnlijke skeletmetastasen, ben je tevens verantwoordelijk voor de toediening

van de microsferen, en ben je betrokken bij de praktische implementatie van de patiëntendosimetrie rondom de holmiumtherapie. Je vormt een waardevolle aanvulling voor de klinische tak van het holmiumteam.

Dr. M.W. Konijnenberg, beste Mark, het dosimetriestuk heeft flink wat tijd en transpiratie gekost, maar uiteindelijk hebben we het gelukkig toch op tijd kunnen afronden, zodat het nog in mijn proefschrift kon worden opgenomen.

Dr. ir. H.W.A.M. de Jong, beste Hugo, bedankt voor je pragmatische input. Binnenkort zal een patiëntenstudie met de holmium microsferen starten, terwijl er aan patiëntendosimetrie op basis van SPECT-beelden nog wel wat te ontwikkelen valt. Hiervoor heb je een aio aangetrokken, Matthijs Elschot, en ik hoop dat zijn werk op niet al te lange termijn voor een nog nauwkeuriger behandeling van de patiënten zal zorgen.

Dr. A. Huisman, beste Albert, bedankt voor de ontspannen samenwerking als het gaat om de vele bloedonderzoeken van de toxiciteitsstudie.

Chris “spieren in rust” Oerlemans en Agnes Paradissis, de *next generation* aio's van de holmiumgroep. Het is opvallend dat er binnen de groep een sterke tendens lijkt te zijn naar de ontwikkeling van steeds kleinere deeltjes: van 30 μm (de microsferen in dit proefschrift) naar 15 μm (“Bultbollen”) naar nano (jullie deeltjes). Ik wens jullie veel succes met je onderzoek.

Prof. dr. J. Kirpensteijn, Dr. B.P. Meij, Prof. dr. G. Voorhout, beste vakbroeders, om meerdere redenen heeft het enkele jaren geduurd vooraleer het mogelijk was geworden om samen veterinaire patiënten te gaan behandelen hier in Utrecht, maar uiteindelijk hebben we kortgeleden toch de eerste twee honden en een kat behandeld. Het begin is gemaakt.

Tjitske Bosma, goed dat jij werd aangetrokken om in de omvangrijke voorbereidende werkzaamheden voor de patiëntenstudie wat structuur te brengen. Ik vond de samenwerking erg plezierig en professioneel.

Dr. T.S.G.A.M. van den Ingh, hartelijk dank voor de assistentie bij het beoordelen van de histologische coupes van de toxiciteitsstudie.

Tom Grimbergen, het was een mooi plan, in een *ex vivo* lever de door de holmium microsferen afgegeven dosis meten met heel kleine TLD-tjes. Alleen bleken

er nogal wat haken en ogen aan te zitten en uiteindelijk is dit plan nooit tot uitvoering gebracht. Niettemin dank voor je vakbekwame inbreng.

Beste diervverzorgers en biotechnici van het Gemeenschappelijk Dierenlaboratorium, dank voor de goede verzorging van de varkens en de biotechnische assistentie bij de experimenten. In het bijzonder hulde aan het 'dreamteam', *i.e.* Hans Vosmeer en (mijn tweede paranimf) Nico Attevelt, ik heb veel van jullie geleerd en jullie flexibiliteit (experimenten die een uur of acht langer dan gepland in beslag namen waren voor jullie geen probleem) altijd hoog gewaardeerd.

Willem van Wolferen en Simon Plomp, heren prosectoren, hartelijk dank, zowel voor het aanleveren van het anatomisch materiaal en de assistentie bij het inbedden en zagen van de levers, als voor al de mooie anekdotes.

Wim van Beek en Jan van Ewijk, dank voor de hulp bij de ontwikkeling van het toedienings-/bestralingsvial.

Raymond Toelanie, dank voor het maken van (de vele versies van) de mooie *artist impressions*.

Alle leuke en bekwame lieden van het Technisch Cluster en van Multimedia Beeld (in het bijzonder Karin, natuurlijk), zeer bedankt voor jullie ondersteuning.

André Dales, Rosanne Varkevisser, Maurits Wondergem, Kitty Bos, Judith van Eeuwijk en Carola van de Bovenkamp, 'mijn' studenten, jullie waren stuk voor stuk leuke exemplaren, allen dank voor het goede werk, bij enkelen van jullie zie ik overigens wel promovenduspotentie.

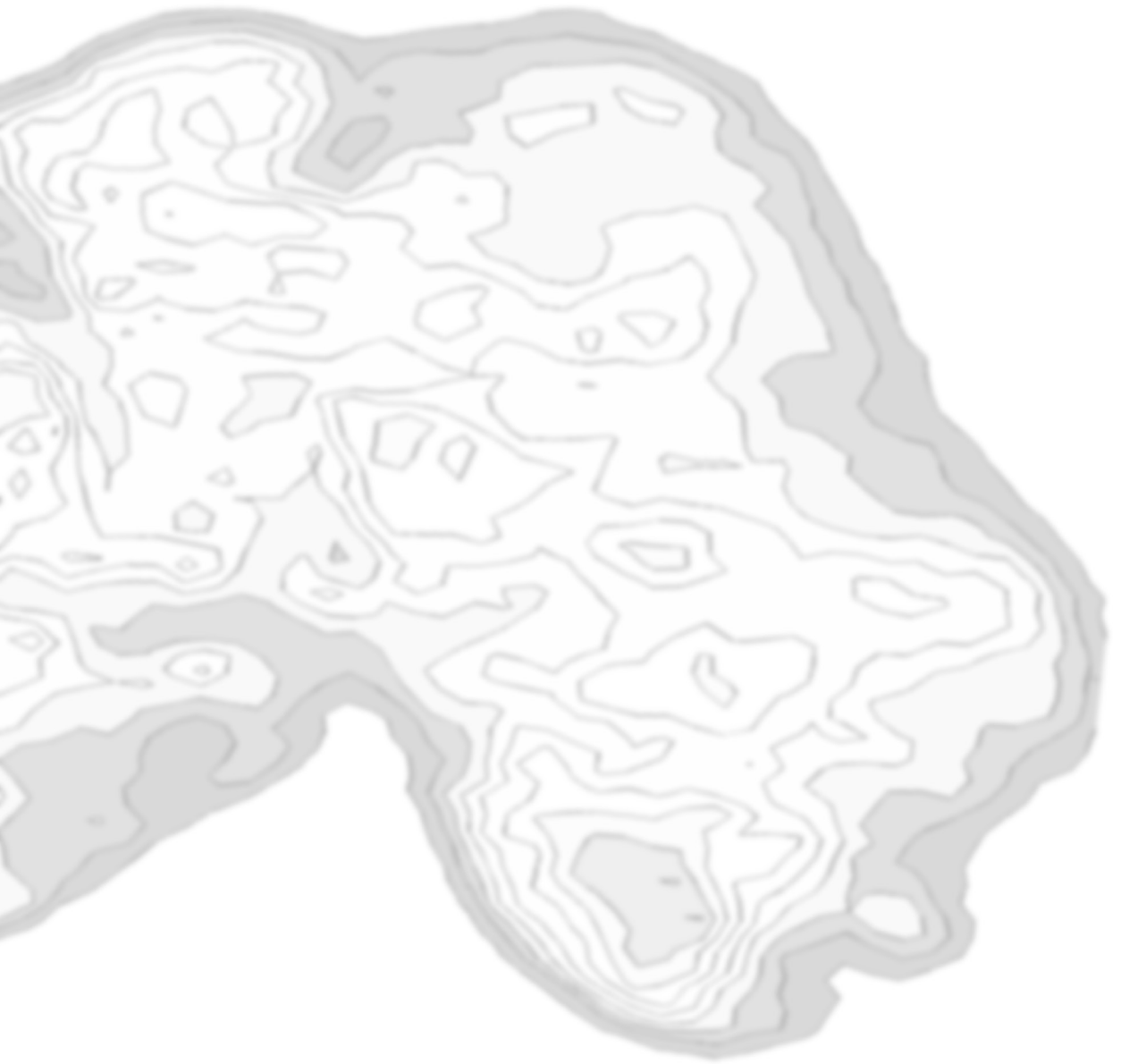
Lieve familie en vrienden, hierbij bied ik mijn excuses aan, want ik heb jullie de afgelopen vijf jaar ietwat verwaarloosd. Dat beloof ik in de aankomende tijd goed te gaan maken.

Last but not least, wil ik alle medewerkers van de afdeling Nucleaire Geneeskunde hartelijk danken, voor hun interesse, de helpende hand indien nodig, maar vooral ook voor de ontzettende goede onderlinge sfeer!

Saluut!

Maarten

**Curriculum vitae
and
list of publications**



CURRICULUM VITAE

De schrijver van dit proefschrift werd geboren op 15 juli 1970 te Amstelveen. De middelbare school werd trapsgewijs doorlopen: in 1986 werd het mavo-examen behaald (Christelijke Mavo Doorn), in 1988 het havo-examen en in 1990 het atheneumexamen (Christelijk Lyceum Zeist). Aanvullende certificaten natuurkunde en scheikunde werden aan het James Boswell Instituut (Universiteit Utrecht) behaald.

In 1992 begon hij met de studie diergeneeskunde aan de Faculteit der Diergeneeskunde van de Universiteit Utrecht. Het propedeutisch examen werd behaald in 1993. Hij was lid van de reductiecommissie (1993-'94) en bestuurslid van de Veterinaire Motorclub (1995-2000). De titel van zijn doctoraalscriptie was "Bijzondere fysiologische kenmerken en veterinaire aspecten van de Europese bruine beer (*Ursus arctos arctos*)". Het doctoraalexamen diergeneeskunde werd behaald in 1999. Het theoretisch deel van de postdoctorale fase werd afgerond in 2000 en het dierenartsexamen (differentiatie gezelschapsdieren) werd uiteindelijk behaald in 2003.

In november 2003 werd een aanvang gemaakt met het promotieonderzoek binnen het holmiumproject op de afdeling Nucleaire Geneeskunde van het Universitair Medisch Centrum Utrecht. De resultaten van dit onderzoek hebben geleid tot dit proefschrift. Naast dit onderzoek was hij sinds november 2007 als klinisch medewerker betrokken bij de voorbereiding van de binnenkort te starten klinische fase I studie met de holmium microsferen. Momenteel oriënteert hij zich op een interessante baan bij een farmaceutisch of biotechnologisch bedrijf.

LIST OF PUBLICATIONS

Full papers

M.A.D. Vente, M.G.G. Hobbelink, A.D. van het Schip, B.A. Zonnenberg, J.F.W. Nijsen. Radionuclide liver cancer therapies: from concept to current clinical status *Anti-Cancer Agents in Medicinal Chemistry* 2007;7:441-459.

M.A.D. Vente, J.F.W. Nijsen, R. de Roos, M.J. van Steenberg, C.N.J. Kaaijk, M.J.J. Koster-Ammerlaan, P.F.A. de Leege, W.E. Hennink, A.D. van het Schip, G.C. Krijger. Neutron activation of holmium poly(L-lactic acid) microspheres for hepatic arterial radioembolization: a validation study
Biomedical Microdevices
Accepted.

M.A.D. Vente, J.F.W. Nijsen, T.C. de Wit, J.H. Seppenwoolde, G.C. Krijger, P.R. Seevinck, A. Huisman, B.A. Zonnenberg, T.S.G.A.M. van den Ingh, A.D. van het Schip. Clinical effects of transcatheter hepatic arterial embolization with holmium-166 poly(L-lactic acid) microspheres in healthy pigs
European Journal of Nuclear Medicine and Molecular Imaging 2008;35:1259-1271.

M.A.D. Vente, T.C. de Wit, M.A.A.J. van den Bosch, W. Bult, P.R. Seevinck, B.A. Zonnenberg, H.W.A.M. de Jong, G.C. Krijger, C.J.G. Bakker, A.D. van het Schip, J.F.W. Nijsen. Holmium-166 poly(L-lactic acid) microsphere radioembolization of the liver: technical aspects studied in a large-animal model
Submitted.

M.W. Konijnenberg, M.A.D. Vente, T.C. de Wit, H.W.A.M. de Jong, A.D. van het Schip, J.F.W. Nijsen. Hepatic dosimetry for holmium-166 poly(L-lactic acid) microspheres: comparison of MIRD, dose-point kernel, and MCNP
Submitted.

M.A.D. Vente, M. Wondergem, I. van der Tweel, M.A.A.J. van den Bosch, B.A. Zonnenberg, M.G.E.H. Lam, A.D. van het Schip, J.F.W. Nijsen. Yttrium-90 microsphere radioembolization for the treatment of liver malignancies: A structured meta-analysis

European Radiology 2009;19:951-959.

M.A.D. Vente, W. Bult, K. Peremans, H. Haers, E. Vandermeulen, P.R. Seevinck, A.D. van het Schip, R. de Roos, C.J.G. Bakker, G.C. Krijger, J.F.W. Nijsen Interstitial microbrachytherapy using small holmium-166 acetylacetonate microspheres for radioablation of intrahepatic malignancies

Submitted.

M.A.D. Vente, M.L.J. Smits, B.A. Zonnenberg, J.F.W. Nijsen, M.A.A.J. van den Bosch. Intra-arterial radioembolization with yttrium-90 microspheres for treatment of unresectable colorectal liver metastases

Dutch Journal of Oncology 2008;5:370-376.

W. Bult, M.A.D. Vente, B.A. Zonnenberg, A.D. van het Schip, J.F.W. Nijsen. Microsphere radioembolization of liver malignancies: current developments

The Quarterly Journal of Nuclear Medicine and Molecular Imaging

Accepted.

Conference contributions

(1st authorship only)

M.A.D. Vente, M.A.A.J. van den Bosch, T.C. de Wit, P.R. Seevinck, B.A. Zonnenberg, G.C. Krijger, A.D. van het Schip, J.F.W. Nijsen. Hepatic arterial embolization with holmium-166 poly(L-lactic acid) microspheres for treatment of liver malignancies: does the distribution of the holmium-166 microspheres scout dose predict the distribution of the therapeutic dose *in vivo*?

Radiological Society of North America 94th Scientific Assembly and Annual Meeting
Chicago, IL, USA, 2008

M.A.D. Vente, W. Bult, T.C. de Wit, P.R. Seevinck, J.H. Seppenwoolde, B.A. Zonnenberg, R. de Roos, G.C. Krijger, A.D. van het Schip, J.F.W. Nijsen. Holmium-166 poly(L-lactic acid) microspheres for treatment of liver malignancies: treatment procedure testing in a large animal model

Beta-Days – Current status in radionuclide therapy
Capri, Italy, 2007

M.A.D. Vente, J.F.W. Nijsen, T.C. de Wit, P.R. Seevinck, R. de Roos, J.H. Seppenwoolde, G.C. Krijger, W. Bult, B.A. Zonnenberg, M.G.G. Hobbelink, C.J.G. Bakker, A.D. van het Schip. Administration procedure testing of holmium-166 microspheres for treatment of liver cancer

Annual Congress of the European Association of Nuclear Medicine
Copenhagen, Denmark, 2007

M.A.D. Vente, J.F.W. Nijsen, T.C. de Wit, J.H. Seppenwoolde, G.C. Krijger, P.R. Seevinck, W. Bult, R. de Roos, B.A. Zonnenberg, M.G.G. Hobbelink, P.P. van Rijk, A.D. van het Schip. Radioembolization of the liver with holmium-166 poly(L-lactic acid) microspheres in healthy pigs

Annual Congress of the European Association of Nuclear Medicine
Athens, Greece, 2006

M.A.D. Vente, S.W. Zielhuis, J.F.W. Nijsen, J.H. Seppenwoolde, G.C. Krijger, T.C. de Wit, C.J. Bakker, B.A. Zonnenberg, A.D. van het Schip, P.P. van Rijk. Biocompatibility of holmium-166 loaded microspheres for the treatment of liver malignancies

Annual Congress of the European Association of Nuclear Medicine
Istanbul, Turkey, 2005

M.A.D. Vente, J.H. Seppenwoolde, J.F.W. Nijsen, S.W. Zielhuis, R. de Roos, B.A. Zonnenberg, A.D. van het Schip, P.P. van Rijk. Transcatheter arterial embolization (TAE) of the liver with holmium loaded microspheres in pigs: a toxicity and biodistribution study

Annual Congress of the European Association of Nuclear Medicine
Helsinki, Finland, 2004

